

Cover Page



Universiteit Leiden



The handle <http://hdl.handle.net/1887/28890> holds various files of this Leiden University dissertation.

Author: Hombrink, Pleun

Title: Identification of minor histocompatibility antigens by reverse immunology

Issue Date: 2014-09-23

**IDENTIFICATION OF MINOR HISTOCOMPATIBILITY
ANTIGENS BY REVERSE IMMUNOLOGY**

Pleun Hombrink

Identification of minor histocompatibility antigens by reverse immunology
© 2014 Pleun Hombrink, Amsterdam

Cover image: Joke Haverkate, 2014, *Steenmannetjes*
kleurenets, combinatie vernis-mou en aquatint techniek

Layout: Liset Westera

Printing: Gildeprint, Enschede, The Netherlands

ISBN: xxx-xx-xxx-xxxx-x

The research described in this thesis was financially supported by the Dutch Cancer Society (grant 07-3825) and the Landsteiner Foundation for Blood Transfusion Research (grant LSBR0713).

Printing of this thesis was financially supported by the Dutch Cancer Society (KWF) and eBioscience.

**IDENTIFICATION OF MINOR HISTOCOMPATIBILITY
ANTIGENS BY REVERSE IMMUNOLOGY**

Proefschrift

ter verkrijging van
de graad van doctor aan de Universiteit Leiden,
op gezag van de Rector Magnificus prof.mr. C.J.J.M. Stolker,
volgens besluit van het College voor Promoties
te verdedigen op dinsdag 23 september 2014
klokke 16:15 uur

door

Pleun Hombrink

geboren te Eindhoven
in 1982

PROMOTIECOMMISSIE

Promotor: Prof. dr. J.H.F. Falkenburg

Co-promotor: Dr. M.H.M. Heemskerk

Overige leden: Prof. dr. R.A.W. van Lier
Prof. dr. B.O. Roep
Dr. T. Mutis

CONTENTS

Chapter 1	General introduction and Aim of the study	7
Chapter 2	High-throughput identification of potential minor histocompatibility antigens by MHC tetramer-based screening: feasibility and limitations	29
Chapter 3	Mixed functional characteristics correlating with TCR-ligand k_{off} -rate of MHC-tetramer reactive T-cells within the naïve T-cell repertoire	73
Chapter 4	Discovery of T-cell epitopes implementing HLA-peptidomics into a reverse immunology approach	99
Chapter 5	Identification of clinically relevant minor histocompatibility antigens within the B-lymphocyte derived HLA-ligandome using a reverse immunology approach	123
Chapter 6	Summary and General discussion	151
Appendices	Nederlandse samenvatting	167
	Dankwoord	179
	Curriculum vitae	181
	List of publications	182



1

GENERAL INTRODUCTION AND AIM OF THE STUDY

GENERAL INTRODUCTION

Allogeneic hematopoietic stem cell transplantation

Allogeneic stem cell transplantation (alloSCT) is considered an effective curative therapy for various hematopoietic malignancies¹⁻³. During this therapy patients receive a transplantation of multipotent hematopoietic stem cells derived from a genetically different donor. Pre-transplantation, patients are conditioned with chemotherapy, irradiation and immune suppression to eradicate malignant cells and to allow engraftment of the donor derived stem cell graft. After conditioning, a donor hematopoietic stem cell graft is transplanted that can fully replace the damaged patient's bone marrow. The efficacy of this therapy is affected by the pre-transplant doses of chemotherapy and irradiation. Conventional myeloablative conditioning includes intensive high-dose treatment aiming at complete eradication of malignant cells and prevention of graft rejecting by residual patient immune cells. This type of conditioning is associated with severe toxicity that can be potentially lethal. As a consequence, older and frailer patients who require a less toxic approach may receive non-myeloablative conditioning with lower-dose treatment^{4,5}. This regimen is characterized by reduced intensity pre-transplantation treatment of patients aiming at sufficient immune suppression to allow donor stem cell engraftment and prevent graft rejection. Post-transplantation, durable engraftment of allogeneic hematopoietic stem cells may be achieved using both regimens followed by complete hematopoietic reconstitution within several weeks. Although both myeloablative and non-myeloablative conditioning aim at pre-transplant reduction of tumor burden, not all malignant cells can be eliminated. Residual malignant cells may remain in the patient and can lead to relapse of disease. As a consequence, both regimens rely on the graft versus leukemia (GvL) effect of donor immune cells to fully eradicate residual malignant cells.

Graft versus leukemia and graft versus host disease

The beneficial role of donor immune cells in controlling durable remission after hematopoietic stem cell transplantation was demonstrated when patients who developed graft versus host disease (GvHD) after alloSCT showed a lower leukemic relapse rate and an increased overall survival^{6,7}. GvHD is a potentially life-threatening complication in which donor immune cells were demonstrated to attack healthy tissues of the host^{8,9}. GvHD causes damage to many organs and especially targets the skin, gastrointestinal tract, liver and lungs. GvHD can be divided in two categories based on the onset of clinical manifestation. Whereas acute GvHD is usually observed within 100 days after transplant, chronic GvHD generally manifests later and may follow acute GvHD. Symptoms of acute GvHD can be divided in 4 grades depending on the severity of target organs inflammation whereas chronic GvHD has features more resembling autoimmune diseases. Although both types of GvHD may be treated with immune suppressive drugs this also increases the risk of infections and leukemic relapse.

The role for T-cells in both GvL as in GvHD was demonstrated by the induction of remission in patients after withdrawal of immune suppression^{10;11}. In addition, depletion of T-cells from the alloSCT graft was shown to be effective in reducing the incidence of GvHD but also resulted in an increased leukemic relapse rate¹²⁻¹⁶. More evidence that GvL was mediated by donor derived T-cells was provided by the induction of sustained remissions in patients with relapsed or persistent leukemia after alloSCT after treatment with donor lymphocyte infusion (DLI) from the original stem cell donor¹⁷. Although this form of immunotherapy, with unmanipulated T-cells, mediates GvL in various hematopoietic malignancies, the susceptibility of different types of malignancies to respond to DLI varies¹⁸⁻²². As T-cells play a crucial role in both the development of GvHD and GvL many strategies aim to minimize their role in GvHD while maintaining their beneficial GvL effect. By comparing different transplantation strategies in which donor grafts were used of either autologous, homozygous twin or allogeneic origin it was demonstrated that merely the presence of T-cells was not sufficient to mediate GvL and that a certain degree of genetic disparity between patient and donor was required^{23;24}. The major determinant for the development of severe GvHD appeared to be disparities in genetic loci within the major histocompatibility complex (MHC), with an increased number of mismatched antigens predicting greater risk for GvHD. In humans, MHC is also called human leukocyte antigen (HLA). The percentage of T-cells within an individual T-cell repertoire that is capable to react with peptides presented in non-self HLA is high and ranges between 1-10%^{25;26}. As a consequence, HLA-matched allo-SCT is preferable over HLA-mismatched allo-SCT to minimize the toxicity associated with more severe GVHD.

Human leukocyte antigens and antigen presentation

HLA-molecules are membrane-spanning heterodimers that are encoded by highly polymorphic genes and as a consequence are extremely variable in their primary structure. There are different classes of HLA and those that correspond to HLA class I are composed of a heavy α -chain and a β_2 microglobulin. In contrast, HLA class II molecules are composed of a homogenous α - and β -chain. HLA-class I molecules present small cytosolic intracellular processed peptides, 8 to 11 amino acids in length, to CD8⁺ T-cells. HLA-class II molecules, which are structurally different, present peptides mainly derived from extracellular proteins, 12-25 amino acids in length, to CD4⁺ T-cells²⁷. Peptides presented by HLA-class I molecules are the product of ubiquitinated proteins^{28;29}. Ubiquitin is a small regulatory protein that post translation binds to proteins and regulates protein turnover as it signals for protein degradation in the proteasome³⁰. Excessive or damaged intracellular proteins can be degraded via proteolysis in proteasomes, specialized protein complexes located in the cytoplasm. Protein degradation yields peptide fragments that are generally translocated by the transporter associated with antigen processing (TAP) into the lumen of the endoplasmic reticulum (ER), where they may be loaded onto an HLA-

class I molecule if they bind into their peptide-binding pocket with sufficient affinity³¹. The peptide-HLA complex is then guided through the ER to the cell surface for presentation to CD8⁺ T-cells³². Peptides derived from autologous proteins are continuously processed and presented at the surface of antigen presenting cells. The repertoire of peptides that is presented is restricted to self HLA-molecules and only represents a subset of the human proteome, all proteins produced from the human genome³³. HLA-class I molecules are continuously expressed on all nucleated cells whereas expression of HLA-class II molecules, which are loaded with peptides generated by a different process called endocytosis, is more restricted to cells derived from the hematopoietic compartment, such as B-cells, monocytes, dendritic cells and macrophages, but can be induced in non-hematopoietic cells under inflammatory conditions^{34;35}. Based on the extremely variable structure of HLA-molecules, it is very unlikely that two randomly selected, non-related, individuals will express identical HLA-molecules. As alloreactive T-cells, recognizing peptides in allo HLA-molecules are present in high frequencies in peripheral blood, HLA-mismatched alloSCT may result in strong allo-HLA immunity³⁶. Therefore, fully HLA-matched individuals, related or unrelated to the patient are ideal alloSCT donors.

T-cells and antigen recognition

The main mediators of GvHD and GvL are believed to be T-cells that play an important role in the adaptive immune response against various pathogens. T-cells are a subpopulation of lymphocytes that can be distinguished from other white blood cells by the presence of a T-cell receptor (TCR), through which they can distinguish self from mutated self and foreign antigenic peptides, presented in the context of HLA-molecules at the surface of antigen presenting cells^{37;38}. The TCR is a transmembrane heterodimer consisting of a TCR α and a TCR β chain that are linked with a disulfide bond and embedded in combination with the CD3 protein complex in the cell membrane. Each of these chains is composed of a variable and a constant region. The rearrangement of these chains during T-cell development and especially the random mutations in the extracellular complementarity-determining regions (CDR) within their variable regions establish a unique antigen-binding site for each TCR. The CD3 protein complex is composed of 3 different CD3 T-cell co-receptor chains (gamma, delta and epsilon) and a CD3 zeta-chain that can associate with the TCR and generate an activation signal upon antigen challenge. Together these molecules are called the TCR complex. The TCR of an individual T-cell is usually specific for a particular peptide-HLA complex. However, since a TCR can be activated by even a few crucial residues of the presented peptide, other peptides with high sequence similarities may also be recognized in a process called molecular mimicry³⁹. Hematopoietic precursor cells are released from the bone marrow and thymus-homing progenitors migrate to the thymus to give rise to the T-cell lineage. After T-cell development in the thymus immune competent naïve T-cells are released in the periphery either committed to the CD4 or CD8 lineage that can home to

nonlymphoid tissues^{40;41}. In the thymus positive selection takes place of T-cells expressing a TCR that is able to engage self-HLA molecules with low affinity that are tolerant for self peptides presented in the context of self-HLA⁴². Subsequently, T-cells with too high affinity to self-peptides in the context of self-HLA are eliminated through programmed cell death⁴³. In the thymus, T-cells are not negatively selected towards peptides derived from mutated or non-self antigens.

For activation of naïve CD8⁺ T-cells several simultaneous signals are required. First, the TCR should bind a non-self peptide presented by HLA class I molecules. This interaction is stabilized by an additional interaction of the CD8 co-receptor molecule with the HLA class I molecule. Secondly, binding of the CD28 co-stimulatory molecules to CD80 and CD86 expressed by the activated antigen presenting cells (APC) is essential. Helper T-cells, expressing a CD4 co-receptor are in addition important for optimal activation of naïve-CD8⁺ T-cells by the induction of expression of CD80 and CD86 on the APCs and by the production of cytokines necessary for the proliferation of CD8⁺ T-cells. Upon activation, CD8⁺ T-cells will start to produce cytokines such as TNF-alpha and IFN-gamma and will be able to lyse the recognized target cells (e.g. infected cells, tumor cells) by a perforin, granzymes and granulysin mediated response^{44;45}. In addition, CD8⁺ T-cells can also induce apoptosis of target cells by binding with their surface expressed FAS ligand to FAS molecules at the surface of target cells. Specific antigen recognition results in a clonal expansion of antigen-specific effector T-cells followed by a rapid contraction when the infection is cleared. After infection, memory T-cells survive that can initiate a faster and more efficient secondary immune response upon re-encounter with the antigenic peptides^{46;47}.

As described previously, T-cell activation is strictly regulated and multiple signals are simultaneously required to induce their effector function. To induce activation, the TCR complex needs to bind to non-self peptide presented on HLA of APC such as dendritic cells (DC). The strength by which a TCR interacts with a peptide-HLA complex is termed TCR affinity. Antigen engagement results in cross-linking of TCR and subsequent phosphorylation of immunoreceptor tyrosine-based activation motifs (ITAM) motifs on the proximal domain of the assembled CD3-TCR complex. This phosphorylation is mediated by protein kinases and initiates a cascade of signaling events that eventually results in translocation of transcription factors into the nucleus and transcription of effector molecules. As the affinity of a single TCR towards a single peptide-HLA complex is relative low, many TCR need to engage with their antigen and cross-link simultaneously to initiate T-cell activation. This results in TCR clustering in the immunological synapse, the interaction site between the APC and a T-cell. During the formation of this ring shaped structure, the TCR co-receptor molecules CD4 or CD8, co-stimulatory and adhesion molecules such as CD28, OX40, ICOS and LFA-1 are also recruited and clustered in protein islands and amplify the signaling process initiated by the TCR^{48;49}. The affinity of the TCR for the presented peptide-HLA complex in combination with additional interactions via co-receptor, co-stimulatory and

adhesion molecules with their APC ligands, determines the overall strength by which a T-cell binds to a target cell, termed T-cell avidity.

The activation of naïve T-cells is strictly regulated by the requirement of both TCR and co-stimulatory molecule stimulation. As a consequence, naïve T-cells can only be properly activated by professional APC that are frequently residing in the draining lymph nodes of infected organs^{50,51}. Upon activation, naïve T-cells gain the capacity to migrate into the infected tissue and exert their effector function. In the absence of co-stimulation, TCR signaling alone will result in anergy of these cells⁵². In contrast, memory T-cells can be activated in the absence of co-stimulation. Although the molecular basis of this increased sensitivity remains unclear, both enhanced downstream signaling of TCR signaling and the expression of more and larger TCR oligomers at the cell surface enable the activation of these cells by every HLA-expressing cell⁵³. As a consequence, memory T-cells can reside in peripheral tissues and epithelial cell layers, the main entry sites for pathogens, and enable long-term immunosurveillance to prevent secondary infections⁵⁴⁻⁵⁶.

Minor histocompatibility antigens

Since T-cell mediated GvHD and GvL may also occur after fully HLA-matched alloSCT, disparities outside the MHC loci can also elicit T-cell reactivity. Detailed analyses of T-cell responses in patients responding to HLA-matched allo-SCT and subsequent DLI have demonstrated that the donor T-cells mediating both GVHD and GVL recognize minor histocompatibility antigens (MiHA) presented in the context of HLA-class I and HLA-class II molecules on the surface of recipient cells⁵⁷⁻⁶⁵. These MiHA are immunogenic peptides derived from polymorphic proteins that differ between donor and recipient due to DNA sequence variations. The most frequent MiHA variations between two individuals are generated by single nucleotide polymorphisms (SNP) in the coding regions of the MiHA encoding genes⁶⁶⁻⁶⁸. When these SNP change the amino acid sequence of the protein they are called “nonsynonymous” while SNP that does not affect this sequence are called “synonymous”. Synonymous SNP in coding regions or those that are located in non-coding regions may still be responsible for T-cell recognition as peptides containing these SNPs may be produced due to differential protein synthesis caused by alterations in reading frame, gene splicing and messenger RNA stability⁶⁹⁻⁷². As humans are diploid, two copies of each autosomal chromosome exist that both contain an allele of the MiHA encoding gene. If both alleles are identical, the MiHA is homozygously expressed. If the alleles are not identical for the SNP, the MiHA is heterozygously expressed. The minor allele frequency indicates the occurrence of the least common allele in a population. If an individual is homozygous for a given MiHA, there may be T-cells present within the T-cell repertoire that recognize the non-self alternative allelic variant of the MiHA with high avidity. If a donor is heterozygous for a given MiHA, T-cells that recognize both allelic variants of the MiHA are depleted from the T-cell repertoire in the thymus.

Variation in the DNA sequence of different individuals is common and is caused by spontaneous mutations, genetic recombination and driven by natural selection. To date, approximately 180 million SNP are listed in the bioinformatics NCBI dbSNP database that are mainly identified by the combined efforts of two massive whole genome sequencing consortiums^{73,74}. On average, 3 million SNP were identified per individual genome. Consequently, two randomly selected individuals will be mismatched for hundreds of thousands of SNP. Despite these astonishing numbers, to date, only 50 MiHA have been identified by different molecular methods of which 44 are expressed at autosomal loci^{68,75}. The *ex vivo* analysis of the recipient T-cell repertoire after allo-SCT for presence of T-cells directed against these MiHA revealed that the presence of these T-cells variable and some MiHA specific T-cells are more frequently observed than others⁷⁶⁻⁷⁹.

MiHA as relevant targets for adoptive immunotherapy

Currently, several strategies are exploited to generate MiHA-specific adoptive immunotherapy. As MiHA specific T-cells can both mediate GvL and GvHD, specificity is crucial. If donor derived T-cells recognize MiHA that are ubiquitously expressed on many tissues they may mediate both GvL and GvHD. However, if this response is directed against MiHA that are exclusively expressed on cells of the hematopoietic system, they may mediate GvL in absence of GvHD⁸⁰. Donor-derived T-cells that target MiHA expressed on hematopoietic cells will selectively eradicate patient hematopoietic cells, including malignant cells. Hence, selective infusion of T-cells reactive with MiHA exclusively expressed on hematopoietic cells is considered an attractive immunotherapy to establish a potent GvL response in absence of GVHD^{81,82}. However, a recent multicenter study demonstrated that although mismatching for hematopoietic restricted MiHA correlates with lower relapse rates, higher relapse-free survival and higher overall survival after allo-SCT, this was only observed in recipients with GvHD and not in those without GvHD. This indicates that adoptive immunotherapy should aim to enhance the GvL effect in a GvHD controllable manner⁸³.

MiHA specific adoptive immunotherapy requires the *ex vivo* generation of sufficient numbers of donor derived high-avidity MiHA-specific T-cells. One way to achieve these numbers is by redirecting the specificity of donor T-cells by gene transfer of MiHA-specific TCR. To prevent the induction of GVHD, the TCR genes should preferentially be transferred into donor T-cells with a known specificity that are unlikely to mediate GVHD, such as virus-specific T-cells^{84,85}. Alternatively, sufficient number of MiHA specific T-cells can be achieved by repeated stimulation of donor T-cells with MiHA-peptide loaded or genetically MiHA gene transduced dendritic cells⁸⁶⁻⁹⁰. Several clinical trials, using adoptive transfer of MiHA-specific T-cells have been performed thus far^{91,92}. Although these therapies appeared to be relatively safe, clinical response is not always observed. A recent phase I trial, that included the adoptive transfer of MiHA-specific T-cells in patients with relapsed

leukemia, demonstrated the induction of a temporary complete morphologic remission in 5 out of 7 patients⁹². Although promising, the assessment of the contribution of adoptively transferred MiHA-specific T-cells to the observed GvL response was complicated due to pre-therapy and concurrent administration of immunosuppressive agents. Unfortunately, the infused cells failed to persist *in vivo* and as a consequence may not protect against future relapsed disease. The observed short life span of the introduced cells may be the result of extensive *in vitro* expansion culture protocols that result in short-lived terminally differentiated cells. Alternatively, MiHA specific T-cells may be isolated from the naïve T-cell repertoire, as these cells are not terminally differentiated upon expansion and may persist longer after infusion⁹³. In a different immunotherapy approach the frequency of MiHA specific T-cells is increased by pre transplant vaccination of donors or by vaccinating patients after DLI with DCs that selectively present hematopoietic restricted MiHA peptides⁹⁴⁻⁹⁶. These strategies aim to stimulate long-term persistence of MiHA specific T-cell responses *in vivo*, and induce GvL without extensive T-cell manipulation. Although currently several MiHA specific immunotherapy strategies are exploited, a major limitation for broad clinical implementation of MiHA is the small number of identified MiHA derived from genes that are exclusively restricted to hematopoietic cells.

Strategies for the molecular identification of hematopoietic MiHA

Over the years, the discovery of MiHA is accelerated by the introduction of novel immunology approaches such as cDNA library screening⁹⁷⁻⁹⁹, genetic linkage analysis^{100;101}, peptide elution from-HLA^{69;102;103}, and genome-wide association studies^{64;104;105}. Collectively, these methods use a forward immunology approach characterized by the isolation of activated T-cells from patients demonstrating a clinical response to DLI after allo-SCT and subsequent elucidation of the genomic locus and peptide sequence of the MiHA recognized. The intrinsic property of these methods is isolation of T-cells with antigen specificities which are not predefined. Stimulated by the emerging availability of public bioinformatics data on human genetic polymorphisms^{73;106}, computer algorithms that predict peptide-HLA binding affinity, TAP transport, proteosomal cleavage and gene expression profiles¹⁰⁷⁻¹¹⁰, an alternative method called “reverse” immunology is increasingly exploited to enhance the efficiency of characterizing hematopoietic MiHA with therapeutic potential. In this approach computational peptide predictions are the starting point and peptide candidates are subsequently screened for their capacity to induce a T-cell specific response¹¹¹⁻¹¹³. This approach has the advantage to specifically screen for T-cells recognizing MiHA that are exclusively expressed by hematopoietic cells. Although this approach have been used extensively to discover tumor associated antigens (TAA), it only resulted in the identification of a few MiHA^{114;115}. Thus far the numbers of immunogenic TAA and MiHA epitopes that were identified by reverse immunology approaches are in contrast with the large panel of candidate epitopes that can be generated using these algorithms. The overall

low efficiency may be explained by the observation that when such epitope predictions are solely based on computer algorithms that predict peptide-HLA binding affinity the vast majority of T-cell responses detected is directed against epitopes that are not naturally processed and presented and as a consequence these T-cells will not kill their target cells¹¹⁶⁻¹¹⁹. One possibility to evade this candidate selection problem is the identification of the HLA-associated peptidome of hematopoietic cells by mass spectrometric analysis. The implementation of HLA-peptidomics into a reverse immunology approach guarantees HLA-restricted processing and presentation of eluted peptide candidates^{33;120;121}.

Although the generation of large panels of candidate epitopes is feasible, predicted MiHA can only be validated by the identification of high-avidity T-cells reactive to these antigens. The use of soluble fluorescently labeled major histocompatibility complex multimers (MHC-tetramers) has become a widely used approach to detect antigen-specific T-cells in a diverse T-cell repertoire¹²². Whereas classical major histocompatibility complex multimer analyses are designed for the detection of immune responses to a few epitopes, large-scale screening of a multitude of different T-cell populations in a single sample is essential to keep up with demands to screen large predicted peptide libraries. The development of technology for high-throughput MHC-tetramer production makes it possible to screen for T-cell reactivity against large panels of potential MiHA by flow cytometry either by combinatorial coding or by extension of the number of fluorescent labels used for MHC-tetramer labeling¹²³⁻¹²⁷. In conclusion, differential tissue distribution of MiHA in patients may elicit high avidity donor derived T-cell reactivity that can mediate in GvL when the tissue distribution of the SNP is restricted to the malignant or hematopoietic compartment. If these MiHA are exclusively expressed on hematopoietic cells, these MiHA are attractive targets for adoptive T-cell therapy of patients with hematological malignancies. To date however, the number of known MiHA that form attractive targets for adoptive T-cell therapy remains limited. The development of efficient techniques to identify MiHA may increase the number of patients that may be treated with MiHA specific immunotherapy. In addition, future applications of MiHA specific immunotherapy may also benefit from increased knowledge of what source of T-cell populations should be used for generation of MiHA specific T-cells that may persist *in vivo* and exert optimal effector functions.

AIM OF THE STUDY

Two decades ago, reverse immunology was postulated as an efficient and high-throughput approach for the identification of strongly immunogenic tumor antigens that could be used in immunotherapy. Encouraged by advances in T-cell culture techniques and the elucidation of structural components underlying the interaction of the T-cell receptor (TCR) of antigen specific T-cells with the peptide presenting major histocompatibility complex (MHC) on target cells, reverse immunology was expected to overcome the limitations of forward immunology approaches. Although promising, a typical reverse immunology approach in which the prediction of putative minor histocompatibility antigens (MiHA) candidates is the starting point and peptide candidates are subsequently screened for their capacity to induce a T-cell specific response appeared to be low efficient in identifying MiHA.

In the past decade, rapid developments in the field of bioinformatics renewed the interest in using reverse immunology for MiHA discovery. The emerging availability of data on genome sequencing, human genetic polymorphism and gene expression profiles resulted in the prediction of large libraries of candidate MiHA for which the specific recognition by T-cell clones must be achieved in *in vitro* assays. In **chapter 2**, we investigate whether the genome-wide prediction of hematopoietic MiHA, coupled to the isolation of T-cell populations that react with these antigens is feasible using a novel technology for the high-throughput production of MHC-tetramers. Although the use of MHC-tetramers to detect antigen-specific T-cells in a diverse T-cell repertoire was already widely used, it was only after the development of UV-induced conditional ligand cleavage that this technology could be used on this scale. To this purpose a large set of putative HLA-A*0201 binding hematopoietic MiHA is produced using various HLA-peptide binding algorithms. To allow high-throughput screening with a large set of MHC-tetramers in PBMC samples with low cell numbers, we first develop an approach to simultaneously isolate T-cells reactive with any of the MHC-tetramers by magnetic pull down, followed by *in vitro* expansion. Subsequently, flow cytometry analysis of antigen-specific T-cell responses in patients with various hematologic malignancies after allo-SCT, followed by functional testing of identified T-cell clones is used to assess the clinical value of predicted MiHA.

Since the frequencies of antigen-specific T-cells in the naïve T-cell repertoire are very low, isolation of antigen specific naïve T-cells is challenging. In **chapter 3** we aim to optimize the generation of naïve repertoire derived antigen-specific T-cell lines based on MHC-tetramer staining and magnetic-bead enrichment. To ensure their biological relevance, we select a variety of immunodominant cytomegalovirus (CMV) epitopes binding to various HLA-molecules (HLA-A1, A2, B7, B8 and B40). In this chapter we describe the functional heterogeneity of isolated CMV-specific T-cells within the total MHC-tetramer positive T-cell populations and focus on the predictive value of MHC-tetramer staining on T-cell reactivity as T-cells within a certain range of high avidity for their cognate ligand are believed to be most effective. We demonstrate that variations in the functional avidity of

the MHC-tetramer positive T-cells correlate with the structural avidity of their cell surface expressed TCR as measured by the dissociation kinetics of antigen specific TCR binding to monomeric peptide-MHC complexes.

Although the rapid developments in the field of bioinformatics encourage the use of reverse immunology approaches, the gigantic amounts of data provided by gene sequence, expression and polymorphisms databases is overwhelming and may result in low efficient prediction of biological relevant MiHA. In **chapter 4**, we investigate the feasibility of implementing mass spectrometry based HLA-peptidomics into a reverse immunology approach as a reliable source for naturally processed and presented peptides. For this purpose HLA class I binding peptides are eluted from transformed B-cells, analyzed by mass spectrometry and matched with a database dedicated to identify polymorphic peptides. The resulting set of HLA-A*0201 binding MiHA candidates will be evaluated for their immunogenic potential in multiple selection steps. Based on these results we will develop an algorithm that can be exploited for the efficient identification of MiHA, that is used and further optimized in **chapter 5** to study the clinically relevance of a new high priority set of eluted HLA-A*0201 and B*0702 MiHA candidates. In this study we will screen the T-cell repertoire of both healthy donors and patients that received an allo-SCT from a HLA-matched donor with a favorable SNP disparity for the availability of high avidity T-cells. Identified MiHA specific T-cells will be tested for their reactivity against primary hematopoietic malignant cells.

Finally, the general discussion describes how our findings may contribute to the improvement of reverse immunology approaches for the identification of clinically relevant MiHA or other T-cell epitopes useful for adoptive T-cell therapies. In addition, novel technologies that have the potential to increase the efficiency of future reverse immunology based epitope discovery studies will be discussed.

REFERENCE LIST

1. Horowitz MM, Gale RP, Sondel PM et al. Graft-versus-leukemia reactions after bone marrow transplantation. *Blood* 1990;75:555-562.
2. Appelbaum FR. Haematopoietic cell transplantation as immunotherapy. *Nature* 2001;411:385-389.
3. Welniak LA, Blazar BR, Murphy WJ. Immunobiology of allogeneic hematopoietic stem cell transplantation. *Annu.Rev Immunol* 2007;25:139-170.
4. Schattenberg AV, Levenska TH. Differences between the different conditioning regimens for allogeneic stem cell transplantation. *Curr.Opin.Oncol.* 2006;18:667-670.
5. Gill S, Porter DL. Reduced-Intensity Hematopoietic Stem Cell Transplants for Malignancies: Harnessing the Graft-Versus-Tumor Effect. *Annu.Rev Med.* 2012
6. Weiden PL, Flournoy N, Thomas ED et al. Antileukemic Effect of Graft-versus-Host Disease in Human Recipients of Allogeneic-Marrow Grafts. *New England Journal of Medicine* 1979;300:1068-1073.
7. Weiden PL, Flournoy N, Sanders JE, Sullivan KM, Thomas ED. Antileukemic effect of graft-versus-host disease contributes to improved survival after allogeneic marrow transplantation. *Transplant.Proc.* 1981;13:248-251.
8. Shlomchik WD. Graft-versus-host disease. *Nat Rev Immunol* 2007;7:340-352.
9. Ferrara JL, Levine JE, Reddy P, Holler E. Graft-versus-host disease. *Lancet* 2009;373:1550-1561.
10. Sullivan KM, Deeg HJ, Sanders J et al. Hyperacute graft-v-host disease in patients not given immunosuppression after allogeneic marrow transplantation. *Blood* 1986;67:1172-1175.
11. Higano CS, Brixey M, Bryant EM et al. Durable complete remission of acute nonlymphocytic leukemia associated with discontinuation of immunosuppression following relapse after allogeneic bone marrow transplantation. A case report of a probable graft-versus-leukemia effect. *Transplantation* 1990;50:175-177.
12. Maraninchi D, Gluckman E, Blaise D et al. Impact of T-cell depletion on outcome of allogeneic bone-marrow transplantation for standard-risk leukaemias. *Lancet* 1987;2:175-178.
13. Apperley JF, Jones L, Hale G et al. Bone marrow transplantation for patients with chronic myeloid leukaemia: T-cell depletion with Campath-1 reduces the incidence of graft-versus-host disease but may increase the risk of leukaemic relapse. *Bone Marrow Transplant.* 1986;1:53-66.
14. Marmont AM, Horowitz MM, Gale RP et al. T-cell depletion of HLA-identical transplants in leukemia. *Blood* 1991;78:2120-2130.
15. Martin PJ, Hansen JA, Buckner CD et al. Effects of in vitro depletion of T cells in HLA-identical allogeneic marrow grafts. *Blood* 1985;66:664-672.
16. Hale G, Cobbold S, Waldmann H. T cell depletion with CAMPATH-1 in allogeneic bone marrow transplantation. *Transplantation* 1988;45:753-759.
17. Kolb HJ, Schattenberg A, Goldman JM et al. Graft-versus-leukemia effect of donor lymphocyte transfusions in marrow grafted patients. *European Group for Blood and Marrow Transplantation Working Party Chronic Leukemia.* *Blood* 1995;86:2041-2050.
18. Kolb HJ, Mittermuller J, Clemm C et al. Donor leukocyte transfusions for treatment of recurrent chronic myelogenous leukemia in marrow transplant patients. *Blood* 1990;76:2462-2465.
19. Mackinnon S, Papadopoulos EB, Carabasi MH et al. Adoptive immunotherapy evaluating escalating doses of donor leukocytes for relapse of chronic myeloid leukemia after bone

- marrow transplantation: separation of graft-versus-leukemia responses from graft-versus-host disease. *Blood* 1995;86:1261-1268.
20. Lokhorst HM, Schattenberg A, Cornelissen JJ, Thomas LL, Verdonck LF. Donor leukocyte infusions are effective in relapsed multiple myeloma after allogeneic bone marrow transplantation. *Blood* 1997;90:4206-4211.
 21. Collins RH, Jr., Shpilberg O, Drobyski WR et al. Donor leukocyte infusions in 140 patients with relapsed malignancy after allogeneic bone marrow transplantation. *J Clin.Oncol.* 1997;15:433-444.
 22. Loren AW, Porter DL. Donor leukocyte infusions for the treatment of relapsed acute leukemia after allogeneic stem cell transplantation. *Bone Marrow Transplant.* 2008;41:483-493.
 23. Zittoun RA, Mandelli F, Willemze R et al. Autologous or allogeneic bone marrow transplantation compared with intensive chemotherapy in acute myelogenous leukemia. European Organization for Research and Treatment of Cancer (EORTC) and the Gruppo Italiano Malattie Ematologiche Maligne dell'Adulto (GIMEMA) Leukemia Cooperative Groups. *N Engl J Med* 1995;332:217-223.
 24. Bruno B, Rotta M, Patriarca F et al. A comparison of allografting with autografting for newly diagnosed myeloma. *N Engl J Med* 2007;356:1110-1120.
 25. Lindahl KF, Wilson DB. Histocompatibility antigen-activated cytotoxic T lymphocytes. II. Estimates of the frequency and specificity of precursors. *J Exp.Med* 1977;145:508-522.
 26. Suchin EJ, Langmuir PB, Palmer E et al. Quantifying the frequency of alloreactive T cells in vivo: new answers to an old question. *J Immunol* 2001;166:973-981.
 27. Engelhard VH. Structure of peptides associated with class I and class II MHC molecules. *Annu. Rev Immunol* 1994;12:181-207.
 28. Hershko A, Ciechanover A. Mechanisms of intracellular protein breakdown. *Annu.Rev Biochem.* 1982;51:335-364.
 29. Hershko A, Ciechanover A, Rose IA. Resolution of the ATP-dependent proteolytic system from reticulocytes: a component that interacts with ATP. *Proc.Natl.Acad.Sci U.S.A* 1979;76:3107-3110.
 30. Goldstein G, Scheid M, Hammerling U et al. Isolation of a polypeptide that has lymphocyte-differentiating properties and is probably represented universally in living cells. *Proc.Natl. Acad.Sci U.S.A* 1975;72:11-15.
 31. Neefjes JJ, Momburg F, Hammerling GJ. Selective and ATP-dependent translocation of peptides by the MHC-encoded transporter. *Science* 1993;261:769-771.
 32. Vyas JM, Van der Veen AG, Ploegh HL. The known unknowns of antigen processing and presentation. *Nat Rev Immunol* 2008;8:607-618.
 33. Falk K, Rotzschke O, Stevanovic S, Jung G, Rammensee HG. Allele-specific motifs revealed by sequencing of self-peptides eluted from MHC molecules. *Nature* 1991;351:290-296.
 34. Klein J, Sato A. The HLA system. First of two parts. *N Engl J Med* 2000;343:702-709.
 35. Klein J, Sato A. The HLA system. Second of two parts. *N Engl J Med* 2000;343:782-786.
 36. Sherman LA, Chattopadhyay S. The molecular basis of allorecognition. *Annu.Rev Immunol* 1993;11:385-402.
 37. Neefjes J, Jongsma ML, Paul P, Bakke O. Towards a systems understanding of MHC class I and MHC class II antigen presentation. *Nat Rev Immunol* 2011;11:823-836.
 38. Jorgensen JL, Reay PA, Ehrich EW, Davis MM. Molecular components of T-cell recognition. *Annu.Rev Immunol* 1992;10:835-873.
 39. Oldstone MB. Molecular mimicry and autoimmune disease. *Cell* 1987;50:819-820.

40. Schwarz BA, Bhandoola A. Trafficking from the bone marrow to the thymus: a prerequisite for thymopoiesis. *Immunological Reviews* 2006;209:47-57.
41. Singer A, Adoro S, Park JH. Lineage fate and intense debate: myths, models and mechanisms of CD4- versus CD8-lineage choice. *Nat Rev Immunol* 2008;8:788-801.
42. Klein L, Hinterberger M, Wirnsberger G, Kyewski B. Antigen presentation in the thymus for positive selection and central tolerance induction. *Nat Rev Immunol* 2009;9:833-844.
43. Huseby ES, Crawford F, White J, Kappler J, Marrack P. Negative selection imparts peptide specificity to the mature T cell repertoire. *Proc.Natl.Acad.Sci U.S.A* 2003;100:11565-11570.
44. Harty JT, Tvinnereim AR, White DW. CD8+ T cell effector mechanisms in resistance to infection. *Annu.Rev Immunol* 2000;18:275-308.
45. Zhang N, Bevan MJ. CD8(+) T cells: foot soldiers of the immune system. *Immunity*. 2011;35:161-168.
46. Gerlach C, Rohr JC, Perie L et al. Heterogeneous differentiation patterns of individual CD8+ T cells. *Science* 2013;340:635-639.
47. King CG, Koehli S, Hausmann B et al. T cell affinity regulates asymmetric division, effector cell differentiation, and tissue pathology. *Immunity*. 2012;37:709-720.
48. Monks CR, Freiberg BA, Kupfer H, Sciaky N, Kupfer A. Three-dimensional segregation of supramolecular activation clusters in T cells. *Nature* 1998;395:82-86.
49. Lillemeier BF, Mortelmaier MA, Forstner MB et al. TCR and Lat are expressed on separate protein islands on T cell membranes and concatenate during activation. *Nat Immunol* 2010;11:90-96.
50. Croft M. Activation of naive, memory and effector T cells. *Curr.Opin.Immunol* 1994;6:431-437.
51. Sallusto F, Lanzavecchia A. The instructive role of dendritic cells on T-cell responses. *Arthritis Res.* 2002;4 Suppl 3:S127-S132.
52. Smith-Garvin JE, Koretzky GA, Jordan MS. T cell activation. *Annu.Rev Immunol* 2009;27:591-619.
53. Kumar R, Ferez M, Swamy M et al. Increased sensitivity of antigen-experienced T cells through the enrichment of oligomeric T cell receptor complexes. *Immunity*. 2011;35:375-387.
54. Ariotti S, Haanen JB, Schumacher TN. Behavior and function of tissue-resident memory T cells. *Adv.Immunol* 2012;114:203-216.
55. Sathaliyawala T, Kubota M, Yudanin N et al. Distribution and Compartmentalization of Human Circulating and Tissue-Resident Memory T Cell Subsets. *Immunity*. 2012
56. Piet B, de Bree GJ, Smids-Dierdorp BS et al. CD8(+) T cells with an intraepithelial phenotype upregulate cytotoxic function upon influenza infection in human lung. *J Clin.Invest* 2011;121:2254-2263.
57. Barth R, Counce S, Smith P, Snell GD. Strong and weak histocompatibility gene differences in mice and their role in the rejection of homografts of tumors and skin. *Ann.Surg.* 1956;144:198-204.
58. Thomas ED, Storb R, Clift RA et al. Bone-marrow transplantation (first of two parts). *N Engl J Med* 1975;292:832-843.
59. Thomas ED, Storb R, Clift RA et al. Bone-marrow transplantation (second of two parts). *N Engl J Med* 1975;292:895-902.
60. Goulmy E, Schipper R, Pool J et al. Mismatches of minor histocompatibility antigens between HLA-identical donors and recipients and the development of graft-versus-host disease after bone marrow transplantation. *N Engl J Med* 1996;334:281-285.

61. Goulmy E. Human minor histocompatibility antigens: new concepts for marrow transplantation and adoptive immunotherapy. *Immunol.Rev.* 1997;157:125-140.
62. Falkenburg JH, van de Corp, Marijt EW, Willemze R. Minor histocompatibility antigens in human stem cell transplantation. *Exp.Hematol.* 2003;31:743-751.
63. Griffioen M, Van Der Meijden ED, Slager EH et al. Identification of phosphatidylinositol 4-kinase type II beta as HLA class II-restricted target in graft versus leukemia reactivity. *Proc. Natl.Acad.Sci.U.S.A* 2008;105:3837-3842.
64. Spaapen RM, Lokhorst HM, van den Oudenalder K et al. Toward targeting B cell cancers with CD4+ CTLs: identification of a CD19-encoded minor histocompatibility antigen using a novel genome-wide analysis. *The Journal of Experimental Medicine* 2008;205:2863-2872.
65. Stumpf AN, Van Der Meijden ED, Van Bergen CA et al. Identification of 4 new HLA-DR-restricted minor histocompatibility antigens as hematopoietic targets in antitumor immunity. *Blood* 2009;114:3684-3692.
66. Feng X, Hui KM, Younes HM, Brickner AG. Targeting minor histocompatibility antigens in graft versus tumor or graft versus leukemia responses. *Trends Immunol.* 2008;29:624-632.
67. Mullally A, Ritz J. Beyond HLA: the significance of genomic variation for allogeneic hematopoietic stem cell transplantation. *Blood* 2007;109:1355-1362.
68. Warren EH, Zhang XC, Li S et al. Effect of MHC and non-MHC donor/recipient genetic disparity on the outcome of allogeneic HCT. *Blood* 2012;120:2796-2806.
69. van Bergen CAM, Kester MGD, Jedema I et al. Multiple myeloma-reactive T cells recognize an activation-induced minor histocompatibility antigen encoded by the ATP-dependent interferon-responsive (ADIR) gene. *Blood* 2007;109:4089-4096.
70. Brickner AG, Evans AM, Mito JK et al. The PANE1 gene encodes a novel human minor histocompatibility antigen that is selectively expressed in B-lymphoid cells and B-CLL. *Blood* 2006;107:3779-3786.
71. Kawase T, Akatsuka Y, Torikai H et al. Alternative splicing due to an intronic SNP in HMSD generates a novel minor histocompatibility antigen. *Blood* 2007;110:1055-1063.
72. Nicholls S, Piper KP, Mohammed F et al. Secondary anchor polymorphism in the HA-1 minor histocompatibility antigen critically affects MHC stability and TCR recognition. *Proc.Natl.Acad. Sci.U.S.A* 2009;106:3889-3894.
73. Smigielski EM, Sirotkin K, Ward M, Sherry ST. dbSNP: a database of single nucleotide polymorphisms. *Nucleic Acids Res.* 2000;28:352-355.
74. The 1000 Genomes Project Consortium. A map of human genome variation from population-scale sequencing. *Nature* 2010;467:1061-1073.
75. Bleakley M, Riddell SR. Exploiting T cells specific for human minor histocompatibility antigens for therapy of leukemia. *Immunol.Cell Biol.* 2011;89:396-407.
76. Van Bergen CA, Rutten CE, Van Der Meijden ED et al. High-throughput characterization of 10 new minor histocompatibility antigens by whole genome association scanning. *Cancer Res.* 2010;70:9073-9083.
77. Hobo W, Broen K, van der Velden WJ et al. Association of disparities in known minor histocompatibility antigens with relapse-free survival and graft-versus-host-disease after allogeneic stem cell transplantation. *Biol.Blood Marrow Transplant.* 2012
78. van Els CA, D'Amaro J, Pool J et al. Immunogenetics of human minor histocompatibility antigens: their polymorphism and immunodominance. *Immunogenetics* 1992;35:161-165.
79. Rufer N, Wolpert E, Helg C et al. HA-1 and the SMCY-derived peptide FIDSYICQV (H-Y) are immunodominant minor histocompatibility antigens after bone marrow transplantation.

- Transplantation 1998;66:910-916.
80. de Bueger M., Bakker A, van Rood JJ, Van der Woude F, Goulmy E. Tissue distribution of human minor histocompatibility antigens. Ubiquitous versus restricted tissue distribution indicates heterogeneity among human cytotoxic T lymphocyte-defined non-MHC antigens. *J.Immunol.* 1992;149:1788-1794.
 81. Warren EH, Greenberg PD, Riddell SR. Cytotoxic T-lymphocyte-defined human minor histocompatibility antigens with a restricted tissue distribution. *Blood* 1998;91:2197-2207.
 82. Spierings E, Goulmy E. Expanding the immunotherapeutic potential of minor histocompatibility antigens. *J Clin Invest* 2005;115:3397-3400.
 83. Spierings E, Kim YH, Hendriks M et al. Multicenter Analyses Demonstrate Significant Clinical Effects of Minor Histocompatibility Antigens on GvHD and GvL after HLA-Matched Related and Unrelated Hematopoietic Stem Cell Transplantation. *Biol.Blood Marrow Transplant.* 2013;19:1244-1253.
 84. Heemskerk MHM, Hoogeboom M, Hagedoorn R et al. Reprogramming of Virus-specific T Cells into Leukemia-reactive T Cells Using T Cell Receptor Gene Transfer. *The Journal of Experimental Medicine* 2004;199:885-894.
 85. van Loenen MM, Hagedoorn RS, Kester MG et al. Kinetic preservation of dual specificity of coprogrammed minor histocompatibility antigen-reactive virus-specific T cells. *Cancer Res.* 2009;69:2034-2041.
 86. Heemskerk MH, Hoogeboom M, de Paus RA et al. Redirection of antileukemic reactivity of peripheral T lymphocytes using gene transfer of minor histocompatibility antigen HA-2-specific T-cell receptor complexes expressing a conserved alpha joining region. *Blood* 2003;102:3530-3540.
 87. Spaapen R, van den Oudenalder K, Ivanov R et al. Rebuilding human leukocyte antigen class II-restricted minor histocompatibility antigen specificity in recall antigen-specific T cells by adoptive T cell receptor transfer: implications for adoptive immunotherapy. *Clin.Cancer Res.* 2007;13:4009-4015.
 88. van Loenen MM, de BR, Hagedoorn RS et al. Optimization of the HA-1-specific T-cell receptor for gene therapy of hematologic malignancies. *Haematologica* 2011;96:477-481.
 89. Brossart P, Spahlinger B, Grunebach F et al. Induction of minor histocompatibility antigen HA-1-specific cytotoxic T cells for the treatment of leukemia after allogeneic stem cell transplantation. *Blood* 1999;94:4374-4376.
 90. Mutis T, Ghoreschi K, Schrama E et al. Efficient induction of minor histocompatibility antigen HA-1-specific cytotoxic T-cells using dendritic cells retrovirally transduced with HA-1-coding cDNA. *Biol.Blood Marrow Transplant.* 2002;8:412-419.
 91. Meij P, Jedema I, van der Hoorn MA et al. Generation and administration of HA-1-specific T-cell lines for the treatment of patients with relapsed leukemia after allogeneic stem cell transplantation: a pilot study. *Haematologica* 2012;97:1205-1208.
 92. Warren EH, Fujii N, Akatsuka Y et al. Therapy of relapsed leukemia after allogeneic hematopoietic cell transplantation with T cells specific for minor histocompatibility antigens. *Blood* 2010;115:3869-3878.
 93. Hinrichs CS, Borman ZA, Gattinoni L et al. Human effector CD8+ T cells derived from naive rather than memory subsets possess superior traits for adoptive immunotherapy. *Blood* 2011;117:808-814.
 94. Li N, Matte-Martone C, Zheng H et al. Memory T cells from minor histocompatibility antigen-vaccinated and virus-immune donors improve GVL and immune reconstitution. *Blood* 2011;118:5965-5976.

95. Levenska H, Schaap N, Maas F et al. Partial T cell-depleted allogeneic stem cell transplantation following reduced-intensity conditioning creates a platform for immunotherapy with donor lymphocyte infusion and recipient dendritic cell vaccination in multiple myeloma. *Biol.Blood Marrow Transplant.* 2010;16:320-332.
96. Zhang Y, Joe G, Zhu J et al. Dendritic cell-activated CD44hiCD8+ T cells are defective in mediating acute graft-versus-host disease but retain graft-versus-leukemia activity. *Blood* 2004;103:3970-3978.
97. Dolstra H, Fredrix H, Maas F et al. A Human Minor Histocompatibility Antigen Specific for B Cell Acute Lymphoblastic Leukemia. *The Journal of Experimental Medicine* 1999;189:301-308.
98. Murata M, Warren EH, Riddell SR. A Human Minor Histocompatibility Antigen Resulting from Differential Expression due to a Gene Deletion. *The Journal of Experimental Medicine* 2003;197:1279-1289.
99. Slager EH, Honders MW, van der Meijden ED et al. Identification of the angiogenic endothelial-cell growth factor-1/thymidine phosphorylase as a potential target for immunotherapy of cancer. *Blood* 2006;107:4954-4960. 100. Warren EH, Otterud BE, Linterman RW et al. Feasibility of using genetic linkage analysis to identify the genes encoding T cell-defined minor histocompatibility antigens. *Tissue Antigens* 2002;59:293-303.
101. Akatsuka Y, Nishida T, Kondo E et al. Identification of a Polymorphic Gene, BCL2A1, Encoding Two Novel Hematopoietic Lineage-specific Minor Histocompatibility Antigens. *The Journal of Experimental Medicine* 2003;197:1489-1500.
102. Rotzschke O, Falk K, Wallny HJ, Faath S, Rammensee HG. Characterization of naturally occurring minor histocompatibility peptides including H-4 and H-Y. *Science* 1990;249:283-287.
103. den Haan JM, Sherman NE, Blokland E et al. Identification of a graft versus host disease-associated human minor histocompatibility antigen. *Science* 1995;268:1476-1480.
104. Kamei M, Nannya Y, Torikai H et al. HapMap scanning of novel human minor histocompatibility antigens. *Blood* 2009;113:5041-5048.
105. Kawase T, Nannya Y, Torikai H et al. Identification of human minor histocompatibility antigens based on genetic association with highly parallel genotyping of pooled DNA. *Blood* 2008;111:3286-3294.
106. The International HapMap Consortium. The International HapMap Project. *Nature* 2003;426:789-796.
107. Lundegaard C, Lamberth K, Harndahl M et al. NetMHC-3.0: accurate web accessible predictions of human, mouse and monkey MHC class I affinities for peptides of length 8-11. *Nucleic Acids Res.* 2008;36:W509-W512.
108. Rammensee H, Bachmann J, Emmerich NP, Bachor OA, Stevanovic S. SYFPEITHI: database for MHC ligands and peptide motifs. *Immunogenetics* 1999;50:213-219.
109. Wu C, Orozco C, Boyer J et al. BioGPS: an extensible and customizable portal for querying and organizing gene annotation resources. *Genome Biol.* 2009;10:R130.
110. Uhlen M, Oksvold P, Fagerberg L et al. Towards a knowledge-based Human Protein Atlas. *Nat Biotechnol.* 2010;28:1248-1250.
111. Celis E, Tsai V, Crimi C et al. Induction of anti-tumor cytotoxic T lymphocytes in normal humans using primary cultures and synthetic peptide epitopes. *Proc.Natl.Acad.Sci.U.S.A* 1994;91:2105-2109.
112. van der Bruggen P, Zhang Y, Chauv P et al. Tumor-specific shared antigenic peptides recognized by human T cells. *Immunol.Rev.* 2002;188:51-64.

113. Maecker B, von B, Anderson KS, Vonderheide RH, Schultze JL. Linking genomics to immunotherapy by reverse immunology--'immunomics' in the new millennium. *Curr.Mol. Med.* 2001;1:609-619.
114. Dolstra H, de Rijke B, Fredrix H et al. Bi-directional allelic recognition of the human minor histocompatibility antigen HB-1 by cytotoxic T lymphocytes. *Eur.J Immunol* 2002;32:2748-2758.
115. Mommaas B, Kamp J, Drijfhout JW et al. Identification of a novel HLA-B60-restricted T cell epitope of the minor histocompatibility antigen HA-1 locus. *J Immunol* 2002;169:3131-3136.
116. Ofran Y, Kim HT, Brusic V et al. Diverse patterns of T-cell response against multiple newly identified human Y chromosome-encoded minor histocompatibility epitopes. *Clin.Cancer Res.* 2010;16:1642-1651.
117. Hombrink P, Hadrup SR, Bakker A et al. High-throughput identification of potential minor histocompatibility antigens by MHC tetramer-based screening: feasibility and limitations. *PLoS.One.* 2011;6:e22523.
118. Popovic J, Li LP, Kloetzel PM et al. The only proposed T-cell epitope derived from the TEL-AML1 translocation is not naturally processed. *Blood* 2011;118:946-954.
119. Broen K, Greupink-Draaisma A, Woestenenk R et al. Concurrent detection of circulating minor histocompatibility antigen-specific CD8+ T cells in SCT recipients by combinatorial encoding MHC multimers. *PLoS.One.* 2011;6:e21266.
120. Hunt DF, Henderson RA, Shabanowitz J et al. Characterization of peptides bound to the class I MHC molecule HLA-A2.1 by mass spectrometry. *Science* 1992;255:1261-1263.
121. Admon A, Barnea E, Ziv T. Tumor antigens and proteomics from the point of view of the major histocompatibility complex peptides. *Mol.Cell Proteomics.* 2003;2:388-398.
122. Altman JD, Moss PAH, Goulder PJR et al. Phenotypic Analysis of Antigen-Specific T Lymphocytes. *Science* 1996;274:94-96.
123. Perfetto SP, Chattopadhyay PK, Roederer M. Seventeen-colour flow cytometry: unravelling the immune system. *Nat Rev.Immunol.* 2004;4:648-655.
124. Rodenko B, Toebe M, Hadrup SR et al. Generation of peptide-MHC class I complexes through UV-mediated ligand exchange. *Nat.Protoc.* 2006;1:1120-1132.
125. Chattopadhyay PK, Price DA, Harper TF et al. Quantum dot semiconductor nanocrystals for immunophenotyping by polychromatic flow cytometry. *Nat Med* 2006;12:972-977.
126. Bakker AH, Hoppes R, Linnemann C et al. Conditional MHC class I ligands and peptide exchange technology for the human MHC gene products HLA-A1, -A3, -A11, and -B7. *Proc. Natl.Acad.Sci.U.S.A* 2008;105:3825-3830.
127. Hadrup SR, Bakker AH, Shu CJ et al. Parallel detection of antigen-specific T-cell responses by multidimensional encoding of MHC multimers. *Nat.Methods* 2009;6:520-526.



**HIGH-THROUGHPUT IDENTIFICATION OF
POTENTIAL MINOR HISTOCOMPATIBILITY
ANTIGENS BY MHC TETRAMER-BASED
SCREENING: FEASIBILITY AND LIMITATIONS**

Pleun Hombrink¹, Chopie Hassan², Michel G.D. Kester¹, Arnoud H. de Ru², Cornelis A.M. van Bergen¹, Harm Nijveen³, Jan W. Drijfhout², J.H. Frederik Falkenburg¹, Mirjam H.M. Heemskerk^{1,5} and Peter A. van Veelen^{2,5}

¹ Department of Hematology, Leiden University Medical Center, Leiden, The Netherlands;

² Department of Immunohematology and Blood Transfusion, Leiden University Medical Center, Leiden, The Netherlands;

³ The Laboratory of Bioinformatics, Wageningen University, Wageningen, The Netherlands

⁵ Shared Senior Authorship

T-cell recognition of minor histocompatibility antigens (MiHA) plays an important role in the graft-versus-tumor (GVT) effect of allogeneic stem cell transplantation (allo-SCT). However, the number of MiHA identified to date remains limited, making clinical application of MiHA reactive T-cell infusion difficult. This study represents the first attempt of genome-wide prediction of MiHA, coupled to the isolation of T-cell populations that react with these antigens. In this unbiased high-throughput MiHA screen, both the possibilities and pitfalls of this approach were investigated. First, 973 polymorphic peptides expressed by hematopoietic stem cells were predicted and screened for HLA-A2 binding. Subsequently a set of 333 high affinity HLA-A2 ligands was identified and post transplantation samples from allo-SCT patients were screened for T-cell reactivity by a combination of pMHC-tetramer-based enrichment and multi-color flow cytometry. Using this approach, 71 peptide-reactive T-cell populations were generated. The isolation of a T-cell line specifically recognizing target cells expressing the MAP4K1_{IMA} antigen demonstrates that identification of MiHA through this approach is in principle feasible. However, with the exception of the known MiHA HMHA1, none of the other T-cell populations that were generated demonstrated recognition of endogenously MiHA expressing target cells, even though recognition of peptide-loaded targets was often apparent. Collectively these results demonstrate the technical feasibility of high-throughput analysis of antigen-specific T-cell responses in small patient samples. However, the high-sensitivity of this approach requires the use of potential epitope sets that are not solely based on MHC binding, to prevent the frequent detection of T-cell responses that lack biological relevance.

INTRODUCTION

Patients with hematological malignancies can be successfully treated with HLA-matched allogeneic stem cell transplantation (allo-SCT) and subsequent donor lymphocyte infusion (DLI)^{1,2}. The graft-versus-leukemia (GVL) effect of this successful immunotherapy is due to recognition by donor T-cells of minor histocompatibility antigens (MiHA) expressed on malignant hematopoietic recipient cells³⁻⁶. These MiHA result from genetic polymorphisms between donor and recipient that alter the HLA-associated peptide repertoire, and are therefore capable to elicit a potent T-cell response in the context of self-HLA⁷. Unfortunately, most MiHA are not solely expressed on hematopoietic cells but display a broad expression pattern in nonmalignant recipient tissues. As a consequence, DLI can induce or enhance graft-versus-host disease (GVHD), one of the main causes of transplant-related morbidity and mortality^{8,9}. It is assumed that the selective infusion of T-cells reactive with MiHA exclusively expressed on recipient hematopoietic cells would help to separate the beneficial GVL effect from GVHD, and identification of MiHA with a hematopoietic expression pattern is therefore of interest.

To date, the number of known MiHA that form attractive targets for antigen-selective cell therapy remains limited. As a consequence of the requirement for both the relevant MiHA mismatch between donor and recipient and expression of the relevant HLA restriction molecule, the percentage of patients that can be treated with such MiHA-selective cell therapy remains low¹⁰. Considering the complex gene expression profiles in hematopoietic cells¹¹ and the enormous number of known allelic polymorphisms¹², the existence of many more clinically applicable MiHA seems reasonable.

Several biochemical and molecular methods have successfully led to the identification of MiHA including peptide elution from HLA, cDNA library screening, genetic linkage analysis, and genome-wide association analysis^{7,13-16}. These methods identified MiHA using a forward immunology approach, based on the characterization of epitopes recognized by T-cells isolated during a GVL response.

The use of soluble fluorescently labeled multimeric peptide-MHC (pMHC) complexes has become a widely used approach to detect antigen-specific T-cells in a diverse T-cell repertoire¹⁷. Furthermore, the development of technology for high-throughput pMHC production^{18,19}, makes it possible to also screen for T-cell reactivity against large panels of potential antigens by flow cytometry either by combinatorial encoding²⁰, or by extension of the number of fluorescent labels used for pMHC tetramer labeling^{21,22}.

In this study we set out to determine whether genome-wide identification of MiHA by pMHC-tetramer screening is feasible. In addition, we assessed whether these screens are possible in an unbiased approach, in which patient are screened with a fixed set of pMHC tetramers. To this purpose, we first predicted a large number of potential MiHA epitopes using HLA-peptide binding algorithms, single nucleotide polymorphism (SNP) data and gene-expression databases. Subsequently, flow cytometry-based high-throughput analysis

of antigen-specific T-cell responses, followed by functional testing of identified T-cell clones was used to assess the clinical value of predicted MiHA. This unbiased screen resulted in the generation of a large number of pMHC tetramer positive T-cell lines. Subsequent functional analysis demonstrated the isolation of two high-affinity T-cell populations specific for the known HMHA-1 MiHA as well as a previously unknown epitope. However, since this novel epitope was not produced to a sufficient level by the endogenous antigen presentation machinery, it should not be considered a *bona fide* MiHA.

Two major conclusions can be drawn from our study: First, high-throughput analysis of antigen-specific T-cell responses in small patient samples is technically feasible using the highly sensitive technologies developed here. Second, when such screens are performed using unbiased peptide sets that are based on epitope binding, irrespective of peptide processing data and SNP status of donor and recipient, the vast majority of T-cell responses detected are of insufficient avidity to allow recognition of endogenously produced antigen, or are directed against epitopes that are not naturally presented to a sufficient extent to allow T-cell recognition.

RESULTS

Identification of genes with a hematopoiesis-restricted expression pattern

In many hematological malignancies it is likely to be essential to therapeutically target not only the differentiated leukemic cells, but also the leukemic stem cell fraction, because of this, genes that are expressed in hematopoietic precursor cells are of interest as a potential source of MiHA, as these genes are likely to be expressed in leukemic precursor cells as well. To obtain a better insight into the gene expression profiles of specific hematopoietic cell fractions, we performed microarray analyses on hematopoietic stem cells purified from bone marrow, G-CSF mobilized peripheral blood and cord blood. Both CD34⁺/CD38⁻ and CD34⁺/CD38⁺ fractions were analyzed, representing early and more committed hematopoietic stem cells, respectively. Subsequently, these data were merged with gene expression data for similar and other cell types from the NCBI GEO database²³, to identify genes expressed in stem cells with a hematological restricted pattern. The robustness of the approach was shown by the identification of known hematopoiesis-restricted MiHA encoding genes such as HMHA-1 and PTPRC (CD45). In addition, ubiquitous and non-hematopoiesis tissue specific genes like KLK2 and GAPD, were also found to have the expected expression profiles, demonstrating that this combined database was sufficiently robust to identify genes with a hematopoiesis-restricted expression pattern (e.g. ITGB2 and FLT3 (Fig. S1A-F). The combined database was subsequently used to identify 79 non-Y-chromosomal genes that are relatively specifically expressed in hematopoiesis-restricted cell subsets (Table S1).

SNP identification in selected genes

The molecular basis for the immunogenicity of most MiHA is formed by amino acid changes in MHC-restricted epitopes that occur as a consequence of single nucleotide polymorphisms. Identification of such SNPs within our 79 hematopoiesis-restricted genes using the NCBI's dbSNP polymorphism database²⁴ revealed 315 SNPs, of which the majority was nonsynonymous. In addition, as MiHA have been reported to also be encoded by alternative reading frames^{5;6} (ARF) we also included synonymous SNPs to ensure no MiHA encoded by ARF were left out. At the time of this SNP selection (dbSNP build 126), allele frequencies were unknown for many of these SNPs, and SNPs with an unknown allele frequency were included.

Prediction of MiHA epitope candidates

To predict potential MiHA epitopes encoded by this set of SNPs, we generated peptide sequences *in silico*, based on the nucleotide sequences of both allelic variants of the SNP. Peptide sequences were generated both from the canonical and from the two alternative forward reading frames, using gene segment encoding ten amino acids N-terminal and C-terminal of the SNP-containing codon. This peptide sequence set was then used to predict 9-, 10- and 11-mer polymorphic HLA-A2 binding peptides using three different HLA-peptide binding algorithms, Syfpeithi²⁵, Bimas²⁶ and netMHC²⁷. Predicted HLA-A2 binding peptides were selected for further testing when at least passing the threshold for one of the three algorithms. Peptides predicted from an ARF were only selected if an upstream alternative start site was detected. In total, 973 unique peptides were selected with a predicted HLA-A2 binding affinity (Table SII). The successful prediction of known MiHA such as HMHA-1, indicated that the quality of the gene-expression and SNP databases combined with HLA-peptide binding algorithms was sufficient to predict putative MiHA (Fig. S1G,H).

Assessing the HLA-A2 binding affinity of predicted MiHA epitopes

To evaluate the HLA-A2 affinity of these predicted MiHA, the set of 973 peptides was synthesized and analyzed using two different MHC binding assays ("MHC ELISA" and "MHC bead assay") that are both based on UV-induced conditional ligand cleavage, followed by peptide affinity dependent rescue of the MHC complex^{18;28,29} (Fig. 1). To set selection thresholds for both binding assays, a number of control peptides with high, intermediate or low HLA-A2 affinity were included. Peptide-MHC rescue scores (RS) were determined in both assays and normalized to the high affinity CMV-pp65_{NLV} peptide³⁰. Results of both assays showed a clear correlation and all control peptides demonstrated the expected HLA-A2 affinity. Based on this analysis, 333 peptides with RS \geq 57 (MHC-ELISA) or RS \geq 60 (MHC-bead assay) were selected (Table SIII).

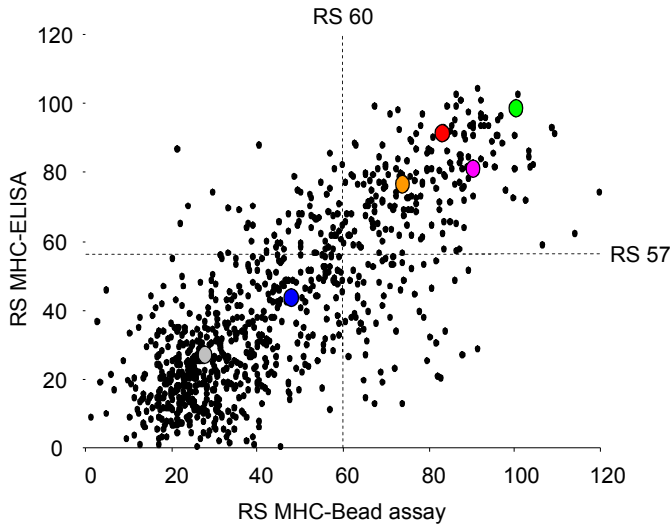


Figure 1. HLA-A2 affinity of predicted peptides measured in parallel by two different assays. HLA-A2 affinity of 973 predicted MiHA peptides was measured in parallel by two different binding assays. Each dot (black) represents a pMHC complex rescued by a tested peptide after UV induced cleavage of a conditional ligand. On the y-axis rescue score (RS) are shown for MHC-ELISA assay. On the x-axis RS are shown for MHC-bead assay. RS are normalized to the HLA-A2 high affinity CMV-pp65_{NLV} peptide and CMV-pp65_{NLV} peptide RS set to 100 for both assays. Selection threshold: RS \geq 57 (MHC-ELISA) and RS \geq 60 (MHC-bead assay). High affinity peptide controls: CMV-NLVPMTATV (green), FLU-GILGFVFTL (pink), EBV-GLCTLVAML (orange) and HA1-VLHDDLLEA (red). Low affinity peptide control: MART1-AAGIGILTV (blue) and negative control A3-gp100-LIYRRRLMK (grey).

Analysis of efficiency and sensitivity for pull down of MiHA specific T-cell populations

Antigen specific T-cells can be present at very low frequencies. MiHA specific T-cell responses may therefore go undetected, especially when analyzed directly *ex vivo* in clinical specimens that often contain only a few million cells and that are generally not obtained during the peak GVL response. To allow high-throughput screening with a very large unbiased set of pMHC tetramers in PBMC samples with low cell numbers, we first developed an approach to simultaneously isolate T-cells reactive with any of the pMHC tetramers, and then expand these T-cells *in vitro*, prior to flow cytometric analysis. To address the sensitivity of this approach, we attempted the detection of a MiHA specific T-cell population in an allo-SCT patient PBMC sample obtained at 15 months after DLI, and in which HMHA-1 specific T-cells were barely detectable (\sim 0.01% of CD8⁺ T-cells) *ex vivo*. After magnetic pull down with the entire PE-labeled 333 pMHC tetramer set and subsequent expansion of the cells, HMHA-1 reactive T-cells were clearly detectable at a frequency of 2.56% of total CD8⁺ T-cells (Fig. S2). Thus, magnetic pull down with large collections of pMHC tetramers can be used to facilitate detection of low-level T-cell responses.

Identification of MiHA specific T-cell populations

Having successfully established the feasibility of our pull down and *in vitro* expansion method for the detection of MiHA specific T-cells in small PBMC samples, we subsequently utilized the entire set of 333 PE-labeled pMHC tetramers to pull down MiHA specific T-cells from 20 HLA-A2 positive allo-SCT patients with various hematologic malignancies. Selected patients all demonstrated a clear graft versus leukemia response after DLL, and samples were obtained at the memory phase of the GVL response, when MiHA specific T-cells are expected to be present but at low frequencies. Following magnetic isolation, isolated cells were expanded *in vitro* until cell numbers allowed the detection of MiHA-reactive T-cell populations by MHC tetramer combinatorial encoding^{19;20;28;31}. For this purpose, a set of fluorescently labeled pMHC tetramers was generated in which each specific pMHC complex was encoded by a unique combination of fluorochromes²⁰, to screen for recognition of all 333 selected epitopes in a limited number of stainings. The total set of selected epitopes was hierarchically clustered to 16 groups of up to 25 unique pMHC complexes according to the order of priority, i.e. SNP frequencies and HLA-A2 affinity (Table SIII).

After pull down and an average of two weeks of expansion, flow cytometric analysis of these samples revealed 71 different pMHC tetramer-reactive T-cell populations, specific for 47 unique pMHC complexes (Table SIV). In most cases, T-cell frequencies varied between 0.02% and 4.9% of total CD8⁺ T-cells. A representative example of a full panel with 25 different 2-color coded pMHC complexes is shown in Fig. 2A, in which 3 potential MiHA-tetramer reactive T-cell populations were observed for the predicted MiHA peptides 89 (0.11%), 104 (0.22%) and 109 (0.17%). In one patient we detected a T-cell population specific for the previously identified HMHA-1H epitope.

To assess the peptide specificity and functional activity of these T-cell populations we selected the 21 most interesting MiHA specific T-cell populations for the generation of cell lines by pMHC tetramer based cell sorting (Fig. 2B-E). We based our selection on favorable SNP allele frequencies according to the dbSNP database and focused on T-cell populations that only showed reactivity with one of the allelic counterparts of a specific peptide. The purity of cell lines generated in this manner was verified by pMHC tetramer staining and 2 representative examples are shown in Fig. S2C,D. We were able to generate cell lines with sufficient purity for subsequent functional assessment for 17 out of 21 selected T-cell populations.

Assessing the functionality of isolated T-cell lines by peptide stimulation

To analyze the functional activity of the isolated pMHC tetramer specific T-cells, we measured IFN γ production upon incubation with peptide-loaded HLA-A2⁺ target cells. As our T-cell isolations were solely based on pMHC tetramer reactivity and not on functional activity, we also measured the overall IFN γ secretion capacity of these cells, by nonspecific stimulation with α CD3/CD28 stimulation beads (Fig. 3A). Although IFN γ production capacity varied,

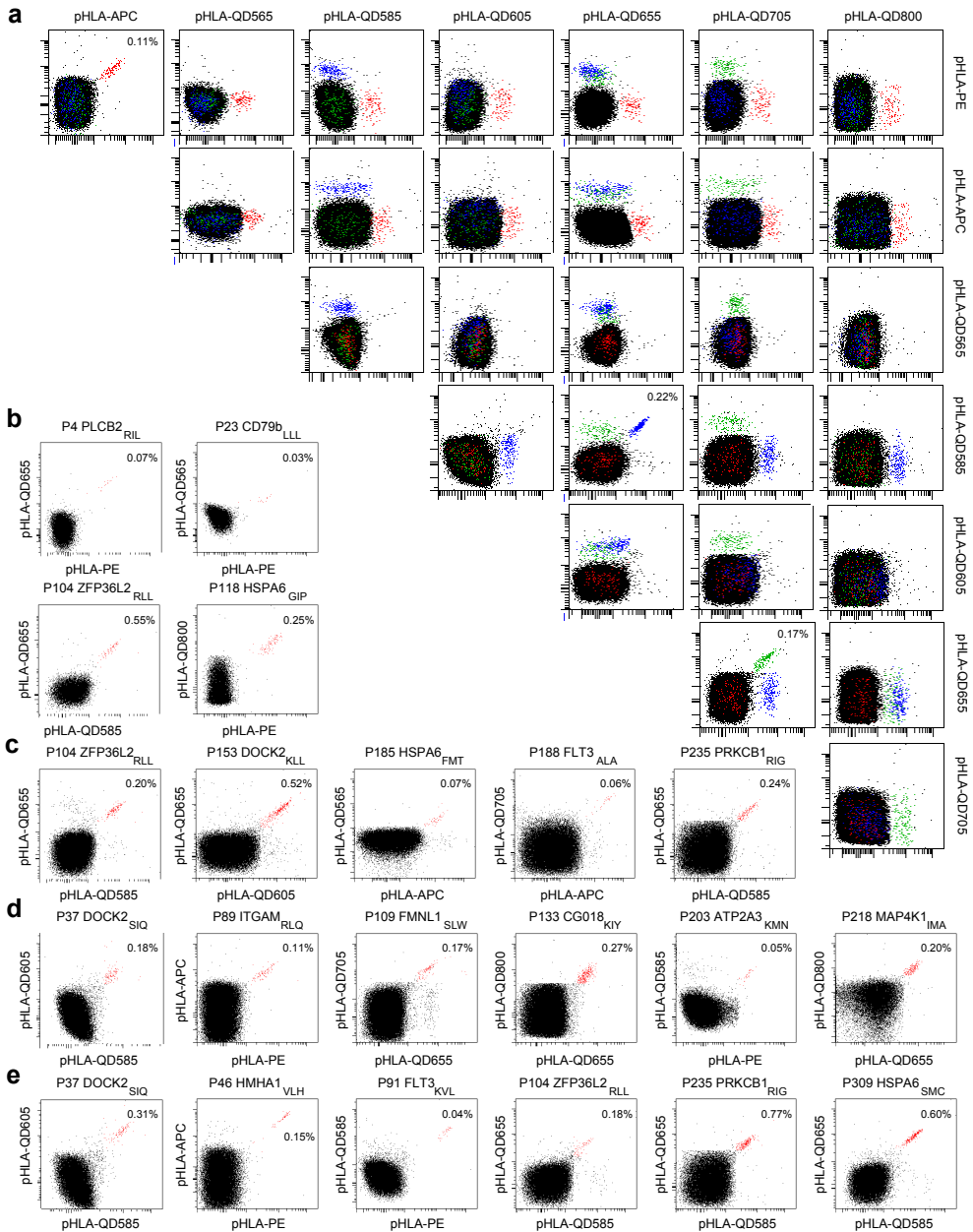


Figure 2. Detection of potential MiHA specific T-cell populations by pMHC tetramer staining. These FACS analyses show the detection of MiHA specific T-cell populations through dual-encoding after pMHC tetramer pull down and *in vitro* expansion. Shown are total CD8⁺ T-cells. All dot plots are shown with bi-exponential axes and display fluorescence intensity for the indicated fluorochromes at the top and right of the plot matrix. Non-pMHC tetramer specific CD8⁺ T-cells are indicated black. Dot plots of pMHC tetramer positive T-cell populations are shown by staining one expanded cell culture with 16 separate panels of up to 25 different dual-color pMHC tetramers. (A) Representative example of pMHC multimer screen panel 5,

peptide specific IFN γ production could be demonstrated for 10 out of 17 pMHC tetramer positive cell lines, including 9 cell lines directed against potential MiHA and one directed against the known HMHA-1 epitope. Six cultures only demonstrated IFN γ production when stimulated with stimulation beads, indicating that these cell lines were not functionally reactive to peptide antigen. In addition, pMHC-tetramer positive cell line P235 PRKCB1_{RIG} totally lacked IFN γ production capacity. Peptide-specificity of the 10 T-cell lines that produced IFN- γ upon peptide stimulation was confirmed by assessing TCR internalization upon stimulation with peptide-loaded target cells (Fig. 3B). TCR downregulation clearly correlated with IFN γ production and was observed for all cell lines that demonstrated peptide specific IFN γ production. Minimal downregulation was observed for the four tested cell lines that lacked peptide specific IFN γ production, as well as the cell line that showed no overall IFN γ producing capacity. Hence, these data indicate that 10 out of 17 tested cell lines are reactive against their specific peptide when added exogenously.

Wide range of peptide affinity observed for pMHC tetramer positive T-cell populations

To examine the ligand sensitivity of the generated peptide specific cell lines, INF- γ production was measured after stimulation with T2 cells that were loaded with a range of peptide concentrations (Fig. 4). In this assay (performed for 8 representative cell lines), peptide concentrations required for T-cell recognition were compared to those required for a previously identified T-cell clone that is specific for the HMHA-1H epitope. This T-cell clone has been demonstrated to be present in a GVL response and was obtained during the subsequent memory phase. The 8 cell lines tested showed a wide range of peptide sensitivity. Specifically, the cell lines specific for P218 MAP4K1_{IMA} and P46 HMHA1_{VLH} were capable of target recognition at low picomolar peptide concentrations, similar to the peptide concentration required for the HMHA-1-specific control T-cell clone. Cell lines specific for P91 FLT3_{KVL}, P309 HSPA6_{SMC} and P188 FLT3_{ALA} required low nanomolar peptide concentrations and those specific for P37 DOCK2_{SIQ}, P203 ATP2A3_{KMN} and P104 ZFP36L2_{RLL} only showed target recognition at high nanomolar peptide concentrations (IC50: \pm 50pM, \pm 5nM and \pm 500nM respectively for the three groups of cell lines). Comparison of the peptide concentration required for T-cell activation and the MHC binding affinity of the different peptides indicated that a requirement for high peptide concentrations to obtain

patient BDY3356. Detection of three dual-labeled potential MiHA specific T-cell populations: P89 ITGAM_{RLQ} (red), P104 ZFP36L2_{RLL} (blue) and P109 FMNL1_{SLW} (green). Frequencies indicate MiHA specific T-cells of total CD8⁺ cells. A selection of 21 potential MiHA specific T-cell populations was made with the highest clinical potential. Selected T-cell populations were derived from allo-SCT patient: OBB1465 (B), JMO2750 (C), BDY3356 (D) and APM4461 (E). Dot plots shown are representative for all detected dual-positive CD8⁺ T-cell populations (red).

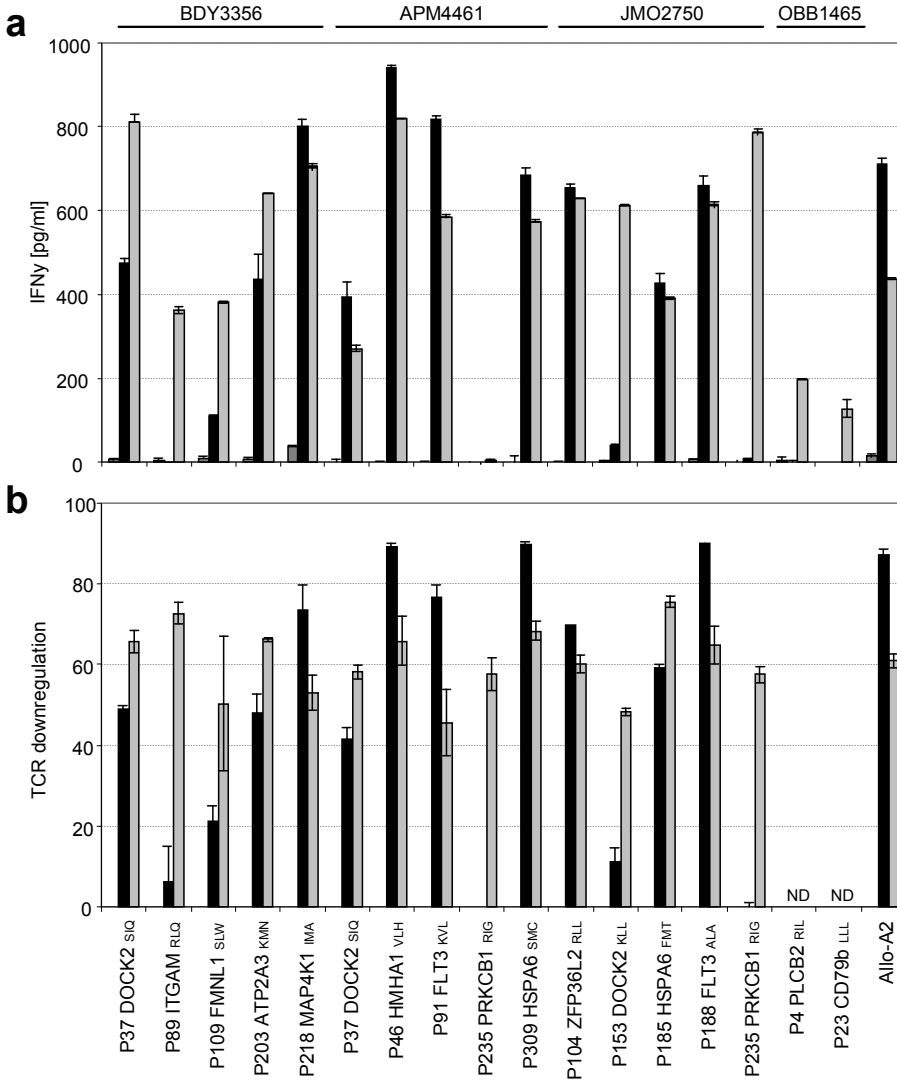


Figure 3. Peptide stimulation leads to IFN γ production and TCR downregulation for 10 out of 17 pMHC tetramer positive cell lines. Isolated pMHC tetramer positive cell lines were stimulated with peptide-loaded HLA-A2* T2 target cells for 18 hours. Data is shown for 17 cell lines that were successfully generated by flowcytometry based cell sorting. Tested cell lines were derived from four different allo-SCT patients as indicated at the top of the graph. As a control an alloreactive CTL clone specific for a HLA-A2 epitope was used (Allo-A2). (A) Antigen specificity and functionality was analyzed by cytokine secretion in a standard IFN γ ELISA. Cell lines were stimulated with non-peptide loaded T2 cells (dark grey), [1 ug/ml] peptide-loaded T2 cells (black) and α CD3/CD28 stimulation beads (light grey). Data are presented as cytokine concentration. (B) Antigen specificity and functionality was analyzed by TCR internalization upon peptide stimulation. Cell lines shown were stimulated with [1 ug/ml] peptide-loaded T2 cells (black) and α CD3/CD28 stimulation beads (light grey). TCR downregulation was normalized to stimulation with non-peptide loaded T2 cell controls. Experiments were performed in duplicate, data are mean \pm SD.

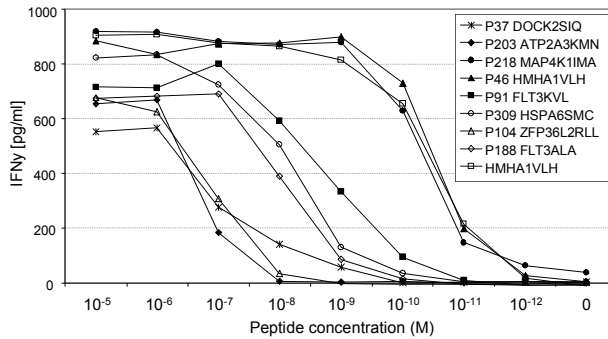


Figure 4. Analysis of peptide affinity of pMHC tetramer positive cell lines. MHC tetramer positive T-cell lines demonstrated a wide range of peptide sensitivity. HLA A2⁺ T2 cells were pulsed with specific MiHA peptide. Peptide concentrations were titrated in 10-fold dilution steps starting from 10ug/ml. T-cell reactivity was analyzed by cytokine secretion in a standard IFN γ ELISA. Data are presented as cytokine concentration. Shown are eight representative generated T-cell lines and a high affinity control clone specific for HMHA-1H (open square). Cell lines APM4461 derived P37 DOCK2_{SIQ} and JMO2750 P185 HSPA6_{FMT} were not tested due to technical limitations.

T-cell activation was not simply due to a lower pMHC affinity. As an example, the peptides recognized by cell-lines P91 FLT3_{KVL} and P203 ATP2A3_{KMN} displayed a comparably high MHC affinity (as measured in Fig. 1) as those of the two highly sensitive cell lines P218 MAP4K1_{IMA} and P46 HMHA1_{VLH}. Thus, the low peptide sensitivity of many of the isolated T-cell lines formed a direct reflection of a low affinity TCR-pMHC interaction.

Isolated T-cell populations are not involved in the clinical response

To determine whether the observed T-cell reactivities could be involved in the clinical response observed after DLI in these patients, we screened the high- and intermediate-avidity T-cell lines for differential recognition of patient- and donor-derived EBV-LCLs and T-cell-blasts. Results are shown for 5 representative T-cell lines isolated from patient BDY3356 and JMO2750 (Fig. 5A,B). Peptide loaded target cells of both donor and recipient origin were recognized by all cell lines. In contrast, all cell lines were unable to recognize recipient target cells, indicating that these cells were not likely to be involved in the GVL response observed in these patients. As a control, all hematopoietic target cells were recognized by an HLA-A2 alloreactive CTL control clone, indicating that HLA-A2 expression was sufficient to allow target-cell recognition. Notably, recognition of recipient cells was also not observed for the HMHA-1 specific cell-line.

To test whether the lack of reactivity that was observed could be explained by absence of the immunogenic MiHA allele variants, we next screened the SNP haplotypes for selected donor-recipient pairs (Table I). For 15 out of the 17 functionally tested cell lines, no SNP haplotype disparities were revealed for the potential MiHA concerned. In

addition, only 7 out of 15 tested cell lines recognized “non-self” antigen variants (i.e. the variant not encoded by the donor genome), whereas 8 cell lines recognized “self” antigen variants. Interestingly, both high-avidity T-cell populations that were isolated (specific for P218 MAP4K1_{IMA} and P46 HMHA1_{VLH}) recognized “non-self” antigen variants, whereas all cell lines that recognized “self” antigen variants were of intermediate or low-avidity. These results suggest a possible role for clonal deletion of high-avidity T-cells specific for these “self” epitopes when they are appropriately processed. Based on these results, we

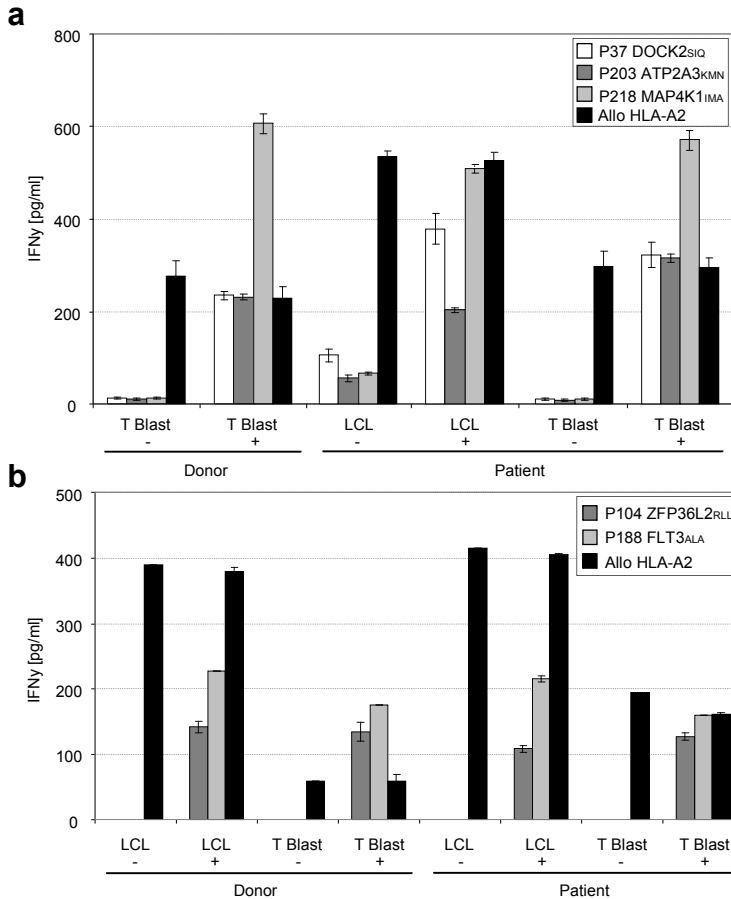


Figure 5. No recognition of hematopoietic donor and recipient target cells by MiHA specific T-cells.

Isolated IFN γ producing cell lines were stimulated with HLA-A2⁺ donor and patient derived hematopoietic target cells for 18 hours. T-cell reactivity was measured in a standard IFN γ ELISA. Data are presented as cytokine concentration. Cell lines shown are representative for all cell lines. As a control for T-cell reactivity an alloreactive HLA-A2 specific CTL clone was used (black). (A) BDY3356 derived cell lines P37 DOCK2_{SIQ} (white), P203 ATP2A3_{KMN} (dark grey) and P218 MAP4K1_{IMA} (light grey) stimulation with donor and recipient T-cell blasts and EBV-LCLs loaded with (+) or without (-) specific peptide [1 μ g/ml]. (B) JMO2750 derived cell lines P104 ZFP36L2_{RLL} (dark grey) and P188 FLT3_{ALA} (light grey) stimulation with donor and recipient T-cell and EBV blasts loaded with (+) or without (-) specific peptide [1 μ g/ml].

Table I. MiHA haplotype disparities in selected donor and recipient pairs

Clone	Gene	Epitope ^α	Epitope allele variant	Donor allele	Patient allele	Disparity ^β	Clonal nature
P4	PLCB2	RI L VGRLR A A	A	AG	AA	no	self
P23	CD79b	LLL S AEVQQHL	A	GG	AG	yes	non-self
P37 (BDY)	DOCK2	S I QNYHPFA	A	AA	AA	no	self
P37 (APM)	DOCK2	S I QNYHPFA	A	AA	AA	no	self
P46	HMHA1	VL H DD LLEA	A	GG	GG	no	non-self
P89	ITGAM	R LQVPVEAV	G	GG	GG	no	self
P91	FLT3	KVLHELFG M DI	A	AA	AA	no	self
P104	ZFP36L2	R LLPLW AALPL	G	GG	GG	no	self
P109	FMNL1	SLWQL G AAVML	G	CC	CG	yes	non-self
P153	DOCK2	KLLQIQL R A	G	GG	GG	no	self
P203	ATP2A3	KMNVFD T NL	A	GG	GG	no	non-self
P218	MAP4K1	I MAIELAEL	A	GG	GG	no	non-self
P235 (APM)	PRKCB1	RIGQRQ E TV	G	AA	AA	no	non-self
P235 (JMO)	PRKCB1	RIGQRQ E TV	G	AA	AA	no	non-self
P309	HSPA6	S MCRFSPL T L	A	AG	AG	no	self

^α Polymorphic residue in red

^β Disparities are indicated in respect to the donor haplotype

hypothesized that the low or intermediate avidity of most MiHA specific cell lines that we generated could explain the inability of these cell lines to recognize endogenously processed antigen. The only two cell lines that were derived from a transplantation setting in which there was a relevant SNP mismatch between the donor and recipient were specific for P23 CD79b_{LLL} and P109 FMNL1_{SLW}. Although these cell lines could theoretically recognize the immunogenic MiHA allele variant of the patient, both cell lines demonstrated no recognition of endogenously processed antigen in the prior functional analyses.

Assessing the MiHA recognition potential of isolated T-cell populations

The above data indicate that unbiased MHC tetramer-based enrichment often results in the isolation of T-cell populations that do not play a role in GVL, as based on the lack of the relevant mismatch. However, this does not exclude that such cell populations could recognize target cells that do express the relevant MiHA allele. To investigate the potential capacity of these MiHA specific T-cell populations to recognize MiHA allele -positive target cells, the cell lines were tested against a panel of SNP-genotyped HLA-A2⁺ EBV-LCLs. Interestingly, the HMHA-1 specific T-cell population, isolated from a transplantation setting in which both donor and recipient were homozygous negative for the immunogenic allele variant of the MiHA, recognized target cells in accordance with their SNP haplotype. Specifically, this tested cell line strongly recognized non-peptide loaded homozygote positive and heterozygote EBV-LCLs, whereas homozygote negative EBV-LCLs were not recognized. In contrast, the second high avidity P218 MAP4K1_{IMA} specific cell-line, as well

as the intermediate avidity cell lines were unable to recognize any target in the SNP-typed EBV-LCL panel.

Lack of target cell recognition by high-avidity T-cells is caused by inappropriate processing and surface presentation of predicted epitope

The P218 MAP4K1_{IMA} specific T-cell population demonstrated efficient recognition of target cells loaded with picomolar concentrations of peptide, whereas no reactivity was observed in accordance with the SNP haplotype of tested targets. To determine whether the inability of this high avidity T-cell line to recognize endogenously processed antigen was due to the inability of the target cells to process and present the MAP4K1_{IMA} epitope, a retroviral minigene vector was constructed that encoded the minimal MAP4K1_{IMA} peptide sequence directly attached to an ER-signal sequence³². In this design, delivery of the potential T-cell epitope to the ER occurs co-translationally, and hence independent of proteasomal processing and TAP transport. As a positive control, a similar minigene was created for the HMHA-1H epitope. HLA-A2⁺ JY cells that are homozygous negative for both the P218 MAP4K1_{IMA} and the HMHA-1H allele were transduced with the two minigene constructs, and demonstrated to be recognized by the HMHA-1 T-cell line as well as by the MAP4K1_{IMA} specific T-cell line (Fig. 6). These results indicate that when endogenous presentation of the predicted MAP4K1_{IMA} epitope is forced, recognition by P218 MAP4K1_{IMA} specific T-cells is strong.

DISCUSSION

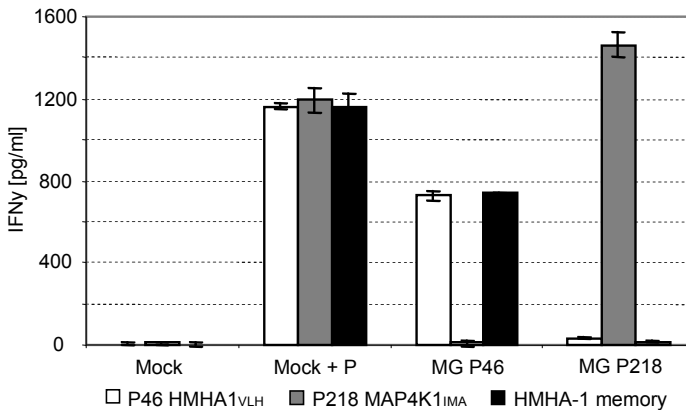


Figure 6. Recognition of EBV target cells by high-avidity MiHA T-cells after minigene transduction.

High-avidity cell lines P46 HMHA1_{VLH} (white) and P218 MAP4K1_{IMA} (grey) were stimulated with HLA-A2⁺ EBV-LCL JY transduced with minigene constructs (MG) encoding minimal peptide sequence directly attached to an ER-signal sequence. T-cell reactivity was measured after 18 hours in a standard IFN γ ELISA. Data are presented as cytokine concentration. The MOCK transduced cells only encoded an ER-signal sequence. As a control for T-cell reactivity an alloreactive HLA-A2 specific CTL clone was used (black).

This study demonstrates the feasibility and limitations of using a reverse immunology approach for the identification of potential MiHA. We combined large scale prediction of HLA-restricted MiHA with functional assessments of these polymorphic epitopes by identifying MiHA specific T-cell populations in a high-throughput unbiased fashion. In this study we used a reverse immunology approach, based on UV-induced peptide exchange technology, in which the predicted MiHA epitopes were the starting point for identification of new MiHA specific T-cell responses. By investigating MiHA source proteins with a hematopoietic tissue restricted expression pattern, we aimed to identify potential CTL epitopes that would selectively target recipient hematopoiesis.

The combined use of three prediction programs resulted in the generation of a synthetic peptide library of 973 experimental peptides encoded by hematopoietic stem cells. The MHC binding capacity of these peptides was verified by UV-induced MHC-peptide exchange. Based on the binding capacity of well studied natural ligands, we estimate that one third of the predicted peptide set could be defined as high affinity, one third as intermediate affinity and one third as low affinity HLA-A2.

To assess the ability of these epitopes to serve as TCR ligands we monitored T-cell responses in a high throughput unbiased fashion using multiplexed fluorescently labeled sets of pMHC complexes. We were able to detect epitope specific T-cell recognition for 71 of the 333 screened pMHC complexes of which 24 epitopes were recognized in multiple and 47 epitopes were recognized in single individuals. Taken into account that these T-cells were isolated from small cell size PBMC samples of allo-SCT patients with only partially reconstituted TCR repertoires, this data highlights both the immense capacity of the TCR repertoire to recognize random HLA-ligands and the high-sensitivity of our enrichment protocol. Unfortunately, most isolated pMHC tetramer positive T-cells appeared to be of low or intermediate avidity. Two cell lines recognized their respective peptide with high avidity. In the case of MAP4K1_{IMA'}, no reactivity against endogenously processed antigen was observed, but cells expressing a minigene encoding this epitope were efficiently recognized, suggesting that inappropriate processing explains the lack of recognition of epitope derived from the parental protein. The second high avidity T-cell population recognized the HMHA-1H epitope, and target cell recognition by the T-cell line fully matched HMHA-1 status.

As the identification of the HMHA-1 and MAP4K1_{IMA} specific T-cell responses in our experiments occurred in a fully unbiased screen, this forms evidence that the type of genome-wide screen developed here can be successful. Nevertheless, the fact that only the HMHA-1 specific T-cell population showed recognition of endogenously produced antigen shows that this discovery process is still highly suboptimal, and we see 3 major areas for improvement for this.

First, the capacity of a specific T-cell to bind to a pMHC tetramer does not necessarily reflect its capacity to elicit potent T-cell reactivity when stimulated with a relevant pMHC complex. In this study only 2 out of the 16 T-cell populations that produced IFN γ upon

nonspecific stimulation also demonstrated IFN γ production (and TCR internalization) at picomolar range peptide concentrations. Importantly, these high-avidity T-cell populations do not necessarily demonstrate a more intense pMHC tetramer staining intensity as compared to low and intermediate avidity T-cell populations, making it difficult to weed out less interesting T-cell populations on the basis of MHC tetramer staining intensity. Thus, alternative strategies are required to obtain a rough estimate of T-cell sensitivity early in the screening process.

Second, in this screen, T-cell populations were isolated using the full set of pMHC tetramer complexes for each sample, irrespective of SNP status of donor and recipient. The frequent encounter of low avidity pMHC tetramer positive T-cells from donors for which this epitope forms a “self” antigen could therefore reflect clonal deletion of high avidity T-cells, due to presentation of the predicted epitopes in the donor thymus. In future screens it seems useful to apply stringent epitope selection criteria to restrict high-throughput analysis to those epitopes that can be considered neo-antigens in a given transplant combination, something that can readily be done by evaluation of donor (and recipient) SNP status.

Third, of the two high avidity T-cell populations isolated, only one could recognize epitopes derived from the endogenous antigen. In this project ligand prediction focused solely on the HLA affinity of predicted peptides and disregarded other aspects of the HLA processing and presentation pathway. As a consequence, many of the predicted epitopes used here may not be part of the natural peptidome and thereby lack biological relevance. In future work, this issue may to some extent be addressed by the use of antigen processing algorithms that predict proteosomal cleavage and TAP-dependent peptide transport^{33,34}. As a second, and in our view even more attractive option, the peptide set used for high-throughput screening could be derived from a database of HLA eluted peptides, thereby guaranteeing presentation of the epitopes concerned.

In conclusion, our isolation and detailed analysis of potential MiHA candidates in a high-throughput fashion has revealed the technical feasibility of this reverse immunology approach. We have demonstrated that TCR repertoires against very large sets of antigens can rapidly be screened. However, the productive use of such high-throughput screening technology will require further improvements. In particular, stringent epitope selection criteria including the availability of high quality databases of MHC ligands and SNP genotypes are likely to be of value to increase the percentage of isolated T-cell populations that is not only pMHC tetramer reactive but also biologically relevant.

ACKNOWLEDGEMENTS

We thank Mireille Toebes for help with the pMHC tetramer production, Jos Urbanus for providing the minigene constructs, Ron Kerkhoven, Daoud Sie and Emilie Casterman for help with the Golden Gate SNP array, Menno van der Hoorn, Guido de Roo and Patrick van

der Holst for flow cytometric cell sorting.

MATERIALS AND METHODS

PBMC samples and T-cell staining. After study approval of the Leiden University Medical Center institutional review board, PBMC samples were obtained from allo-SCT patients during the memory phase of a graft versus leukemia response after DLI as determined by mixed hematopoietic chimerism and/or quantitative BCR-ABL analysis after approval of the Leiden University Medical Center institutional review board and informed consent according to the Declaration of Helsinki. Informed consent form all participants involved in this study were written for samples obtained since 2003 and verbal for older samples when guidelines provided no written consent. PBMC were isolated by Ficoll gradient centrifugation, and frozen in liquid nitrogen. For T-cell staining of approximately 1×10^6 PBMC a final concentration of $2 \mu\text{g}/\text{mL}$ per pMHC tetramer was added and incubated for 15 min at 37°C . Next, antibody-mix consisting of CD8-Alexa700 (Caltag) and CD4-, CD14-, CD16-, CD19- and CD40-FITC (BD) was added and cells were incubated for 30 min at 4°C . Prior to flow cytometry, cells were washed twice and Propidium Iodide (PI) was added to allow dead cell exclusion. Dual-encoding pMHC tetramer analysis was performed as previously described²⁰.

Gene expression of hematopoietic cell fractions by microarray analysis. Hematopoietic precursor CD34⁺ cells were isolated by MACS (Miltenyi) from bone marrow; G-CSF mobilized peripheral blood and cord blood PBMC according to manufacturer's protocol. Total RNA was isolated using Trizol (Invitrogen) and transcribed into cDNA by reverse transcriptase (Invitrogen) using oligo-dT primers (Roche Diagnostics). Microarray analysis of gene expression profiles in CD34⁺/CD38⁻ and CD34⁺/CD38⁺ fractions was performed by Affymetrix U133 array according to the manufacturer's instructions. Additional gene expression information was retrieved from the NCBI Gene Expression Omnibus database²³.

Prediction of HLA-A2* MiHA ligands. The following prediction algorithms were applied to the peptide candidates: Syfpeithi²⁵, Bimas²⁶ and netMHC²⁷. Peptides with a score of ≥ 19 (Syfpeithi), ≥ 1 (Bimas) and ≤ 875 (netMHC) were considered to have potential HLA-A2* binding capacities. SNP data was retrieved from NCBI's dbSNP polymorphism database²⁴. Amino acid sequences were obtained from NCBI Entrez engine.

Generation of peptide-MHC complexes. All peptides were synthesized in-house using standard Fmoc chemistry or purchased from Pepscan (Pepscan Presto). The UV-sensitive building block J was synthesized as described¹⁸. Recombinant HLA-A2 heavy chain and human $\beta_2\text{m}$ light chain were in-house produced in *Escherichia coli*. MHC class I refolding was performed as previously described with minor modifications²⁰. MHC class I complexes were purified by gel-filtration HPLC in PBS. Peptide-MHC complexes were generated by MHC-peptide exchange. Prefolded UV-labile pMHC complexes ($100 \mu\text{g}/\text{ml}$) were subjected to 366nm UV light (Camag) for 1 h in presence of the specific peptide

(200 μ M)^{19,28}. After exchange, samples were spun at 16,000g for 5 min and supernatants were used for pMHC tetramer formation. The peptide HLA-A2⁺ binding affinity was assessed using two different HLA-binding assays in parallel; MHC-ELISA and MHC bead as previously described^{18,29}. For generation of pMHC tetramers, 8 different fluorochrome-streptavidin (SA) conjugates were used as previously described²⁰. Phycoerythrin (PE), allophycocyanin (APC) and the quantum dots (QD); QD565, QD585, QD605, QD655, QD705 and QD800 were used (Invitrogen). Complexes were stored at 4°C and prior to use pMHC tetramers were spun at 17,000g for 2 min.

Isolation of MiHA specific T-cells by pMHC tetramer pull down. Prior to isolation of peptide-specific T-cells, pMHC tetramers were made coupled to SA-PE. PBMC were stained with pMHC tetramers for 1 hour at 4°C. Subsequently, cells were washed and incubated with anti-PE Ab coated magnetic beads (Miltenyi). Cells were then isolated by MACS (Miltenyi), using an LS column, following the manufacturer's protocol. Eluted cells were washed and cultured in Iscove Modified Dulbecco Medium (IMDM; Lonza BioWhittaker) supplemented with 5% human serum, 5% fetal calf serum (FCS; Cambrex), 100 IU/mL IL-2 (Chiron), 10ng/mL IL-15 (Peprotech). Eluted cells were cultured per 5000 cells with 2x10⁴ irradiated autologous feeder cells and 5000 anti-CD3/CD28 Dynabeads (Invitrogen) in 96-well plates. Cultures were split at least twice a week. After 2-3 weeks, cell cultures were analyzed for peptide-specific T-cell populations by pMHC tetramer flow cytometry. Subsequently pMHC tetramer reactive T-cell populations were sorted on a FACSaria (Becton Dickinson) into 96 well plates containing 1x10⁵ irradiated feeder cells supplemented with 0.5 μ g/mL phytohaemagglutinin (PHA; Biochrom AG) as previously described³⁵.

Flow cytometry. Data acquisition was performed on an LSR-II flow cytometer (Becton Dickinson) with FACS Diva software using the following 11-color instrument settings: 488nm laser: PI: 685LP, 695/40; PE: 550LP, 575/26; FITC: 505LP, 530/30; SSC: 488/10. 633nm laser: Alexa700: 685LP, 730/45; APC: 660/20. 405nm laser: QD800: 770LP, 800/30; QD705: 680LP, 710/50; QD655: 635LP, 660/40; QD605: 595LP, 650/12. 355nm laser: QD585: 575LP, 585/15; QD565: 545LP: 560/20. Approximately 200,000 lymphocytes were recorded for each analysis. To identify antigen-specific T-cells we followed the gating strategy as described in Fig. S2.

IFN γ release assay. MiHA specific T-cell lines (1x10⁴) were stimulated with HLA-A2⁺ T2 cells, EBV-LCLs or T-cell blasts (2,5x10⁴) in 96 well plates for 18h at 37°C and 5% CO₂. Peptide pulsing was performed by incubating stimulator cells for 1 h with synthetic peptides (1 μ g/ml) in IMDM containing 2% FCS and cells were washed twice before use. Cytokine release was measured by IFN γ ELISA (Sanquin) according to the manufacturer's instructions.

REFERENCES

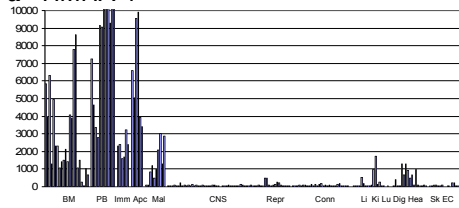
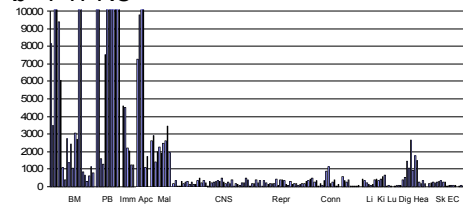
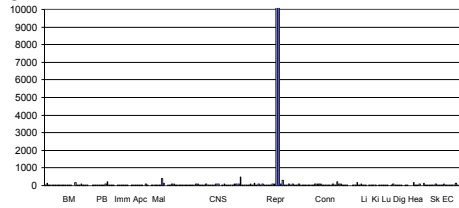
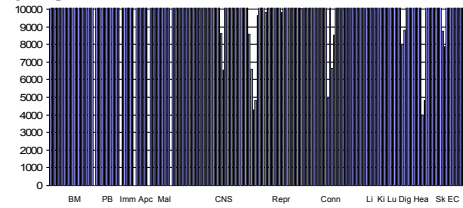
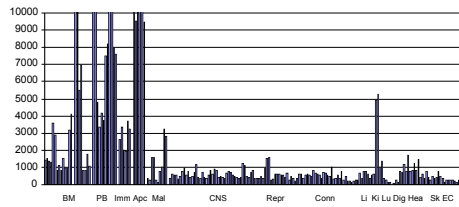
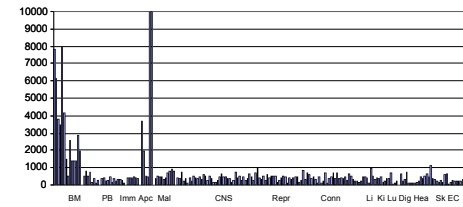
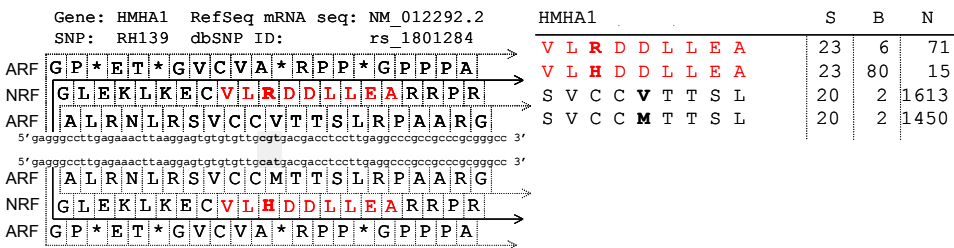
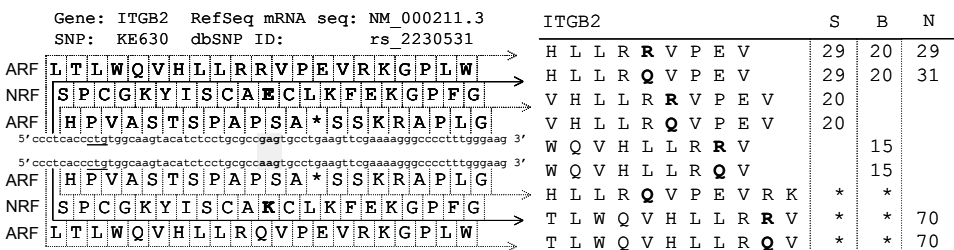
1. Porter DL, Roth MS, McGarigle C, Ferrara J, Antin JH. Induction of Graft-versus-Host Disease as Immunotherapy for Relapsed Chronic Myeloid Leukemia. *N Engl J Med* 1994;330:100-106.
2. Kolb HJ, Schattenberg A, Goldman JM et al. Graft-versus-leukemia effect of donor lymphocyte transfusions in marrow grafted patients. European Group for Blood and Marrow Transplantation Working Party Chronic Leukemia [see comments]. *Blood* 1995;86:2041-2050.
3. Marijt WAE, Heemskerk MHM, Kloosterboer FM et al. Hematopoiesis-restricted minor histocompatibility antigens HA-1- or HA-2-specific T cells can induce complete remissions of relapsed leukemia. *Proceedings of the National Academy of Sciences of the United States of America* 2003;100:2742-2747.
4. de Rijke B, van Horssen-Zoetbrood A, Beekman JM et al. A frameshift polymorphism in P2X5 elicits an allogeneic cytotoxic T lymphocyte response associated with remission of chronic myeloid leukemia. *J Clin Invest* 2005;115:3506-3516.
5. Slager EH, Honders MW, van der Meijden ED et al. Identification of the angiogenic endothelial-cell growth factor-1/thymidine phosphorylase as a potential target for immunotherapy of cancer. *Blood* 2006;107:4954-4960.
6. van Bergen CAM, Kester MGD, Jedema I et al. Multiple myeloma-reactive T cells recognize an activation-induced minor histocompatibility antigen encoded by the ATP-dependent interferon-responsive (ADIR) gene. *Blood* 2007;109:4089-4096.
7. Falkenburg JH, van de Corp, Marijt EW, Willemze R. Minor histocompatibility antigens in human stem cell transplantation. *Exp.Hematol.* 2003;31:743-751.
8. Reddy P, Ferrara JLM. Immunobiology of acute graft-versus-host disease. *Blood Reviews* 2003;17:187-194.
9. Ferrara JL, Levine JE, Reddy P, Holler E. Graft-versus-host disease. *Lancet* 2009;373:1550-1561.
10. Spierings E, Goulmy E. Expanding the immunotherapeutic potential of minor histocompatibility antigens. *J Clin Invest* 2005;115:3397-3400.
11. Watkins NA, Gusnanto A, de BB et al. A HaemAtlas: characterizing gene expression in differentiated human blood cells. *Blood* 2009;113:e1-e9.
12. The UniProt Consortium. The Universal Protein Resource (UniProt) in 2010. *Nucl.Acids Res.* 2010;38:D142-D148.
13. Van Bergen CA, Rutten CE, Van Der Meijden ED et al. High-throughput characterization of 10 new minor histocompatibility antigens by whole genome association scanning. *Cancer Res.* 2010;70:9073-9083.
14. Mullally A, Ritz J. Beyond HLA: the significance of genomic variation for allogeneic hematopoietic stem cell transplantation. *Blood* 2007;109:1355-1362.
15. Dierselhuis M, Goulmy E. The relevance of minor histocompatibility antigens in solid organ transplantation. *Curr.Opin.Organ Transplant.* 2009;14:419-425.
16. Kawase T, Nannya Y, Torikai H et al. Identification of human minor histocompatibility antigens based on genetic association with highly parallel genotyping of pooled DNA. *Blood* 2008;111:3286-3294.
17. Altman JD, Moss PAH, Goulder PJR et al. Phenotypic Analysis of Antigen-Specific T Lymphocytes. *Science* 1996;274:94-96.
18. Rodenko B, Toebe M, Hadrup SR et al. Generation of peptide-MHC class I complexes through UV-mediated ligand exchange. *Nat.Protoc.* 2006;1:1120-1132.

19. Bakker AH, Hoppes R, Linnemann C et al. Conditional MHC class I ligands and peptide exchange technology for the human MHC gene products HLA-A1, -A3, -A11, and -B7. *Proc. Natl. Acad. Sci. U.S.A* 2008;105:3825-3830.
20. Hadrup SR, Bakker AH, Shu CJ et al. Parallel detection of antigen-specific T-cell responses by multidimensional encoding of MHC multimers. *Nat. Methods* 2009;6:520-526.
21. Chattopadhyay PK, Price DA, Harper TF et al. Quantum dot semiconductor nanocrystals for immunophenotyping by polychromatic flow cytometry. *Nat Med* 2006;12:972-977.
22. Perfetto SP, Chattopadhyay PK, Roederer M. Seventeen-colour flow cytometry: unravelling the immune system. *Nat Rev. Immunol.* 2004;4:648-655.
23. Edgar R, Domrachev M, Lash AE. Gene Expression Omnibus: NCBI gene expression and hybridization array data repository. *Nucl. Acids Res.* 2002;30:207-210.
24. Smigielski EM, Sirotkin K, Ward M, Sherry ST. dbSNP: a database of single nucleotide polymorphisms. *Nucleic Acids Res.* 2000;28:352-355.
25. Rammensee H, Bachmann J, Emmerich NP, Bachor OA, Stevanovic S. SYFPEITHI: database for MHC ligands and peptide motifs. *Immunogenetics* 1999;50:213-219.
26. Parker KC, Bednarek MA, Coligan JE. Scheme for ranking potential HLA-A2 binding peptides based on independent binding of individual peptide side-chains. *J Immunol* 1994;152:163-175.
27. Nielsen M, Lundegaard C, Worning P et al. Reliable prediction of T-cell epitopes using neural networks with novel sequence representations. *Protein Sci.* 2003;12:1007-1017.
28. Toebes M, Coccoris M, Bins A et al. Design and use of conditional MHC class I ligands. *Nat. Med.* 2006;12:246-251.
29. Eijssink C, Kester MG, Franke ME et al. Rapid assessment of the antigenic integrity of tetrameric HLA complexes by human monoclonal HLA antibodies. *J Immunol Methods* 2006;315:153-161.
30. Hadrup SR, Toebes M, Rodenko B et al. High-throughput T-cell epitope discovery through MHC peptide exchange. *Methods Mol. Biol.* 2009;524:383-405.
31. Hadrup SR, Schumacher TN. MHC-based detection of antigen-specific CD8(+) T cell responses. *Cancer Immunol. Immunother.* 2010
32. Wolkers MC, Brouwenstijn N, Bakker AH, Toebes M, Schumacher TN. Antigen bias in T cell cross-priming. *Science* 2004;304:1314-1317.
33. Kessler JH, Melief CJ. Identification of T-cell epitopes for cancer immunotherapy. *Leukemia* 2007;21:1859-1874.
34. Lin HH, Ray S, Tongchusak S, Reinherz EL, Bruscia V. Evaluation of MHC class I peptide binding prediction servers: applications for vaccine research. *BMC. Immunol.* 2008;9:8.
35. Amir AL, D'Orsogna LJ, Roelen DL et al. Allo-HLA reactivity of virus-specific memory T cells is common. *Blood* 2010;115:3146-3157.

SUPPLEMENTARY INFORMATION

2

Figure S1. Gene expression profiles and MiHA prediction of hematopoiesis-restricted genes obtained with microarray analysis. Gene expression profiles of CD34⁺/CD38⁻ and CD34⁺/CD38⁺ hematopoietic precursor cell populations. On the x-axis 100 different tissues or cell material are shown, clustered by organ system. On the y-axis the mRNA expression of the gene is shown. SC: stem cells, BM: bone marrow, PB: peripheral blood, Imm: immunological tissues, Apc: antigen presenting cells, Mal: hematological malignancies, CNS: central nervous system. Repr: reproductive organs, Gla: endocrine glands: Conn: connective tissues, Li: liver, Lu: lung, Dig: digestive tracts, Hea: heart, SK: skin, EC: endothelial cells. (A,B) HMHA-1 and PTPRC (CD45) have a clear hematopoiesis-restricted gene expression pattern. (C) Prostate kallikrein 2 (KLK2) demonstrate a tissue-specific gene expression pattern. (D) glyceraldehyde-3-phosphate dehydrogenase (GAPD) is ubiquitously expressed. (E,F) Integrin beta 2 (ITGB2) and FMS-like tyrosine kinase 3 (FLT3) were identified as genes (2 out of 78) with a hematopoiesis-restricted gene expression pattern by data-mining the combined microarray database. MiHA prediction based on peptide sequences representing the nucleotide sequences of both allelic variants of a SNP using three HLA-peptide binding algorithms. Polymorphic residue encoding triplet is highlighted (grey) and start-codon is underlined. ARF: alternative reading frame, NRF: normal reading frame S: Syfpeithi²⁵, B: Bimas²⁶, N: netMHC²⁷. (*): Only N was used to predict 11-mers HLA-binding. Selection threshold S: binding score (BS) ≥ 19 , B: BS ≥ 1 , N: BS ≤ 500 . (G) Prediction of MHMA-1 epitopes for RH139 polymorphism. Described immunogenic MiHA epitope; MHMA-1H and allelic variant are highlighted (red). (H) Prediction of ITGB2 epitopes for KE630 polymorphism.

a HMHA-1**b** PTPRC**c** KLK2**d** GAPD**e** ITGB2**f** FLT3**g** Prediction of HMHA-1 epitopes**h** Prediction of ITGB2 epitopes

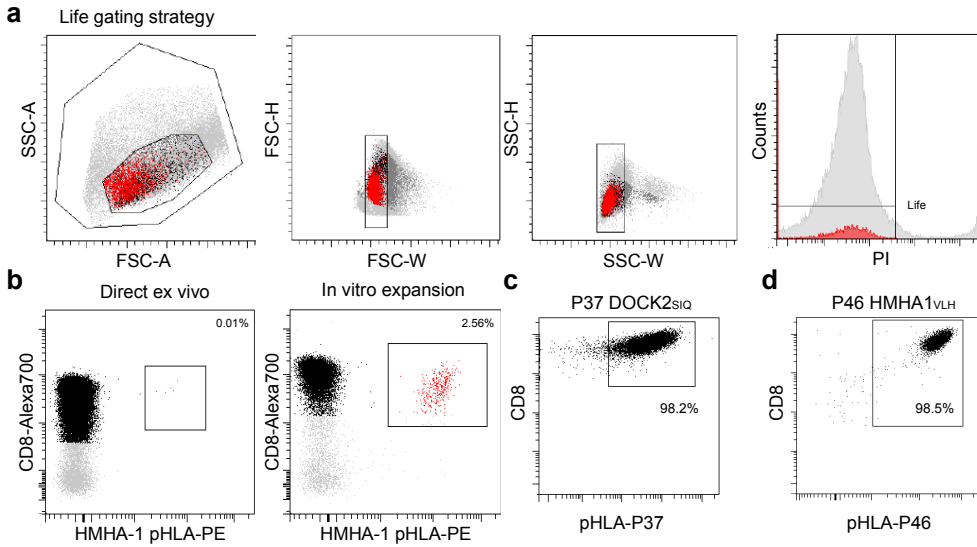


Figure S2. Flowcytometric analysis of pMHC tetramer specific cell lines. Flowcytometric analysis of HMHA-1 specific T-cells in an allo-SCT patient sample obtained 15 months after DLI, during the memory phase of the GVL response. (a) Life gating strategy to reduce background pMHC tetramer staining. FSC and SSC width and height channels were used to reduce background staining. Propidium iodide (PI) was used as a death cell marker. In all plots total lymphocytes are grey, total CD8⁺ T-cells are black and pMHC tetramer positive T-cells are highlighted red. Dot plots are shown with bi-exponential axes and display fluorescence intensity for the indicated fluorochromes. (b) Flowcytometric analysis of HMHA-1 specific T-cells after pull down and *in vitro* expansion. pMHC tetramer positive T-cell frequencies are expressed as total CD8⁺ T-cells. (c,d) Flowcytometric purity analysis of pMHC tetramer specific cell lines. Dot plots show total lymphocytes (black). Dot plots are shown with bi-exponential axes and display fluorescence intensity for the specific pMHC tetramer complexes on the x-axis and CD8 expression on the Y-axis. Shown frequencies indicate pMHC tetramer positive T-cells out of total lymphocytes. (c) BDY3356 derived CD8⁺ cell line: P37 DOCK2_{SIQ}. (d) APM4461 derived CD8⁺ cell line: P46 HMHA1_{VLH}. Dot plots shown are representative for all generated cell lines.

Table S1. Identified genes with a hematopoiesis-associated expression pattern

Gene symbol	Official full name	mRNA accession	Protein accession
AIF1	Allograft inflammatory factor 1	NM_001623.3	NP_001614.3
AREG	Amphiregulin	NM_001657.2	NP_001648.1
ARHGAP4	Rho GTPase activating protein 4	NM_001164741.1	NP_001158213.1
ARHGAP15	Rho GTPase activating protein 15	NM_018460.3	NP_060930.3
ARHGAP25	Rho GTPase activating protein 25	NM_01007231.1	NP_001007232.1
ATP2A3	Sarcoplasmic/endoplasmic reticulum calcium ATPase 3 isoform a	NM_005173.2	NP_005164.2
BTK	Bruton agammaglobulinemia tyrosine kinase	NM_000061.2	NP_000052.1
CBFA2T3	Protein CBFA2T3 isoform MTG16b	NM_005187.4	NP_005178.4
CCL3	Chemokine (C-C motif) ligand 3	NM_002983.2	NP_002974.1
CD37	CD37 molecule	NM_001774.2	NP_001765.1
CD48	CD48 molecule	NM_001778.2	NP_001769.2
CD52	CD52 molecule	NM_001803.2	NP_001794.2
CD69	CD69 molecule	NM_001781.2	NP_001772.1
CD79b	CD79b molecule, immunoglobulin-associated beta	NM_000626.2	NP_000617.1
CD83	CD83 molecule	NM_001040280.1	NP_001035370.1
CENTB1	ArfGAP with coiled-coil, ankyrin repeat and PH domains 1	NM_014716.3	NP_055531.1
CG018	NEDD4 binding protein 2-like 1	NM_001079691.1	NP_001073159.1
CORO1A	Coronin, actin binding protein, 1A	NM_001193333.2	NP_001180262.1
CPVL	Carboxypeptidase, vitellogenic-like	NM_019029.2	NP_061902.2
CRHBP	Corticotropin releasing hormone binding protein	NM_001882.3	NP_001873.2
CSF3R	Colony stimulating factor 3 receptor	NM_000760.3	NP_000751.1
CXorf9	SAM and SH3 domain containing 3	NM_018990.3	NP_061863.1
DOCK2	Dedicator of cytokinesis 2	NM_004946.2	NP_004937.1
DOK2	Docking protein 2	NM_003974.2	NP_003965.2
DUSP22	Dual specificity phosphatase 22	NM_020185.3	NP_064570.1
EVI2B	Ecotropic viral integration site 2B	NM_006495.3	NP_006486.3
FCER1A	Fc fragment of IgE, high affinity I, receptor for; alpha polypeptide	NM_002001.2	NP_001992.1
FLT3	Fms-related tyrosine kinase 3	NM_004119.2	NP_004110.2
FMNL1	Formin-like 1	NM_005892.3	NP_005883.2
FNBP1	Formin binding protein 1	NM_015033.2	NP_055848.1
FOSB	FBJ murine osteosarcoma viral oncogene homolog B	NM_001114171.1	NP_001107643.1
GATA2	GATA binding protein 2	NM_001145661.1	NP_001139133.1
GMFG	Glia maturation factor, gamma	NM_004877.2	NP_004868.1
GNA15	Guanine nucleotide binding protein, alpha 15	NM_002068.2	NP_002059.2
HMHA-1	Histocompatibility minor HA-1	NM_012292.2	NP_036424.2
HOXA9	Homeobox A9	NM_152739.3	NP_689952.1
HSPA6	Heat shock 70kDa protein 6	NM_002155.3	NP_002146.2
ICAM3	Intercellular adhesion molecule 3	NM_002162.3	NP_002153.2
IL2RG	Interleukin 2 receptor, gamma	NM_000206.2	NP_000197.1
IQGAP2	IQ motif containing GTPase activating protein 2	NM_006633.2	NP_006624.2
ISG20	Interferon stimulated exonuclease gene 20kDa	NM_002201.4	NP_002192.2
ITGAL	Integrin, alpha L	NM_001114380.1	NP_001107852.1
ITGAM	Integrin, alpha M	NM_000632.3	NP_000623.2
ITGB2	Integrin, beta 2	NM_000211.3	NP_000202.2
KCNAB2	Voltage-gated potassium channel subunit beta-2 isoform 1	NM_003636.2	NP_003627.1
LAT2	Linker for activation of T-cells family member 2	NM_014146.3	NP_054865.2
LCP2	Lymphocyte cytosolic protein 2	NM_005565.3	NP_005556.1
LOC81691	Putative RNA exonuclease NEF-sp isoform 2	NM_001144924.1	NP_001138396.1
LRMP	Lymphoid-restricted membrane protein	NM_006152.2	NP_006143.2
LTB	Lymphotoxin-beta isoform a	NM_002341.1	NP_002332.1
LYN	Tyrosine-protein kinase Lyn isoform B	NM_001111097.1	NP_001104567.1
MAP4K1	Mitogen-activated protein kinase kinase kinase 1 isoform 1	NM_001042600.1	NP_001036065.1
MCM5	DNA replication licensing factor MCM5	NM_006739.3	NP_006730.2
MPL	Thrombopoietin receptor precursor	NM_005373.2	NP_005364.1
NCF4	Neutrophil cytosol factor 4 isoform 1	NM_000631.4	NP_000622.2
NUP210	Nuclear pore membrane glycoprotein 210 precursor	NM_024923.2	NP_079199.2
PIK3CD	Phosphatidylinositol-4,5-bisphosphate 3-kinase catalytic subunit delta isoform	NM_005026.3	NP_005017.3
PIM2	Serine/threonine-protein kinase pim-2	NM_006875.3	NP_006866.2
PLCB2	1-Phosphatidylinositol-4,5-bisphosphate phosphodiesterase beta-2	NM_004573.2	NP_004564.2
PLEK	Pleckstrin	NM_002664.2	NP_002655.2
PRKCB1	Protein kinase C beta type isoform 2	NM_002738.6	NP_002729.2
PSD4	PH and SEC7 domain-containing protein 4	NM_012455.2	NP_036587.2
PSMB10	Proteasome subunit beta type-10 proprotein	NM_002801.2	NP_002792.1
PSMB8	Proteasome subunit beta type-8 isoform E1 proprotein	NM_004159.4	NP_004150.1
PTPN22	Tyrosine-protein phosphatase non-receptor type 22 isoform 3	NM_001193431.1	NP_001180360.1
PTPN6	Tyrosine-protein phosphatase non-receptor type 6 isoform 1	NM_002831.5	NP_002822.2
PTPRC	Receptor-type tyrosine-protein phosphatase C isoform 1 precursor	NM_002838.3	NP_002829.2
PTPRCAP	Protein tyrosine phosphatase receptor type C-associated protein	NM_005608.2	NP_005599.1
RASGRP2	RAS guanyl-releasing protein 2	NM_153819.1	NP_722541.1
RGS1	Regulator of G-protein signaling 1	NM_002922.3	NP_002913.3
SELL	L-selectin precursor	NM_000655.4	NP_000646.2
SELPLG	P-selectin glycoprotein ligand 1	NM_003006.3	NP_002997.1
SEPT6	Septin-6 isoform B	NM_015129.5	NP_055944.2
SF1	Splicing factor 1 isoform 6	NM_001178030.1	NP_001171501.1
SOCS2	Suppressor of cytokine signaling 2	NM_003877.3	NP_003868.1
SP110	Sp110 nuclear body protein isoform d	NM_001185015.1	NP_001171944.1
SYNGR1	Synaptogyrin-1 isoform 1a	NM_004711.4	NP_004702.2
TNRC5	Protein canopy homolog 3 precursor	NM_006586.3	NP_006577.2
ZFP36L2	Zinc finger protein 36, C3H1 type-like 2	NM_006887.4	NP_008818.3

Table SII. Total MiHA epitopes predicted by HLA-peptide binding algorithm

Gene symbol	Residue Change	RefSNP accession	dbSNP AH [†]	Minor Frequency [‡]	Reading Frame	Length	Peptide Sequence [†]
AIF	RG 14	rs2736182	0,22	0,01	NRF	10	DLQGGKAFGL
AIF	RG 14	rs2736182	0,22	0,01	NRF	10	DLOGGKAFRL
AIF	RG 14	rs2736182	0,22	0,01	NRF	11	GLLKAQQEERL
AIF	RG 14	rs2736182	0,22	0,01	NRF	9	LQGGKAFGL
AIF	RG 14	rs2736182	0,22	0,01	NRF	9	LQGGKAFRL
AIF	RG 14	rs2736182	0,22	0,01	NRF	11	RLLKAQQEERL
AREG	PP 10	rs1615111	0,18	0,02	ARF	9	AGAGGAVAL
AREG	PP 10	rs1615111	0,18	0,02	ARF	9	AGASGAVAL
AREG	PP 10	rs1615111	0,18	0,02	ARF	9	ATAGAGGAV
AREG	PP 10	rs1615111	0,18	0,02	ARF	9	ATAGASGAV
AREG	PP 10	rs1615111	0,18	0,02	ARF	11	ATAGASGAVAL
AREG	PT 76	rs7656521	0,09	0,01	NRF	10	AAHPPLHLSL
AREG	PT 76	rs7656521	0,09	0,01	NRF	10	AAHTPGLHSL
AREG	PT 76	rs7656521	0,09	0,01	NRF	9	AHPPLHLSL
AREG	PT 76	rs7656521	0,09	0,01	NRF	9	AHTPGLHSL
AREG	FF 177	rs2291715	0,22	N.D.	ARF	9	ILVNGVGKS
AREG	FF 177	rs2291715	0,22	N.D.	ARF	11	NVSKNILVNGV
AREG	FF 177	rs2291715	0,22	N.D.	ARF	11	NVSKNISVNGV
AREG	FF 177	rs2291715	0,22	N.D.	ARF	9	SKNILVNGV
AREG	FF 177	rs2291715	0,22	N.D.	ARF	9	SKNISVNGV
ARHGAP4	VA 104	rs5987182	0,14	0,00	NRF	9	LLSPLHCWA
ARHGAP4	VA 104	rs5987182	0,14	0,00	NRF	10	LLSPLHCWAVL
ARHGAP4	VA 104	rs5987182	0,14	0,00	NRF	10	LLSPLHCWVV
ARHGAP4	VA 104	rs5987182	0,14	0,00	NRF	11	LLSPLHCWVVL
ARHGAP4	VA 104	rs5987182	0,14	0,00	NRF	9	LSPPLHCWAV
ARHGAP4	VA 104	rs5987182	0,14	0,00	NRF	9	PLHCWAVLL
ARHGAP4	VA 104	rs5987182	0,14	0,00	NRF	9	PLHCWVLL
ARHGAP4	VA 104	rs5987182	0,14	0,00	NRF	10	SLLSPLHCWA
ARHGAP4	VA 104	rs5987182	0,14	0,00	NRF	11	SLLSPLHCWAV
ARHGAP4	VA 104	rs5987182	0,14	0,00	NRF	10	SLLSPLHCWV
ARHGAP4	VA 104	rs5987182	0,14	0,00	NRF	11	SLLSPLHCWVV
ARHGAP4	VA 104	rs5987182	0,14	0,00	NRF	10	SPLHCWVLL
ARHGAP4	VV 523	rs2070098	N.D.	0,00	ARF	9	ACAPGGGEL
ARHGAP4	VV 523	rs2070098	N.D.	0,00	ARF	9	ACAPRGEL
ARHGAP4	VV 523	rs2070098	N.D.	0,00	ARF	10	APGGGELHSL
ARHGAP4	VV 523	rs2070098	N.D.	0,00	ARF	10	APRGELHSL
ARHGAP4	VV 523	rs2070098	N.D.	0,00	ARF	10	SLCPWSWRAA
ARHGAP4	VV 523	rs2070098	N.D.	0,00	ARF	10	SLCPWWRRAA
ARHGAP15	LF 438	rs11538443	N.D.	0,00	NRF	11	FLRAENETGNM
ARHGAP15	LF 438	rs11538443	N.D.	0,00	NRF	9	GIVFGPTFL
ARHGAP15	LF 438	rs11538443	N.D.	0,00	NRF	9	GIVFGPTLL
ARHGAP15	LF 438	rs11538443	N.D.	0,00	NRF	10	IVFGPTFLRA
ARHGAP15	LF 438	rs11538443	N.D.	0,00	NRF	10	IVFGPTLLRA
ARHGAP15	LF 438	rs11538443	N.D.	0,00	ARF	10	KLGDCIWYLL
ARHGAP15	LF 438	rs11538443	N.D.	0,00	ARF	11	KLGDCIWYLS
ARHGAP15	LF 438	rs11538443	N.D.	0,00	ARF	11	KLGDCIWYTPS
ARHGAP15	LF 438	rs11538443	N.D.	0,00	NRF	11	LRAENETGNM
ARHGAP15	LF 438	rs11538443	N.D.	0,00	NRF	10	SLGIVFGPTL
ARHGAP15	LF 438	rs11538443	N.D.	0,00	NRF	9	TLLRAENET
ARHGAP15	LF 438	rs11538443	N.D.	0,00	NRF	11	TLLRAENETGN
ARHGAP25	AA 384	rs17604346	0,01	0,02	ARF	9	MLLKTSEFL
ARHGAP25	AA 384	rs17604346	0,01	0,02	ARF	11	MLLKTSEFLGQ
ARHGAP25	RS 555	rs4241344	0,43	0,27	NRF	10	KLILCRVWSK
ARHGAP25	RS 555/MT 556	Combination	0,43/0,44	0,27/N.D.	NRF	9	SLQSTVQEL
ARHGAP25	RS 555	rs4241344	0,43	0,27	NRF	9	SLQRMVQEL
ARHGAP25	RS 555	rs4241344	0,43	0,27	NRF	9	SLQSMVQEL
ARHGAP25	RS 555	rs4241344	0,43	0,27	NRF	11	SLQSMVQELRK
ARHGAP25	RS 555	rs4241344	0,43	0,27	NRF	10	SMVQELRKEI
ARHGAP25	MT 556	rs10177248	0,44	N.D.	NRF	9	MVQELRKEI
ARHGAP25	MT 556	rs10177248	0,44	N.D.	NRF	10	RMVQELRKEI
ARHGAP25	MT 556	rs10177248	0,44	N.D.	NRF	9	SLQRTVQEL
ARHGAP25	MT 556	rs10177248	0,44	N.D.	NRF	9	TVQELRKEI
ATP2A3	W*stop 77	rs17846878	N.D.	0,00	ARF	9	ALVSFVLAW
ATP2A3	W*stop 77	rs17846878	N.D.	0,00	NRF	9	LCCPLIRG
ATP2A3	W*stop 77	rs17846878	N.D.	0,00	ARF	10	LCCPLIRGG
ATP2A3	W*stop 77	rs17846878	N.D.	0,00	ARF	9	LCCPLVRG
ATP2A3	W*stop 77	rs17846878	N.D.	0,00	ARF	10	LCCPLVRGG
ATP2A3	LL 302	rs9915542	N.D.	0,00	ARF	10	CLLQDRRGL
ATP2A3	LL 302	rs9915542	N.D.	0,00	ARF	9	LLQDRRGL
ATP2A3	AA 424	rs1800911	N.D.	0,44	ARF	10	RLWTTTRPRV
ATP2A3	ND 458	rs9913158	N.D.	0,00	NRF	9	KMNVDL
ATP2A3	ND 458	rs9913158	N.D.	0,00	NRF	9	KMNVDNL
ATP2A3	ND 458	rs9913158	N.D.	0,00	NRF	9	NVFDLQA
ATP2A3	ND 458	rs9913158	N.D.	0,00	NRF	10	NVFDLQAL
ATP2A3	ND 458	rs9913158	N.D.	0,00	NRF	9	NVFDNLQA
ATP2A3	ND 458	rs9913158	N.D.	0,00	NRF	10	NVFDNLQAL
ATP2A3	ND 458	rs9913158	N.D.	0,00	NRF	9	NLQALSRV
ATP2A3	DE 519	rs12946879	N.D.	0,00	NRF	11	KMFVKGAPDSV
ATP2A3	DE 519	rs12946879	N.D.	0,00	NRF	11	KMFVKGAPESV
ATP2A3	DE 519	rs12946879	N.D.	0,00	NRF	11	MFVKGAPESVI
ATP2A3	CR 674	rs9895012	N.D.	0,07	ARF	10	LLLRPRGART

ATP2A3	CR 674	rs9895012	N.D.	0,07	ARF	11	LLLRPRGARTQ
ATP2A3	CR 674	rs9895012	N.D.	0,07	NRF	9	RTA C CFARV
ATP2A3	CR 674	rs9895012	N.D.	0,07	NRF	9	RTA R CFARV
ATP2A3	HQ 869	rs11654827	0,01	0,00	NRF	10	INFYHLRNFL
ATP2A3	HQ 869	rs11654827	0,01	0,00	NRF	10	INFY Q LRNFL
ATP2A3	RR 1034	rs887387	0,43	0,34	ARF	9	GT G WSLRCV
ATP2A3	RR 1034	rs887387	0,43	0,34	ARF	9	WE Q GGVSGV
ATP2A3	RR 1034	rs887387	0,43	0,34	ARF	9	WE S GGVSGV
BTK	SS 318	rs5991926	N.D.	0,00	ARF	10	CL C LLNPQGT
BTK	SS 318	rs5991926	N.D.	0,00	ARF	10	KL A NIQCLCL
BTK	SS 318	rs5991926	N.D.	0,00	ARF	10	KL A NIQ C PCL
BTK	SS 318	rs5991926	N.D.	0,00	ARF	10	LANIQ C LLCL
BTK	SS 318	rs5991926	N.D.	0,00	ARF	10	QSWQI S V C V
BTK	SS 318	rs5991926	N.D.	0,00	ARF	10	QSWQI S V R V
BTK	CY 361	rs28935478	N.D.	0,00	NRF	11	ELIN Y HQHNSA
BTK	CY 361	rs28935478	N.D.	0,00	ARF	11	SL S SLTAISTT
BTK	CY 361	rs28935478	N.D.	0,00	ARF	10	SL S SLTAIST
BTK	CY 361	rs28935478	N.D.	0,00	ARF	11	SL S SLTISTT
BTK	CY 361	rs28935478	N.D.	0,00	ARF	10	SL S SLTIST
BTK	CY 361	rs28935478	N.D.	0,00	ARF	11	SLT A ISTTLQD
BTK	CY 361	rs28935478	N.D.	0,00	ARF	9	SLT A ISTTL
BTK	CY 361	rs28935478	N.D.	0,00	ARF	9	SLT T ISTTL
BTK	CC 633	rs1135363	N.D.	0,21	ARF	11	TV A GMRKQMSV
BTK	CC 633	rs1135363	N.D.	0,21	ARF	11	TV V GMRKQMSV
BTK	CC 633	rs1135363	N.D.	0,21	ARF	10	V V GMRKQMSV
BTK	CC 633	rs1135363	N.D.	0,21	ARF	10	Y I PSCT V AGM
CCL3	PP 60	rs1130371	0,43	0,04	ARF	11	TL R RAASAP S L
CCL3	GS 69	rs5029408	N.D.	0,07	NRF	9	FL T K R G R Q V
CCL3	GS 69	rs5029408	N.D.	0,07	NRF	9	FL T K R S R Q V
CCL3	GS 69	rs5029408	N.D.	0,07	NRF	11	FL T K R S R Q V CA
CD37	CC 7	rs11545491	N.D.	0,00	ARF	11	EL P Q P HQ V L P L
CD37	CC 7	rs11545491	N.D.	0,00	ARF	11	EL S Q P HQ V L P L
CD37	CC 7	rs11545491	N.D.	0,00	ARF	10	L P Q P HQ V L P L
CD37	CC 7	rs11545491	N.D.	0,00	ARF	10	L S Q P HQ V L P L
CD37	II 38	rs354021	0,21	0,18	ARF	10	HL D PH R Q D Q L
CD48	LL 16	rs11541827	N.D.	0,01	ARF	9	F V S G S G IA I
CD48	LL 16	rs11541827	N.D.	0,01	ARF	10	F V S G S G IA I A
CD48	LL 16	rs11541827	N.D.	0,01	ARF	9	F V S G S G IA T
CD48	LL 16	rs11541827	N.D.	0,01	ARF	10	F V S G S G IA T A
CD48	QE 102	rs2295615	0,26	N.D.	ARF	10	AL Y IS K V Q KE
CD48	QE 102	rs2295615	0,26	N.D.	ARF	10	AL Y IS K V Q K L
CD48	QE 102	rs2295615	0,26	N.D.	ARF	11	K Q D N ST Y IM R V
CD48	QE 102	rs2295615	0,26	N.D.	ARF	11	K V Q K ED N ST Y I
CD48	QE 102	rs2295615	0,26	N.D.	ARF	11	K V Q K Q D N S T Y I
CD48	LL 150	rs17851383	N.D.	0,00	ARF	9	LL F ET V MC D
CD48	LL 150	rs17851383	N.D.	0,00	ARF	10	LL F ET V MC D T
CD48	LL 150	rs17851383	N.D.	0,00	ARF	10	LL S ET V MC D T
CD52	SN 40	rs1071849	0,46	0,28	NRF	11	N I SG G IF L FF V
CD52	SN 40	rs1071849	0,46	0,28	NRF	11	Q T SS P AS S SS I
CD52	SN 40/MI 41	Combination	0,46/0,46	0,28/N.D.	NRF	11	Q T SS P AS S SS M
CD52	SN 40	rs1071849	0,46	0,28	NRF	11	S I GG I FL F FF V
CD52	MI 41	rs17645	0,46	N.D.	NRF	10	I S GG I FL F FF V
CD52	MI 41	rs17645	0,46	N.D.	NRF	10	M S GG I FL F FF V
CD52	MI 41	rs17645	0,46	N.D.	NRF	11	N M SG G IF L FF V
CD52	MI 41	rs17645	0,46	N.D.	NRF	11	Q T SS P AS S SN I
CD52	MI 41	rs17645	0,46	N.D.	NRF	11	Q T SS P AS S SN M
CD69	NN 166	rs11052883	0,066	0,04	ARF	9	KE F NN W F V
CD69	NN 166	rs11052883	0,066	0,04	ARF	9	KE F NN W F N V
CD69	NN 166	rs11052883	0,066	0,04	ARF	9	K V T G S D K C V
CD69	NN 166	rs11052883	0,03	0,04	ARF	10	L T T G S T L Q L
CD69	NN 166	rs11052883	0,03	0,04	ARF	10	L T T G S K L Q L
CD69	NN 166	rs11052883	0,03	0,04	ARF	11	N L T T G S T L Q L
CD69	NN 166	rs11052883	0,066	0,04	ARF	11	N L T T G S K L Q L
CD69	NN 166	rs11052883	0,066	0,04	ARF	9	N V T G S D K C V
CD69	NN 166	rs11052883	0,03	0,04	ARF	11	Q M A K N L T T G S T
CD69	NN 166	rs11052883	0,066	0,04	ARF	9	S K L Q L T S V
CD69	NN 166	rs11052883	0,03	0,04	ARF	9	S T L Q L T S V
CD69	NN 166	rs11052883	0,03	0,04	ARF	11	S T L Q L T S V F F
CD69	NN 166	rs11052883	0,03	0,04	ARF	9	T T G S T L Q L
CD79b	LL 20	rs11555057	N.D.	0,00	ARF	9	PL D GG V A A
CD79b	LL 20	rs11555057	N.D.	0,00	ARF	9	PL D GG V A V
CD79b	LL 20	rs11555057	N.D.	0,00	ARF	10	PL D GG V A A V
CD79b	CC 122	rs2070776	0,47	0,27	ARF	10	GL R T M A S T S V
CD79b	CC 122	rs2070776	0,47	0,27	ARF	10	L L L P A E V Q Q H
CD79b	CC 122	rs2070776	0,47	0,27	ARF	11	L L L P A E V Q Q H L
CD79b	CC 122	rs2070776	0,47	0,27	ARF	11	L L L S A E V Q Q H L
CD79b	CC 122	rs2070776	0,47	0,27	ARF	10	L L L P A E V Q Q H L
CD79b	CC 122	rs2070776	0,47	0,27	ARF	10	L L L S A E V Q Q H L
CD79b	CC 122	rs2070776	0,47	0,27	ARF	11	S G L R T M A S T S V
CD79b	CC 122	rs2070776	0,47	0,27	ARF	11	T M A S T S A S R S A
CD79b	CC 122	rs2070776	0,47	0,27	ARF	11	T M A S T S V S R S A
CD79b	KE 217	rs1063625	N.D.	0,00	NRF	10	D I V T L R T G E V
CD79b	KE 217	rs1063625	N.D.	0,00	NRF	10	D I V T L R T G K V
CD79b	KE 217	rs1063625	N.D.	0,00	NRF	9	R T G E V K W S V
CD79b	KE 217	rs1063625	N.D.	0,00	NRF	9	R T G K V K W S V
CD79b	KE 217	rs1063625	N.D.	0,00	NRF	11	T L R T G E V K W S V
CENTB1	YY 166	rs3809828	0,13	0,07	ARF	9	W V P G T G T G L

CENTB1	YY 166	rs3809828	0.13	0.07	ARF	9	WVSGTG TGL
CORO1A	DH 80	rs11555342	N.D.	0.00	ARF	9	GLWPHSPCA
CORO1A	DH 80	rs11555342	N.D.	0.00	ARF	9	GLWRHSPCA
CORO1A	DH 80	rs11555342	N.D.	0.00	NRF	9	TVCGDTAPV
CORO1A	DH 80	rs11555342	N.D.	0.00	NRF	9	TVCGHTAPV
CORO1A	LL 404	rs11555339	N.D.	0.00	ARF	10	WLRTPKEP GV
CORO1A	PT 443	rs1053574	0.04	0.00	NRF	9	EMRKLQATV
CORO1A	PT 443	rs1053574	0.04	0.00	NRF	9	KLOAPVQEL
CORO1A	PT 443	rs1053574	0.04	0.00	NRF	9	KLOATVQEL
CORO1A	PT 443	rs1053574	0.04	0.00	NRF	9	TVQELQKRL
CPVL	QP 112	rs11542982	N.D.	0.00	NRF	10	QGGSSMFLG
CPVL	RH 398	rs1052200	0.3	0.15	NRF	9	AAALTEHSL
CPVL	RH 398	rs1052200	0.3	0.15	NRF	9	AAALTERSL
CPVL	RH 398	rs1052200	0.3	0.15	NRF	10	ALTEHSLMGM
CPVL	RH 398	rs1052200	0.3	0.15	NRF	10	ALTERSLMGM
CPVL	RH 398	rs1052200	0.3	0.15	NRF	11	IVAALTEHSL
CPVL	RH 398	rs1052200	0.3	0.15	NRF	11	IVAALTERSL
CPVL	VA 435	rs7313	0.47	0.42	NRF	9	EVAGYIROV
CPVL	VA 435	rs7313	0.47	0.42	ARF	11	LVTSGKRVTSI
CPVL	VA 435	rs7313	0.47	0.42	ARF	9	LVTSGKWVT
CPVL	VA 435	rs7313	0.47	0.42	NRF	9	RQAGDFHQV
CPVL	VA 435	rs7313	0.47	0.42	NRF	9	RQVDFHQV
CPVL	VA 435	rs7313	0.41	0.42	ARF	10	RVTSIRLFEV
CPVL	VA 435	rs7313	0.47	0.42	ARF	10	VTSGKRVTSI
CPVL	VA 435	rs7313	0.47	0.42	ARF	10	VTSGKWVTSI
CPVL	VA 435	rs7313	0.41	0.42	ARF	10	WVTSIRLFEV
CPVL	VA 435	rs7313	0.47	0.42	ARF	9	WLVTSGKRV
CPVL	VA 435	rs7313	0.47	0.42	ARF	10	WLVTSGKRV
CPVL	VA 435	rs7313	0.47	0.42	ARF	9	WLVTSGKWV
CPVL	VA 435	rs7313	0.47	0.42	ARF	10	WLVTSGKWV
CSF3R	VV 36	rs3918011	0.01	0.01	ARF	11	FTWGI PSQPPA
CSF3R	VV 36	rs3918011	0.01	0.01	ARF	10	SQPPSFTWGI
CSF3R	VV 36	rs3918011	0.01	0.01	ARF	10	SQPPSFTWGI
CSF3R	VV 36	rs3918011	0.01	0.01	ARF	11	STWGI PSQPPA
CSF3R	VV 36	rs3918011	0.01	0.01	ARF	9	SVSQPSFT
CSF3R	AA 242	rs3918017	0.02	N.D.	ARF	11	LLPRQAAYS CA
CSF3R	ND 320	rs3918018	0.07	0.13	ARF	9	APAWPLEQL
CSF3R	ND 320	rs3918018	0.07	0.13	ARF	9	APAWPLERL
CSF3R	ND 320	rs3918018	0.07	0.13	ARF	10	LAPAWPLEQL
CSF3R	ND 320	rs3918018	0.07	0.13	ARF	10	LAPAWPLERL
CSF3R	RQ 346	rs3917974	0.04	N.D.	NRF	9	QLDPRTVQL
CSF3R	RQ 346	rs3917974	0.04	N.D.	NRF	10	RQLDPRTVQL
CSF3R	RQ 346	rs3917974	0.04	N.D.	NRF	9	RQLDPRTVQL
CSF3R	RR 418	rs3917980	0.4	N.D.	ARF	10	ITQPGPLAPL
CSF3R	RR 418	rs3917980	0.4	N.D.	ARF	10	ITQPGPLVPL
CSF3R	RR 418	rs3917980	0.4	N.D.	ARF	9	TQPGPLAPL
CSF3R	RR 418	rs3917980	0.4	N.D.	ARF	9	TQPGPLVPL
CSF3R	QR 440	rs3918020	0.35	0.00	NRF	11	AMADDPHSLWV
CSF3R	QR 440	rs3918020	0.35	0.00	NRF	11	AMARDPHSLWV
CSF3R	QR 440	rs3918020	0.35	0.00	NRF	9	AMADDPHSL
CSF3R	QR 440	rs3918020	0.35	0.00	NRF	9	AMARDPHSL
CSF3R	QR 440	rs3918020	0.35	0.00	NRF	9	AQDPHSLWV
CSF3R	QR 440	rs3918020	0.35	0.00	NRF	10	MAQDPHSLWV
CSF3R	QR 440	rs3918020	0.35	0.00	NRF	10	MARDPHSLWV
CSF3R	HD 510	rs3917991	0.12	0.02	ARF	9	LVPGHGGT
CSF3R	HD 510	rs3917991	0.12	0.02	ARF	9	SLVPAHHGT
CSF3R	HD 510	rs3917991	0.12	0.02	ARF	10	SLVPAHHGT
CSF3R	HD 510	rs3917991	0.12	0.02	ARF	9	SLVPAHHGT
CSF3R	HD 510	rs3917991	0.12	0.02	ARF	10	SLVPAHHGT
DOCK2	QQ 784	rs13155521	0.05	0.06	ARF	9	SIQNYHPFA
DOCK2	YY 1438	rs17647491	0.02	0.04	ARF	10	IQLCAKVPLL
DOCK2	YY 1438	rs17647491	0.02	0.04	ARF	9	IQLCAKVPL
DOCK2	YY 1438	rs17647491	0.02	0.04	ARF	10	IQLRAKVPLL
DOCK2	YY 1438	rs17647491	0.02	0.04	ARF	9	IQLRAKVPL
DOCK2	YY 1438	rs17647491	0.02	0.04	ARF	9	KLLQIQLCA
DOCK2	YY 1438	rs17647491	0.02	0.04	ARF	11	KLLQIQLCAKV
DOCK2	YY 1438	rs17647491	0.02	0.04	ARF	11	KLLQIQLRAKV
DOCK2	YY 1438	rs17647491	0.02	0.04	ARF	9	KLLQIQLRA
DOCK2	YY 1438	rs17647491	0.02	0.04	ARF	10	LLQIQLCAKV
DOCK2	YY 1438	rs17647491	0.02	0.04	ARF	10	LLQIQLRAKV
DOCK2	YY 1438	rs17647491	0.02	0.04	ARF	9	LQIQLCAKV
DOCK2	YY 1438	rs17647491	0.02	0.04	ARF	9	LQIQLRAKV
DOCK2	YY 1438	rs17647491	0.02	0.04	ARF	10	QIQLCAKVPL
DOCK2	YY 1438	rs17647491	0.02	0.04	ARF	10	QIQLRAKVPL
DOCK2	YY 1438	rs17647491	0.02	0.04	ARF	9	QLCAKVPLL
DOCK2	YY 1438	rs17647491	0.02	0.04	ARF	9	QLRAKVPLL
DOCK2	YY 1438	rs17647491	0.018	0.04	ARF	9	RLSTNPTM
DOCK2	YY 1438	rs17647491	0.018	0.04	ARF	9	RLSTNPTM
DOCK2	RR 1632	rs1045168	0.34	0.29	ARF	10	LTLTGEWAA
DOCK2	RR 1632	rs1045168	0.34	0.29	ARF	10	LTLTGEWAV
DOCK2	RR 1632	rs1045168	0.34	0.29	ARF	9	LTLTGEWAA
DOCK2	RR 1632	rs1045168	0.34	0.29	ARF	9	LTLTGEWAV
DOCK2	RR 1632	rs1045168	0.34	0.29	ARF	10	TTGEWAVPGL
DOCK2	PA 152	rs1140295	N.D.	0.00	ARF	10	SQSAPTRNFL
DOCK2	PA 152	rs1140295	N.D.	0.00	NRF	10	TVGPHKEFV
DOCK2	PA 152	rs1140295	N.D.	0.00	NRF	10	TVGPHKEFPV
DOCK2	PA 152	rs1140295	N.D.	0.00	NRF	9	VGPHKEFV
DOCK2	PA 152	rs1140295	N.D.	0.00	NRF	9	VGPHKEFPV

DOK2	PA 152	rs1140295	N.D.	0,00	NRF	11	VTVGP ^H PK ^E F ^A V
DOK2	PA 152	rs1140295	N.D.	0,00	NRF	11	VTVGP ^H PK ^E F ^P V
DOK2	PT 336	rs7824139	N.D.	0,00	ARF	10	ALR ^R PC ^P LDL
DOK2	PT 336	rs7824139	N.D.	0,00	ARF	10	ALR ^S PC ^P LDL
DOK2	PT 336	rs7824139	N.D.	0,00	NRF	10	PLYDSIEE ^P L
DOK2	PT 336	rs7824139	N.D.	0,00	NRF	9	PLYDSIEE ^T L
DOK2	PT 336	rs7824139	N.D.	0,00	NRF	10	PLYDSIEE ^T L
DOK2	PT 336	rs7824139	N.D.	0,00	NRF	9	TLPPRPD ^H I
DOK2	AA 387	rs17853066	0,03	N.D.	ARF	10	LLASSMSS ^Q L
DOK2	AA 387	rs17853066	0,03	N.D.	ARF	11	LLASSMSS ^Q L ^G
DOK2	AA 387	rs17853066	0,03	N.D.	ARF	9	QLGRIS ^L LL
DOK2	AA 387	rs17853066	0,03	N.D.	ARF	10	QLGRIS ^L LLA
DOK2	AA 387	rs17853066	0,03	N.D.	ARF	9	RAGFLC ^F WL
DOK2	AA 387	rs17853066	0,03	N.D.	ARF	11	SMSSQLGRIS ^L
DOK2	AA 387	rs17853066	0,03	N.D.	ARF	9	SMSSQLGR ^I
DOK2	AA 387	rs17853066	0,03	N.D.	ARF	11	SMSSQ ^P GRIS ^L
DOK2	AA 387	rs17853066	0,03	N.D.	ARF	9	SQ ^L GRIS ^L LL
DOK2	AA 387	rs17853066	0,03	N.D.	ARF	10	SQ ^L GRIS ^L LL
DOK2	AA 387	rs17853066	0,03	N.D.	ARF	11	TLLASSMSS ^Q L
DOK2	AA 387	rs17853066	0,03	N.D.	ARF	9	WAGFLC ^F WL
DOK2	AS 394	rs2242241	0,01	0,30	ARF	9	RAGFLC ^F WL
DUSP22	HR 119	rs7768224	0,07	0,00	ARF	9	CMLGDPV ^P T
DUSP22	HR 119	rs7768224	0,07	0,00	ARF	10	MLGDPV ^P T ^T
DUSP22	HR 119	rs7768224	0,07	0,00	ARF	9	RMPCT ^P CM ^L
DUSP22	HR 119	rs7768224	0,07	0,00	ARF	9	RMPCT ^P CV ^L
DUSP22	HR 119	rs7768224	0,07	0,00	ARF	10	VLGDPV ^P T ^T
DUSP22	PP 172	rs1129085	0,24	0,37	ARF	9	SGNSEV ^L GL
DUSP22	PP 172	rs1129085	0,24	0,37	ARF	9	SRNSEV ^L GL
EVI2B	VI 161	rs17882145	0,01	0,00	NRF	10	QIPSRK ^Q V ^T V
EVI2B	VI 161	rs17882145	0,01	0,00	NRF	10	SVQIPSRK ^Q V
EVI2B	VI 161	rs17882145	0,01	0,00	NRF	9	VQIPSRK ^Q V
EVI2B	GC 340	rs17884293	0,01	0,00	ARF	9	CL ^D HLP ^F WI
EVI2B	GC 340	rs17884293	0,01	0,00	ARF	9	CL ^H HLP ^F WI
EVI2B	GC 340	rs17884293	0,01	0,00	NRF	9	GL ^P PP ^P LL
EVI2B	GC 340	rs17884293	0,01	0,00	NRF	10	LP ^P PP ^P LL ^D L
EVI2B	GC 340	rs17884293	0,01	0,00	ARF	9	MMQVCL ^H L
EVI2B	GC 340	rs17884293	0,01	0,00	ARF	10	VCL ^H HLP ^F WI
FCER1A	VA 230	rs17851282	N.D.	0,00	NRF	9	FISTQQ ^Q A ^T
FCER1A	VA 230	rs17851282	N.D.	0,00	NRF	11	FISTQQ ^Q A ^T FL
FCER1A	VA 230	rs17851282	N.D.	0,00	NRF	11	FISTQQ ^Q V ^T FL
FCER1A	VA 230	rs17851282	N.D.	0,00	NRF	10	GLFISTQQ ^Q A
FCER1A	VA 230	rs17851282	N.D.	0,00	NRF	10	GLFISTQQ ^Q V
FCER1A	VA 230	rs17851282	N.D.	0,00	NRF	11	ISTQQ ^Q A ^T FL ^L
FCER1A	VA 230	rs17851282	N.D.	0,00	NRF	11	ISTQQ ^Q V ^T FL ^L
FCER1A	VA 230	rs17851282	N.D.	0,00	NRF	9	QQ ^A T ^F LL ^K I
FCER1A	VA 230	rs17851282	N.D.	0,00	NRF	9	QQ ^V T ^F LL ^K I
FCER1A	VA 230	rs17851282	N.D.	0,00	NRF	9	TQQ ^Q A ^T FL ^L
FCER1A	VA 230	rs17851282	N.D.	0,00	NRF	9	TQQ ^Q V ^T FL ^L
FLT3	GD 7	rs12872889	0,5	N.D	NRF	9	ALAR ^D AG ^T V
FLT3	GD 7	rs12872889	0,5	N.D	NRF	11	ALAR ^D AG ^T V ^P L
FLT3	GD 7	rs12872889	0,5	N.D	NRF	9	ALAR ^G AG ^T V
FLT3	GD 7	rs12872889	0,5	N.D	NRF	11	ALAR ^G AG ^T V ^P L
FLT3	GD 7	rs12872889	0,5	N.D	NRF	10	GAG ^T V ^P LL ^V L
FLT3	GD 7	rs12872889	0,5	N.D	NRF	10	LAR ^D AG ^T V ^P L
FLT3	GD 7	rs12872889	0,5	N.D	NRF	10	LAR ^G AG ^T V ^P L
FLT3	GD 7	rs12872889	0,5	N.D	NRF	9	R ^D AG ^T V ^P LL
FLT3	GD 7	rs12872889	0,5	N.D	NRF	9	R ^G AG ^T V ^P LL
FLT3	DD 96	rs7338903	0,08	0,22	ARF	9	SMPQGT ^F FPV
FLT3	DD 96	rs7338903	0,08	0,22	ARF	9	S ^T PQGT ^F FPV
FLT3	DD 96	rs7338903	0,08	0,22	ARF	10	W ^S MPQGT ^F FPV
FLT3	DD 96	rs7338903	0,08	0,22	ARF	10	W ^S T ^P QGT ^F FPV
FLT3	MT 227	rs1933437	0,49	0,41	NRF	9	KVLH ^E L ^F G ^M
FLT3	MT 227	rs1933437	0,49	0,41	NRF	11	KVLH ^E L ^F G ^M D ^I
FLT3	MT 227	rs1933437	0,49	0,41	NRF	9	KVLH ^E L ^F G ^T
FLT3	MT 227	rs1933437	0,49	0,41	NRF	11	KVLH ^E L ^F G ^T D ^I
FLT3	MT 227	rs1933437	0,49	0,41	NRF	10	VLH ^E L ^F G ^M D ^I
FLT3	MT 227	rs1933437	0,49	0,41	NRF	10	VLH ^E L ^F G ^T D ^I
FMNL1	NN 170	rs7209538	N.D.	0,00	ARF	10	MTWRAQ ^T M ^G L
FMNL1	NN 170	rs7209538	N.D.	0,00	ARF	10	MTWRAQ ^T T ^G L
FMNL1	NN 170	rs7209538	N.D.	0,00	ARF	9	RMTWRAQ ^T M
FMNL1	NN 170	rs7209538	N.D.	0,00	ARF	11	RMTWRAQ ^T M ^G L
FMNL1	NN 170	rs7209538	N.D.	0,00	ARF	9	RMTWRAQ ^T T
FMNL1	NN 170	rs7209538	N.D.	0,00	ARF	11	RMTWRAQ ^T T ^G L
FMNL1	SS 336	rs12940312	N.D.	0,13	ARF	10	F ^G G ^E H ^E L ^P C ^L
FMNL1	SS 336	rs12940312	N.D.	0,13	ARF	10	F ^S G ^E H ^E L ^P C ^L
FMNL1	SS 336	rs12940312	N.D.	0,13	ARF	9	G ^T F ^G G ^E H ^E L
FMNL1	SS 336	rs12940312	N.D.	0,13	ARF	9	G ^T F ^S G ^E H ^E L
FMNL1	SS 336	rs12940312	N.D.	0,13	ARF	9	TLWY ^I Q ^W R ^T
FMNL1	SS 336	rs12940312	N.D.	0,13	ARF	9	TLWY ^I R ^W R ^T
FMNL1	RP 511	rs4792898	N.D.	0,38	NRF	9	ILPVA ^V A ^T R
FMNL1	RP 511	rs4792898	N.D.	0,38	ARF	10	QL ^G A ^A V ^M L ^R L
FMNL1	RP 511	rs4792898	N.D.	0,38	ARF	10	QL ^R A ^A V ^M L ^R L
FMNL1	RP 511	rs4792898	N.D.	0,38	ARF	9	SLW ^Q L ^G A ^A V
FMNL1	RP 511	rs4792898	N.D.	0,38	ARF	10	SLW ^Q L ^G A ^A V ^M
FMNL1	RP 511	rs4792898	N.D.	0,38	ARF	11	SLW ^Q L ^G A ^A V ^M L
FMNL1	RP 511	rs4792898	N.D.	0,38	ARF	9	SLW ^Q L ^R A ^A V

FMNL1	RP 511	rs4792898	N.D.	0,38	ARF	10	SLWQLRAAVM
FMNL1	RP 511	rs4792898	N.D.	0,38	ARF	11	SLWQLRAAVML
FMNL1	RP 511	rs4792898	N.D.	0,38	ARF	9	WQLGAAVML
FMNL1	RP 511	rs4792898	N.D.	0,38	ARF	9	WQLRAAVML
FMNL1	EK 667	rs11555736	N.D.	0,00	NRF	11	ELNDEEVLQEL
FMNL1	EK 667	rs11555736	N.D.	0,00	NRF	11	ELNDEKVLQEL
FMNL1	EK 667	rs11555736	N.D.	0,00	NRF	10	LNDEEVLQEL
FMNL1	EK 667	rs11555736	N.D.	0,00	NRF	10	LNDEKVLQEL
FMNL1	EK 667	rs11555736	N.D.	0,00	NRF	11	TVFTELNDEEV
FMNL1	EK 667	rs11555736	N.D.	0,00	NRF	11	TVFTELNDEKV
FBNP1	SS 136	rs17519205	0,15	0,08	ARF	9	LAGSSLNLV
FBNP1	SS 136	rs17519205	0,15	0,08	ARF	9	LAGSSLNPV
FBNP1	SS 136	rs17519205	0,15	0,08	ARF	9	LVKGDNLAI
FBNP1	SS 136	rs17519205	0,15	0,08	ARF	9	NLVKGDNLAI
FBNP1	SS 136	rs17519205	0,15	0,08	ARF	10	NLVKGDNLAI
FBNP1	SS 136	rs17519205	0,15	0,08	ARF	11	NLVKGDNLNAIA
FBNP1	SS 136	rs17519205	0,15	0,08	ARF	10	NLVKGDNLNAI
FBNP1	SS 136	rs17519205	0,15	0,08	ARF	10	RLAGSSLNLV
FBNP1	SS 136	rs17519205	0,15	0,08	ARF	10	RLAGSSLNPV
FBNP1	SS 136	rs17519205	0,15	0,08	ARF	9	RLAGSSLNL
FBNP1	SS 136	rs17519205	0,15	0,08	ARF	11	SRLAGSSLNLV
FBNP1	SS 136	rs17519205	0,15	0,08	ARF	11	SRLAGSSLNPV
FBNP1	SS 136	rs17519205	0,15	0,08	ARF	11	GLLRQSTHRRG
FOSB	SG 33	rs28381241	0,01	N.D.	ARF	11	GLLRQSTHRRG
FOSB	SG 33	rs28381241	0,01	N.D.	ARF	11	GLLRQSTHRRG
FOSB	SG 33	rs28381241	0,01	N.D.	ARF	11	LLRQSTHRRGL
FOSB	SG 33	rs28381241	0,01	N.D.	ARF	11	LLRQSTHRRGL
FOSB	AA 39	rs2282695	0,48	0,27	ARF	11	GLLRQSTHRRG
FOSB	AA 39	rs2282695	0,48	0,27	ARF	11	GLLRQSTHRRR
FOSB	AA 39	rs2282695	0,48	0,27	ARF	11	LLRQSTHRRGL
FOSB	AA 39	rs2282695	0,48	0,27	ARF	11	LLRQSTHRRRL
GATA2	TA 164	rs2335052	0,35	0,15	ARF	10	GLPHYPYNPL
GATA2	TA 164	rs2335052	0,35	0,15	ARF	10	GLPHYPYSSL
GATA2	TA 164	rs2335052	0,35	0,15	ARF	10	NPLWIPPFRL
GATA2	TA 164	rs2335052	0,35	0,15	NRF	11	SLTPTAHSGS
GATA2	TA 164	rs2335052	0,35	0,15	NRF	11	SLTPTATHSGS
GATA2	TA 164	rs2335052	0,35	0,15	NRF	11	SPLWIPPFRL
GATA2	GG 480	rs1126560	N.D.	0,00	NRF	10	GLGNRWTSRT
GATA2	GG 480	rs1126560	N.D.	0,00	NRF	9	VQHGDHRHGL
GATA2	GG 480	rs1126560	N.D.	0,00	NRF	9	VQHGDHRHGV
GATA2	GG 480	rs1126560	N.D.	0,00	NRF	10	AAACPPPLAST
GNA15	IM 187	rs2230330	0,04	0,01	ARF	10	AAAYPPLAST
GNA15	IM 187	rs2230330	0,04	0,01	ARF	10	AAAYPPLAST
GNA15	IM 187	rs2230330	0,04	0,01	ARF	9	AACPPLAST
GNA15	IM 187	rs2230330	0,04	0,01	ARF	9	AAYPPLAST
GNA15	IM 187	rs2230330	0,04	0,01	NRF	9	VLRSPPTT
GNA15	IM 187	rs2230330	0,04	0,01	NRF	11	VLRSPPTTGI
GNA15	IM 187	rs2230330	0,04	0,01	NRF	11	VLRSPMPTTGI
GNA15	LL 232	rs2074865	0,45	0,09	ARF	9	RDRPHLPSL
GNA15	LL 339	rs1637656	0,26	0,21	ARF	10	RTIPTPFQPL
GNA15	LL 339	rs1637656	0,26	0,21	ARF	10	RTIPTPLQPL
GNA15	LL 339	rs1637656	0,26	0,21	ARF	9	TIPTPFQPL
GNA15	LL 339	rs1637656	0,26	0,21	ARF	9	TIPTPLQPL
HSPA6	GV 96	rs428614	N.D.	0,00	ARF	9	FMTSSWGGGA
HSPA6	GV 96	rs428614	N.D.	0,00	ARF	11	FMTSSWGGAPL
HSPA6	GV 96	rs428614	N.D.	0,00	ARF	9	FMTSSWGGGA
HSPA6	GV 96	rs428614	N.D.	0,00	ARF	11	FMTSSWGGAPL
HSPA6	AA 216	rs391145	0,412	N.D.	ARF	9	FSPLLTVSL
HSPA6	AA 216	rs391145	0,412	N.D.	ARF	10	RFSPLTLVSL
HSPA6	AA 216	rs391145	0,412	N.D.	ARF	11	RFSPLTLVSLV
HSPA6	AA 216	rs391145	0,412	N.D.	ARF	11	SMCRFSPLTL
HSPA6	AA 216	rs391145	0,412	N.D.	ARF	11	SMCRFSPLTLV
HSPA6	AA 216	rs391145	0,412	N.D.	ARF	11	SMCRFSPLTPV
HSPA6	LP 276	rs393027	0,42	0,49	NRF	11	LSSTQATLEI
HSPA6	LP 276	rs393027	0,42	0,49	NRF	11	RLSSSTQATL
HSPA6	LP 276	rs393027	0,42	0,49	NRF	11	RTPSSTQATL
HSPA6	LP 276	rs393027	0,42	0,49	NRF	11	TLSSTQATL
HSPA6	LP 276	rs393027	0,42	0,49	NRF	10	TLSSTQATL
HSPA6	KT 297	rs41297718	0,02	0,06	NRF	10	FEQVDFYKSI
HSPA6	KT 297	rs41297718	0,02	0,06	NRF	10	FEQVDFYTSI
HSPA6	KT 297	rs41297718	0,02	0,06	ARF	11	GLLHVHHSCLP
HSPA6	KT 297	rs41297718	0,02	0,06	ARF	11	GLLQVHHSCLP
HSPA6	KT 297	rs41297718	0,02	0,06	ARF	10	LLHVHHSCLP
HSPA6	KT 297	rs41297718	0,02	0,06	ARF	10	LLQVHHSCLP
HSPA6	KT 297	rs41297718	0,02	0,06	ARF	9	LQVHHSCLP
HSPA6	KT 297	rs41297718	0,02	0,06	NRF	9	SLFEGVDFYK
HSPA6	KT 297	rs41297718	0,02	0,06	NRF	10	SLFEGVDFYT
HSPA6	KT 297	rs41297718	0,02	0,06	ARF	9	WTSTRPSLV
HSPA6	KT 297	rs41297718	0,02	0,06	ARF	9	WTSTSPSLV
HSPA6	VG 447	rs450363	0,47	0,00	NRF	11	FIQVYGERAM
HSPA6	VG 447	rs450363	0,47	0,00	NRF	10	FIQVYVERA
HSPA6	VG 447	rs450363	0,47	0,00	NRF	11	FIQVYVERAM
HSPA6	VG 447	rs450363	0,47	0,00	NRF	9	GVFIQVYV
HSPA6	VG 447	rs450363	0,47	0,00	NRF	10	QVYGERAMT
HSPA6	VG 447	rs450363	0,47	0,00	NRF	10	QVYVERAMT
HSPA6	SI 464	rs388218	0,08	N.D.	ARF	9	FELIGIPPA
HSPA6	SI 464	rs388218	0,08	N.D.	ARF	9	FELSGIPPA
HSPA6	SI 464	rs388218	0,08	N.D.	ARF	10	LLGRFELIGI
HSPA6	SI 464	rs388218	0,08	N.D.	ARF	10	LLGRFELSGI
HSPA6	SI 464	rs388218	0,08	N.D.	ARF	11	NLLGRFELIGI
HSPA6	SI 464	rs388218	0,08	N.D.	ARF	11	NLLGRFELSGI

HSPA6	SI 464	rs388218	0,08	N.D.	ARF	9	NLLGRFELI
HSPA6	SI 464	rs388218	0,08	N.D.	NRF	9	SLASLLPHV
HSPA6	SI 464	rs388218	0,08	N.D.	NRF	9	VLNSLASLL
HSPA6	SI 464	rs388218	0,08	N.D.	NRF	9	VLNSVASLL
HSPA6	HR 471	rs41299256	0,06	N.D.	NRF	9	GIPPAPHGV
HSPA6	HR 471	rs41299256	0,06	N.D.	NRF	9	GIPPAPRGV
HSPA6	HR 471	rs41299256	0,06	N.D.	ARF	9	SVASLLPHV
HSPA6	VM 527	rs452004	0,04	N.D.	ARF	10	KIPEEDRRKV
HSPA6	VM 527	rs452004	0,04	N.D.	NRF	9	KMQDKCREV
HSPA6	VM 527	rs452004	0,04	N.D.	NRF	10	KMQDKCREVL
HSPA6	VM 527	rs452004	0,04	N.D.	NRF	9	KVQDKCREV
HSPA6	VM 527	rs452004	0,04	N.D.	NRF	10	KVQDKCREVL
HSPA6	EK 528	rs570189	0,02	N.D.	NRF	11	RMVHEAEQYEA
HSPA6	ED 562	rs753856	0,24	N.D.	NRF	11	SLQEESLRDKI
HSPA6	ED 562	rs753856	0,24	N.D.	NRF	10	SLQEESLRLEK
HSPA6	ED 562	rs753856	0,24	N.D.	NRF	9	SLQEESLRLEKI
HSPA6	ED 562	rs753856	0,24	N.D.	NRF	9	SLRDKIPEE
HSPA6	ED 562	rs753856	0,24	N.D.	NRF	9	SLRDKIPEE
HSPA6	QR 577	rs368844	0,49	0,14	NRF	9	KCQEVLAWL
HSPA6	QR 577	rs368844	0,49	0,14	NRF	9	KCREVLAWL
HSPA6	QR 577	rs368844	0,49	0,14	NRF	9	KMQDKQEV
HSPA6	QR 577	rs368844	0,49	0,14	NRF	10	KMQDKQEVVL
ICAM3	AA 2	rs281414	0,02	0,21	ARF	10	ALCQNGHGT
ICAM3	AA 2	rs281414	0,02	0,21	ARF	11	ALCQNGHHGTI
ICAM3	AA 2	rs281414	0,02	0,21	ARF	10	ALCQNGYHGT
ICAM3	AA 2	rs281414	0,02	0,21	ARF	11	ALCQNGYHGTI
ICAM3	AA 2	rs281414	0,02	0,21	ARF	9	SLSEWLPWY
ICAM3	AA 2	rs281414	0,02	0,21	ARF	10	SLSEWLPWYH
ICAM3	AA 2	rs281414	0,02	0,21	ARF	10	SLSEWLPWYH
ICAM3	VI 63	rs17697947	0,044	0,00	NRF	11	IALETSLSKEL
ICAM3	VI 63	rs17697947	0,044	0,00	NRF	11	VALETSLSKEL
ICAM3	SS 103	rs2304240	0,27	N.D.	ARF	9	LQWLPDNRL
ICAM3	SS 103	rs2304240	0,27	N.D.	ARF	10	LQWLPDNRL
ICAM3	SS 103	rs2304240	0,27	N.D.	ARF	9	LQWLSDNRL
ICAM3	SS 103	rs2304240	0,27	N.D.	ARF	10	LQWLSDNRL
ICAM3	SS 103	rs2304240	0,27	N.D.	ARF	11	SVLQWLPDNRL
ICAM3	SS 103	rs2304240	0,27	N.D.	ARF	11	SVLQWLSDNRL
ICAM3	SS 103	rs2304240	0,27	N.D.	ARF	10	VLQWLPDNRL
ICAM3	SS 103	rs2304240	0,27	N.D.	ARF	10	VLQWLSDNRL
ICAM3	GR 115	rs7258015	0,26	N.D.	NRF	11	GLPERVELAPL
ICAM3	GR 115	rs7258015	0,26	N.D.	NRF	9	GLPERVELA
ICAM3	GR 115	rs7258015	0,26	N.D.	NRF	10	ITVYGLPERV
ICAM3	GR 115	rs7258015	0,26	N.D.	NRF	10	ITVYRLPERV
ICAM3	GR 115	rs7258015	0,26	N.D.	NRF	9	RLPERVELA
ICAM3	GR 115	rs7258015	0,26	N.D.	NRF	11	SLPERVELAPL
ICAM3	GR 115	rs7258015	0,26	N.D.	NRF	9	SSNITVYGL
ICAM3	GR 115	rs7258015	0,26	N.D.	NRF	9	TVYGLPERV
ICAM3	GR 115	rs7258015	0,26	N.D.	NRF	9	TVYRLPERV
ICAM3	GR 115	rs7258015	0,26	N.D.	NRF	9	YGLPERVEL
ICAM3	GR 115	rs7258015	0,26	N.D.	NRF	9	YRLPERVEL
ICAM3	GD 143	rs2304237	0,29	0,00	ARF	9	SPCAAKWRV
ICAM3	GD 143	rs2304237	0,29	0,00	ARF	10	TSPCAAKWRV
ICAM3	ST 525	rs2230399	0,19	0,13	NRF	11	HVREESTYLP
ICAM3	ST 525	rs2230399	0,19	0,13	NRF	11	HVREETTYLP
ICAM3	ST 525	rs2230399	0,19	0,13	ARF	9	TMLGRRAPI
ICAM3	ST 525	rs2230399	0,19	0,13	ARF	9	TMLGRRPPI
IL2RG	EK 109	rs17875899	0,02	0,00	NRF	10	YLFSEITSG
IL2RG	EK 109	rs17875899	0,02	0,00	NRF	10	YLFSEITSG
IQGFAP2	LL 154	rs10036913	0,46	0,44	ARF	9	ILHSRTEFI
IQGFAP2	LL 154	rs10036913	0,46	0,44	ARF	11	ILHSRTEFISV
IQGFAP2	LL 154	rs10036913	0,46	0,44	ARF	9	ILHSRTEFV
IQGFAP2	LL 154	rs10036913	0,46	0,44	ARF	11	ILHSRTEFVSV
IQGFAP2	AA 524	rs2431351	0,5	0,42	ARF	9	FGWMRYSKL
IQGFAP2	AA 524	rs2431351	0,499	0,42	ARF	9	KLSMRPTWT
IQGFAP2	DE 527	rs2431352	0,14	N.D.	NRF	11	EIQQAVDDANV
IQGFAP2	DE 527	rs2431352	0,14	N.D.	NRF	11	EIQQAVDEANV
IQGFAP2	DE 527	rs2431352	0,14	N.D.	NRF	10	IQQAVDDANV
IQGFAP2	DE 527	rs2431352	0,14	N.D.	NRF	10	IQQAVDEANV
IQGFAP2	DE 527	rs2431352	0,14	N.D.	NRF	9	QQAVDDANV
IQGFAP2	DE 527	rs2431352	0,14	N.D.	NRF	9	QQAVDEANV
IQGFAP2	DE 527	rs2431352	0,14	N.D.	NRF	9	QQAVDEANV
IQGFAP2	DD 597	rs2910819	0,5	0,40	ARF	11	CLVMVHGSNST
IQGFAP2	DD 597	rs2910819	0,5	0,40	ARF	11	CLVTVHGSNST
IQGFAP2	DD 597	rs2910819	0,5	0,40	ARF	10	LVMVHGSNST
IQGFAP2	DD 597	rs2910819	0,5	0,40	ARF	9	VMVHGSNST
IQGFAP2	FL 629	rs2455230	0,5	0,40	NRF	9	SCFYKESWL
IQGFAP2	FL 629	rs2455230	0,5	0,40	NRF	9	SCLYKESWL
IQGFAP2	VI 724	rs2431363	0,48	0,42	NRF	9	FIDNTDSIV
IQGFAP2	VI 724	rs2431363	0,48	0,42	NRF	11	FIDNTDSIVKI
IQGFAP2	VI 724	rs2431363	0,48	0,42	NRF	9	FIDNTDSVV
IQGFAP2	VI 724	rs2431363	0,48	0,42	NRF	11	FIDNTDSVVKI
IQGFAP2	VI 724	rs2431363	0,48	0,42	NRF	11	SIVKIQSWFRM
IQGFAP2	VI 724	rs2431363	0,48	0,42	NRF	11	SVVKIQSWFRM
IQGFAP2	WR 1379	rs17681908	0,04	0,00	NRF	9	KIQRNRLT
IQGFAP2	WR 1379	rs17681908	0,04	0,00	NRF	9	KIQRNRLWT
IQGFAP2	WR 1379	rs17681908	0,04	0,00	NRF	11	NLRTLQGTGHV
IQGFAP2	WR 1379	rs17681908	0,04	0,00	NRF	9	NLWTLQGTGHV
IQGFAP2	WR 1379	rs17681908	0,04	0,00	NRF	11	RTLQGTGHV

IQGAP2	WR 1379	rs17681908	0,04	0,00	NRF	9	WTLEQTGHV
ITGAL	RT 791	rs2230433	0,49	0,22	NRF	11	RAIRLRTAFASL
ITGAL	RT 791	rs2230433	0,49	0,22	NRF	11	TALRLRTAFASL
ITGAL	PP 1152	rs11574950	0,05	N.D.	ARF	9	HLGKRLGIL
ITGAM	RH 77	rs1143679	0,08	0,15	NRF	9	HLQVPVEAV
ITGAM	RH 77	rs1143679	0,08	0,15	NRF	11	HLQVPVEAVNM
ITGAM	RH 77	rs1143679	0,08	0,15	NRF	10	IHLQVPVEAV
ITGAM	RH 77	rs1143679	0,08	0,15	NRF	10	IRLQVPVEAV
ITGAM	RH 77	rs1143679	0,08	0,15	NRF	9	RLQVPVEAV
ITGAM	RH 77	rs1143679	0,08	0,15	NRF	11	RLQVPVEAVNM
ITGAM	RS 343	rs3087444	0,02	0,00	ARF	11	EVAAPLSMRCL
ITGAM	RS 343	rs3087444	0,02	0,00	ARF	11	RVLRQEVAAPL
ITGAM	RS 343	rs3087444	0,02	0,00	ARF	11	RVLRQEV EAPL
ITGAM	RS 343	rs3087444	0,02	0,00	ARF	10	VAAPLSMRCL
ITGAM	RS 343	rs3087444	0,02	0,00	ARF	10	VAAPLSMRCL
ITGAM	RS 343	rs3087444	0,02	0,00	ARF	10	VLRQEVAAPL
ITGAM	RS 343	rs3087444	0,02	0,00	ARF	10	VLRQEV EAPL
ITGAM	MT 441	rs11861251	0,2	0,16	NRF	9	AMFRONTGM
ITGAM	MT 441	rs11861251	0,2	0,16	NRF	9	AMFRONTGT
ITGAM	MT 441	rs11861251	0,2	0,16	NRF	9	GMWESNANV
ITGAM	MT 441	rs11861251	0,2	0,16	NRF	9	GMWESNANV
ITGAM	SP 1146	rs1143678	0,42	0,17	NRF	10	MMSEGGPPGA
ITGAM	SP 1146	rs1143678	0,42	0,17	NRF	10	MMSEGGSPGA
ITGB2	GG 273	rs2230528	0,25	N.D.	ARF	10	SISRATESWA
ITGB2	GG 273	rs2230528	0,25	N.D.	ARF	10	SISRATG SWA
ITGB2	VV 367	rs2230529	0,23	0,23	ARF	11	TINSPPGSSWI
ITGB2	VV 367	rs2230529	0,23	0,23	ARF	11	TINSPPGY SWI
ITGB2	WR 586	rs5030672	N.D.	0,01	NRF	10	TEGCLNPWRV
KCNAB2	EK 88	rs2229003	0,5	N.D.	ARF	10	GINLFDTAEV
KCNAB2	EK 88	rs2229003	0,5	N.D.	ARF	10	GINLFDTAKV
KCNAB2	EK 88	rs2229003	0,5	N.D.	ARF	9	INLFDTAEV
KCNAB2	EK 88	rs2229003	0,5	N.D.	ARF	9	INLFDTAKV
KCNAB2	EK 88	rs2229003	0,5	N.D.	ARF	10	KVYAAGKAEV
KCNAB2	EK 88	rs2229003	0,5	N.D.	ARF	10	NLFDTAEVYA
KCNAB2	EK 88	rs2229003	0,5	N.D.	ARF	11	NLFDTAEVYAA
KCNAB2	EK 88	rs2229003	0,5	N.D.	ARF	10	NLFDTAKVYA
KCNAB2	EK 88	rs2229003	0,5	N.D.	ARF	11	NLFDTAKVYAA
KCNAB2	AA 92	rs2229004	0,14	0,00	ARF	9	QLARLKWYW
KCNAB2	AA 92	rs2229004	0,14	0,00	ARF	11	SIQOKSTQLAR
KCNAB2	AA 92	rs2229004	0,14	0,00	ARF	9	SIQOKSTQL
KCNAB2	AA 92	rs2229004	0,14	0,00	ARF	11	SSIQOKSTQLA
KCNAB2	GG 122	rs2229005	0,05	0,00	ARF	10	LLGRKGGDGA
KCNAB2	GG 122	rs2229005	0,05	0,00	ARF	10	LLGWKGGDGA
KCNAB2	SS 344	rs2229002	0,49	0,35	ARF	9	HLP LSTRLI
KCNAB2	SS 344	rs2229002	0,49	0,35	ARF	10	HLP LSTRLIV
KCNAB2	SS 344	rs2229002	0,49	0,35	ARF	9	RLP LSTRLI
KCNAB2	SS 344	rs2229002	0,49	0,35	ARF	10	RLP LSTRLIV
LCP2	QQ 326	rs315717	0,49	0,48	ARF	10	MMKMMCKIDL
LCP2	QQ 326	rs315717	0,49	0,48	ARF	10	MMKMMCKIDL
LRMP	GE 25	rs1129442	N.D.	0,00	NRF	10	LLQSR EYSSL
LRMP	GE 25	rs1129442	N.D.	0,00	NRF	10	LLQSRGYSSL
LRMP	GE 25	rs1129442	N.D.	0,00	NRF	9	LQSR EYSSL
LRMP	GE 25	rs1129442	N.D.	0,00	NRF	9	LQSRGYSSL
LRMP	GE 25	rs1129442	N.D.	0,00	NRF	11	SLQSR EYSSL
LRMP	GE 25	rs1129442	N.D.	0,00	NRF	11	SLQSRGYSSL
LRMP	SC 197	rs1908946	0,5	N.D.	NRF	9	NCLKLLESL
LRMP	SC 197	rs1908946	0,5	N.D.	NRF	10	NLKEITNCL
LRMP	SC 197	rs1908946	0,5	N.D.	NRF	10	NLKEITNSL
LRMP	SC 197	rs1908946	0,5	N.D.	NRF	9	NCLKLLESL
LRMP	SC 197	rs1908946	0,5	N.D.	NRF	11	SLK LLES LTP I
LRMP	FS 322	rs1129443	N.D.	0,00	NRF	9	FLPRNIGNA
LRMP	FS 322	rs1129443	N.D.	0,00	NRF	11	FLPRNIGNAGM
LRMP	FS 322	rs1129443	N.D.	0,00	NRF	9	LRRVTIASL
LRMP	FS 322	rs1129443	N.D.	0,00	NRF	11	SSLRRVTIAFL
LRMP	FS 322	rs1129443	N.D.	0,00	NRF	11	SSLRRVTIASL
LRMP	FS 322	rs1129443	N.D.	0,00	NRF	9	SLPRNIGNA
LRMP	FS 322	rs1129443	N.D.	0,00	NRF	11	SLPRNIGNAGM
LRMP	FS 322	rs1129443	N.D.	0,00	NRF	10	SLRRVTIAFL
LRMP	FS 322	rs1129443	N.D.	0,00	NRF	10	SLRRVTIASL
LRMP	FS 322	rs1129443	N.D.	0,00	NRF	9	TIASLPRNI
LTB	GA 69	rs4647186	0,01	0,04	NRF	9	DLRPLPAA
LTB	GA 69	rs4647186	0,01	0,04	ARF	10	KQISAPGSQL
LTB	GA 69	rs4647186	0,01	0,04	ARF	10	KQISGPGSQL
LTB	GA 69	rs4647186	0,01	0,04	ARF	9	QISAPGSQL
LTB	GA 69	rs4647186	0,01	0,04	ARF	9	QISGPGSQL
LTB	RS 84	rs4647186	0,01	0,04	NRF	9	DLSPLPAA
LTB	TT 117	rs2229698	0,4	0,00	ARF	9	GVSDERDAV
LTB	TT 117	rs2229698	0,4	0,00	ARF	10	GVSDERDAVL
LTB	TT 117	rs2229698	0,4	0,00	ARF	9	GVSDERDSV
LTB	TT 117	rs2229698	0,4	0,00	ARF	10	GVSDERDSVL
LTB	DA 122	rs2229699	0,17	N.D.	NRF	11	FLTSGTQFSDA
LTB	DA 122	rs2229699	0,17	N.D.	NRF	9	TQFSDA EGL
LTB	DA 122	rs2229699	0,17	N.D.	NRF	9	TQFSDDEGL
LTB	FF 231	rs4248165	0,01	0,01	ARF	9	GLCEREDLL
LTB	FF 231	rs4248165	0,01	0,01	ARF	9	GLCEREDLL
LTB	FF 231	rs4248165	0,01	0,01	ARF	9	SVTPIWWT L
LTB	FF 231	rs4248165	0,01	0,01	ARF	9	TLREGRPSL
LTB	FF 231	rs4248165	0,01	0,01	ARF	10	WTLREGRPSL
LYN	KK 233	rs2227980	0,22	0,03	ARF	10	VLPVSHRSHGI

LYN	KK 233	rs2227980	0.22	0.03	ARF	11	VLVPSHRSHGI
LYN	II 358	rs7001291	N.D.	0.00	ARF	9	RLQREWHTL
LYN	II 358	rs7001291	N.D.	0.00	ARF	9	TLSGRTTFT
LYN	II 379	rs1050875	N.D.	0.00	ARF	11	LMFWSPSHSCA
LYN	II 379	rs1050875	N.D.	0.00	ARF	10	SCAKLQILAL
MAP4K1	MT 204	rs17847696	N.D.	0.00	NRF	10	DIWSLGI MAI
MAP4K1	MT 204	rs17847696	N.D.	0.00	NRF	10	DIWSLGI TAI
MAP4K1	MT 204	rs17847696	N.D.	0.00	NRF	10	GIMAIELAEI
MAP4K1	MT 204	rs17847696	N.D.	0.00	NRF	10	GITAIELAEI
MAP4K1	MT 204	rs17847696	N.D.	0.00	NRF	9	IMAIELAEI
MAP4K1	MT 204	rs17847696	N.D.	0.00	NRF	9	ITAIELAEI
MAP4K1	MT 204	rs17847696	N.D.	0.00	NRF	9	SLGIMAIEL
MAP4K1	MT 204	rs17847696	N.D.	0.00	NRF	10	SLGIMAIELA
MAP4K1	MT 204	rs17847696	N.D.	0.00	NRF	9	SLGTAIEL
MAP4K1	MT 204	rs17847696	N.D.	0.00	NRF	10	SLGTAIELA
MCM5	ST 180	rs2307340	0.08	0.17	ARF	11	AAAAATPSATL
MCM5	ST 180	rs2307340	0.08	0.17	ARF	10	AAAAATPSATL
MCM5	ST 180	rs2307340	0.08	0.17	ARF	10	AAAAATPSPTL
MCM5	ST 180	rs2307340	0.08	0.17	ARF	9	AAAAATPSATL
MCM5	ST 180	rs2307340	0.08	0.17	ARF	9	AAAAATPSPTL
MCM5	ST 180	rs2307340	0.08	0.17	NRF	10	LTNIAMRPGI
MCM5	ST 180	rs2307340	0.08	0.17	NRF	11	TLSNIAMRPGI
MCM5	ST 180	rs2307340	0.08	0.17	NRF	11	TLNIAMRPGI
MCM5	LL 188	rs2230932	0.04	N.D.	ARF	10	TLPCALALRA
MCM5	LL 188	rs2230932	0.04	N.D.	ARF	10	TLPCALASRA
MCM5	VI 258	rs2230933	0.03	0.00	NRF	10	KVIPGNRVTI
MCM5	VI 258	rs2230933	0.03	0.00	NRF	10	KVVPGNRVTI
MCM5	VI 258	rs2230933	0.03	0.00	NRF	9	VIPGNRVTI
MCM5	VI 258	rs2230933	0.03	0.00	NRF	9	VVPGNRVTI
MCM5	VI 258	rs2230933	0.03	0.00	NRF	9	YLCDKVI PG
MCM5	VI 258	rs2230933	0.03	0.00	NRF	10	YLCDKVI PG
MCM5	VI 258	rs2230933	0.03	0.00	NRF	9	YLCDKVVPG
MCM5	VI 258	rs2230933	0.03	0.00	NRF	10	YLCDKVVPG
MCM5	KK 569	rs133427	0.19	N.D.	ARF	10	LLPSE MWPPA
MCM5	KK 569	rs133427	0.19	N.D.	ARF	11	LLPSE MWPPA
MCM5	KK 569	rs133427	0.19	N.D.	ARF	10	LLPSE VWPPA
MCM5	KK 569	rs133427	0.19	N.D.	ARF	11	LLPSE VWPPA
MPL	KN 39	rs17292650	0.04	0.00	ARF	9	GIRLRAPEL
MPL	KN 39	rs17292650	0.04	0.00	ARF	9	GIRLRAPEV
MPL	KN 39	rs17292650	0.04	0.00	ARF	9	RLRAPELFL
MPL	KN 39	rs17292650	0.04	0.00	ARF	9	RLRAPEVFL
MPL	KN 39	rs17292650	0.04	0.00	NRF	11	SLLASDSEPLK
MPL	KN 39	rs17292650	0.04	0.00	NRF	11	SLLASDSEPLN
MPL	PP 70	rs6086	N.D.	0.00	ARF	10	CMPT HGRSPV
MPL	PP 70	rs6086	N.D.	0.00	ARF	10	CMPT RGRSPV
MPL	PP 70	rs6086	N.D.	0.00	ARF	10	CLP TGEAPCL
MPL	VM 114	rs12731981	0.03	0.03	NRF	10	FLHLWVKNV
MPL	VM 114	rs12731981	0.03	0.03	NRF	9	HLWVKNMFL
MPL	VM 114	rs12731981	0.03	0.03	NRF	9	HLWVKNVFL
MPL	VM 114	rs12731981	0.03	0.03	NRF	9	NMFLNQTRT
MPL	VM 114	rs12731981	0.03	0.03	NRF	9	PLHLWVKNV
MPL	VM 114	rs12731981	0.03	0.03	ARF	10	SAAPLGEECV
MPL	VM 114	rs12731981	0.03	0.03	ARF	10	SAAPLGEELYV
MPL	EE 230	rs16830693	0.13	0.01	ARF	9	SRPPQVEKL
MPL	TP 275	rs28928908	N.D.	0.00	NRF	10	GSWGSWSL PV
MPL	TP 275	rs28928908	N.D.	0.00	NRF	10	GSWGSWSL TV
MPL	TP 275	rs28928908	N.D.	0.00	ARF	9	GSWSL TVTV
MPL	TP 275	rs28928908	N.D.	0.00	ARF	9	WLLGILVPH
N4BP2L1	IL 141	rs1062947	N.D.	0.00	NRF	9	ALENNYEVI
N4BP2L1	IL 141	rs1062947	N.D.	0.00	NRF	9	ALENNYEVL
N4BP2L1	IL 141	rs1062947	N.D.	0.00	NRF	11	VMALENNYEVI
N4BP2L1	IL 141	rs1062947	N.D.	0.00	NRF	11	VMALENNYEVL
NCF4	SS 23	rs10854695	0.23	0.01	ARF	10	MMLPS QPTLL
NCF4	SS 23	rs10854695	0.23	0.01	ARF	11	MMLPS QPTLLT
NCF4	SS 23	rs10854695	0.23	0.01	ARF	10	MMLPS RPTLL
NCF4	SS 23	rs10854695	0.23	0.01	ARF	11	MMLPS RPTLLT
NCF4	SS 23	rs10854695	0.23	0.01	ARF	9	MLPS QPTLL
NCF4	SS 23	rs10854695	0.23	0.01	ARF	10	MLPS QPTLLT
NCF4	SS 23	rs10854695	0.23	0.01	ARF	9	MLPS RPTLL
NCF4	SS 23	rs10854695	0.23	0.01	ARF	10	MLPS RPTLLT
NCF4	SS 23	rs10854695	0.23	0.01	ARF	9	MMLPS QPTL
NCF4	SS 23	rs10854695	0.23	0.01	ARF	9	MMLPS RPTL
NCF4	SS 23	rs10854695	0.23	0.01	ARF	10	RMMLPS QPTL
NCF4	SS 23	rs10854695	0.23	0.01	ARF	10	RMMLPS RPTL
NCF4	SN 118	rs9610595	N.D.	0.00	NRF	11	AYMKSLLNLPV
NCF4	SN 118	rs9610595	N.D.	0.00	NRF	9	AYMKSLLSL
NCF4	SN 118	rs9610595	N.D.	0.00	NRF	11	AYMKSLLSLPV
NCF4	SN 118	rs9610595	N.D.	0.00	NRF	9	LNLNPVWVL
NCF4	SN 118	rs9610595	N.D.	0.00	NRF	10	LNLNPVWVLM
NCF4	SN 118	rs9610595	N.D.	0.00	NRF	9	LLSLNPVWVL
NCF4	SN 118	rs9610595	N.D.	0.00	NRF	10	LLSLNPVWVLM
NCF4	SN 118	rs9610595	N.D.	0.00	NRF	10	NAYMKSLLNL
NCF4	SN 118	rs9610595	N.D.	0.00	NRF	10	NAYMKSLLSL
NCF4	SN 118	rs9610595	N.D.	0.00	NRF	10	SLLNLPVWVL
NCF4	SN 118	rs9610595	N.D.	0.00	NRF	11	SLLNLPVWVLM
NCF4	SN 118	rs9610595	N.D.	0.00	NRF	10	SLLSLPVWVL
NCF4	SN 118	rs9610595	N.D.	0.00	NRF	11	SLLSLPVWVLM

NCF4	SN 118	rs9610595	N.D.	0,00	NRF	9	SLLNLPVWV
NCF4	SN 118	rs9610595	N.D.	0,00	NRF	9	SLLSLPVWV
NCF4	SN 118	rs9610595	N.D.	0,00	NRF	10	VSLLNLPVWV
NCF4	SN 118	rs9610595	N.D.	0,00	NRF	10	VSLSLPVWV
NCF4	SN 118	rs9610595	N.D.	0,00	NRF	10	YMKSLNLPV
NCF4	SN 118	rs9610595	N.D.	0,00	NRF	10	YMKSLSLPV
NCF4	SS 299	rs11552115	0,26	N.D.	ARF	9	GIWFGCCQM
NCF4	SS 299	rs11552115	0,26	N.D.	ARF	9	GIWFGCCRM
NCF4	EA 304	rs5995361	N.D.	0,00	NRF	10	ALMVRQARGL
NCF4	EA 304	rs5995361	N.D.	0,00	NRF	10	ELMVRQARGL
NCF4	EA 304	rs5995361	N.D.	0,00	NRF	9	LLSDEDVAL
NCF4	EA 304	rs5995361	N.D.	0,00	NRF	10	LLSDEDVALM
NCF4	EA 304	rs5995361	N.D.	0,00	NRF	11	LLSDEDVALMV
NCF4	EA 304	rs5995361	N.D.	0,00	NRF	9	LLSDEDVEL
NCF4	EA 304	rs5995361	N.D.	0,00	NRF	10	LLSDEDVELM
NCF4	EA 304	rs5995361	N.D.	0,00	NRF	11	LLSDEDVELMV
NCF4	EA 304	rs5995361	N.D.	0,00	NRF	10	RLLSDEDVAL
NCF4	EA 304	rs5995361	N.D.	0,00	NRF	11	RLLSDEDVALM
NCF4	EA 304	rs5995361	N.D.	0,00	NRF	10	RLLSDEDVEL
NCF4	EA 304	rs5995361	N.D.	0,00	NRF	11	RLLSDEDVELM
NCF4	FF 320	rs1858	0,11	N.D.	ARF	9	PLPEAPLPL
NCF4	FF 320	rs1858	0,11	N.D.	ARF	9	PLPEAPL
NCF4	TT 337	rs28669668	0,09	0,00	ARF	9	QLQGLQHD
NCF4	TT 337	rs28669668	0,09	0,00	ARF	9	QLQGLQHN
NCF4	TT 337	rs28669668	0,09	0,00	ARF	9	QCHELTVSL
NCF4	TT 337	rs28669668	0,09	0,00	ARF	9	RCHELTVSL
NUP210	VA 755	rs6795271	0,31	0,38	ARF	10	CLSTPAPSWT
NUP210	VA 755	rs6795271	0,31	0,38	NRF	10	LVPVYTSPL
NUP210	VA 755	rs6795271	0,31	0,38	ARF	10	RLSTPAPSWT
NUP210	VA 755	rs6795271	0,31	0,38	NRF	11	TLPVYTSPL
NUP210	VA 755	rs6795271	0,31	0,38	NRF	11	TLVPVYTSPL
NUP210	LR 786	rs2280084	0,47	0,39	ARF	11	ATATPCWTWLL
NUP210	LR 786	rs2280084	0,47	0,39	ARF	11	ATATPGWTWLL
NUP210	LR 786	rs2280084	0,47	0,39	ARF	9	ATPCWTWLL
NUP210	LR 786	rs2280084	0,47	0,39	ARF	9	ATPGWTWLL
NUP210	AP 821	rs2280085	0,36	0,16	NRF	10	IEALPMQLV
NUP210	AP 821	rs2280085	0,36	0,16	NRF	10	IEALPMQLV
NUP210	AP 821	rs2280085	0,36	0,16	NRF	10	IEPELPMQLV
NUP210	AP 821	rs2280085	0,36	0,16	NRF	10	IEPELPMQLV
NUP210	AP 821	rs2280085	0,36	0,16	NRF	10	SIEALPMQL
NUP210	AP 821	rs2280085	0,36	0,16	NRF	10	SIEPELPMQL
NUP210	AP 821	rs2280085	0,36	0,16	NRF	11	VLASIEALPM
NUP210	AP 821	rs2280085	0,36	0,16	NRF	11	VLASIEPELPM
NUP210	AP 821	rs2280085	0,36	0,16	NRF	9	VLASIEAL
NUP210	AP 821	rs2280085	0,36	0,16	NRF	9	VLASIEPEL
NUP210	PL 966	rs2271503	N.D.	0,00	NRF	10	CLVFLAPAKA
NUP210	PL 966	rs2271503	N.D.	0,00	NRF	10	CLVFPAPAKA
NUP210	PL 966	rs2271503	N.D.	0,00	NRF	11	CLVFPAPAKAV
NUP210	PL 966	rs2271503	N.D.	0,00	NRF	9	DCLVFLAPA
NUP210	PL 966	rs2271503	N.D.	0,00	NRF	9	FLAPAKAVV
NUP210	PL 966	rs2271503	N.D.	0,00	NRF	11	FLAPAKAVVYV
NUP210	PL 966	rs2271503	N.D.	0,00	NRF	11	IMHDLCLVFL
NUP210	PL 966	rs2271503	N.D.	0,00	NRF	10	LVFLAPAKAV
NUP210	PL 966	rs2271503	N.D.	0,00	NRF	11	LVFLAPAKAVV
NUP210	PL 966	rs2271503	N.D.	0,00	NRF	10	LVFPAPAKAV
NUP210	PL 966	rs2271503	N.D.	0,00	NRF	11	LVFPAPAKAVV
NUP210	PL 966	rs2271503	N.D.	0,00	NRF	10	LAPAKAVVYV
NUP210	PL 966	rs2271503	N.D.	0,00	NRF	11	MHDLCLVFLA
NUP210	PL 966	rs2271503	N.D.	0,00	NRF	10	MHDLCLVFL
NUP210	FF 1016	rs2271504	0,47	0,39	NRF	9	ILPLHGPEA
NUP210	FF 1016	rs2271504	0,47	0,39	NRF	9	ILPLYGPEA
NUP210	FF 1016	rs2271504	0,47	0,39	ARF	11	PLHGPEAPSSL
NUP210	FF 1016	rs2271504	0,47	0,39	ARF	11	PLYGPEAPSSL
NUP210	FF 1016	rs2271504	0,47	0,39	NRF	10	QILPLHGPEA
NUP210	FF 1016	rs2271504	0,47	0,39	NRF	10	QILPLYGPEA
NUP210	FF 1016	rs2271504	0,47	0,39	ARF	10	SLPNTSPLWT
NUP210	FF 1016	rs2271504	0,47	0,39	ARF	10	SLPNTSPSWT
NUP210	IM 1096	rs2271505	0,01	0,00	NRF	9	LLIGATIQT
NUP210	IM 1096	rs2271505	0,01	0,00	NRF	10	LLIGATIQVT
NUP210	IM 1096	rs2271505	0,01	0,00	NRF	11	LLIGATIQVTS
NUP210	IM 1096	rs2271505	0,01	0,00	NRF	9	LLIGATMQV
NUP210	IM 1096	rs2271505	0,01	0,00	NRF	10	LLIGATMQVT
NUP210	IM 1096	rs2271505	0,01	0,00	NRF	11	LLIGATMQVTS
NUP210	IM 1096	rs2271505	0,01	0,00	NRF	10	TLLIGATIQT
NUP210	IM 1096	rs2271505	0,01	0,00	NRF	11	TLLIGATIQVT
NUP210	IM 1096	rs2271505	0,01	0,00	NRF	10	TLLIGATMQV
NUP210	IM 1096	rs2271505	0,01	0,00	NRF	11	TLLIGATMQVT
NUP210	IM 1096	rs2271505	0,01	0,00	NRF	9	VTLLIGATI
NUP210	IM 1096	rs2271505	0,01	0,00	NRF	11	VTLLIGATIQT
NUP210	IM 1096	rs2271505	0,01	0,00	NRF	11	VTLLIGATMQV
NUP210	CC 1444	rs2271509	0,5	0,46	ARF	9	ALSAQSAWA
NUP210	CC 1444	rs2271509	0,5	0,46	ARF	9	RAPPTTPVL
NUP210	CC 1444	rs2271509	0,5	0,46	ARF	9	RAPPTPAL
NUP210	CC 1444	rs2271509	0,5	0,46	ARF	9	VLSAQSAWA
NUP210	SL 1752	rs354479	0,19	N.D.	NRF	9	FITYTVGVV
NUP210	SL 1752	rs354479	0,19	N.D.	NRF	9	YTVGVLDPA
NUP210	MV 1787	rs354478	0,5	0,46	NRF	10	AIPTVYAFVV
NUP210	MV 1787	rs354478	0,05	0,46	ARF	10	LLWVIAVGPV

PIK3CD	TT 226	rs2230735	0.04	0.00	ARF	11	GLCPAEEGHGV
PIK3CD	TT 226	rs2230735	0.04	0.00	ARF	11	GLCPAEEGH ^S V
PIK3CD	AA 345	rs28730672	N.D.	0.00	ARF	10	WAFPRQRDAV
PIK3CD	CR 437	rs28730673	N.D.	0.01	NRF	9	KTGE ^C CLYM
PIK3CD	CR 437	rs28730673	N.D.	0.01	NRF	9	KTGE ^R CLYM
PIK3CD	CR 437	rs28730673	N.D.	0.01	NRF	9	QLKTGE ^C CL
PIK3CD	CR 437	rs28730673	N.D.	0.01	NRF	9	QLKTGE ^R CL
PIK3CD	YY 936	rs11121484	0.4	0.06	ARF	11	SVSHSSSP ^M TTL
PIK3CD	YY 936	rs11121484	0.4	0.06	ARF	11	SVSHSSSP ^T TTL
PLCB2	TT 477	rs2229691	0.46	0.23	ARF	9	APPPV ^R IL
PLCB2	TT 477	rs2229691	0.46	0.23	ARF	11	FLAPPPV ^R IL
PLCB2	TT 477	rs2229691	0.46	0.23	ARF	9	ILVGR ^L RAA
PLCB2	TT 477	rs2229691	0.46	0.23	ARF	10	ILVGR ^L RAAA
PLCB2	TT 477	rs2229691	0.46	0.23	ARF	10	LAPPPV ^R IL
PLCB2	TT 477	rs2229691	0.46	0.23	ARF	10	RILVGR ^L RAA
PLEK	NK 97	rs3816281	0.5	0.29	NRF	9	D ^I KKA ^I KCI
PLEK	NK 97	rs3816281	0.5	0.29	NRF	9	D ^I NKA ^I KCI
PLEK	NK 97	rs3816281	0.5	0.29	ARF	10	G ^I S ^I R ^P L ^N AL
PLEK	NK 97	rs3816281	0.5	0.29	ARF	10	G ^I S ^R R ^P L ^N AL
PRKCB1	RR 238	rs17847891	N.D.	0.00	ARF	9	RIGQR ^R QTV
PRKCB1	RR 238	rs17847891	N.D.	0.00	ARF	9	RIGQR ^K TV
PRKCB1	II 508	rs17847876	N.D.	0.00	ARF	10	RLH ^C PRDN ^C L
PRKCB1	II 508	rs17847876	N.D.	0.00	ARF	10	RLH ^R PRDN ^C L
PRKCB1	PS 563	rs17847879	N.D.	0.00	NRF	9	PMSKEA ^V AI
PRKCB1	PS 563	rs17847879	N.D.	0.00	NRF	9	SMSKEA ^V AI
PSD4	PP 58	rs3738908	0.02	0.50	ARF	10	LLN ^Q PD ^K M ^F L
PSD4	PP 58	rs3738908	0.02	0.50	ARF	10	LLN ^L PD ^K M ^F L
PSD4	PP 58	rs3738908	0.02	0.50	ARF	9	LLN ^L PD ^K M ^F L
PSD4	PP 58	rs3738908	0.02	0.50	ARF	11	NL ^L PD ^K M ^F L ^P GA
PSD4	PP 58	rs3738908	0.02	0.50	ARF	9	TLLN ^L PD ^K M
PSD4	PP 58	rs3738908	0.02	0.50	ARF	11	TLLN ^L PD ^K M ^F L
PSD4	PP 58	rs3738908	0.02	0.50	ARF	9	TLLN ^Q PD ^K M
PSD4	PP 58	rs3738908	0.02	0.50	ARF	11	TLLN ^Q PD ^K M ^F L
PSD4	DE 124	rs17857060	N.D.	0.00	ARF	10	QA ^A EHSIT ^R V
PSD4	DE 124	rs17857060	N.D.	0.00	ARF	10	SQA ^E HSIT ^R V
PSD4	SS 216	rs3748914	0.49	N.D	ARF	10	KTQ ^G KTAA ^S L
PSD4	SS 216	rs3748914	0.49	N.D	ARF	10	KTQ ^G KTAV ^S L
PSD4	AG 269	rs4849167	0.49	0.37	NRF	9	AAS ^D SHAG ^V
PSD4	AG 269	rs4849167	0.49	0.37	ARF	10	GLQ ^T PMQV ^G L
PSD4	AG 269	rs4849167	0.49	0.37	NRF	9	GAS ^D SHAG ^V
PSD4	AG 269	rs4849167	0.49	0.37	ARF	10	LLES ^A FP ^G RL
PSD4	AG 269	rs4849167	0.49	0.37	ARF	10	LLES ^A FP ^G RL
PSD4	AG 269	rs4849167	0.752	0.37	ARF	10	RLQ ^T PMQV ^G L
PSD4	AG 269	rs4849167	0.49	0.37	NRF	11	SW ^A AS ^D SHAG ^V
PSD4	AG 269	rs4849167	0.49	0.37	ARF	11	VLL ^E S ^A FP ^G RL
PSD4	AG 269	rs4849167	0.49	0.37	ARF	11	VLL ^E S ^A FP ^G RL
PSD4	AG 269	rs4849167	0.49	0.37	NRF	10	W ^A AS ^D SHAG ^V
PSD4	GG 422	rs2241976	0.49	0.38	ARF	9	W ^A PP ^G IS ^L
PSD4	GG 422	rs2241976	0.49	0.38	ARF	9	W ^T PP ^G IS ^L
PSMB8	ST 70	rs17220206	0.06	N.D	NRF	9	EMA ^H GT ^S T ^L
PSMB8	ST 70	rs17220206	0.06	N.D	NRF	9	EMA ^H GT ^T T ^L
PSMB8	ST 70	rs17220206	0.06	N.D	NRF	11	QIEMA ^H GT ^S T ^L
PSMB8	ST 70	rs17220206	0.06	N.D	NRF	11	QIEMA ^H GT ^T T ^L
PSMB8	ST 70	rs17220206	0.06	N.D	NRF	11	STLAF ^K FQ ^H GV
PSMB8	ST 70	rs17220206	0.06	N.D	NRF	11	TTLAF ^K FQ ^H GV
PSMB8	LL 163	rs11540143	N.D.	0.00	ARF	10	PLY ^G QYD ^L LV
PSMB10	LL 107	rs20549	0.42	0.32	ARF	9	GVQ ^D GAT ^R V
PSMB10	GG 151	rs14178	0.23	0.04	ARF	10	AAL ^R CASP ^W L
PSMB10	GG 151	rs14178	0.23	0.04	ARF	10	AAL ^R RASP ^W L
PSMB10	GG 151	rs14178	0.23	0.04	ARF	9	AL ^R CASP ^W L
PSMB10	GG 151	rs14178	0.23	0.04	ARF	10	AL ^R CASP ^W L ^L
PSMB10	GG 151	rs14178	0.23	0.04	ARF	9	AL ^R RASP ^W L
PSMB10	GG 151	rs14178	0.23	0.04	ARF	10	AL ^R RASP ^W L ^L
PTPN22	RR 620	rs2476601	0.25	0.00	NRF	11	PV ^R T ^P ES ^F IV ^V
PTPN22	RR 620	rs2476601	0.25	0.00	NRF	11	PV ^W T ^P ES ^F IV ^V
PTPN22	RR 620	rs2476601	0.25	0.00	NRF	9	RT ^P ES ^F IV ^V
PTPN22	RR 620	rs2476601	0.25	0.00	NRF	9	WT ^P ES ^F IV ^V
PTPN6	PL 28	rs11547853	N.D.	0.00	ARF	10	RL ^G PV ^A RT ^R V
PTPN6	PL 28	rs11547853	N.D.	0.00	ARF	11	SR ^L GPV ^A RT ^R V
PTPN6	PL 28	rs11547853	N.D.	0.00	ARF	11	SW ^L GPV ^A RT ^R V
PTPN6	PL 28	rs11547853	N.D.	0.00	ARF	10	STV ^A S ^R LG ^P V
PTPN6	PL 28	rs11547853	N.D.	0.00	ARF	10	STV ^A S ^W LG ^P V
PTPN6	PL 28	rs11547853	N.D.	0.00	ARF	9	TV ^A S ^R LG ^P V
PTPN6	PL 28	rs11547853	N.D.	0.00	ARF	9	TV ^A S ^W LG ^P V
PTPN6	PL 28	rs11547853	N.D.	0.00	ARF	10	W ^L GPV ^A RT ^R V
PTPN6	VV 85	rs1048596	N.D.	0.00	ARF	10	TL ^S SRV ^C CR ^T
PTPN6	VV 85	rs1048596	N.D.	0.00	ARF	10	TL ^S SRV ^S CR ^T
PTPN6	VV 85	rs1048596	N.D.	0.00	ARF	10	VL ^H SAAG ^C AA
PTPN6	VV 85	rs1048596	N.D.	0.00	ARF	10	VL ^H SAAG ^C PA
RASGRP2	II 83	rs11231864	N.D.	0.00	ARF	10	NV ^P PPQ ^V LD ^L
RASGRP2	II 83	rs11231864	N.D.	0.00	ARF	11	QV ^L D ^F RL ^P SG ^V
RASGRP2	II 83	rs11231864	N.D.	0.00	ARF	11	QV ^L D ^L RL ^P SG ^V
RASGRP2	II 83	rs11231864	N.D.	0.00	ARF	10	VLD ^F RL ^P SG ^V
RASGRP2	II 83	rs11231864	N.D.	0.00	ARF	10	VLD ^L RL ^P SG ^V
RASGRP2	GG 583	rs2230414	0.35	N.D	ARF	9	AL ^A GEAP ^L G
RASGRP2	GG 583	rs2230414	0.35	N.D	ARF	9	AL ^E GEAP ^L G
RASGRP2	GG 583	rs2230414	0.35	N.D	ARF	9	SL ^C PAL ^A GE
RASGRP2	GG 583	rs2230414	0.35	N.D	ARF	10	SL ^C PAL ^A GEA

RASGRP2	GG 583	rs2230414	0,35	N.D	ARF	9	SLCPALEGE
RASGRP2	GG 583	rs2230414	0,35	N.D	ARF	10	SLCPALEGEA
SELL	GG 22	rs4987279	0,04	0,00	ARF	10	LMEHLQVVGL
SELL	GG 22	rs4987279	0,04	0,00	ARF	10	LMEHLQVVGV
SELL	LL 107	rs1051091	0,38	0,17	ARF	11	LLKKQRTGEMV
SELL	LL 107	rs1051091	0,38	0,17	ARF	9	NLLKKQRT
SELL	LL 107	rs1051091	0,38	0,17	ARF	9	NLLKKQRT
SELL	LL 107	rs1051091	0,38	0,17	ARF	11	SLKKQRTGEMV
SELL	FL 193	rs1131498	0,29	0,28	NRF	9	QLVIQCEPL
SELL	SP 213	rs2229569	0,26	0,09	NRF	11	ELGTMDCETHPL
SELL	SP 213	rs2229569	0,26	0,09	NRF	11	ELGTMDCETHSL
SELL	SP 213	rs2229569	0,26	0,09	NRF	9	GTMDCETHPL
SELL	SP 213	rs2229569	0,26	0,09	NRF	9	GTMDCETHSL
SELL	SP 213	rs2229569	0,26	0,09	ARF	9	SJLFGKLQQL
SELL	SP 213	rs2229569	0,26	0,09	ARF	10	SJLFGKLQQL
SELPLG	IM 62	rs2228315	0,34	0,07	NRF	10	FLPETEPEI
SELPLG	IM 62	rs2228315	0,34	0,07	NRF	11	FLPETEPEIL
SELPLG	IM 62	rs2228315	0,34	0,07	NRF	10	FLPETEPEM
SELPLG	IM 62	rs2228315	0,34	0,07	NRF	11	FLPETEPEML
SELPLG	IM 62	rs2228315	0,34	0,07	NRF	9	ILRNSTDTT
SELPLG	IM 62	rs2228315	0,34	0,07	NRF	11	ILRNSTDTTPL
SELPLG	IM 62	rs2228315	0,34	0,07	NRF	11	MLRNSTDTTPL
SELPLG	VM 264	rs7300972	0,08	0,00	NRF	11	LSMEPTTKRGL
SELPLG	VM 264	rs7300972	0,08	0,00	NRF	11	LSVEPTTKRGL
SELPLG	VM 264	rs7300972	0,08	0,00	NRF	10	SMEPTTKRGL
SELPLG	VM 264	rs7300972	0,08	0,00	NRF	11	SVEPTTKRGL
SEPT6	PL 406	rs17856302	N.D.	0,40	ARF	11	ELLSQSGSQAQ
SEPT6	PL 406	rs17856302	N.D.	0,40	ARF	9	LLSQSGSQA
SEPT6	PL 406	rs17856302	N.D.	0,40	NRF	9	RLLSCPSRA
SEPT6	PL 406	rs17856302	N.D.	0,40	NRF	9	RLLSCSPRA
SF1	PP 499	rs2277308	N.D.	0,00	ARF	11	PMTATAAASA
SF1	PP 499	rs2277308	N.D.	0,00	ARF	11	PVATATAAASA
SF1	PP 499	rs2277308	N.D.	0,00	ARF	9	SLWSSSPMA
SF1	PP 499	rs2277308	N.D.	0,00	ARF	10	SLWSSSPMAT
SF1	PP 499	rs2277308	N.D.	0,00	ARF	11	SLWSSSPMATT
SF1	PP 499	rs2277308	N.D.	0,00	ARF	9	SLWSSSPVA
SF1	PP 499	rs2277308	N.D.	0,00	ARF	10	SLWSSSPVAT
SF1	PP 499	rs2277308	N.D.	0,00	ARF	11	SLWSSSPVATT
SF1	PP 499	rs2277308	N.D.	0,00	ARF	11	FSDHPAVPWA
SOCS2	GE 7	rs7956250	N.D.	0,01	ARF	10	WQSRDTPILL
SP110	RW 112	rs1129411	N.D.	0,08	NRF	10	YEWQSRDTP
SP110	RW 112	rs1129411	N.D.	0,08	NRF	10	YEWQSRDTP
SP110	VA 128	rs11556887	0,11	N.D.	NRF	10	GLAEGSSLHT
SP110	VA 128	rs11556887	0,11	N.D.	NRF	10	GLAEGSSLHT
SP110	VA 128	rs11556887	0,11	N.D.	NRF	10	ILLEAPTGLA
SP110	VA 128	rs11556887	0,11	N.D.	NRF	11	ILLEAPTGLA
SP110	VA 128	rs11556887	0,11	N.D.	NRF	10	ILLEAPTGLV
SP110	VA 128	rs11556887	0,11	N.D.	NRF	11	ILLEAPTGLVE
SP110	VA 128	rs11556887	0,11	N.D.	NRF	9	LLEAPTGLV
SP110	VA 206	rs28930679	0,05	N.D.	NRF	11	KMNAEEDSEEM
SP110	VA 206	rs28930679	0,05	N.D.	NRF	11	KMNVEEDSEEM
SP110	KE 207	rs9061	0,31	0,11	NRF	11	KMNAKEDSEEM
SP110	RG 299	rs1365776	0,52	0,44	NRF	9	SLPRGTASS
SP110	RG 299	rs1365776	0,52	0,44	NRF	9	SLPRGTASS
SP110	LS 303	rs17856567	N.D.	0,00	NRF	9	SLPRGTASS
SP110	SL 425	rs3948464	0,29	0,10	NRF	11	RLLKKEKKEKDI
SP110	MT 523	rs1135791	0,41	0,45	NRF	9	NIRCEGRTL
SP110	MT 523	rs1135791	0,41	0,45	NRF	9	NIRCEGRTL
SP110	CC 577	rs13018234	0,12	N.D.	ARF	10	ELHLLQDEEV
SP110	IM 579	rs3948463	0,05	0,08	ARF	10	ELHLLQDEEV
SP110	IM 579	rs3948463	0,05	0,08	ARF	11	ELHLLQDEEVFRK
SP110	IM 579	rs3948463	0,05	0,08	ARF	11	ELHLLQDEEVFRK
SP110	IM 579	rs3948463	0,05	0,08	NRF	10	MLW SCTFCRI
SP110	IM 579	rs3948463	0,05	0,08	NRF	10	MLW SCTFCRM
SP110	IM 579	rs3948463	0,05	0,08	NRF	11	RMLW SCTFCRI
SP110	IM 579	rs3948463	0,05	0,08	NRF	11	RMLW SCTFCRM
SYNGR1	LF 153	rs1062695	N.D.	0,00	NRF	10	AIALSFFSI
SYNGR1	LF 153	rs1062695	N.D.	0,00	NRF	9	ALSFFSIFT
SYNGR1	LF 153	rs1062695	N.D.	0,00	NRF	11	ALSFFSIFTWA
SYNGR1	LF 153	rs1062695	N.D.	0,00	NRF	10	AIAF SFFSI
SYNGR1	LF 153	rs1062695	N.D.	0,00	NRF	9	AIAF SFFSI
SYNGR1	LF 153	rs1062695	N.D.	0,00	NRF	9	AIALSFFSI
SYNGR1	LF 153	rs1062695	N.D.	0,00	NRF	10	F SFFSIFTWA
SYNGR1	LF 153	rs1062695	N.D.	0,00	NRF	10	IAF SFFSIFT
SYNGR1	LF 153	rs1062695	N.D.	0,00	NRF	10	IALSFFSIFT
SYNGR1	LF 153	rs1062695	N.D.	0,00	ARF	9	LLFLHLHL
SYNGR1	LF 153	rs1062695	N.D.	0,00	ARF	9	PLFLHLHL
SYNGR1	LF 153	rs1062695	N.D.	0,00	NRF	10	RLLFLHLHL
SYNGR1	KQ 164	rs11548411	N.D.	0,09	ARF	9	FTWAGKAVL
SYNGR1	KQ 164	rs11548411	N.D.	0,09	ARF	9	FTWAGQAVL
SYNGR1	KQ 164	rs11548411	N.D.	0,09	ARF	10	GGCAGLPAV
SYNGR1	KQ 164	rs11548411	N.D.	0,09	ARF	10	HLGGPGCAGL
SYNGR1	KQ 164	rs11548411	N.D.	0,09	ARF	10	HLGGGCAGL
SYNGR1	KQ 164	rs11548411	N.D.	0,09	ARF	9	LGPGCAGL
SYNGR1	KQ 164	rs11548411	N.D.	0,09	ARF	10	SIFTWAGKAV
SYNGR1	KQ 164	rs11548411	N.D.	0,09	ARF	11	SIFTWAGKAVL
SYNGR1	KQ 164	rs11548411	N.D.	0,09	ARF	10	SIFTWAGQAV
SYNGR1	KQ 164	rs11548411	N.D.	0,09	ARF	11	SIFTWAGQAVL
ZFP36L2	II 203	rs8098	0,08	0,08	ARF	10	AVPHLSYHWL

ZFP36L2	II 203	rs8098	0,08	0,08	ARF	10	HLSYH R LLPL
ZFP36L2	II 203	rs8098	0,08	0,08	ARF	10	HLSYH W LLPL
ZFP36L2	II 203	rs8098	0,08	0,08	ARF	9	R LLPLWAAAL
ZFP36L2	II 203	rs8098	0,08	0,08	ARF	11	R LLPLWAAALP
ZFP36L2	II 203	rs8098	0,08	0,08	ARF	9	W LLPLWAAAL
ZFP36L2	II 203	rs8098	0,08	0,08	ARF	11	W LLPLWAAALP
ZFP36L2	LL 254	rs7933	0,5	0,32	ARF	10	A APQPQLLGL
ZFP36L2	LL 254	rs7933	0,5	0,32	ARF	10	GLPAGAAA Q A
ZFP36L2	LL 254	rs7933	0,5	0,32	ARF	10	GLPAGAAA V
ZFP36L2	LL 254	rs7933	0,5	0,32	ARF	11	QVAPQPQLLGL
ZFP36L2	LL 254	rs7933	0,5	0,32	ARF	10	V APQPQLLGL
HMH41 (red)	RH 139	rs1801284	0,04	0,37	NRF	9	V L HDDLLEA
ADIR-F (N.D.)	FL 13	rs2296377	0,28	0,03	ARF	11	SVAPALAL F PA
CMV (green)	none	no polymorphism	-	N.D.	NRF	9	NLVPMVATV
EBV (orange)	none	no polymorphism	-	N.D.	NRF	9	GLCTLVAML
FLU (pink)	none	no polymorphism	-	N.D.	NRF	9	GILGFVFTL
HY (N.D.)	none	no polymorphism	-	N.D.	NRF	9	FIDSYICQV
Mart-1 (blue)	none	no polymorphism	-	N.D.	NRF	9	AAGIGILTV
A3-GP100 (grey)	none	no polymorphism	-	N.D.	NRF	9	LIYRRRLMK

^a dbSNP average heterozygosity (build126)

^b SNP frequency obtained from customized SNP genotyping array. Data represents the allele frequency of 100 Dutch individuals

^c Peptide sequences are provided with polymorphic residue in red

Table SIII. Dual-encoding pMHC tetramer scheme

Peptide number	Gene symbol	Peptide Sequence ^a	RS MHC-ELISA ^b	RS MHC-Bead ^c	Tetramer group	Dual-color encoding
1	NUP210	MIHDLCLVFL	71	38	1	PE & Q565
2	NUP210	CLVFPAPAKAV	56	51		PE & Q585
3	PSD4	VLLSEAFPGGL	73	79		PE & Q605
4	PLCB2	RILVGRRLRAA	84	79		PE & Q655
5	HSPA6	SLASLLPHV	88	101		PE & Q705
6	CSF3R	TQPGPLVPL	70	63		PE & Q800
7	HSPA6	GIPPAPHGV	73	98		APC & Q565
8	ARHGAP15	KLGDICIWTYL	78	39		APC & Q605
9	GNA15	RTIPTPLQL	74	56		APC & Q655
10	CPVL	ALTEHSLMGM	22	86		APC & Q800
11	ICAM3	ALCQNGYHGTI	61	66		Q565 & Q605
12	PSD4	TLLNQPDKMFL	104	84		Q565 & Q655
13	PSD4	LLNQPDKMFL	82	21		Q565 & Q705
14	SELL	GTMDCTHPL	120	74		Q585 & Q605
15	ZFP36L2	WLLPLWAAALPL	81	77		Q585 & Q655
16	MPL	RLRAPEVFL	66	31		Q585 & Q705
17	HSPA6	GLLQVHHSCPL	84	33		Q605 & Q705
18	NCF4	MMLPSQPTLL	86	95		Q605 & Q800
19	NCF4	M L P S Q P T L L	50	56		Q655 & Q705
20	MCM5	YLCDKVIIPG	96	90		Q655 & Q800
21	HY	FIDSYICQV	N.D.	N.D.		Q705 & Q800
22	CPVL	RQVGDFFHQV	79	76	2	PE & APC
23	CD79b	LLLSAEVQQHL	89	97		PE & Q565
24	KCNAB2	NLFDTAKVYA	95	85		PE & Q585
25	HSPA6	NLLGRFELIGI	65	70		PE & Q605
26	HSPA6	VLNSVASLL	107	58		PE & Q655
27	NUP210	DCLVFLAPA	46	57		PE & Q705
28	NUP210	QILPLHGPEA	63	51		PE & Q800
29	ICAM3	VLQWLSDNRL	59	43		APC & Q585
30	ARHGAP 25	SLQRMVQEL	92	96		APC & Q605
31	SP110	ELHLLQDEEV	26	25		APC & Q655
32	NUP210	VLASIEPELPM	70	55		APC & Q705
33	SELPLG	FLPETEPEPM	94	93		APC & Q800
34	ICAM3	TMLGRRPPI	69	88		Q565 & Q605
35	SELL	S L F G K L Q L Q L	42	60		Q565 & Q655
36	FBNP1	L A G S S L N P V	67	99		Q565 & Q705
37	DOCK2	S I Q N Y H P F A	60	51		Q585 & Q605
38	ZFP36L2	H L S Y H R L L P L	77	44		Q585 & Q655
39	DOCK2	K L L Q I Q L R A K V	49	78		Q585 & Q705
40	DOCK2	K L L Q I Q L C A	103	72		Q605 & Q655
41	HSPA6	S L F E G V D F Y T	77	77		Q605 & Q705
42	FLT3	S M P Q G T F P V	63	87		Q605 & Q800
43	SF1	S L W S S S P M A	101	102		Q655 & Q705
44	CD48	L L F E T V M C D T	100	72		Q655 & Q800
45	HSPA6	F M T S S W W R A P L	N.D.	73		Q705 & Q800
46	HMHA1	V L H D D L L E A	83	91	3	PE & APC
47	IQGAP2	S V V K I Q S W F R M	59	62		PE & Q565
48	KCNAB2	N L F D T A E V Y A A	50	59		PE & Q585
49	ITGAL	T A L R L T A F A S L	64	34		PE & Q605
50	LCP2	M M K M M C I K D L	36	69		PE & Q655
51	HSPA6	N L L G R F E L I	65	76		PE & Q705
52	CSF3R	T Q P G P L A P L	76	79		PE & Q800
53	ZFP36L2	G L P A G A A A A Q A	35	54		APC & Q565
54	DOCK2	T L T T G E W A V	68	73		APC & Q605
55	SP110	M L W S C T F C R M	63	88		APC & Q655
56	ITGAM	M M S E G G P P G A	59	63		APC & Q705
57	NUP210	V L A S I E P E L	79	96		APC & Q800
58	ICAM3	A L C Q N G Y H G T	56	74		Q565 & Q605
59	PSD4	T L L N L P D K M F L	93	93		Q565 & Q655
60	PSD4	L L N L P D K M F L	88	26		Q565 & Q705
61	HSPA6	L L Q V H H S C P L	33	-14		Q585 & Q605
62	BTK	Y I P S C T V V G M	52	66		Q585 & Q655
63	ZFP36L2	R L L P L W A A L	88	71		Q585 & Q705
64	EVI2B	L P P P P P L L D L	69	19		Q605 & Q800
65	EVI2B	D L P P P P P L L	41	58		Q655 & Q705
66	ARHGAP4	S L C P W S W R A A	90	78		Q655 & Q800
67	ADIR-1F	S V A P A L A L F P A	N.D.	N.D.		Q705 & Q800
68	CPVL	R Q A G D F H Q V	81	86	4	PE & APC
69	CD79b	L L L P A E V Q Q H L	84	99		PE & Q565

70	KCNAB2	NLFDTAEVYA	81	90	PE & Q585
71	PLCB2	FLAPPPVRL	70	44	PE & Q605
72	HSPA6	VLNSLASLL	86	49	PE & Q655
73	CSF3R	ITQPGPLVPL	82	75	PE & Q705
74	NUP210	ILPLHGPEA	64	43	PE & Q800
75	ICAM3	VLQWLFDNRL	67	52	APC & Q585
76	ITGAM	GTWESNAV	52	74	APC & Q605
77	GNA15	TIPTPLQPL	67	66	APC & Q655
78	NUP210	VLASIEAELPM	87	57	APC & Q705
79	SELPLG	FLPETEPPEI	96	90	APC & Q800
80	ICAM3	TMLGRRAPI	50	58	Q565 & Q605
81	FNBP1	RLAGSSSLNPV	91	104	Q565 & Q655
82	FNBP1	LAGSSSLNV	71	79	Q565 & Q705
83	ZFP36L2	WLLPLWAAL	97	96	Q585 & Q655
84	DOCK2	RLTSTNPTT	67	75	Q585 & Q705
85	NCF4	MMLPSQPTLLT	52	70	Q605 & Q655
86	BTK	CLCLLNPPQGT	18	21	Q605 & Q705
87	NCF4	MMLPSRPTL	79	61	Q605 & Q800
88	N4BP2L1	KLYSENLTLA	122	86	Q655 & Q705
89	ITGAM	RLQVPVEAV	58	81	PE & APC
90	ARHGAP4	SLLSPLHCWAV	82	71	PE & Q565
91	FLT3	KVLHELFGMDI	84	79	PE & Q585
92	LRMP	SLKLLLESTPI	90	93	PE & Q605
93	HSPA6	LLGRFELIGI	82	54	PE & Q655
94	LRMP	NCLKLLES	59	51	PE & Q705
95	HSPA6	FIQVYEVERA	77	80	PE & Q800
96	NCF4	RMMLPSQPTL	72	80	APC & Q565
97	NUP210	RAPPTPAL	65	80	APC & Q585
98	ARHGAP 25	SLQSTVQEL	91	94	APC & Q605
99	SP110	MLWSTCFCRI	100	81	APC & Q655
100	NUP210	VLASIEAEL	86	99	APC & Q800
101	FNBP1	SRLAGSSSLNPV	90	90	Q565 & Q655
102	FNBP1	RLAGSSSLN	91	73	Q565 & Q705
103	SP110	ILLEAPTGLV	78	73	Q585 & Q605
104	ZFP36L2	RLLPLWAALPL	88	64	Q585 & Q655
105	ARHGAP 25	MLLKTSEFL	92	101	Q585 & Q705
106	DOCK2	QLCAKVPLL	94	82	Q605 & Q655
107	IL2RG	YLFSKEITSG	88	76	Q605 & Q705
108	HSPA6	LLHVHHSCLP	61	26	Q605 & Q800
109	FMNL1	SLWQLGAAVML	96	95	Q655 & Q705
110	SYNGR1	FTWAGKAVL	100	90	Q655 & Q800
111	CD48	FVSGSGIAIA	N.D.	99	Q705 & Q800
112	CD79b	TMASTSVSRSA	53	72	PE & APC
113	IQGAP2	FIDNTDSVV	49	74	PE & Q565
114	PSD4	VLLESAFPGR	72	55	PE & Q585
115	PSD4	RLQTPMQVGL	87	65	PE & Q605
116	HSPA6	SVASLLPHV	88	90	PE & Q655
117	CSF3R	ITQPGPLAPL	73	83	PE & Q705
118	HSPA6	GIPPAPRGV	71	96	PE & Q800
119	DOCK2	LTLTTEGWAV	59	68	APC & Q585
120	ITGAM	GMWESNAV	73	73	APC & Q605
121	CPVL	ALTERSLMGM	72	23	APC & Q705
122	LTB	FLTSGTQFSDA	61	68	APC & Q800
123	HSPA6	LIFDLGGGT	52	48	Q565 & Q605
124	FNBP1	RLAGSSSLNV	84	93	Q565 & Q655
125	SELL	GTMDCTHSL	87	57	Q565 & Q705
126	NCF4	ALMVRQARGL	74	45	Q585 & Q605
127	CD69	STLQGLTSV	74	78	Q585 & Q655
128	DOCK2	RLTSTNPTM	43	50	Q585 & Q705
129	NCF4	MMLPSRPTLLT	45	58	Q605 & Q655
130	NCF4	MMLPSRPTLL	78	93	Q605 & Q705
131	NCF4	MMLPSQPTL	90	94	Q605 & Q800
132	SYNGR1	FTWAGQAVL	95	81	Q655 & Q705
133	N4BP2L1	KIYSENKLA	104	82	Q655 & Q800
134	CSF3R	AMARDPHSLWV	N.D.	104	Q705 & Q800
135	CPVL	RVTSIRLFEV	54	66	PE & APC
136	IQGAP2	SIVKIQSWFRM	55	77	PE & Q565
137	FLT3	VLHELFGMDI	76	90	PE & Q585
138	ITGAL	RALRLTAFASL	92	29	PE & Q605
139	PSD4	LLESAFPGL	57	68	PE & Q655
140	PLCB2	ILVGRLLRAA	104	86	PE & Q705
141	LRMP	SLLQSR EYSSL	74	13	PE & Q800
142	SELL	QLVIQCEPL	67	65	APC & Q565

143	NUP210	LLW WIAVGPV	80	80	APC & Q585
144	ARHGAP 25	SLQ SMVQEL	93	96	APC & Q605
145	BTK	KLANIQC PCL	87	77	APC & Q655
146	PSMB10	ALR CASPWL	65	26	APC & Q705
147	SEPLPG	FLPETEPEML	69	60	APC & Q800
148	FBNP1	SRLAGSS LNLV	77	72	Q565 & Q655
149	PSD4	LNLPDKMFL	64	58	Q565 & Q705
150	SP110	ILLEAPTGLA	66	71	Q585 & Q605
151	ZFF36L2	HLSYHWLLPL	80	25	Q585 & Q655
152	DOCK2	KLLQIQ LCAKV	53	66	Q585 & Q705
153	DOCK2	KLLQIQ LRA	83	20	Q605 & Q655
154	IL2RG	YLFSE EITSG	88	75	Q605 & Q705
155	HSPA6	VLVEG STRI	74	55	Q605 & Q800
156	N4BP2L1	KLYSEN LKLA	108	93	Q655 & Q705
157	CD48	LLSETVMCDT	100	81	Q655 & Q800
158	CD48	FVSGSDIATA	110	91	PE & APC
159	KCNAB2	MIMASTSSI	91	92	PE & Q565
160	NUP210	IMIHD LCLA	104	86	PE & Q585
161	NCF4	LLSDEDV AL	92	97	PE & Q605
162	ARHGAP 25	SLQR TVQEL	87	84	PE & Q655
163	EVI2B	LLFLLQMMQV	77	104	PE & Q705
164	NCF4	RLLSDEDV ELM	67	64	APC & Q565
165	EVI2B	LLQMMQVCL	74	91	APC & Q585
166	FMNL1	SLWQLGA AVM	76	61	APC & Q605
167	CORO1A	KLQAPVQEL	79	53	APC & Q655
168	LYN	RLQREWHTL	69	54	APC & Q705
169	RASGRP2	VLD FRLPSGV	51	43	APC & Q800
170	PTPN6	STVASRLGPV	72	74	Q565 & Q605
171	NCF4	RCHELTVSL	33	69	Q565 & Q655
172	NCF4	SLLSLPVVWLM	74	48	Q565 & Q705
173	N4BP2L1	MALENNYEV	59	83	Q585 & Q605
174	MAP4K1	SLGIMAIEL	71	70	Q585 & Q655
175	SEPT6	RLSCPSPRA	53	64	Q585 & Q705
176	FCER1A	ISTQQQATFLL	56	55	Q605 & Q655
177	DUSP22	MLGDPVPTPT	41	88	Q605 & Q705
178	SP110	ELHLLQDKEV	23	47	Q655 & Q800
179	ATP2A3	KMFVKGAPESV	N.D.	98	Q705 & Q800
180	N4BP2L1	KIYSEN LTLA	92	95	PE & APC
181	N4BP2L1	TMKIYSEN LTL	88	83	PE & Q565
182	FMNL1	SLWQLGA AV	88	91	PE & Q655
183	EVI2B	MMQVCLHHL	84	65	PE & Q705
184	NUP210	LLIGATMQV	88	81	PE & Q800
185	HSPA6	FMTSSWVRA	82	78	APC & Q565
186	IQGAP2	ILHSRTEFI	80	81	APC & Q605
187	LRMP	FLPRNIGNA	62	79	APC & Q655
188	FLT3	ALARGAGTVPL	76	73	APC & Q705
189	NCF4	PLPEAPLSL	77	91	APC & Q800
190	NCF4	AISANIADI	47	56	Q565 & Q605
191	EVI2B	LLFLLQMMQI	65	74	Q565 & Q655
192	DOK2	TLPPRPDHI	54	66	Q565 & Q705
193	NCF4	LLSDEDV ELMV	62	68	Q585 & Q605
194	DOK2	LLASSMSSQL	62	59	Q585 & Q655
195	NUP210	IMIHD LCLV	60	54	Q605 & Q655
196	DOK2	QLGRISLLL	63	37	Q605 & Q705
197	CSF3R	AQDPHSLWV	60	64	Q605 & Q800
198	ARHGAP15	FLRAENETGNM	39	64	Q655 & Q705
199	FMNL1	QLRAAVMLRL	65	19	Q655 & Q800
200	CSF3R	AMAQDPHSLWV	N.D.	103	Q705 & Q800
201	N4BP2L1	KLYSEN LTL	94	92	PE & APC
202	MPL	HLWVKNVFL	109	93	PE & Q565
203	ATP2A3	KMNVFDTNL	89	89	PE & Q585
204	BTK	SLTAISTTL	83	80	PE & Q705
205	EVI2B	FLLQMMQVCL	86	82	APC & Q565
206	SF1	SLWSSSPVAT	69	84	APC & Q585
207	IQGAP2	ILHSRTEFV	77	86	APC & Q605
208	NCF4	SLLNLPVWV	73	92	APC & Q705
209	PIK3CD	SVSHSSPMTL	76	52	APC & Q800
210	N4BP2L1	TMKLYSEN LTL	73	91	Q565 & Q605
211	ARHGAP4	PLHCWV VLL	70	77	Q565 & Q655
212	DUSP22	CMLGDPVPT	57	86	Q565 & Q705
213	CD79b	PLDGGVAAA	45	65	Q585 & Q605
214	BTK	HLASEKVYAI	68	65	Q585 & Q705
215	CCL3	FLTKRGRQV	54	56	Q605 & Q655

216	PTPN6	RLGPVARTRV	48	68	Q605 & Q800
217	BTK	SLTTISTTL	92	84	Q655 & Q705
218	MAP4K1	IMAIELAEI	92	93	Q655 & Q800
219	ATP2A3	KMFVKGAPDSV	N.D.	106	Q705 & Q800
220	EVI2B	FLQMMQICL	91	90	PE & APC
221	EVI2B	QMMQVCLHHL	87	65	PE & Q585
222	CSF3R	AMAQDPHSL	83	62	PE & Q605
223	NUP210	FLAPAKAVVYV	88	85	PE & Q705
224	BTK	KLANIQCLCL	89	51	PE & Q800
225	NUP210	TIMIHDLCLA	85	72	APC & Q565
226	IQGAP2	KIQRNLWTL	76	69	APC & Q585
227	ITGAM	VLRQEVAAPL	89	84	APC & Q605
228	NCF4	LLSDEDVALM	76	72	APC & Q655
229	EVI2B	ICLHHLPFWI	80	79	APC & Q705
230	EVI2B	VCLHHLPFWI	57	75	APC & Q800
231	ITGAM	RVLRQEVAAPL	74	79	Q565 & Q605
232	LRMP	LQSRGYSSL	72	70	Q565 & Q655
233	N4BP2L1	VMALENNYEV	60	72	Q565 & Q705
234	NUP210	TLLIGATIQVT	69	48	Q585 & Q605
235	PRKCB1	RIGQRQETV	63	63	Q585 & Q655
236	ARHGAP4	LLSPLHCWAV	77	70	Q585 & Q705
237	ZFP36L2	RLRPLCCTA	56	58	Q605 & Q655
238	NUP210	LLIGATIQV	59	71	Q605 & Q705
239	NUP210	TLLIGATIQV	68	81	Q605 & Q800
240	MPL	HLWVKNMFL	104	82	PE & APC
241	DOK2	TLLASSMSSL	74	80	PE & Q585
242	NCF4	RLSDEDVALM	77	68	PE & Q655
243	CD79b	TLRTGEVKKWSV	69	62	PE & Q800
244	ITGB2	RLGGAALPRV	73	95	APC & Q565
245	BTK	LASEKVYTI	62	67	APC & Q585
246	ATP2A3	RLWTTTRPRV	68	68	APC & Q655
247	MAP4K1	GIMAIELAEI	81	81	APC & Q705
248	NUP210	LLIGATIQVT	71	46	APC & Q800
249	SEPT6	RLSCSSPRA	58	56	Q565 & Q605
250	IQGAP2	ILHSRTEFISV	66	70	Q565 & Q655
251	NUP210	LAPAKAVVYV	67	72	Q565 & Q705
252	LTB	DLSPLPAA	62	61	Q585 & Q655
253	IQGAP2	KIQRNLRTL	66	39	Q585 & Q705
254	PIK3CD	KTGECCLYM	84	86	Q605 & Q655
255	NUP210	TLLIGATMQV	87	83	Q605 & Q705
256	FMNL1	SLWQLRAAV	86	91	Q605 & Q800
257	N4BP2L1	KLYSENKL	93	90	Q655 & Q705
258	NCF4	SLLSLPVVW	80	87	Q655 & Q800
259	CORO1A	KLQATVQEL	89	81	PE & APC
260	SF1	SLWSSSPVA	86	102	PE & Q565
261	SF1	SLWSSSPMATT	75	83	PE & Q585
262	EVI2B	MMQICLHHL	97	74	PE & Q605
263	EVI2B	LLQMMQICL	87	87	PE & Q655
264	N4BP2L1	KIYSENKL	83	81	PE & Q705
265	NUP210	CLAFPAPAKA	20	23	APC & Q565
266	NCF4	RLSDEDVEL	85	93	APC & Q585
267	SYNGR1	SIFTWAGKAVL	81	46	APC & Q655
268	ITGAM	RVLRQEVAAPL	66	79	APC & Q705
269	CORO1A	GLWRHSPCA	114	62	Q565 & Q605
270	LRMP	SLLQSRGYSSL	69	72	Q565 & Q655
271	LTB	GLREREDLL	65	48	Q565 & Q705
272	NCF4	QLQGLQHNA	53	51	Q585 & Q605
273	HSPA6	FMTSSWVGA	65	67	Q585 & Q655
274	N4BP2L1	AVMALENNYEV	64	85	Q605 & Q655
275	NUP210	VTLIGATIQV	63	78	Q605 & Q705
276	CD79b	LLSAEVQQHL	65	34	Q655 & Q800
277	CD48	KQDNSTYIMRV	N.D.	124	Q705 & Q800
278	DOK2	SMSSQLGRISL	86	76	PE & APC
279	NCF4	LLSDEDVEL	85	92	PE & Q585
280	NUP210	IMIHDLCVFL	81	64	PE & Q605
281	NUP210	LLIGATMQVT	74	53	PE & Q655
282	SF1	SLWSSSPVATT	70	81	PE & Q705
283	LTB	GLCEREDLL	75	72	PE & Q800
284	PSD4	AQAEHSITRV	78	61	APC & Q605
285	CCL3	FLTKRGGQV	64	75	APC & Q705
286	NUP210	CLVFLAPAKA	50	67	Q565 & Q655
287	SF1	SLWSSSPMAT	88	100	Q585 & Q605
288	N4BP2L1	KIYSENLT	91	94	Q585 & Q655

289	ARHGAP4	SLLSPLHCW A	86	81	Q605 & Q655
290	NCF4	RLLSDEDV A L	85	71	Q605 & Q705
291	EVI2B	GLP P PPPLL	80	85	Q605 & Q800
292	NUP210	CLVFP A PAKA	72	69	Q655 & Q705
293	NCF4	SLL N LPVWVLM	85	66	Q655 & Q800
294	MCM5	YLC D KV V PG	97	88	PE & APC
295	NUP210	VTLLIGAT M QV	88	84	PE & Q565
296	ARHGAP4	L L SPLHCW A	50	65	PE & Q585
297	NCF4	L L SDEDV E LM	83	69	PE & Q605
298	EVI2B	Q M M Q IC L H H L	82	59	PE & Q655
299	SYNGR1	S I FTWAG Q AVL	84	58	PE & Q705
300	FMNL1	S L W Q L R A A V M L	58	48	APC & Q565
301	NUP210	F L APAKAVV	85	83	APC & Q585
302	CD79b	R T G E V K W S V	67	79	APC & Q605
303	BTK	L A S E K V V A I	72	69	APC & Q655
304	CSF3R	A M A R D P H S L	72	53	APC & Q800
305	NCF4	L L N L P V V V L	38	65	Q565 & Q605
306	FMNL1	R M T W R A Q T M	79	38	Q565 & Q655
307	CCL3	F L T K R S G Q V	69	77	Q565 & Q705
308	PRKCB1	S M S K E A V A I	68	65	Q585 & Q605
309	HSPA6	S M C R F S P L T L	61	69	Q585 & Q655
310	IQGAP2	N L W T L E Q T G H V	60	82	Q585 & Q705
311	HSPA6	K C Q E V L A W L	82	30	Q605 & Q705
312	NUP210	T L L I G A T M Q V T	45	41	Q605 & Q800
313	PTPN6	T L S S R V C C R T	72	34	Q655 & Q705
314	NUP210	L V F L APAKAVV	53	67	Q655 & Q800
315	NCF4	L L SDEDV A LMV	70	82	PE & APC
316	N4BP2L1	A L E N N Y E V L	71	63	PE & Q565
317	EVI2B	C L H H L P F W I	41	33	PE & Q585
318	PTPN6	S T V A S W L G P V	75	64	PE & Q605
319	CCL3	F L T K R S R Q V	64	76	PE & Q655
320	ARHGAP4	P L H C W A V L L	69	77	PE & Q800
321	PTPN6	T V A S R L G P V	73	61	APC & Q565
322	CCL3	F L T K R S G Q V C A	61	59	APC & Q605
323	SP110	L L E A P T G L V	75	69	APC & Q655
324	NCF4	V S L L S L P V V V	56	60	APC & Q800
325	ARHGAP15	K L G D C I W T Y P S	N.D.	105	Q565 & Q655
326	NUP210	M I H D L C L A F P A	N.D.	128	Q565 & Q705
327	PSD4	N L P D K M F L P G A	N.D.	124	Q585 & Q605
328	ARHGAP15	K L G D C I W T Y L S	N.D.	91	Q585 & Q655
329	HSPA6	G V F I Q V Y E V	N.D.	103	Q585 & Q705
330	LYN	L M F W S P S H S C A	N.D.	102	Q605 & Q705
331	MCM5	T L T N I A M R P G L	N.D.	74	Q605 & Q800
332	RASGRP2	Q V L D L R L P S G V	N.D.	107	Q655 & Q705
333	NUP210	A T A T P C W T W L L	N.D.	86	Q655 & Q800

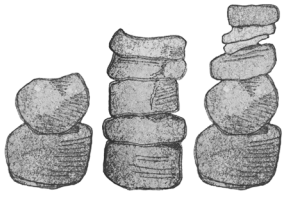
^a Peptide sequences are provided with polymorphic residue in red

^b RS are normalized to the HLA-A2 high affinity CMV-pp65_{NLV} peptide

Table SIV. Total pMHC tetramer-reactive T-cell populations revealed after pull down and two weeks of expansion

Allo-SCT patient	pMHC tetramer group	Dual-color encoding	CD8+ T cell frequency	Peptide number	Allo-SCT patient	pMHC tetramer group	Dual-color encoding	CD8+ T cell frequency	Peptide number
APM4461 12 weeks ^a	1	QD655 & PE	0,36	4	OBB1465 12 weeks	1	APC & QD565	0,09	7
	2	QD585 & QD605	0,31	37		2	PE & QD655	0,07	4
	3	QD605 & PE	0,04	25		3	QD585 & QD705	0,21	39
	4	APC & PE	0,15	46		4	PE & QD565	0,03	23
	5	APC & PE	0,06	68		5	PE & QD605	0,27	71
		PE & QD585	0,04	91		6	QD705 & QD585	0,04	84
		PE & QD605	n.t.	92		7	PE & QD655	0,17	93
		QD585 & QD655	0,18	104		8	QD585 & QD655	0,55	104
		PE & QD605	0,42	115		9	PE & QD800	0,25	118
		PE & APC	4,9	135		10	QD585 & QD705	0,04	128
		APC & QD565	0,04	185		11	PE & QD705	0,07	163
		QD585 & QD655	0,77	235		12	PE & QD800	0,35	184
		QD565 & APC	0,19	265		13	QD605 & QD655	0,15	195
		QD585 & QD655	0,6	309		14	QD605 & QD705	0,05	238
	BDY3356 16 weeks	2	APC & PE	0,07		22	1	APC & QD565	0,04
3		QD605 & QD585	0,177	37	2	QD705 & QD605	0,06	255	
4		APC & PE	0,05	68	3	QD605 & QD800	0,06	291	
5		QD655 & QD585	0,215	104	4	QD655 & QD705	0,07	292	
		APC & PE	0,11	89	5	QD585 & PE	0,27	2	
		QD705 & QD655	0,17	109	6	QD705 & PE	0,02	5	
		QD655 & QD800	0,27	133	7	QD585 & QD705	0,19	84	
		QD655 & QD705	0,53	156	8	APC & PE	0,2	68	
		APC & QD565	0,03	185	9	QD585 & QD655	0,2	104	
		PE & QD585	0,05	203	10	QD655 & QD705	0,14	109	
		QD705 & APC	0,05	208	11	QD585 & QD705	0,62	128	
		QD655 & QD800	0,2	218	12	QD605 & QD655	0,52	153	
		QD705 & APC	0,04	229	13	QD585 & QD605	0,15	150	
		PE & QD605	0,04	25	14	APC & PE	0,08	135	
LBK5266 16 weeks		2	APC & PE	0,05	68	1	QD705 & PE	0,07	163
	3	PE & QD705	0,08	163	2	QD705 & APC	0,06	188	
	4	QD585 & QD605	0,19	213	3	QD565 & APC	0,07	185	
	5	PE & QD705	0,08	163	4	QD585 & QD655	0,24	235	
	6	QD705 & APC	0,06	229	5	QD565 & APC	0,08	265	
	7	QD605 & QD655	0,13	254	6	QD655 & QD705	0,34	292	
	8	PE & QD655	0,15	281	7	QD605 & PE	0,04	25	
					8	PE & QD705	0,1	163	

^a Allo-SCT patient PBMC samples were obtained at the indicated time point after DLI



MIXED FUNCTIONAL CHARACTERISTICS CORRELATING WITH TCR-LIGAND K_{OFF} -RATE OF TETRAMER REACTIVE T-CELLS WITHIN THE NAÏVE T-CELL REPERTOIRE

Pleun Hombrink¹, Yotam Raz¹, Michel G.D. Kester¹, Renate de Boer¹, Bianca Weißbrich³, Peter A. von dem Borne¹, Dirk H. Busch³, Ton N.M. Schumacher², J.H. Frederik Falkenburg¹ and Mirjam H.M. Heemskerk¹

¹Department of Hematology, Leiden University Medical Center, Leiden, The Netherlands;

²Division of Immunology, The Netherlands Cancer Institute, Amsterdam, The Netherlands;

³Institute for Medical Microbiology, Immunology and Hygiene, Technische Universität München, Munich, Germany

The low frequency of antigen-specific naïve T-cells has challenged numerous laboratories to develop various techniques to study the naïve T-cell repertoire. Here we combine the generation of naïve repertoire-derived antigen-specific T-cell lines based on MHC-tetramer staining and magnetic-bead enrichment with in-depth functional assessment of the isolated T-cells. Cytomegalovirus (CMV) specific T-cell lines were generated from seronegative individuals. Generated T-cell lines consisted of a variety of immunodominant CMV-epitope specific oligoclonal T-cell populations restricted to various HLA-molecules (HLA-A1, A2, B7, B8 and B40), and the functional and structural avidity of the CMV-specific T-cells was studied. Although all CMV-specific T-cells were isolated based on their reactivity towards a specific peptide-MHC complex, we observed a large variation in the functional avidity of the MHC-tetramer positive T-cell populations, which correlated with the structural avidity measured by the recently developed *Streptamer* k_{off} -rate assay. Our data demonstrate that MHC-tetramer staining is not always predictive for the sensitivity of specific T-cell reactivity, and challenge the sole use of MHC-tetramers as an indication of the peripheral T-cell repertoire, independent of the analysis of functional activity or structural avidity parameters.

INTRODUCTION

The almost unlimited size of the T-cell repertoire enables the adaptive immune system to protect the individual against a wide range of pathogens. T-cells can recognize pathogen derived antigens when presented on the cell membrane by the major histocompatibility antigen complex (MHC) via their unique T-cell receptor. An adequate T-cell receptor repertoire size is crucial for the immune system to continuously respond to new threats. The immense size of the T-cell receptor repertoire is accomplished by somatic recombination of the genes encoding the two different T-cell receptor heterodimer chains and is shaped by central tolerance to an estimated range of 10^6 to 10^7 unique T-cell receptors¹. After exposure to novel pathogen, immune surveying naïve T-cells that encounter their cognate antigen become activated, initiate a robust immune response and differentiate into memory T-cells. Precursor frequencies of antigen specific naïve T-cells are reported to influence both primary and memory T-cell responses to infection²⁻⁴.

The frequencies of distinct naïve T-cell clones are extremely low and these low numbers have complicated the possibilities to study the naïve T-cell repertoire^{5,6}. Quantification of preexisting antigen-specific T-cell numbers have been established by several functional assays such as limiting dilution analysis and repeated *in vitro* stimulations with antigen-loaded dendritic cells⁷⁻¹¹. In addition, MHC-class-I tetramers have been used to identify antigen-specific CD8⁺ T-cells in the memory and naïve repertoire¹²⁻¹⁵. However, the fact that functional CD8⁺ T-cells responding to infection can generally be identified by MHC-tetramer staining within the memory T-cell repertoire does not imply that T-cells identified in the naïve repertoire by MHC-tetramer staining are also generally antigen responsive. As we previously reported that MHC-tetramer positive T-cells within *in vitro* generated primary immune responses could demonstrate impaired T-cell reactivity^{16,17}, we aim to address this issue. Our observations may put the MHC-tetramer based quantification of naïve antigen specific T-cells into a different perspective. Functional characterization of antigen-specific naïve T-cells may provide insight into the natural avidity range of T-cells present within a MHC-tetramer positive T-cell repertoire in the absence of *in vivo* antigen exposure and subsequent selection of high-avidity T-cell clones. In addition it may help to understand intrinsic differences observed between T-cells derived from the memory or the naïve compartment^{18,19}.

In this report we present a method for the generation of naïve repertoire derived antigen-specific T-cell lines based on the combined use of MHC-tetramer staining and magnetic-bead enrichment. This method was used for the generation of functional CMV-specific T-cell lines from seronegative individuals within four weeks. We studied the functional characteristics of MHC-tetramer positive CMV-specific T-cells derived from the naïve compartment. Although the enriched T-cells were isolated based on their reactivity towards specific MHC-tetramers, we observed a large avidity variation within the isolated oligoclonal naïve T-cell populations. Part of the CMV-specific T-cells derived from the naïve

repertoire exhibited equal antigen-specific functionality as well as high MHC-tetramer staining as their memory response derived counterparts. However MHC-tetramer staining was not always predictive for antigen reactivity of isolated T-cells, since also functional non-reacting T-cells appeared MHC-tetramer positive. Our data indicate that when MHC-tetramers are used to isolate antigen-specific T-cells in an unbiased T-cell repertoire, both high and low-avidity T-cells may be isolated including T-cells that react to peptide in the context of MHC-tetramers but are functional non-reacting.

RESULTS

Isolation of CMV-specific T-cells by MHC-tetramer pull down from seronegative individuals

Primary CMV-specific T-cell lines were generated from peripheral blood mononuclear cells (PBMCs) of CMV-unexposed healthy donors as defined by CMV serology and confirmed by absence of MHC-tetramer positive T-cells. Four CMV-unexposed donors were selected for in duplicate generation of primary CMV-specific T-cell lines, by incubating 100×10^6 PBMCs with a set of CMV-specific MHC-tetramers, followed by enrichment of MHC-tetramer positive cells on a magnetic column. The set of MHC-tetramers covered 10 immunodominant CMV epitopes distributed over 5 HLA alleles that are most common among Dutch populations (HLA-A*0101, A*0201, B*0702, B*0801 and B*4001). The set of MHC-tetramers used for pull down was adjusted to the HLA-typing of each donor. After isolation of the MHC-tetramer enriched fraction, T-cells were expanded using anti-CD3/CD28 beads in the presence of irradiated autologous feeder cells, IL-2 and IL-15 for 14 days, and analyzed by multiparametric flow cytometry²¹.

After MHC-tetramer enrichment and subsequent expansion of all in duplicate generated T-cell lines, we were able to detect MHC-tetramer positive CD8⁺ T-cells specific for 8 out of 10 CMV-epitopes in one or more of the CMV-unexposed individuals covering all 5 selected HLA alleles (Table I). In all cases MHC-tetramer positive T-cell frequencies were low and varied between 0.01% and 2.3% of total CD8⁺ T-cells. A representative flow cytometric analysis of one T-cell line with the full panel of 11 different 2-color coded MHC-tetramers is shown in Fig. 1, in which 5 CMV-specific populations of the 8 CMV MHC-tetramer populations searched for were observed. In addition, a positive control HBV-specific T-cell population was detected.

After two weeks of expansion, additional MHC-tetramer isolations were performed to increase the frequencies of MHC-tetramer positive T-cells. For each donor, with the exception of donor B, the cell line with the most abundant MHC-tetramer positive T-cell populations was selected for a second pull down. For all donors, repeated pull down using the identical set of MHC-tetramers as was used for the initial isolation, resulted in increased frequencies of MHC-tetramer positive T-cells (Table I). CMV-specific MHC-tetramer positive

Table I. CMV-specific CD8⁺ T-cells after first and second MHC-tetramer pull down

Donor	HLA	1st Pull down										2nd Pull down											
		Experiment	pp65-Y5E	pp50-VTE	IE1-VLE	pp65-NLV	pp65-TPR	pp65-RPH	IE1-QIK	IE1-ELR	pp65-HER	pp65-CED	pp65-Y5E	pp50-VTE	IE1-VLE	pp65-NLV	pp65-TPR	pp65-RPH	IE1-QIK	IE1-ELR	pp65-HER	pp65-CED	
A	A*01																						
	A*02																						
	B*07																						
	B*27	S1	0.04	0	0	0.08	0.04	0	-	-	-	-	-	-	-	-	-	-	-	-	-	-	-
		S2	0	0	0.02	0	0	-	-	-	-	-	-	-	-	-	-	-	-	-	-	-	-
B	A*01																						
	A*02																						
	B*07																						
	B*08	S1	0.02	0	0	0.02	0	0	0.03	0	0	0.03	0	-	-	-	-	-	-	-	-	-	-
		S2	0.02	0.01	0	0.01	0	0	0.1	0.01	-	-	-	-	-	-	-	-	-	-	-	-	-
C	A*02																						
	A*03																						
	B*07																						
	B*40	S1	-	-	0	0.03	0	0	-	-	-	2.3	0	-	-	-	-	-	-	-	44	0	-
		S2	-	-	0	0.1	0	0	-	-	0	0	-	-	-	-	-	-	-	-	-	-	
D	A*01																						
	A*02																						
	B*07																						
	B*08	S1	0.3	0	0.1	0.2	0.01	0	0.2	0.01	0	0.2	0.01	-	-	-	-	-	-	-	-	-	-
		S2	0	0	0	0.05	0	0	0	0	0	0	-	-	-	-	-	-	-	-	-	-	-

Frequencies indicate percentage of total CD8⁺ T-cells.

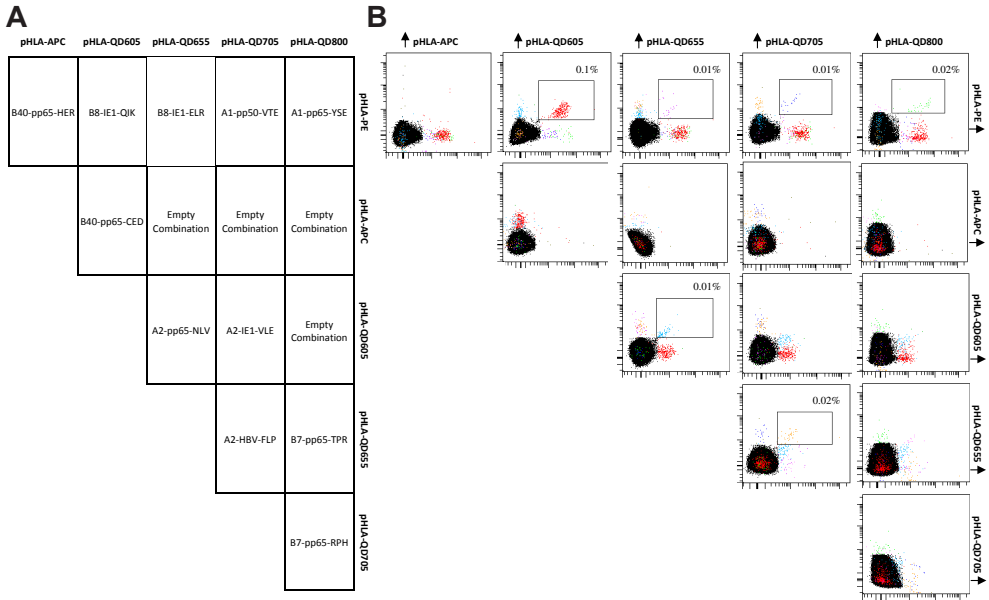


Figure 1. Dual color MHC-tetramer analysis of generated cell lines. CMV-specific T-cells were detected by dual-color MHC-tetramer screening after pull down and *in vitro* expansion. All dot plots are shown with bi-exponential axes and display fluorescence intensity for the indicated fluorochromes at the top and side of the plot matrix. Non MHC-tetramer specific CD8⁺ T-cells are indicated in black. (A) Schematic overview of dual-color MHC-tetramer screen covering 11 different CMV and HBV epitopes. Each peptide-MHC complex was encoded by a unique combination of fluorochromes, to screen for recognition of all epitopes in a single staining. (B) Representative example of MHC-tetramer screen of the pull down S1 derived T-cell line from donor B with a panel of 11 different dual-color MHC-tetramer combinations. Shown are total CD8⁺ T-cells. Specific MHC-tetramer positive T-cells will appear double positive for the respective peptide-HLA-fluorochrome combination. To determine the efficiency of the pull down protocol, we included in some experiments a human hepatitis B virus (HBV)-derived epitope. Detected are 6 dual-labeled CMV- and HBV-specific T-cell populations: IE1-QIK (red), IE1-ELR (pink), pp50-VTE (dark blue), pp65-YSE (green), pp65-NLV (blue) and HBV-FLP (orange). Indicated percentages are frequencies of gated double MHC-tetramer positive T-cell populations of the total CD8⁺ T-cells.

T-cell frequencies increased to 9.74%, 21.9%, 44.0% and 51.4% of total CD8⁺ T-cells for donor A, B, C and D, respectively. Testing with individual MHC-tetramers revealed that 10 of 14 previously detected populations were increased in frequency after an extra round of MHC-tetramer pull down. The frequency of 1 population remained similar (Donor D; B7-pp65-TPR), and 3 populations decreased or became undetectable (Donor B, C and D; A2-pp65-NLV). Four MHC-tetramer positive populations were newly discovered after the second pull down (Donor A; A1-p50-VTE, Donor B; A1-pp50-VTE and B8-IE1-ELR and Donor D; B7-pp65-RPH). Although the prevalence of some populations remained low after repeated MHC-tetramer isolation, most frequencies allowed functional assessment.

Precursor frequencies of MHC-tetramer positive T-cells affect the enriched T-cell line composition

Although the composition of the in duplicate generated T-cell lines was relatively similar for each CMV-unexposed donor, the absence of MHC-tetramer positive T-cells specific for some well-described immunodominant epitopes was remarkable. To investigate whether the composition of the generated cell lines was affected by differences in precursor frequencies of antigen-specific T-cells, unavailable donor TCR repertoire or reflected low reproducibility of the MHC-tetramer pull down method we performed a comparative analysis of 10 pull down experiments, all starting with 100×10^6 PBMCs from another CMV-unexposed donor (donor E). Consistent with the previous results, MHC-tetramer positive T-cell populations were detected in each of the 10 generated cell lines (Table II). A1-pp65-YSE MHC-tetramer positive T-cells were detected in each cell line, whereas, A1-pp50-VTE, A2-pp65-NLV or A2-IE1-VLE MHC-tetramer positive T-cells were detected in 1 or 2 of the 10 T-cell lines. Importantly, the composition of the T-cell lines cannot be considered as direct calculations of antigen-specific precursor frequencies as they are analyzed after *in vitro* expansion and its accuracy may be affected by selective expansion of specific T-cell clones. However, for A1-pp65-YSE specific T-cells a minimal number of 1 cell per 100×10^6 PBMCs, corresponding with 14×10^6 CD8⁺ T-cells stained positive with the specific MHC-tetramer.

Table II. CMV-specific CD8⁺ T-cells frequencies after 10 parallel MHC-tetramer pull down experiments

Donor	HLA	Experiment	1st Pull down			
			HLA-A*01		HLA-A*02	
			pp65-YSE	pp50-VTE	IE1-VLE	pp65-NLV
E	A*01 A*02 B*51 B*57	S1	0.48	0.16	0	0
		S2	0.72	0	0	0
		S3	0.27	0	0	0
		S4	0.26	0	0	0
		S5	0.33	0	0	0
		S6	0.62	0	0	0.04
		S7	0.53	0	0	0
		S8	0.37	0	0	0
		S9	0.36	0	0.01	0
		S10	0.36	0.17	0	0.01

Frequencies indicate percentage of total CD8⁺ T-cells

The precursor frequencies of T-cells specific for any of the other 3 CMV epitopes tested in donor E may be estimated to be at least 5-fold lower. Based on these data we speculate that, the composition of the T-cell lines, enriched from a fixed PBMCs number, is affected by variable precursor frequencies.

T-cell lines show CMV-specific IFN- γ production, but MHC-tetramer positive T-cells respond different

To assess the functionality of the enriched MHC-tetramer positive T-cell populations we stimulated the T-cell lines from the 4 donors with peptide loaded target cells and measured overnight IFN- γ production. As may be expected from the low frequencies of MHC-tetramer positive T-cells in the cell lines generated after one round of pull down, no or only marginal IFN- γ production was observed when these cell lines were stimulated with the different peptides for donor A, B and C (Fig. 2A-C). Only the enriched S1 T-cell line derived from donor D demonstrates a low IFN- γ response directed against the A1-pp65-YSE peptide

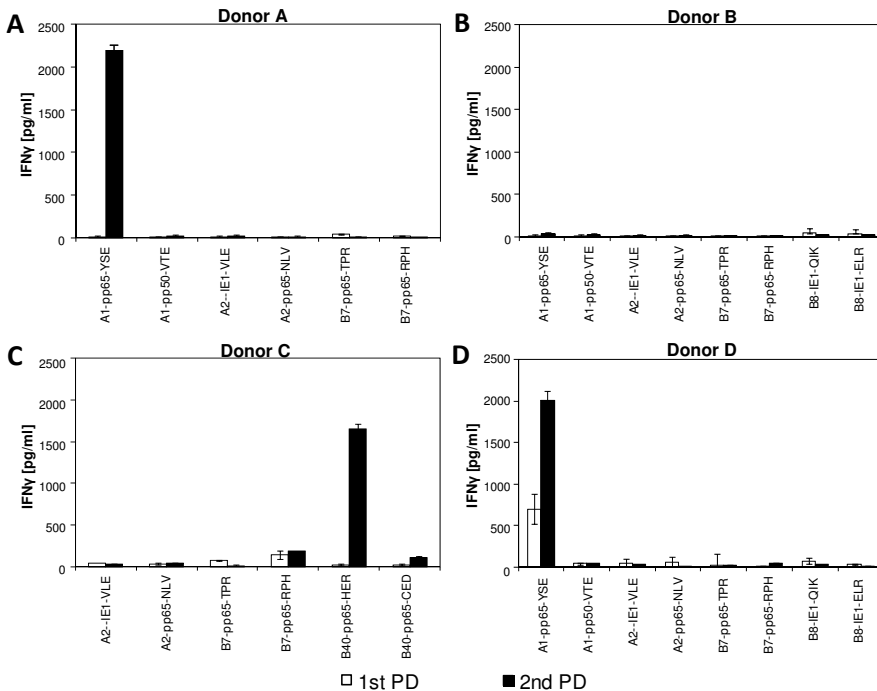


Figure 2. Stimulation assay MHC-tetramer enriched T-cell lines. Enriched CMV-specific T-cell lines derived from (A) donor A, (B) donor B, (C) donor C and (D) donor D were stimulated with single HLA-molecule transduced K562 target cells loaded with specific peptide after one and two rounds of MHC-tetramer pull down. T-cell reactivity was analyzed by measuring the secreted IFN- γ concentration in a standard ELISA. Data are shown as mean/median + SD/SEM of 3 replicates and are from one experiment representative of 2 performed.

(Fig. 2D). Increase in the frequency of the MHC-tetramer positive T-cell populations by a second pull down did result in a peptide-specific IFN- γ production for 3 of the 4 tested cell lines derived from donor A, C and D. However, not all T-cell populations present in these T-cell lines demonstrated to produce IFN- γ upon peptide-specific stimulation. The T-cell line derived from donor A, C and D that were enriched by second pull down harboring 4, 1 and 7 different CMV-specific T-cell populations, appeared only reactive to one peptide: A1-pp65-YSE, B40-pp65-HER and A1-pp65-YSE, respectively. Although for donor A and C the observed single peptide reactivity could be explained by the absence of other high frequent MHC-tetramer positive T-cell populations, donor D obtained 4 populations with frequencies above 2% of total CD8⁺ T-cells but appeared only reactive to A1-pp65-YSE stimulation. In addition both the high frequent A1-pp65-YSE (10,4%) and B8-IE1-QIK (11%) specific T-cell populations in donor B appeared unable to produce IFN- γ upon specific peptide stimulation.

To investigate whether the lack of IFN- γ production by some of the MHC-tetramer positive T-cell populations was due to their low frequencies or whether these T-cells were incapable to produce IFN- γ upon peptide-specific stimulation, we generated single MHC-tetramer specific T-cell lines. For this purpose, different donor E-derived T-cell lines were used for a second enrichment with single MHC-tetramers. This resulted in the generation of 7 T-cell lines specific for 3 CMV-epitopes with frequencies varying from 5.1% to 24.6% of total MHC-tetramer positive T-cells. T-cells specific for the A2-IE1-VLE epitope were lost after isolation. Subsequently, the single MHC-tetramer enriched T-cell lines were tested in a peptide titration assay to assess their peptide specificity and avidity (Fig. 3A). Four of the 7 enriched T-cell lines demonstrated a clear sigmoid shape antigen-dose response with variable half-maximum response (EC50). The enriched T-cell lines S10 A1-pp50-VTE (13.2%) and S1 A1-pp65-YSE (16.1%) demonstrated EC50 values between 1 and 5ng/ml, comparable with those of 3 high-avidity memory control clones, T-cell lines S8 A1-pp65-YSE (18.5%) and S1 A1-pp50-VTE (24.6%) demonstrated EC50 values of approximately 300 ng/ml. No peptide-specific IFN- γ production was observed for S6 A1-pp65-YSE (14.0%), S6 A2-pp65-NLV (5.2%) and S10 A2-pp65-NLV (5.1%) even when these T-cell lines were exposed to very high peptide concentrations. Stimulation with a panel of CMV-protein transduced target cells demonstrated that all T-cell lines that demonstrated peptide induced IFN- γ production were capable of recognizing endogenously presented peptide, irrespective of variable EC50 values (Fig. 3B-D). In addition, we screened the reactive and functional non-reactive MHC-tetramer positive T-cell lines for their capacity to produce 17 other cytokines, chemokines and growth factors besides IFN- γ upon activation (data not shown). Unlike the reactive T-cell lines the functional non-reactive T-cell lines were not capable of producing other cytokines. These data indicate that functional heterogeneity exists among the different MHC-tetramer positive T-cell lines generated from an identical donor, and that this did not correlate with the frequencies of the specific T-cell populations.

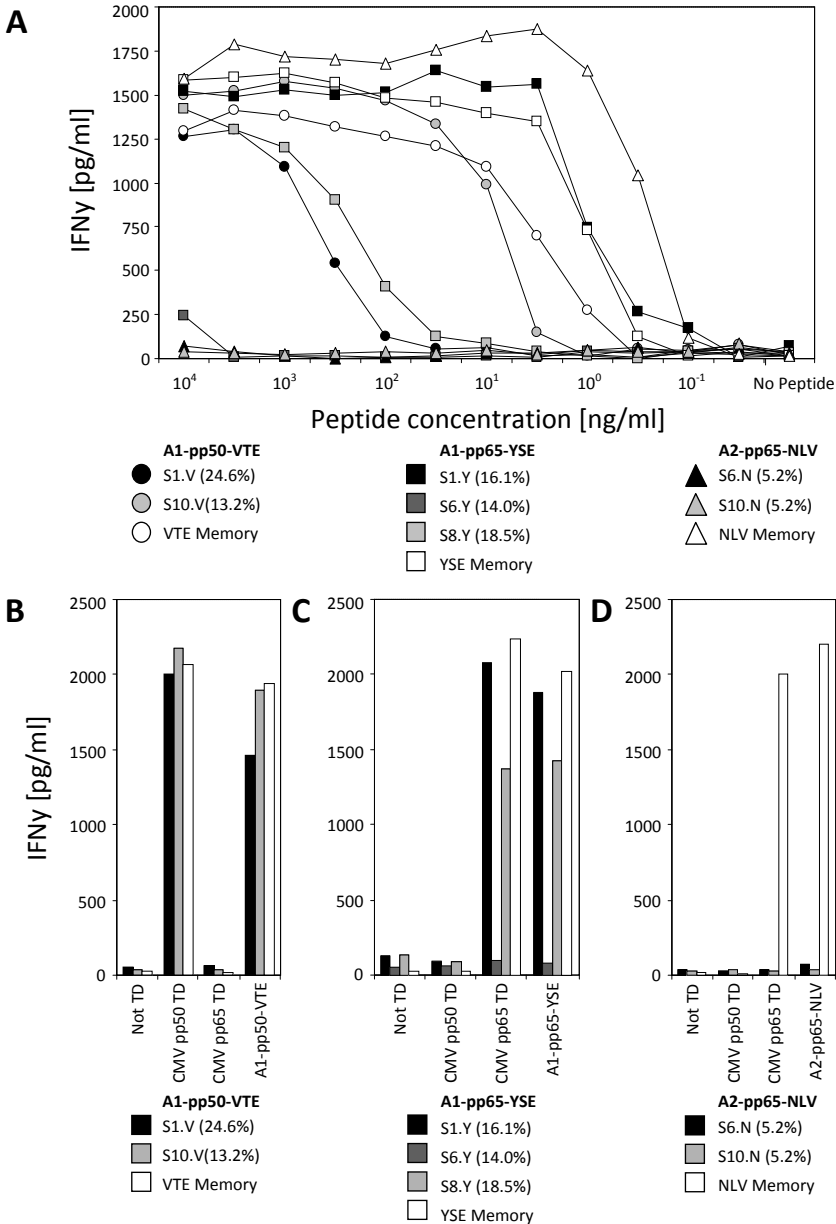
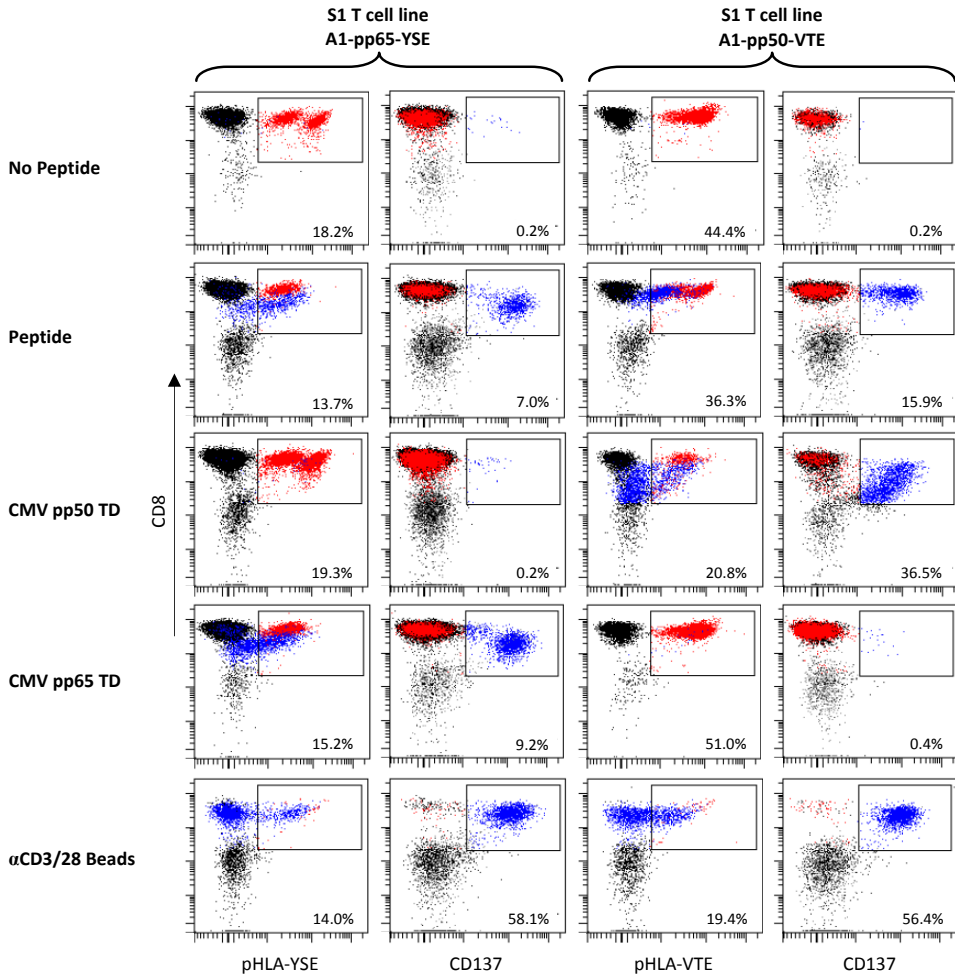


Figure 3. Avidity analysis of MHC-tetramer positive T-cell lines. Single MHC-tetramer positive T-cell lines demonstrated a wide range of peptide sensitivity. Single MHC-tetramer positive T-cell lines were generated from donor E and stimulated with (A) peptide-pulsed or (B) pp50, (C,D) pp65 CMV protein-transduced (TD) HLA-A*0101⁺ and HLA-A*0201⁺ EBV-LCL cells. Specific CMV-peptide was titrated in 3-fold dilution steps starting from 10 μ g/ml. T-cell reactivity was analyzed by measuring the overnight IFN- γ secretion in a standard ELISA. For each epitope a control clone derived from the memory compartment of a CMV experienced donor was used. Data are shown from one experiment.

To assess whether all MHC-tetramer positive T-cells within a single T-cell line contributed equally to the CMV-specific response, the T-cell lines were antigen specifically activated and the individual T-cells within the T-cell lines were screened for CMV-specific T-cell activation by measuring the efficiency of TCR internalization and induction of the activation marker CD137. The results shown in Fig. 4 demonstrate that variable parts of the total MHC-tetramer positive T-cell population revealed activation induced expression of CD137 and decreased MHC-tetramer staining intensity. For the S1 A1-pp65-YSE T-cell line containing 18.2% MHC-tetramer positive T-cells only 7.0% and 9.2% of CD8⁺ T-cells, corresponding with 38% to 51% of total MHC-tetramer positive cells, demonstrated activation induced CD137 expression when stimulated with peptide loaded or CMV-protein transduced target cells, respectively, and clearly downregulated their TCR as measured by decreased MHC-tetramer staining intensity. Comparable results were obtained with the S1 A1-pp50-VTE T-cell line containing 44.4% MHC-tetramer positive T cells as 15.9% and 36.5% of CD8⁺ T-cells, corresponding with 36% to 82% of total MHC-tetramer positive cells, demonstrated activation induced CD137 expression when stimulated with either peptide loaded or CMV-protein transduced stimulator cells, respectively. Furthermore, for the S6 A2-pp65-NLV T-cell line that previously showed no peptide-specific IFN- γ production, only marginal T-cell activation could be observed when stimulated with CMV-specific antigen. Irrespective of their specificity, all tested T-cell lines demonstrated strong activation by α CD3/28 beads, indicating their intrinsic capacity to become activated via TCR-mediated stimulation. Activated T-cells demonstrated a clear downregulation of MHC-tetramer staining after overnight stimulation. These data indicate that a substantial part of the MHC-tetramer positive T-cells fail to respond to specific antigen stimulation.

Functional heterogeneity by variable TCR-ligand k_{off} rate of MHC-tetramer reactivity T-cell clones

To study the functional heterogeneity observed among the isolate MHC-tetramer positive T-cells we analyzed the TCR $V\beta$ -usage of the MHC-tetramer positive T-cell lines derived from donor E by staining the cells with MHC-tetramer in combination with a $V\beta$ -antibody kit. At least 6 different TCR's could be identified within the 3 enriched A1-pp65-YSE MHC-tetramer positive T-cell lines S1, S6 and S8. For A1-pp50-VTE and A2-pp65-NLV MHC-tetramer positive T-cells, 3 and 2 different TCR $V\beta$ -usage were detected, respectively. T-cell clones representing the oligoclonal TCR spectrum were generated by single cell sorting and analyzed for their MHC-tetramer specificity. For the 6 A1-pp65-YSE specific T-cell clones variable MHC-tetramer reactivity was demonstrated when stained with a fixed MHC-tetramer concentration (Fig. 5A). The reactivity range varied between the S1.5.Y TCR $V\beta$ ND T-cell clone demonstrating high MHC-tetramer staining relatively similar to that of the YSE-memory control clone, and S6.12.Y TCR $V\beta$ 22 T-cell clone demonstrating a 2.5 fold lower MHC-tetramer reactivity. As a control for nonspecific MHC-tetramer staining a VTE-



memory control clone was stained with the A1-pp65-YSE specific MHC-tetramer.

Subsequently, expanding T-cell clones were analyzed for antigen reactivity by stimulating the clones with titrated concentration of peptide. For the A1-pp65-YSE specific T-cell clones a wide avidity range was demonstrated. Two representative T-cell clones expressing 2 different TCRs (S1.11.Y TCR V β 4 and S1.5.Y TCR V β ND) exhibited a high avidity recognition pattern similar to that of the memory control clone, 1 T-cell clone (S6.4.Y TCR V β 17) demonstrated only marginal IFN- γ production when stimulated with very high peptide concentrations and 3 T-cell clones (S6.25.Y TCR V β ND, S6.6.Y TCR V β 2 and S6.12.Y TCR V β 22) demonstrated no peptide recognition (Fig. 5B). No different cytokine profiles were observed when these T-cell clones were screened for their capacity to produce other cytokines besides IFN- γ (data not shown). All the high avidity T-cell clones were capable of recognizing endogenously presented peptide. Similar results were obtained for A1-

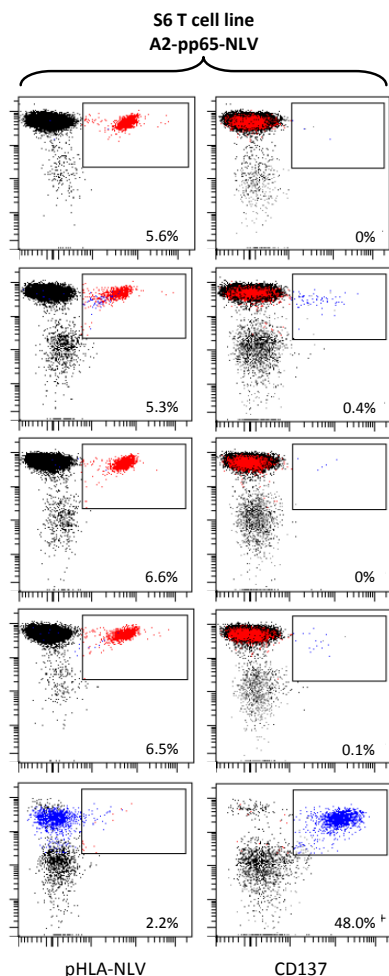


Figure 4. Flow cytometric analysis of stimulated CMV-specific T-cell lines. To demonstrate antigen specificity and functionality of the donor E-derived MHC-tetramer positive T-cell lines the cell lines were co-cultured with peptide pulsed (1 $\mu\text{g}/\text{ml}$), CMV-protein transduced (TD) HLA-A*0101⁺ and HLA-A*0201⁺ EBV-LCL or $\alpha\text{CD}3/28$ stimulation beads. TCR internalization and activation induced CD137 expression was analyzed by flow cytometry after 18 hours. Data are shown for the representative cell lines S1-A1-pp50-VTE, S1-A1-pp65-YSE and S6-A2-pp65-NLV. All dot plots are shown with bi-exponential axes and display fluorescence intensity for the indicated MHC-tetramer or cell markers. Most EBV-LCLs are deleted by CD19⁺ back-gating. However some EBV-LCL contamination remains and is indicated as CD8⁺ black dots. Non MHC-tetramer positive CD8⁺ T-cells are indicated black. T-cells expressing CD137 expression after stimulation are indicated blue. MHC-tetramer positive T-cells that do not express CD137 are indicated in red. Frequencies of MHC-tetramer⁺ or CD137⁺ T-cells are indicated and are percentages of total CD8⁺ T-cells. Data shown are representative of 3 experiments performed.

pp50-VTE specific T-cell clones expressing different TCRs as 2 out of 3 clones demonstrated high avidity peptide recognition and 1 clone demonstrated no peptide reactivity. No IFN- γ production was observed for T-cell clones specific for A2-pp65-NLV (data not shown).

To analyze whether the observed MHC-tetramer reactivity correlated with the detected T-cell avidity we compared the results of both assays obtained for various A1-pp65-YSE specific T-cell clones expressing different TCRs (Fig. 5C). Although the high avidity TCR $\text{V}\beta\text{ND}$ expressing specific T-cell clones demonstrated relatively similar MHC-tetramer reactivity compared to YSE memory control clone, the high avidity TCR $\text{V}\beta 4$ expressing T-cell clones demonstrated a significant 2-fold lower MHC-tetramer reactivity (YSE M: $P = 0.003$, $\text{V}\beta\text{ND}$: $P = 0.004$, as determined by the unpaired t-test; $P < 0.05$). The MHC-tetramer reactivity of the TCR $\text{V}\beta 4$ expressing T-cell clones was relatively similar to that of the nonfunctional TCR $\text{V}\beta 2$, $\text{V}\beta 22$, and part of the S6 derived $\text{V}\beta\text{ND}$ T-cell clones and even

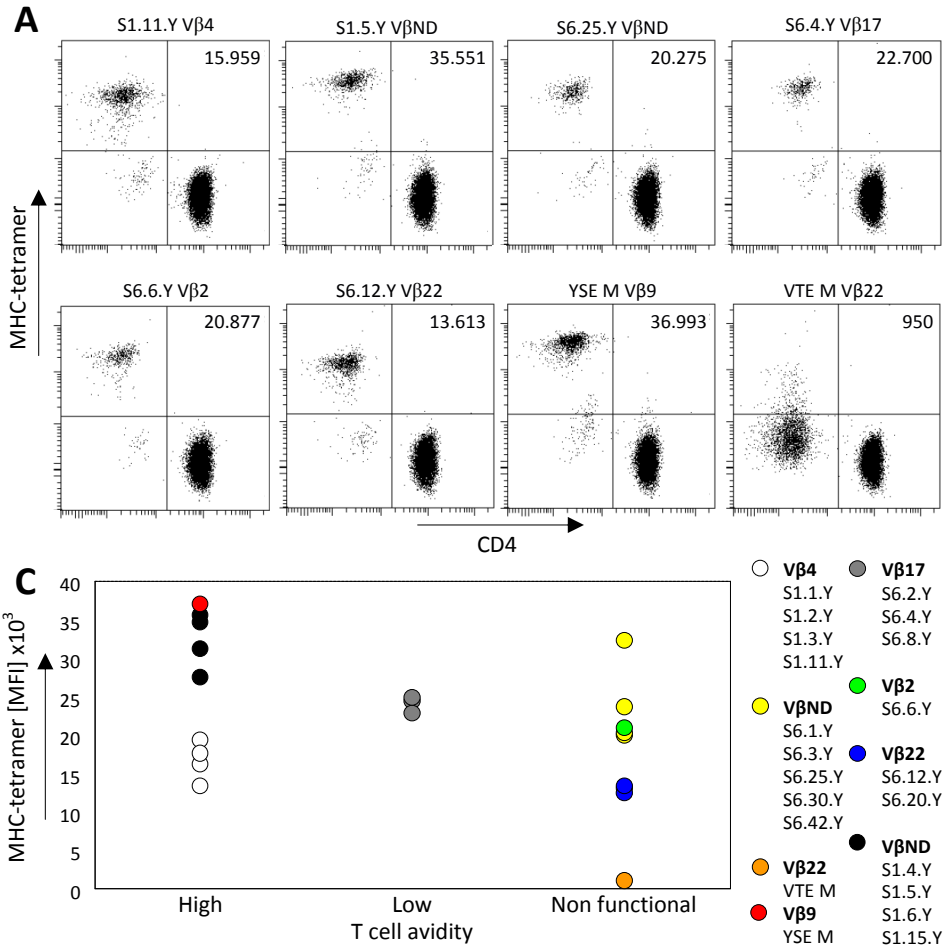
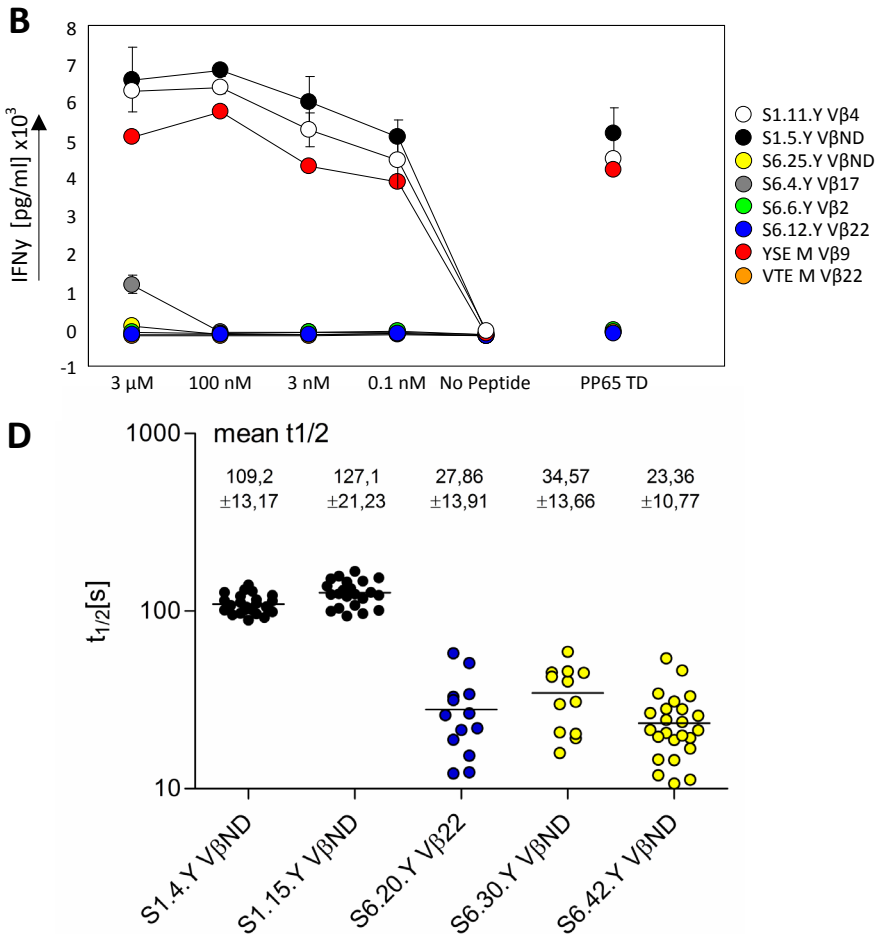


Figure 5. MHC-tetramer reactivity and structural TCR binding avidity of A1-PP65-YSE specific T-cell clones. Clonally expanded donor E-derived A1-pp65-YSE specific T-cell clones were compared with a memory control clone and demonstrated a wide range of functional heterogeneity. (A) Flow cytometric analysis of 6 representative A1-pp65-YSE specific T-cell clones expressing different TCRs is shown. For flow cytometry T-cell clones were mixed 1:5 with CD4⁺ T-cells prior to incubation with PE-coupled MHC-tetramer to prevent aggregate formation. Included are a high-avidity A1-pp65-YSE memory and a non-specific A1-pp50-VTE memory control clone. The MFI of the CD4-MHC-tetramer⁺ population is indicated in the upper right quadrant. (B) A1-pp65-YSE specific T-cell clones were stimulated with HLA-A*0101 and HLA-A*0201 positive EBV-LCLs pulsed with a titrated concentration of A1-pp65-YSE peptide starting with a concentration of 3 μ M. As a control for high avidity recognition of endogenously presented peptide, T-cells were stimulated with pp65 protein transduced target cells. T-cell reactivity was analyzed by measuring the IFN- γ production



after overnight stimulation in a standard ELISA. Data are shown as mean + SD/SEM of 3 replicates and are from one experiment representative of 2 performed. (C) Relationship between MHC-tetramer reactivity and T-cell avidity. High avidity T-cell clones were defined by their capacity to recognize endogenously presented peptide. Low avidity T-cell clones were defined by their capacity only to respond to high peptide concentrations and non functional T-cell clones demonstrated no IFN- γ production when stimulated with specific peptide. Data shown are from one representative experiment out of two experiments performed. (D) koff rate assay of 5 representative T-cell clones. The $t_{1/2}$ of 12 to 24 single cells of each T-cell clone stained with the HLA*0101/PP65-YSE Streptamer is shown. The values above symbols indicate the mean $t_{1/2}$ with standard deviation (\pm SD) for each measurement. The MFI of the tetramer staining of these T-cell clones was S1.4: MFI 27.500, S1.15: MFI 31.200, S6.20: MFI 13.000, S6.30: MFI 24.060, and S6.42: MFI 32.450. Data shown are from one experiment.

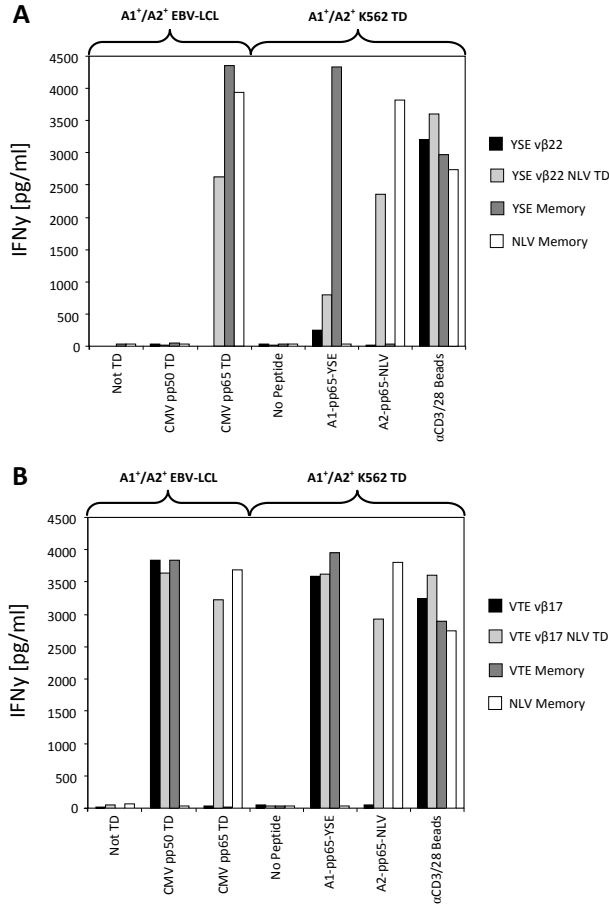


Figure 6. Stimulation assay TCR transduced T-cell clones. After clonal expansion a high-affinity pp65-NLV specific TCR was introduced in (A) low avidity T-cell clone YSE-Vβ22 and (B) high avidity clone VTE-Vβ17. TCR-transduced T-cell clones were stimulated with CMV PP50 or PP65 transduced (TD) HLA-A1 and -A2 positive EBV-LCL or peptide pulsed (1 μg/ml) K562 transduced with HLA-A1 and -A2 for 18 hours. Endogenous and introduced TCR-reactivity was analyzed by cytokine secretion in a standard IFN-γ ELISA. As a control for overall IFN-γ production, T-cells were nonspecifically stimulated with αCD3/28 beads. Data are shown from one experiment representative of 2 performed.

significant lower than that of the low avidity TCR Vβ17 expressing T-cell clone ($P = 0.008$), demonstrating that functionality of T-cells does not correlate with the intensity of MHC-tetramer staining.

To prove that the observed functional heterogeneity was not due to intrinsic differences between the TCR-bearing T-cells such as their naïve or memory phenotype, or coreceptor and adhesion molecule expression differences, we performed a *Streptamer*-based k_{off} rate assay in which the dissociation kinetics of monomeric peptide-MHC molecules

from different T-cell clones was measured²¹ (Fig. 5D). Representative nonfunctional T-cell clones (S6.30.Y V β ND, S6.42.Y V β ND, and S6.20.Y V β 22) exhibited very fast $t_{1/2}$ values, whereas the functional T-cell clones S1.4.Y V β ND and S1.15.Y V β ND bound the peptide-MHC complex for longer periods. Although all these T-cell clones exhibited positive MHC tetramer reactivity (S6.30: MFI 24.060, S6.42: 32.450, S6.20: MFI 13.000, S1.4: MFI 27.500, S1.15: MFI 31.200), they demonstrated differential functional avidity that correlated with the k_{off} rates of monomeric peptide-MHC complexes as a readout for structural TCR binding strength.

In addition, to confirm that the incapacity of T-cells to functionally react to cell-surface presented peptide-MHC complexes despite their ability to bind to MHC-tetramer and capacity to produce IFN- γ upon non-specific α CD3/28 is due to a low-affinity TCR and not caused by a different differentiation state of the tested T-cells, we introduced a high-affinity pp65-NLV specific TCR into the non-responsive A1-pp65-YSE specific V β 22 expressing T-cell clone by retroviral transduction²². Upon specific stimulation of the introduced TCR with peptide pulsed and CMV-protein transduced target cells, the TCR transduced T-cells were able to produce significant amounts of IFN- γ , which was not observed by stimulating the endogenous A1-pp65-YSE TCR (Fig. 6A). Introduction of the high affinity pp65-NLV specific TCR into the functional A1-pp50-VTE specific TCR V β 17 expressing T-cell clone, resulted in IFN- γ production after stimulation of both the introduced and endogenous TCR (Fig. 6B). These results indicate that these functionally non-responsive T-cells are intrinsically capable of reacting to peptide-MHC-complexes when a high-affinity TCR is introduced.

DISCUSSION

In this study CMV specific T-cells were isolated from 5 healthy CMV unexposed individuals. High-avidity CMV-specific T-cell reactivity was observed for T-cell lines generated from 4 out of 5 individuals when stimulated with endogenous antigen. Based on specific TCR V β -chain expression MHC-tetramer positive T-cell clones representing the oligoclonal TCR spectrum were generated by single cell sorting. The clonally expanded T-cell clones demonstrated a wide avidity range for their specific antigens. As the selected PBMCs donors were CMV-unexposed no previous clonal selection has taken place among T-cell clones competing for cognate antigen, narrowing the range CMV specific T-cells towards a few immunodominant clones that can efficiently clear infection²³. The *in vitro* generated T-cell lines were solely selected based on TCR-MHC-tetramer with no subsequent selection for CMV reactivity. As the TCR diversity in the naïve repertoire has been reported to be at least 100-fold higher compared to the memory T-cell repertoire and high avidity T-cells are selectively enriched in the memory subset a substantial part of the isolated T-cells will be of low-avidity^{5,11}. The composition of the generated T-cell lines most likely reflected the broad MHC-tetramer positive T-cell repertoire before antigen driven T-cell selection.

It has been reported that frequencies of antigen specific naïve T-cells affect the

response kinetics to primary infection and regulate immunodominance^{2;24-27}. Although we assessed T-cell precursor frequencies by indirect quantification, we demonstrate that the number of isolated MHC-tetramer positive T-cells was not predictive for the number of functional CMV specific T-cells. The isolation of high avidity T-cells was not restricted to the most frequently detected A1-pp65-YSE specific T-cells, and a substantial part of the less frequently detected A1-pp50-VTE specific T-cells demonstrated high CMV functional reactivity. The precursor frequency of A2-pp65-NLV specific naïve T-cells have been described by direct MHC-tetramer analysis to be 1 in 600 thousand (0.6×10^{-6}) CD8⁺ T-cells and conserved among individuals¹⁴. We estimated the precursor frequency even 55-fold lower to be 1 in 33 million CD8⁺ T-cells and we only isolated non-functional T-cells. Our data indicate that irrespective to quantitative measurements we need to assess the quality of MHC-tetramer positive T-cells to be able to predict response kinetics of the naïve T-cell repertoire to primary infections.

To study the impact of variable precursor frequencies of CMV-specific naïve T-cells on the shaping of a protective memory repertoire we analyzed 40 seropositive donors by MHC-tetramer staining for the prevalence of CMV-specific T-cells (Table III). The frequent detection of A1-pp65-YSE specific memory T-cells in 14 of the 17 individuals was in line with the frequent detection of high-avidity T-cells specific for this epitope in seronegative donors. In contrast, no correlation was observed for the detection of T-cells specific for A2-pp65-NLV as a memory response specific for this epitope was frequently observed in 20 of the 24 individuals but no functional T-cells were isolated from seronegative donors. Apparently high avidity T-cells restricted to these immunodominant epitopes are available in the majority of individual T-cell repertoires. However, the success rate for finding these T-cells in the naïve repertoire may be affected by their low precursor frequencies. The incapacity to isolate functional A2-pp65-NLV from the naïve repertoire was also reported by Hanley et al²⁸. These data indicate that the observed precursor frequencies of high-avidity CD8⁺ T-cells within an unprimed naïve repertoire may not directly reflect the shape of the late-phase memory repertoire after *in vivo* antigen exposure. *In vivo* priming by antigen presenting cells and subsequent cytokine-driven expansion of specific T-cell clones may result in uneven clonal expansion of different T-cell clones.

The frequent isolation of low avidity T-cells with high MHC-tetramer staining addresses the question whether a correlation between TCR-MHC-tetramer reactivity and the avidity of a specific T-cell exists and whether MHC-tetramer staining can function as a predictive value for T-cell functionality. Although MHC-tetramer reactivity of a given TCR may be predictive for its functionality when memory T-cells are compared, the observation that A1-pp65-YSE and A1-pp50-VTE specific T-cell clones demonstrated no strict correlation between MHC-tetramer reactivity and T-cell avidity suggest that this may be different for an unbiased CMV-inexperienced T-cell repertoire. We demonstrated that high avidity CMV-specific T-cells derived from the naïve T-cell repertoire showed relatively similar MHC-

Table III. Direct MHC-tetramer analysis of CMV-specific CD8⁺ T-cells in 40 seropositive donors

Donor	HLA				HLA-A*01		HLA-A*02		HLA-B*07		HLA-B*08	
	A*0101	A*0201	B*0702	B*0801	pp65-YSE	pp50-VTE	IE1-VLE	pp65-NLV	pp65-TPR	pp65-RPH	IE1-QIK	IE1-ELR
1	+	-	-	-	0.14	0	-	-	-	-	-	-
2	-	+	+	-	-	-	0.01	0	0.06	0.02	-	-
3	+	-	-	+	0.15	0.14	-	-	-	-	0.07	0
4	-	+	-	-	-	-	0.09	0.02	-	-	-	-
5	-	+	+	-	-	-	0.49	0	0	0.01	-	-
6	+	-	-	+	0.9	0.03	-	-	-	-	2.5	0
7	+	+	-	+	0.6	0.05	0.06	0	-	-	0.1	0
8	-	-	+	-	-	-	-	0.13	0.74	-	-	-
9	+	-	-	+	0.11	0.07	-	-	-	-	0	0.64
10	+	-	-	+	0.02	0.04	-	-	-	-	0	0.64
11	-	+	-	-	-	-	0.76	0.3	-	-	-	-
12	-	+	-	-	-	-	0.1	0	-	-	-	-
13	-	+	-	+	-	-	0.65	0	-	-	0	0
14	-	+	+	-	-	-	0.9	0	0.06	0.3	-	-
15	+	+	-	+	1.2	0.01	0.36	0	-	-	0.3	2.1
16	-	-	+	-	-	-	-	-	0.16	0.07	-	-
17	+	+	+	+	0.58	0.02	0	0	0.5	0.27	0	0
18	+	+	+	+	0.54	0	0.03	0	0.51	0.02	0.02	0
19	-	-	+	-	-	-	-	-	0.81	0.06	-	-
20	+	-	-	+	0	0.06	-	-	-	-	0.01	0
21	-	+	+	-	-	-	0.06	0	0	0.06	-	-
22	-	+	+	-	-	-	0.11	0	0.35	0.11	-	-
23	-	+	-	+	-	-	0.3	0	-	-	0.2	0
24	-	-	+	-	-	-	-	-	0.05	0.01	-	-
25	+	+	-	+	0.01	0	0	0	-	-	0.01	0
26	-	-	+	-	-	-	-	-	0.36	0.56	-	-
27	-	+	-	+	-	-	0.46	0	-	-	0.03	0.54
28	+	+	-	+	0.05	0.02	0.22	0	-	-	0.01	0
29	+	-	-	+	0.35	0.02	-	-	-	-	0.02	0
30	-	+	-	-	-	-	0.12	0.07	-	-	-	-
31	+	+	-	+	0.13	0.02	0.19	0	-	-	1.3	0
32	-	+	-	-	-	-	0.15	0	-	-	-	-
33	-	-	+	-	-	-	-	-	0.07	0.03	-	-
34	+	-	-	+	0.42	0.06	-	-	-	-	0.22	0.24
35	-	+	+	-	-	-	0	0	0.15	0.7	-	-
36	-	+	+	-	-	-	0	0.06	0.36	0.68	-	-
37	-	-	+	-	-	-	-	-	0	0.1	-	-
38	+	-	-	-	0.13	0.03	-	-	-	-	-	-
39	-	+	-	+	-	-	0.68	0	-	-	0.9	0
40	+	+	-	+	0.05	0.02	0.12	0	-	-	0.33	0
MHC-tetramer positive					16/17	14/17	20/24	4/24	13/16	16/16	15/19	5/19
Average frequency					0.32	0.04	0.26	0.14	0.29	0.27	0.27	0.88

Frequencies indicate percentage of total CD8⁺ T-cells

tetramer reactivity as high avidity T-cells obtained from a memory response. In addition, low or nonfunctional T-cell clones could demonstrate comparable or even increased MHC-tetramer staining when compared to high-avidity T-cell clones with the same specificity and obtained from the same individual. Non-responsiveness of MHC-tetramer positive T-cell clones has also been reported by others for tetramer positive T-cell-derived from the naïve repertoire^{24;29}. The discrepancy between MHC-tetramer reactivity and T-cell functionality may be explained by the staining with multimerized MHC-peptide complexes. Multimerization of MHC-peptide complexes alter the TCR-MHC-peptide dissociation on- and off-rate kinetics and may result in increased binding avidity of the multimerized MHC-peptide complex to surface TCR³⁰. By measuring the TCR binding strength to monomeric peptide-MHC complexes we demonstrated that the dissociation kinetics correlated with the observed functional avidity of the different T-cell clones, and that this was independent of the intensity of MHC-tetramer reactivity.

In conclusion, the method described in this study may find application in studying the naïve T-cell repertoire before antigen driven T-cell selection. Our data put a critical note to the direct monitoring of the shape of the peripheral naïve T-cell repertoire independent of the analysis of functional activity or structural avidity parameters.

ACKNOWLEDGEMENTS

We thank Menno van der Hoorn, Guido de Roo and Patrick van der Holst for flow cytometric cell sorting and MHC-tetramer analysis of CMV seropositive donor cohort.

MATERIALS AND METHODS

Culture conditions and cells. Peripheral blood was obtained from different individuals with informed consent (Sanquin Reagents, Amsterdam, The Netherlands). All experiments were approved by the local medical ethics committees. Blood samples were HLA-typed by high-resolution genomic DNA-typing and serological immunoassay was performed using the AxSYM microparticle enzyme immunoassay (Abbott, Abbott Park, IL) for the detection of anti-CMV IgG/IgM antibodies. Peripheral blood mononuclear cells (PBMCs) were isolated by Ficoll gradient separation and cryopreserved for further use. Donor samples were included when CMV serology was negative and when the frequencies of MHC-tetramer positive T-cells appeared less than 0.01% of total CD8⁺ T-cells. T-cells were cultured in Iscove's Modified Dulbecco's Media (IMDM: Lonza, Basel, Switzerland) containing 5% human serum, 5% fetal bovine serum (FBS), 2 mM L-glutamine, 100 U/ml penicillin, and 100 µg/ml streptomycin (Invitrogen, Carlsbad, CA) supplemented with 100 IU/ml IL-2 (Proleukin; Chiron, Amsterdam, The Netherlands). Feeder fractions were irradiated with 50 Gy. Stable Epstein-Barr virus-transformed lymphoblastoid B-cell lines (EBV-LCL) and phytohemagglutinine (PHA) blasts were generated using standard procedures.

Generation of peptide-MHC complexes. All peptides were synthesized in-house using standard Fmoc chemistry. Recombinant HLA-A*0201 heavy chain and human β_2m light chain were in-house produced in *Escherichia coli*. MHC class I refolding was performed as previously described with minor modifications³¹. MHC class I complexes were purified by gel-filtration HPLC in PBS and stored at 4°C.

Isolation of CMV-specific T-cells by MHC-tetramer pull down. Prior to isolation PBMCs samples were stained with PE-coupled MHC-tetramers for 1 hour at 4°C. Subsequently, cells were washed and incubated with anti-PE antibody coated magnetic beads (Miltenyi Biotec, Bergisch Gladbach, Germany). Cells were then isolated by magnetic activated cell sorting (MACS) using an LS column, following the manufacturer's protocol (Miltenyi). Eluted cells were cultured per 5000 cells with 5×10^4 irradiated (50 Gy) autologous feeder cells in presence of 100 IU/ml IL-2, 5ng/ml IL-15 (Biosource) and 11.000 anti-CD3/CD28 Dynabeads (Invitrogen) for polyclonal stimulation in 96-well plates. Cultures were refreshed at least twice a week. After 2 weeks, cell cultures were analyzed for peptide-specific T-cell populations by MHC-tetramer flow cytometry. Subsequently MHC-tetramer pull down and expansion procedure was repeated or MHC-tetramer positive T-cell populations were sorted on a FACSAria (BD Biosciences, San Diego, USA) into 96 well plates containing 1×10^5 irradiated feeder cells supplemented with 0.5 µg/mL PHA.

Flow cytometry and T-cell staining. Data acquisition was performed on an LSR-II flow cytometer (BD) with FACS Diva software using the following 11-color instrument settings: 488 nm laser: PI: 685LP, 695/40; PE: 550LP, 575/26; FITC: 505LP, 530/30; SSC: 488/10. 633 nm laser: Alexa700: 685LP, 730/45; APC: 660/20. 405 nm laser: QD800: 770LP, 800/30; QD705: 680LP, 710/50; QD655: 635LP, 660/40; QD605: 595LP, 650/12. 355 nm laser: QD585: 575LP, 585/15; QD565: 545LP: 560/20. Approximately

1×10^6 PBMCs were stained for each analysis with a final concentration of $2 \mu\text{g}/\text{mL}$ per MHC-tetramer in $100 \mu\text{l}$ Phosphate buffered saline (PBS) with 5% (v/v) pasteurized plasma protein solution (GPO). Next, antibody-mixtures consisting of CD8-Alexa700 (Caltag-MedSystems, Buckingham, UK), CD4-, CD14-, CD19-FITC or CD137-allophycocyanin (BD) were added and cells were incubated for 30 min at 4°C . Prior to flow cytometry, cells were washed twice. For dual-encoding MHC-tetramer staining a set of fluorescently labeled MHC-tetramers was generated in which each specific peptide-MHC complex was encoded by a unique combination of two fluorochromes, to screen for recognition of all CMV-epitopes in a single sample. For assessment of TCR-V β -chain usage the TCR-V β repertoire kit was used (Beckman Coulter, Takeley, UK) according to the manufactory protocol.

Functional analysis. For analysis of IFN- γ production, 5000 T-cells were cocultured with 25.000 target cells loaded with different concentrations of CMV, control peptides or with artificial Ag-presenting beads. To test the functional activity of the T-cells against target cells presenting endogenously processed antigen, we used K562 transduced with single HLA molecules or EBV-LCL transduced with a retroviral vector containing a CMV-pp65/-pp50 or -IE1 expression construct as target cells³². Peptide loading was performed by incubating target cells for 1 hour in 96 well plates at 37°C and 5% CO_2 in IMDM containing 2% FBS and cells were washed twice before use. After 24 h, supernatants were harvested, and the concentration of IFN- γ was measured by an enzyme-linked immunosorbent assay (Sanquin Reagents). For FACS analysis of activation induced TCR internalization 10.000 effector cells were incubated with 50.000 target cells.

TCR gene transfer. The construction of the retroviral vector encoding the TCR chains of the CMV-pp65 specific T-cell clone have been described earlier³³. The high-affinity CMV-TCR-AV18 T-cell receptor was transduced in the selected T-cell clones two days after stimulation as previously described. Marker gene eGFP and NGF-R double positive T-cells were subsequently sorted³⁴.

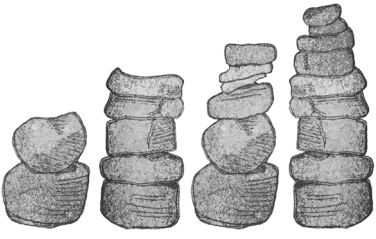
k_{off} -rate assays. The dissociation kinetics of monomeric pMHC molecules bound to cell surface expressed TCRs was determined using the *Streptamer*-based k_{off} rate assay that was recently described²¹. In short, T-cell clones were incubated with *Strep*-Tactin Allophycocyanin (APC) and HLA*0101/PP65-YSE Atto565 double labeled *Streptamers* for 45 min on ice. To prevent internalization of MHC molecules, *Streptamer*-stained cells were constitutively kept at 4°C . Fluorescence images were taken on a Leica SP5 confocal laser scanning microscope before and every 10 seconds after the addition of D-biotin until complete dissociation of the MHCs.

REFERENCES

1. Davis, M.M. and Bjorkman, P.J., T-cell antigen receptor genes and T-cell recognition. *Nature* 1988. 334: 395-402.
2. Obar, J.J., Khanna, K.M., and Lefrancois, L., Endogenous naive CD8+ T cell precursor frequency regulates primary and memory responses to infection. *Immunity*. 2008. 28: 859-869.
3. La Gruta, N.L., Rothwell, W.T., Cukalac, T., Swan, N.G., Valkenburg, S.A., Kedzierska, K., Thomas, P.G., et al., Primary CTL response magnitude in mice is determined by the extent of naive T cell recruitment and subsequent clonal expansion. *J Clin. Invest* 2010. 120: 1885-1894.
4. Kwok, W.W., Tan, V., Gillette, L., Littell, C.T., Soltis, M.A., LaFond, R.B., Yang, J., et al., Frequency of epitope-specific naive CD4(+) T cells correlates with immunodominance in the human memory repertoire. *J Immunol* 2012. 188: 2537-2544.
5. Arstila, T.P., Casrouge, A., Baron, V., Even, J., Kanellopoulos, J., and Kourilsky, P., A direct estimate of the human alphabeta T cell receptor diversity. *Science* 1999. 286: 958-961.
6. Goldrath, A.W. and Bevan, M.J., Selecting and maintaining a diverse T-cell repertoire. *Nature* 1999. 402: 255-262.
7. Peterson, D.A., DiPaolo, R.J., Kanagawa, O., and Unanue, E.R., Quantitative analysis of the T cell repertoire that escapes negative selection. *Immunity*. 1999. 11: 453-462.
8. Teh, H.S., Harley, E., Phillips, R.A., and Miller, R.G., Quantitative studies on the precursors of cytotoxic lymphocytes. I. Characterization of a clonal assay and determination of the size of clones derived from single precursors. *J. Immunol.* 1977. 118: 1049-1056.
9. Blattman, J.N., Antia, R., Sourdive, D.J., Wang, X., Kaech, S.M., Murali-Krishna, K., Altman, J.D., et al., Estimating the precursor frequency of naive antigen-specific CD8 T cells. *J. Exp. Med.* 2002. 195: 657-664.
10. Ho, W.Y., Nguyen, H.N., Wolf, M., Kuball, J., and Greenberg, P.D., In vitro methods for generating CD8+ T-cell clones for immunotherapy from the naive repertoire. *J. Immunol. Methods* 2006. 310: 40-52.
11. Geiger, R., Duhon, T., Lanzavecchia, A., and Sallusto, F., Human naive and memory CD4+ T cell repertoires specific for naturally processed antigens analyzed using libraries of amplified T cells. *J. Exp. Med.* 2009. 206: 1525-1534.
12. Altman, J.D., Moss, P.A., Goulder, P.J., Barouch, D.H., McHeyzer-Williams, M.G., Bell, J.I., McMichael, A.J., et al., Phenotypic analysis of antigen-specific T lymphocytes. *Science*. 1996. 274: 94-96. *J. Immunol.* 2011. 187: 7-9.
13. Hataye, J., Moon, J.J., Khoruts, A., Reilly, C., and Jenkins, M.K., Naive and Memory CD4+ T Cell Survival Controlled by Clonal Abundance. *Science* 2006. 312: 114-116.
14. Alanio, C., Lemaitre, F., Law, H.K., Hasan, M., and Albert, M.L., Enumeration of human antigen-specific naive CD8+ T cells reveals conserved precursor frequencies. *Blood* 2010. 115: 3718-3725.
15. Seah, S.G., Sutherland, R.M., La Gruta, N.L., Brown, L.E., Carrington, E.M., Belz, G.T., Brady, J.L., et al., The linear range for accurately quantifying antigen-specific T-cell frequencies by tetramer staining during natural immune responses. *Eur. J Immunol* 2011. 41: 1499-1500.
16. Hombrink, P., Hadrup, S.R., Bakker, A.H., Kester, M.G.D., Falkenburg, J.H.F., von dem Borne, P.A., Schumacher, T.N.M., et al., High-Throughput Identification of Potential Minor Histocompatibility Antigens by MHC Tetramer-Based Screening: Feasibility and Limitations. *PLoS ONE* 2011. 6: e22523.
17. Amir, A.L., van der Steen, D.M., van Loenen, M.M., Hagedoorn, R.S., de Boer, R., Kester, M.D., de Ru, A.H., et al., PRAME-specific Allo-HLA-restricted T cells with potent antitumor reactivity

- useful for therapeutic T-cell receptor gene transfer. *Clin.Cancer Res.* 2011. 17: 5615-5625.
18. Hinrichs,C.S., Borman,Z.A., Cassard,L., Gattinoni,L., Spolski,R., Yu,Z., Sanchez-Perez,L., et al., Adoptively transferred effector cells derived from naive rather than central memory CD8+ T cells mediate superior antitumor immunity. *Proc.Natl.Acad.Sci.U.S.A* 2009. 106: 17469-17474.
 19. Berard,M. and Tough,D.F., Qualitative differences between naive and memory T cells. *Immunology* 2002. 106: 127-138.
 20. Hadrup,S.R., Bakker,A.H., Shu,C.J., Andersen,R.S., van Veluw,J., Hombrink,P., Castermans,E., et al., Parallel detection of antigen-specific T-cell responses by multidimensional encoding of MHC multimers. *Nat.Methods* 2009. 6: 520-526.
 21. Nauwerth,M., Weißbrich B, and Knall,B., TCR-ligand k_{off} -rate predicts protective capacity of antigen-specific CD8⁺ T cells for adoptive transfer. *Sci Transl Med* 2013. 5: 192ra87.
 22. Heemskerck,M.H.M., Hoogeboom,M., Hagedoorn,R., Kester,M.G.D., Willemze,R., and Falkenburg,J.H.F., Reprogramming of Virus-specific T Cells into Leukemia-reactive T Cells Using T Cell Receptor Gene Transfer. *The Journal of Experimental Medicine* 2004. 199: 885-894.
 23. Busch,D.H. and Pamer,E.G., T cell affinity maturation by selective expansion during infection. *J.Exp.Med.* 1999. 189: 701-710.
 24. Ford,M.L., Koehn,B.H., Wagener,M.E., Jiang,W., Gangappa,S., Pearson,T.C., and Larsen,C.P., Antigen-specific precursor frequency impacts T cell proliferation, differentiation, and requirement for costimulation. *J.Exp.Med.* 2007. 204: 299-309.
 25. Moon,J.J., Chu,H.H., Pepper,M., McSorley,S.J., Jameson,S.C., Kedl,R.M., and Jenkins,M.K., Naive CD4(+) T cell frequency varies for different epitopes and predicts repertoire diversity and response magnitude. *Immunity.* 2007. 27: 203-213.
 26. Tan,A.C., La Gruta,N.L., Zeng,W., and Jackson,D.C., Precursor frequency and competition dictate the HLA-A2-restricted CD8+ T cell responses to influenza A infection and vaccination in HLA-A2.1 transgenic mice. *J Immunol* 2011. 187: 1895-1902.
 27. Day,E.B., Charlton,K.L., La Gruta,N.L., Doherty,P.C., and Turner,S.J., Effect of MHC class I diversification on influenza epitope-specific CD8+ T cell precursor frequency and subsequent effector function. *J Immunol* 2011. 186: 6319-6328.
 28. Hanley,P.J., Cruz,C.R., Savoldo,B., Leen,A.M., Stanojevic,M., Khalil,M., Decker,W., et al., Functionally active virus-specific T cells that target CMV, adenovirus, and EBV can be expanded from naive T-cell populations in cord blood and will target a range of viral epitopes. *Blood* 2009. 114: 1958-1967.
 29. Derby,M.A., Wang,J., Margulies,D.H., and Berzofsky,J.A., Two intermediate-avidity cytotoxic T lymphocyte clones with a disparity between functional avidity and MHC tetramer staining. *Int.Immunol* 2001. 13: 817-824.
 30. Knabel,M., Franz,T.J., Schiemann,M., Wulf,A., Villmow,B., Schmidt,B., Bernhard,H., et al., Reversible MHC multimer staining for functional isolation of T-cell populations and effective adoptive transfer. *Nat.Med.* 2002. 8: 631-637.
 31. Burrows,S.R., Kienzle,N., Winterhalter,A., Bharadwaj,M., Altman,J.D., and Brooks,A., Peptide-MHC class I tetrameric complexes display exquisite ligand specificity. *J Immunol* 2000. 165: 6229-6234.
 32. Amir,A.L., D'Orsogna,L.J., Roelen,D.L., van Loenen,M.M., Hagedoorn,R.S., de Boer,R., van der Hoorn,M.A., et al., Allo-HLA reactivity of virus-specific memory T cells is common. *Blood* 2010. 115: 3146-3157.
 33. Heemskerck,M.H., Hoogeboom,M., de Paus,R.A., Kester,M.G., van der Hoorn,M.A., Goulmy,E.,

- Willemze,R., et al., Redirection of antileukemic reactivity of peripheral T lymphocytes using gene transfer of minor histocompatibility antigen HA-2-specific T-cell receptor complexes expressing a conserved alpha joining region. *Blood* 2003. 102: 3530-3540.
34. Kuball,J., Dossett,M.L., Wolf,I., Ho,W.Y., Voss,R.H., Fowler,C., and Greenberg,P.D., Facilitating matched pairing and expression of TCR chains introduced into human T cells. *Blood* 2007. 109: 2331-2338.



4

Journal of Immunology 2013

DISCOVERY OF T-CELL EPITOPES IMPLEMENTING HLA-PEPTIDOMICS INTO A REVERSE IMMUNOLOGY APPROACH

Pleun Hombrink¹, Chopie Hassan², Michel G.D. Kester¹, Arnoud H. de Ru², Cornelis A.M. van Bergen¹, Harm Nijveen³, Jan W. Drijfhout², J.H. Frederik Falkenburg¹, Mirjam H.M. Heemskerk^{1,5} and Peter A. van Veelen^{2,5}

¹ Department of Hematology, Leiden University Medical Center, Leiden, The Netherlands;

² Department of Immunohematology and Blood Transfusion, Leiden University Medical Center, Leiden, The Netherlands;

³ The Laboratory of Bioinformatics, Wageningen University, Wageningen, The Netherlands

⁵ Shared Senior Authorship

T-cell recognition of minor histocompatibility antigens (MiHA) plays an important role in the graft-versus-tumor (GVT) effect of allogeneic stem cell transplantation (allo-SCT). Selective infusion of T-cells reactive for hematopoiesis-restricted MiHA presented in the context of HLA class I or II molecules may help to separate the GVT effects from graft-versus-host disease (GVHD) effects after allo-SCT. Over the years, increasing numbers of MiHA have been identified by forward immunology approaches that are characterized by the isolation of T-cells with antigen specificities which are not predefined. As the tissue distribution of MiHA affects the clinical outcome of T-cell responses against these antigens it would be beneficial to identify predefined MiHA that are exclusively expressed on malignant cells. Therefore, several reverse immunology approaches have been explored for the prediction of MiHA. Thus far, these approaches frequently resulted in the identification of T-cells directed against epitopes that are not naturally processed and presented. In this study we established a method for the identification of biologically relevant MiHA implementing mass spectrometry based HLA-peptidomics into a reverse immunology approach. For this purpose HLA class I binding peptides were eluted from transformed B-cells, analyzed by mass spectrometry and matched with a database dedicated to identify polymorphic peptides. This resulted in a set of 40 MiHA candidates that was evaluated in multiple selection steps. The identification of LB-NISCH-1A demonstrated the technical feasibility of our approach. Based on these results we present an approach that can be of value for the efficient identification of MiHA or other T-cell epitopes.

INTRODUCTION

Over the past decades, allogeneic stem cell transplantation (allo-SCT) and subsequent donor lymphocyte infusion (DLI) has proven to be a valuable therapeutic regimen to treat hematological malignancies^{1,2}. Eradication of tumor burden and long-term remission in patients with hematological malignancies including leukemia has been attributed to the recognition of malignant cells by donor T-cells. Detailed analyses of T-cell immune responses in patients responding to DLI have demonstrated that the donor T-cells recognize minor histocompatibility antigens (MiHA) presented in the context of HLA molecules on malignant cells. These MiHA are peptides derived from polymorphic proteins that differ between donor and recipient due to single nucleotide polymorphisms (SNP)³⁻⁵. Whether donor T-cells mediate beneficial graft-versus-leukemia (GVL) responses or harmful graft-versus-host-disease (GVHD) is likely to depend on the tissue distribution of the target antigen. If the donor T-cell response is directed against MiHA that are ubiquitously expressed it may mediate GVHD⁶, a major cause of transplant-related morbidity and mortality^{7,8}, whereas selective infusion of T-cells reactive with MiHA exclusively expressed on hematopoietic cells is considered an attractive therapy to establish a GVL response in absence of GVHD⁹.

Over the years, increasing numbers of MiHA have been identified by cDNA library screening¹⁰⁻¹², genetic linkage analysis¹³⁻¹⁵, peptide elution from HLA¹⁶⁻¹⁸ and genome-wide association analysis¹⁹⁻²¹. Collectively, these methods use a forward immunology approach characterized by the isolation of activated T-cells from patients demonstrating a clinical response to DLI after allo-SCT and subsequent elucidation of the antigens recognized. The intrinsic property of these methods is isolation of T-cells with antigen specificities which are not predefined. As a consequence, many MiHA specific T-cells were isolated that recognized at least some non-hematopoietic cells, marking them inappropriate for adoptive transfer as they may mediate GVHD toxicity.

To increase the efficiency of characterizing MiHA with therapeutic potential, we and others have used an alternative approach called reverse immunology in which peptide predictions are the starting point and peptide candidates are subsequently screened for their capacity to induce a T-cell specific response²²⁻²⁴. This approach has the advantage to specifically screen for T-cells recognizing MiHA that are exclusively expressed by hematopoietic cells. However, we and others have previously reported that when such peptide predictions are solely based on computer algorithms that predict peptide-HLA binding affinity and proteolytic cleavage, the vast majority of T-cell responses detected is directed against epitopes that are not naturally processed and presented and as a consequence will not kill their target cells^{25,26}. The identification of the HLA-associated peptidome of hematopoietic cells by mass spectrometric analysis evades this peptide selection problem. The implementation of HLA-peptidomics into a reverse immunology approach guarantees HLA-restricted processing and presentation of eluted peptide candidates²⁷⁻²⁹.

In this study we investigated whether the identification of biologically relevant MiHA is feasible by merging HLA-peptidomics, single nucleotide polymorphism (SNP) databases, MHC-tetramer technology and multi-parametric flow-cytometric analysis into an efficient selection algorithm. For this purpose peptide elution experiments were performed resulting in the generation of a large set of eluted peptides. Subsequently, this library was screened for potential MiHA using a database dedicated to identify polymorphic peptides³⁰. A set of 40 MiHA candidates was synthesized and subsequently evaluated by mass spectrometric analysis, SNP validation and peptide-HLA binding assays. After evaluation, 12 polymorphic peptides were selected for MHC-tetramer production³¹⁻³³. Subsequently, MHC-tetramer positive T-cells lines were generated from healthy peripheral blood mononuclear cells (PBMC) donors by magnetic activated cell sorting (MACS). Flow cytometry-based analysis of antigen-specific T-cells, followed by functional testing of identified T-cell clones demonstrated the immunogenic potential of eluted MiHA and resulted in the isolation of high avidity T-cell clones specific for a novel MiHA.

The identification of the LB-NISCH-1A MiHA demonstrated the technical feasibility of our HLA-peptidomics based reverse immunology approach. In addition, by establishing strict selection criteria we could create an algorithm that can be exploited to selectively target T-cells specific for MiHA with a defined tissue distribution.

RESULTS

Selection of MiHA candidates from eluted peptide set

To establish a database of eluted peptides 4 EBV-LCL cell lines were expanded and lysed prior to use. Subsequently, HLA-A*0201 molecules were isolated by BB7.2 monoclonal antibody covalently linked to protein A beads and ligands were eluted by acid treatment³⁴. The complex ligand pool was fractionated by C18 reverse-phase HPLC and subsequently analyzed by on-line tandem mass spectrometry for sequencing. Tandem mass spectra were matched to the Human Short Peptide Variation Database (HSPVdb) for polymorphic peptide identification using the Mascot search engine^{30,40}. Peptide sequences encoded by both the normal and alternative reading frames were identified with a length of 7 to 14 amino acids allowing methionine oxidation, a minimal Best Mascot Ion score (BMI) of 20 and a mass accuracy of 10 parts per million (ppm). The HSPVdb database is specifically designed to address all peptide variations and only contains mRNA sequence fragments covering each polymorphism. As a consequence non-polymorphic mRNA regions are not included. This may result in false positive assignment of eluted non-polymorphic peptides to polymorphic mRNA regions. Therefore, as a first check, the tandem mass spectra were matched against both the HSPVdb and the regular IPIhuman database³⁶. Polymorphic peptide assignments were only allowed if the HSPVdb peptide identification confidence score was greater than the IPIhuman confidence score. As some amino acid sequences are conserved among the

human genome we further screened the MiHA candidates for sequence alignment with homologous genes and selected for those peptides that were uniquely encoded by a single gene of the human genome. In addition, MiHA candidates were only allowed to contain one polymorphism and as a consequence most peptides encoded by very polymorphic genes such as HLA, taste and olfactory receptor genes were excluded. The top 40 of identified MiHA candidates was selected and synthesized by standard Fmoc chemistry (Table SI)⁴¹.

Validation of eluted MiHA candidates

For final confirmation of the identity of the MiHA candidates the tandem mass spectra of the eluted peptides were compared with their synthetic counterparts. For 23 peptides, representing 58% of the MiHA candidates a perfect match confirmed the identification of the eluted peptides (Table I). For 10 peptides, representing 25% of the MiHA candidates, the tandem mass spectra did clearly differ, indicating that the peptide assignment was wrong. The assignment of 7 candidates MiHA could not be confirmed due to poor spectral quality. These candidates remained in the study until subsequent selection steps proved otherwise.

To confirm whether the SNP haplotype of the elution target cells corresponded with the allelic variant of the eluted peptides, we screened the 4 EBV-LCL cell lines for the respective set of polymorphisms using an Illumina Human1M-duo array supplemented with KASPar SNP genotyping assays. No SNP haplotype disparities were revealed for all the 30 remaining MiHA candidates. In addition a panel of 100 Dutch individuals was analyzed to evaluate the SNP allele frequencies of the remaining MiHA candidates (Table I). Although their existence was suggested by the NCBI dbSNP database⁴², we could not verify the SNP for 7 candidates and these non-polymorphic peptides were excluded from the potential MiHA list.

Assessment of the HLA-A*0201 affinity of eluted MiHA candidates

Although low affinity polymorphic peptides may be eluted from the HLA-peptidome these can not be validated as MiHA due to the necessity to isolate T-cells reactive to these peptides via MHC-tetramer isolation. Therefore in our MiHA identification method we analyzed the remaining MiHA candidates for their HLA-A*0201 affinity using a binding assay that is based on UV-induced conditional ligand cleavage^{32;39}. In this assay recombinant HLA-monomers that are prefolded around a UV-labile ligand, are subsequently exposed to UV in the presence of one of the MiHA candidate peptides. The UV-induced degradation of the conditional ligand will result in rapid disintegration of the HLA-monomer, a process that may be prevented by the affinity dependent binding of the presented MiHA candidate peptide into the empty binding-groove of the HLA-molecule (Fig. 1). After UV-exchange HLA-monomer rescue scores (R) were normalized to the high HLA-A*0201 affinity CMV-PP65-NLV peptide. A selection threshold was set based on the 40% HLA-rescue score that

Table I. Validation of peptide identification

No.	Peptide ^α	PPM ^β	BMI ^γ	MS status	Eluted MiHA Allele		Allelic MiHA variant		netMHC (nM)
1	APOBEC3F-1S	0,0	30	confirmed	S	0.48%	A	0.52%	19
2	APOBEC3F-1A	0,8	31	confirmed	A	0.52%	S	0.48%	19
3	ASNS-1A	0,3	27	confirmed	A	1.0%	T	0%	2199
4	ATF6-1L	0,3	48	mismatch	L	-	S	-	10
5	ATP10D-1I	0,4	39	confirmed	I	0.15%	V	0.85%	1893
6	ATR-1M	3,4	29	doubt	M	0.46%	T	0.54%	80
7	BRD3-1L	1,0	46	mismatch	L	-	P	-	23528
8	CDC26-1F	0,0	34	confirmed	F	0.68%	S	0.32%	66
9	CHRNA9-1P	0,4	29	doubt	P	0.56%	L	0.44%	7597
10	CMPK1-1S	0,7	27	confirmed	S	0.97%	I	0.03%	1578
11	DDX41-1A	0,3	97	confirmed	A	1.0%	G	0%	65
12	GPR180-1L	3,3	42	mismatch	L	-	P	-	1436
13	GTF3C5-1S	0,1	50	confirmed	S	1.0%	L	0%	10
14	GUCA1C-1M	1,4	49	mismatch	M	-	L	-	17114
15	HIVEP1-1S	0,6	34	doubt	S	0.09%	N	0.91%	310
16	MAGEF1-1A	0,8	55	confirmed	A	1.0%	T	0%	60
17	MAP4K1-1L	1,8	75	confirmed	L	1.0%	Deletion	0%	158
18	NISCH-1A	0,0	39	confirmed	A	0.17%	V	0.83%	12
19	NISCH-1V	0,9	40	confirmed	V	0.83%	A	0.17%	12
20	NUFIP1-1S	0,2	41	confirmed	S	0.52%	R	0.48%	25213
21	OR13G1-1M	3,9	29	mismatch	M	-	L	-	222
22	OR6C65-1T	1,8	31	doubt	T	0.16%	A	0.84%	5945
23	PARP10-1L	0,7	56	confirmed	L	0.66%	P	0.34%	96
24	PEMT-1V	2,5	31	doubt	V	0.53%	I	0.47%	nd
25	PKD1-1V	0,0	37	mismatch	V	-	I	-	nd
26	PLEK-1K	1,0	30	confirmed	K	0.68%	R	0.32%	23170
27	PRH1-1I	0,0	34	confirmed	I	0.64%	S	0.36%	109
28	PRRG2-1G	6,9	27	mismatch	G	-	C	-	19627
29	RNASE8-1P	1,5	39	confirmed	P	0.39%	S	0.61%	1948
30	RPL19-1L	0,0	66	confirmed	L	1.0%	F	0%	7
31	SFI1-1L	0,8	38	confirmed	L	0.75%	P	0.25%	21311
32	SSTR4-1V	0,0	23	mismatch	V	-	F	-	114
33	TARS-1V	0,1	78	confirmed	V	1.0%	I	0%	12
34	TARS-2V	0,3	31	mismatch	V	-	I	-	24411
35	TMC06-1T	3,2	33	mismatch	T	-	S	-	7798
36	TRIM9-1L	0,0	33	doubt	L	0.39%	F	0.61%	1629
37	TYK2-1L	0,9	33	doubt	L	0.54%	V	0.46%	nd
38	UCRC-1I	0,0	53	confirmed	I	0.94%	V	0.06%	63
39	USP31-1S	0,2	31	confirmed	S	0.34%	A	0.66%	nd
40	ZNF610-1V	0,2	56	confirmed	V	0.09%	L	0.91%	nd

^α MiHA nomenclature

^β Parts-Per-Million: Difference between observed and exact ion mass

^γ Best-Mascot-Ion-Score: Match between observed MS spectrum and stated peptide

Non- and Immunogenic Allele indicated by amino acid code, allele frequencies are calculated by direct counting in a panel of 100 Dutch individuals

Predicted netMHC affinity (nM), Strong binder ≤50; Weak binder ≤500

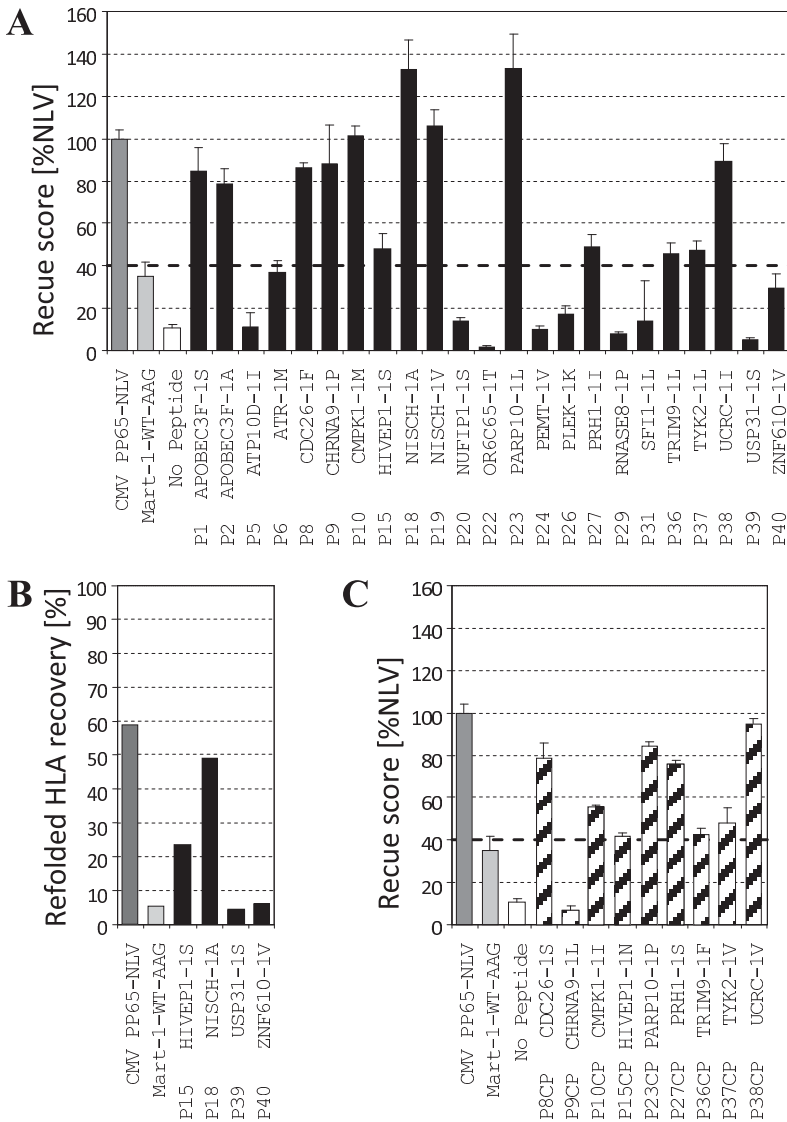


Figure 1. HLA-A*0201 binding affinity of eluted MiHA candidates. (A) HLA-A*0201 binding affinity of 23 confirmed MiHA candidates was measured by a binding assay that is based on UV-exchange monomer technology. After UV-exchange the HLA-monomer rescue score was normalized to the high affinity CMV PP65-NLV (NLVPMVATV) peptide which was set to 100%. Selection threshold was set to 40% HLA recovery based on the low affinity MART-1-WT-AAG (AAGIGILTV) peptide. As negative control no rescue peptide was added. Experiment was performed in triplicate, data are mean \pm SD. (B) The HLA-A*0201 recovery of 2 high- and 2 low-affinity eluted peptides was normalized to the input of total HLA heavy chain and β 2M complex after conventional HLA-refolding. (C) HLA-A*0201 binding affinity of 9 predicted allelic MiHA variants (CP) was measured by the UV-exchange monomer based binding assay.

was demonstrated by the low HLA-A*0201 affinity MART-1-WT-AAG peptide as only a modified MART-1-ELA peptide analog can be used for successful MHC-tetramer formation. For 13 out of the residual 23 MiHA candidates rescue scores above 40% were obtained. Thus, although eluted from HLA-A*0201, a substantial number of 10 validated peptides demonstrated rescue scores beneath the MART-1-WT-EAA based selection threshold, corresponding with low HLA-A*0201 binding affinity.

Next, we analyzed whether these low affinity peptides could be used for MHC-tetramer formation by conventional HLA-refolding. In this assay we tested a representative high-, intermediate and two low-affinity MiHA candidate peptides for their capacity to support stable refolding of the heavy chain and β 2m recombinant subunits of a HLA-A*0201 complex. HLA-recovery levels of 23.5%, 49.0%, 4.5% and 6% were obtained for P15 HIVEP-1S, P18 NISCH-1A, P39 USP31-1S and P40 ZNF610-1V respectively. For the control peptides CMV-PP65-NLV and MART-1-WT-AAG, HLA-recovery levels of 58.8% and 5.4% were obtained (Fig. 1B). These results indicate that for the high- and intermediate affinity peptides, MHC-tetramer formation can be achieved using both the conventional and conditional HLA-monomer formation methods. However, as the two tested low-affinity peptides demonstrated low HLA-recovery scores comparable to the negative control MART-1-WT-AAG peptide, no peptide-HLA-monomer complex remains for MHC-tetramer formation. As a consequence, the low-affinity peptides were removed from the MiHA candidate list and 13 MiHA candidates remained for further validation.

Isolation of peripheral blood derived MiHA-specific T-cells by MHC-tetramer pull down

For the two MiHA candidates encoded by the APOBEC3F and NISCH gene, see Table I, peptides expressing both allelic variants of the SNP were eluted. As bi-directional T-cell recognition of both allelic MiHA variants has been reported^{43;44}, we hypothesized that the prediction of the allelic variants of the remaining high affinity eluted MiHA candidates could be a valuable contribution to our candidate list. We therefore synthesized the predicted allelic MiHA variants of the remaining MiHA candidates and tested them for HLA-A*0201 affinity. With the exception of the allelic CHRNA9-1L variant, demonstrating low peptide-HLA affinity, all predicted allelic MiHA variants demonstrated similar affinity as their eluted counterpart (Fig. 1C). Subsequently, with the exception of both TRIM9 variants, MHC-tetramers were successfully generated for all peptides and bringing the total number of MHC-tetramers up to 19, specific for 12 eluted and 7 predicted allelic MiHA variants.

Next, MiHA-specific T-cell lines were generated by incubating 100×10^6 PBMC from 14 healthy donors with a specific set of MHC-tetramers, followed by enrichment of MHC-tetramer positive cells on a magnetic column. To increase the isolation frequency of high-affinity T-cell populations, the set of MHC-tetramers was specifically adjusted to each PBMC sample to cover only those MiHA for which the encoding SNP was screened homozygous

Table II. MHC-tetramer pull down scheme.

Peptide ^α	APOEC3F_1S	APOEC3F_1A	CDC26_1F	CDC26_1S	CHRNA9_1P	CMFK1_1I	HIVEP1_1S	NISCH_1A	PARP10_1L	PARP10_1P	PRH1_1I	PRH1_1S	TYK2_1L	UCRC_1V
DAR 7250						-/-	-/-	-/-	-/-	-/-	-/-	-/-	-/-	-/-
DBS 7251	-/-	-/-	-/-	-/-	-/-	-/-	0,79	-/-	-/-	-/-	-/-	-/-	-/-	-/-
DCU 7252	-/-	-/-	-/-	-/-	-/-	-/-	-/-	-/-	-/-	-/-	-/-	-/-	-/-	-/-
DDT 7253	-/-	-/-	-/-	-/-	-/-	-/-	-/-	-/-	-/-	-/-	-/-	-/-	-/-	-/-
DEK 7269	-/-	-/-	-/-	-/-	-/-	-/-	-/-	-/-	-/-	-/-	-/-	-/-	-/-	-/-
DFH 7270	-/-	-/-	-/-	-/-	-/-	-/-	-/-	-/-	-/-	-/-	-/-	-/-	-/-	-/-
DG1' 7271	-/-	-/-	-/-	-/-	-/-	1,19	-/-	-/-	-/-	-/-	-/-	-/-	0,19	-/-
DHX 7272	-/-	-/-	-/-	-/-	-/-	0,22	-/-	-/-	0,09	-/-	-/-	-/-	-/-	-/-
DIA 7274	-/-	-/-	-/-	-/-	-/-	-/-	0,01	-/-	-/-	-/-	-/-	-/-	-/-	-/-
DJG 7275	-/-	-/-	-/-	-/-	-/-	-/-	-/-	-/-	-/-	-/-	-/-	-/-	-/-	-/-
DKI 7276	-/-	-/-	-/-	-/-	-/-	-/-	0,02	-/-	-/-	-/-	-/-	-/-	-/-	-/-
DLH 7277	-/-	-/-	-/-	-/-	-/-	-/-	-/-	-/-	-/-	-/-	-/-	-/-	-/-	-/-
DMI 7280	-/-	-/-	-/-	-/-	-/-	0,02	-/-	-/-	-/-	-/-	-/-	-/-	-/-	-/-
DNJ 7281	-/-	-/-	-/-	-/-	-/-	0,03	0,02	-/-	0,07	-/-	-/-	-/-	-/-	-/-
Average	3	7	2	8	4	13	11	7	1	4	1	5	4	14

^α Bold: eluted MiHA variant; Normal: predicted allelic MiHA variant

negative in the respective donor (Table II). Due to unfavorable allele frequencies of some SNP encoding MiHA, no homozygous negative individuals were available for the CMPK1-1S, HIVEP1-1N, NISCH-1V, TYK2-1V and UCRC-1I MiHA candidates. After 14 days of expansion either one or more MHC-tetramer positive T-cell populations were detected in 7 of the generated T-cell lines by flow cytometry (FACS). In total 11 different MHC-tetramer positive T-cell populations were detected specific for the eluted HIVEP1-1S and NISCH-1A and predicted PARP10-1P and UCRC-1V allelic MiHA variants. Overall MHC-tetramer positive T-cell frequencies varied between 0.01% and 1.19% of total CD8⁺ T-cells (Table II). Representative examples for each of these MiHA candidates are shown in Fig. 2A. For each MHC-tetramer positive T-cell population a purified T-cell line was generated by FACS cell sorting (from now on referred to as “purified T-cell lines”). Purity varied between 95% and 100% of total T-cells.

MHC-tetramer positive T-cell lines demonstrate MiHA-specific IFN- γ production

To assess the reactivity of the purified MHC-tetramer positive T-cell lines we stimulated them with T2 target cells loaded with either one of the allelic MiHA variants separately in a titration assay and measured overnight IFN- γ production. For each MiHA candidate the T-cell line demonstrating the highest avidity for the specific peptide that was used for MHC-

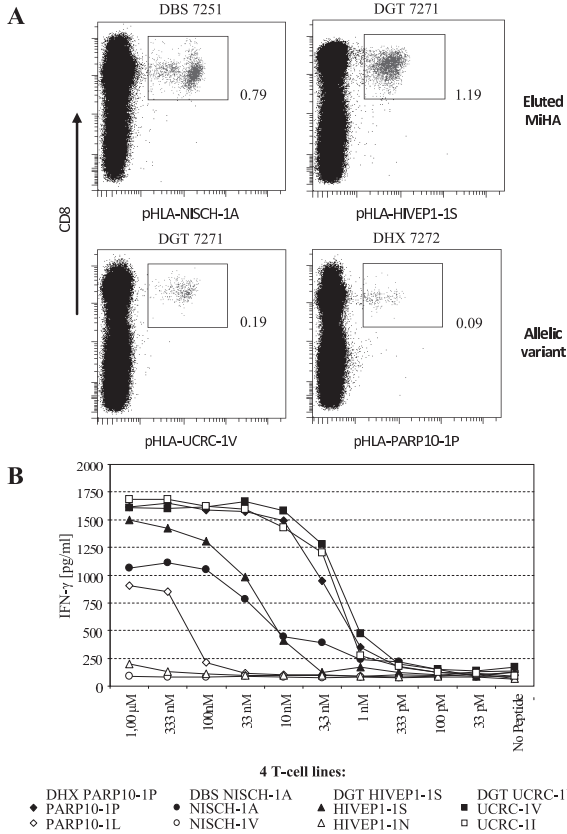


Figure 2. Purified MHC-tetramer positive T-cell lines demonstrate MiHA specific IFN- γ production after peptide stimulation.

(A) Detection of MiHA specific T-cell populations by FACS analysis after MHC-tetramer pull down and *in vitro* expansion for 14 days. Representative examples are shown of MHC-tetramer positive T-cell populations detected in the indicated T-cell lines and specific for 4 unique MiHA of which two were eluted (upper part) and two were predicted allelic variants (lower part). All dot plots display fluorescence intensity for CD8 and specific MHC-tetramer staining. MHC-tetramer positive T-cells are indicated black, total lymphocytes are indicated gray. Frequencies indicate MiHA specific T-cells of total CD8⁺ cells. (B) Purified MHC-tetramer positive T-cell lines were generated by FACS sort and stimulated with HLA-A*0201 positive T2 target cells loaded with titrated concentrations of peptides for 18 hours [E:T] 5000:25000. For each specificity the purified MHC-tetramer positive T-cell line is shown that demonstrated the highest avidity when tested against their specific (black) or allelic MiHA variant peptide (white). IFN- γ production was measured by standard ELISA.

tetramer isolation is shown in Fig. 2B. Tested T-cell lines demonstrated variable peptide avidity and a half maximum response (IC₅₀) of ± 3 nM was obtained for the high-avidity DHA PARP10-1P and DGT UCRC-1V T-cell lines. The DGT HIVEP1-1S and DBS NISCH-1A T-cell lines demonstrated an approximately 10-fold lower peptide sensitivity of ± 30 nM. As the MiHA candidates were eluted from HLA they are expected to be of biological relevance. As a consequence, high-avidity T-cells reactive to one allelic variant of the candidate MiHA are not expected to recognize the other allelic variant due to clonal deletion of high avidity T-cells directed towards potential self antigens. When stimulated with both allelic variants of the MiHA candidates, the DGT HIVEP1-1S and DBS NISCH-1A T-cell lines did not demonstrate any recognition of their allelic MiHA variants; however the DHA PARP10-1P T-cell line demonstrated low avidity recognition of the PARP10-1L variant and the DGT UCRC-1V T-cell line demonstrated equally high avidity peptide recognition of both allelic MiHA variants. Apparently the valine (V) to isoleucine (I) substitution at position 6 in the UCRC decamer peptide did not affect recognition by the UCRC specific MHC-tetramer positive T-cells. These data indicate, that either the allelic UCRC-1I variant is not processed

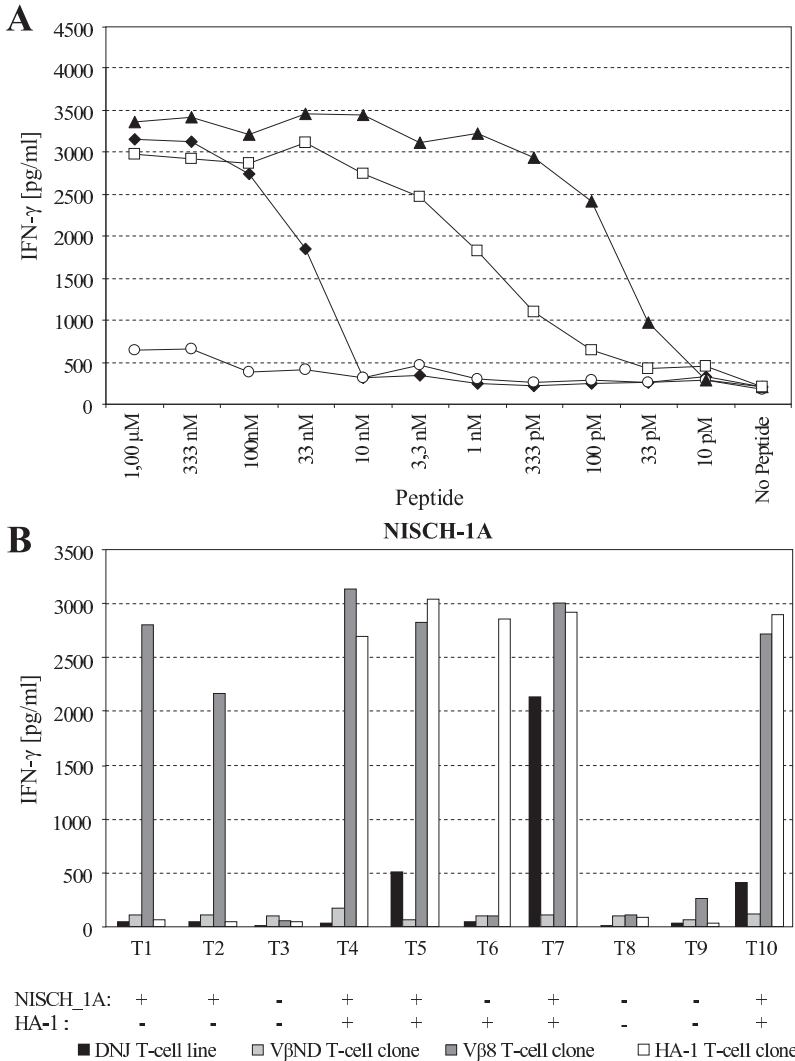


Figure 3. High avidity MHC-tetramer positive T-cell clone demonstrates MiHA positive target cell recognition. (A) Donor DNJ7281 derived NISCH-1A purified MHC-tetramer positive T-cell line and generated Vβ8 and VβND restricted T-cell clones were stimulated with peptide-loaded HLA-A*0201 positive T2 target cells for 18 hours [E:T] 5000:25000. Peptide concentrations were titrated in 3-fold dilution steps starting from 1 μM. MiHA specificity and peptide reactivity was analyzed by cytokine secretion in a standard IFN-γ ELISA. (B) Donor DNJ7281 derived NISCH-1A purified MHC-tetramer positive T-cell line (black) and generated Vβ8 and VβND restricted T-cell clones (light and dark grey) were stimulated with a panel of 10 HLA-A*0201 positive and SNP genotyped EBV-LCL target cells positive (+) or negative (-) for the indicated MiHA for 18 hours. T-cell reactivity was measured by standard IFN-γ ELISA. As a control for MiHA specific T-cell reactivity a high avidity HA-1 specific T-cell clone was used (white).

and presented in the context of HLA to allow clonal deletion, or that the identity of the UCRC-1V is wrongly assessed by MS analysis and therefore lacks biological relevance.

Next, the purified T-cell lines were stimulation with a panel of 10 SNP genotyped and HLA-A*0201 positive EBV-LCL target cells to screen for MiHA specific reactivity against endogenously presented peptide. Although IFN- γ production was observed after stimulation with some MiHA positive target cells, no MHC-tetramer positive T-cell lines demonstrated recognition of each MiHA positive target cell throughout the whole EBV-LCL panel (Fig. S1).

4

Detection of high-avidity MiHA specific T-cell clones among the total MHC-tetramer positive T-cell population

To investigate whether the lack of endogenously presented peptide recognition by the purified MHC-tetramer positive T-cell lines was due to an overall low-avidity of the isolated MHC-tetramer specific T-cells or could be the result of the presence of low frequent high avidity T-cells within the T-cell lines, we studied the clonal composition of the generated T-cell lines with a TCR V β -usage antibody kit. Although the applied kit only covered up to 60% of all known V β -chains, we were able to demonstrate the oligoclonal composition of all the purified MHC-tetramer positive T-cell lines. For the DNJ NISCH-1A T-cell line a minimum number of 3 different clones was identified. For T-cells within this particular T-cell line; 88.8% used TCR V β 14, 0.6% used TCR V β 8 and 10.6% used an unknown TCR V β -chain. With the exception of TCR V β 14, single T-cell clones were successfully generated for the other two clones by FACS sorting. Subsequently, generated T-cell clones were stimulated with peptide-loaded T2 cells in a titration assay and their avidity was compared to that of the oligoclonal T-cell line and a HA-1 control clone obtained from a memory response after allo-SCT (Fig. 3A). The NISCH-1A TCR V β 8 and HA-1 control T-cell clone demonstrated high avidity peptide recognition with IC50 \pm 100 pM and \pm 1 nM respectively, approximately 100-fold higher than that of the oligoclonal T-cell line. In contrast, the T-cell clone with an unknown TCR V β -chain did not demonstrate any peptide recognition.

Next, the generated DNJ NISCH-1A specific T-cell clones were stimulated with a panel of SNP genotyped EBV-LCL, as previously described, for recognition of endogenously presented peptide. Upon stimulation and according to the peptide-avidity recognition patterns, only the DNJ NISCH-1A derived TCR V β 8 positive T-cell clone, representing 0.6% of the total cell line, demonstrated high IFN- γ production when stimulated with target cells positively expressing the NISCH-1A MiHA (Fig. 3B). Apparently, the majority of T-cells within this MHC-tetramer positive T-cell line were of insufficient avidity to recognize endogenously presented peptide. Also for the other specificities T-cell clones were generated, however no other T-cell clone was able to recognize endogenously presented peptide. The identification of a MiHA-specific high-avidity T-cell clone demonstrated that this reverse immunology approach can be successfully used for the identification of new MiHA.

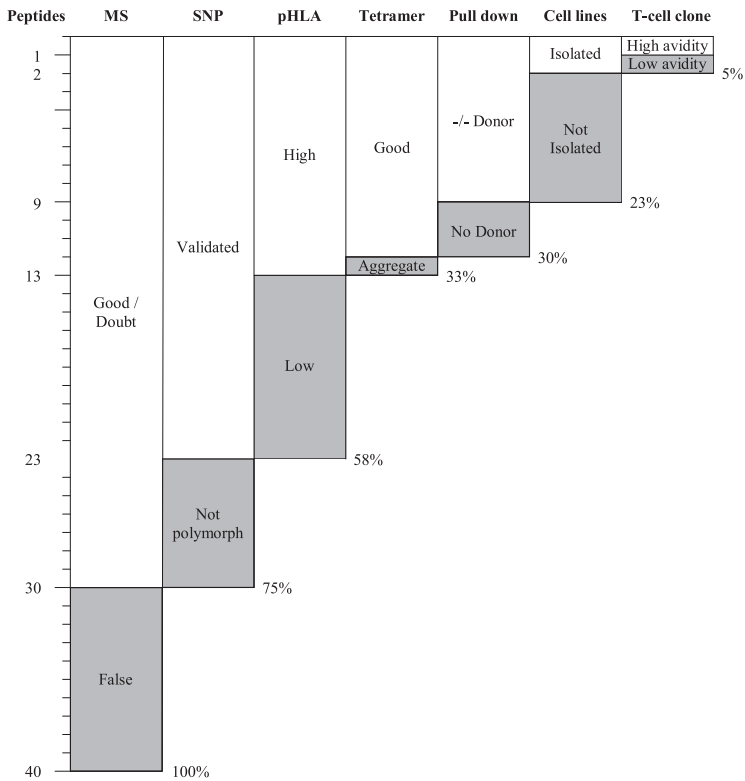


Figure 4. MiHA selection strategy by numbers of eluted peptide candidates. This figure describes the MiHA selection strategy as applied in this study. By setting broad selection thresholds the figure demonstrates the countdown of MiHA candidates following 7 selection steps. The number of residual MiHA candidate that remained in list after each selection step is indicated at the left. Percentages indicate the residual peptides as part of the initial set of 40 eluted MiHA candidates (right). Selection steps (from left to right): First, Mass spectrometry (MS) based validation of eluted peptides. Second, analysis of SNP encoded MiHA allele frequencies in a panel of 100 Dutch individuals. Third, analysis of the HLA-A*0201 affinity of eluted peptides. Fourth, generation of MHC-tetramers. Fifth, selection of donors that are homozygous negative (-/-) for the SNP encoding MiHA and could be used for MHC-tetramer pull down experiments. Sixth, FACS analysis of expansion T-cell cultures for the detection of MHC-tetramer positive T-cells. Seventh, generation of MHC-tetramer positive T-cell clones and subsequent functional assessment to detect high avidity T-cells.

DISCUSSION

The aim of this study was the development of an efficient algorithm for the identification of MiHA. To establish this algorithm we applied broad selection thresholds in each selection step of our pipeline approach starting from epitope selection to the identification of antigen-specific T-cells. We started our approach by selecting the top 40 eluted MiHA candidates and ended with the identification of LB-NISCH-1A (Fig. 4). Although this yield is encouraging when compared to some previous reverse immunology based studies^{25,26}, the majority of MiHA candidates were lost during the first three selection steps as a

consequence of wrongly assigned tandem mass spectrometry, incorrect SNP information in dbSNP and the incapacity to generate MHC-tetramers for some eluted peptides. By careful step-by-step evaluation we can increase the efficiency of our algorithm.

Initially, peptides were assigned from the tandem mass spectra using a generally considered broad criterium of a BMI of >20 , and a tight mass accuracy criterium of <10 ppm. Validation of the identification of the MiHA candidates by comparison of the tandem mass spectra of the eluted peptides with their synthetic counterparts, illustrated that 10 of the 40 MiHA (25%) appeared to be false positive (Fig. 4). By setting more stringent conditions (Table SII), this number could be reduced to 22% (BMI >30) and 18% (mass deviation <2 ppm). Combination of these conditions can further reduce the false positive identification rate to 13% with only 4 of the selected 30 MiHA candidates being false positive. Setting

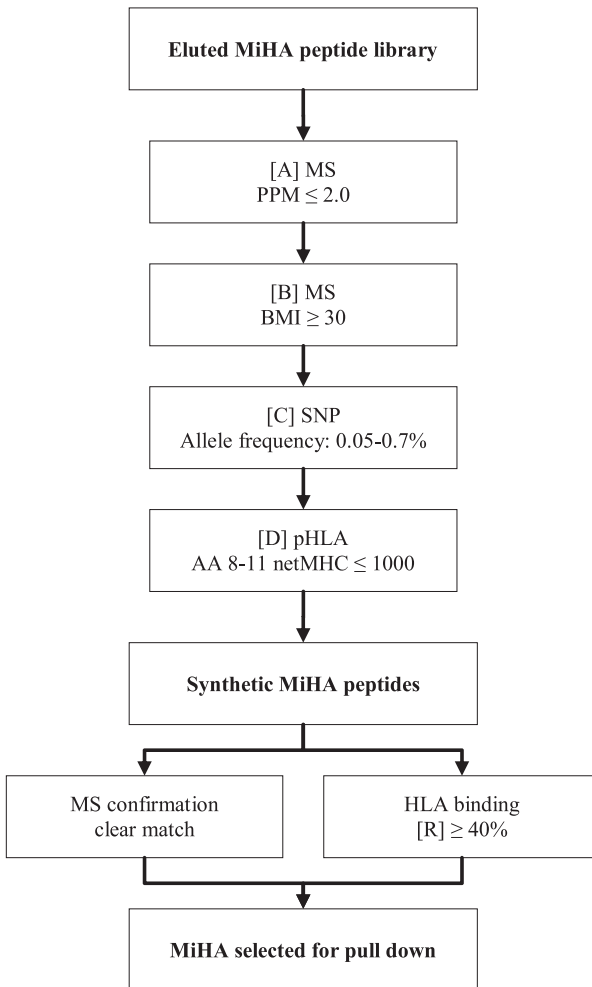


Figure 5. Selection algorithm for discovery of MiHA implementing HLA-peptidomics into a reverse immunology approach. By setting tight selection criteria for both the theoretical and functional evaluation of MiHA candidates an efficient selection algorithm was established. For theoretical evaluation of MiHA candidates before peptide synthesis, MS based thresholds are set for BMI, ppm and peptide length. Tandem mass spectra of eluted peptides will be matched against both the HSPVdb and the regular IPIhuman database. Polymorphic peptide assignments will only be allowed if the HSPVdb peptide identification confidence score is greater than the IPIhuman confidence score. Selection threshold for SNP encoding MiHA allele frequency will be set between 0.05% and 0.7% and the netMHC algorithm will be used to predict peptide-HLA binding affinity. For final confirmation of the identity of the MiHA candidates the tandem mass spectra of the eluted peptides will be compared with their synthetic counterparts. Subsequently, peptide-HLA binding affinity will be analyzed and high-affinity peptides will be selected for MHC-tetramer pull down experiments.

these conditions will increase the MiHA candidate selection efficiency. For peptides encoded by alternative reading frames a similar false positive identification rate (29%) was obtained as that of peptides encoded by the normal reading frame (21%) (Table SII). These results indicate that alternative reading frame peptides may be a valuable contribution to the MiHA candidate list when evaluated according to our algorithm.

To increase the clinical relevance of MiHA candidates, only those SNP could be selected with allele frequencies between 0.05% and 0.07% to allow a relative MiHA mismatch change of 10% between unrelated donors and recipients. By setting this selection threshold, three MiHA candidates for which no homozygous negative donors could be found would have been excluded from the candidate list to further increase the efficiency of our selection algorithm.

The use of HLA-peptidomics as starting point guarantees appropriate processing and HLA-dependent presentation of eluted peptides. However 10 out of 23 MS validated MiHA candidates demonstrated lower peptide-HLA-complex recovery rates than the negative control MART-1-WT-AAG peptide, known for its incapacity to be used for MHC-tetramer formation⁴⁵ (Fig. 4). Although the identity of these low-affinity HLA-A*0201 binding peptides may either be correctly or wrongly assigned by MS analysis, these MiHA candidates could not be validated due to the incapacity to generate MHC-tetramers needed for isolation of high avidity T-cells directed to these antigens. As MHC-tetramers are essential to our approach, these low HLA-affinity peptides should be removed before MiHA candidate selection and synthesis. One possible solution may be the incorporation of a peptide-HLA binding algorithm such as netMHC. With the exception of peptide 6, none of the 10 peptides demonstrating low HLA-recovery were predicted to have HLA-A*0201 binding motifs (predicted affinity >500 nM) when analyzed using this algorithm (Table I). In contrast, HLA-A*0201 binding motifs were confirmed for 10 of the 13 peptides that demonstrated high peptide-HLA-complex recovery, including the MiHA candidates for which specific T-cell populations were detected, indicating that the use of peptide-HLA binding algorithms may be a valuable contribution to the MiHA candidate identification efficiency of our algorithm.

The purified MHC-tetramer positive T-cell lines demonstrated a wide avidity range when stimulated with peptide loaded T2 target cells. However, when stimulated with EBV-LCL target cells, these T-cell lines appeared to be incapable of recognizing endogenously presented peptide. Assessment of the TCR V β -chain usage demonstrated the oligoclonal nature of the MHC-tetramer positive T-cell populations and subsequent functional assessment of single T-cell clones demonstrated that the lack of response, observed for the MHC-tetramer positive T-cell lines was due to the presence of low frequent high-avidity T-cells within the T-cell lines. Only a 0.6% subset of the purified DNJ NISCH-1A specific T-cell line appeared reactive to endogenously presented peptide, in contrast to the purified MHC-tetramer positive T-cell line that predominantly consisted of low-avidity T-cells.

The technical feasibility of our approach was demonstrated by the identification of the LB-NISCH-1A MiHA. By introducing several evaluation steps and setting tight selection criteria a more efficient MiHA identification algorithm can be achieved for the identification of MiHA using a reverse immunology approach (Fig. 5). This new algorithm would allow the efficient selection of the most relevant MiHA candidates within a set of eluted peptides that fulfill to all criteria. Increased selection efficiency would allow the screening of T-cell repertoires for circulating T-cells specific for larger amounts of relevant MiHA candidates. In combination with strict gene of interest selection, this algorithm may be of significance for future identification of MiHA.

ACKNOWLEDGEMENTS

We thank Yotam Raz for help with T-cell culture, Cornelis van Bergen for help with SNP genotyping, Menno van der Hoorn, Guido de Roo and Patrick van der Holst for flow cytometric cell sorting.

MATERIALS AND METHODS

Culture conditions and cells. Peripheral blood was obtained from different individuals after informed consent (Sanquin Reagents, Amsterdam, The Netherlands and Leiden University Medical Center, Leiden, The Netherlands). All experiments were approved by the local medical ethics committees. Blood samples were HLA-typed by high-resolution genomic DNA-typing. Peripheral blood mononuclear cells (PBMC) were isolated by Ficoll gradient separation and cryopreserved for further use. T-cells were cultured in T-cell medium consisting of Iscove's Modified Dulbecco's Media (IMDM: Lonza, Basel, Switzerland) supplemented with 5% human serum (HS), 5% fetal bovine serum (FBS), 100 IU/ml IL-2 (Proleukin; Chiron, Amsterdam, The Netherlands), 2 mM L-glutamine, 100 U/ml penicillin, and 100 µg/ml streptomycin (Invitrogen, Carlsbad, CA). Epstein-Barr virus-transformed lymphoblastoid B-cell lines (EBV-LCL) and phytohemagglutinine (PHA; Murex Diagnostics, Dartford, U.K) blasts were generated using standard procedures.

Peptide library of HLA-class I eluted peptides. The peptides used for this study are derived from a large peptide library that was recently established. In short: Peptide elution, reverse phase high-performance liquid chromatography (RP-HPLC), and mass spectrometry (MS) were carried out as previously described^{16;18}. Briefly, 60 x 10⁹ HLA-A*0201 and HLA-B*0702 positive EBV-LCL were washed with ice cold PBS and stored at -80°C until use. After freeze drying, peptide-HLA-class I complexes were purified by affinity chromatography. Subsequently, peptides were eluted from HLA-molecules, and separated from the HLA heavy chain fragments and β2-microglobulin by size filtration. The peptide mixture was subjected to 3 rounds of fractionation and after the third fractionation, the peptide masses present in the fractions were determined and sequenced by tandem MS. The tandem mass spectra were matched against the International Protein Index (IPI) human database version

3.87, using the mascot search engine version 2.2.04 (Matrix Science, London, UK), with a precursor mass tolerance of 2 ppm and a product ion tolerance of 0.8 Da. For finding polymorphic peptides the tandem mass spectra were matched against the HSPVdb³⁰, specifically designed for finding polymorphic peptides.

The dissolved fractions were analyzed by on-line nano-HPLC mass spectrometry with a system, consisting of a conventional Agilent 1100 gradient HPLC system (Agilent, Waldbronn, Germany). The mass spectrometer was an LTQ-FT Ultra (Thermo, Bremen, Germany) and was operated in datadependent mode, automatically switching between MS and MS/MS acquisition.

SNP genotyping assays. A panel of 100 HLA-A*0201 positive Dutch EBV-LCL was selected for SNP screening as previously described³⁶. Briefly, genomic DNA was isolated from 5×10^6 EBV-LCL cells using Gentra Puregene Cell Kit (Qiagen) and PCR-free whole genome amplification (WGA) was performed. The DNA samples were subsequently fragmented, purified, and hybridized to Illumina Human1M-duo arrays containing probes for 1.1 million SNPs (Illumina). After hybridization, the bead arrays were stained and fluorescence intensities were quantified on an Illumina Bead Array 500GX Scanning Station. Raw data were analyzed using Illumina Genome Studio software, and SNP genotype reports were generated using the Plink software (<http://pngu.mgh.harvard.edu/~purcell/plink>, version 1.03; ref. 30). For SNP that were not present on the Illumina Human1M-duo array, a KASPar SNP genotyping assay was performed according to the manufacturer's protocol.

Generation of peptide-MHC complexes. All peptides were synthesized in-house using standard Fmoc chemistry. Recombinant HLA-A*0201 heavy chain and human β_2m light chain were in-house produced in Escherichia coli. MHC class I refolding was performed as previously described with minor modifications³⁷. MHC class I complexes were purified by gel-filtration HPLC in PBS and stored at 4°C. The peptide HLA-A*0201 binding affinity was assessed by subjecting prefolded UV-sensitive peptide-MHC complexes (100 µg/ml) to 366nm UV light (Camag) for 1 h in presence of the specific peptide (200 µM)³⁸. As controls the CMV PP65 NLVPMVATV and wild-type MART1 AAGIGILTV peptide were used. After exchange, samples were spun at 16,000g for 5 min and supernatants were used to assess HLA-monomer rescue using a bead assay as previously described³⁹.

Isolation of MiHA specific T-cells by MHC-tetramer pull down. Prior to isolation PBMC samples were stained with PE-coupled MHC-multimers for 1 hour at 4°C. Subsequently, cells were washed and incubated with anti-PE antibody coated magnetic beads (Miltenyi Biotec, Bergisch Gladbach, Germany). PE-positive T-cells were isolated by magnetic activated cell sorting (MACS) using an LS column, according to the manufacturer's protocol (Miltenyi). Isolated PE-positive cells were cultured (5000 cells/well) with 5×10^4 irradiated (50Gy) autologous feeder cells in T-cell medium supplemented with 100 IU/ml IL-2, 5ng/ml IL-15 (Biosource) and 11.000 anti-CD3/CD28 Dynabeads (Invitrogen) in 96-round bottomed well plates. Cultures were refreshed twice a week. After 2 weeks, T-cell cultures were analyzed for MHC-multimer positive T-cell population by MHC-multimer combinatorial coding flow cytometry. For the second MHC-multimer pull down the procedure was performed using the

identical set of PE-coupled MHC-multimers. MHC-multimer positive T-cell populations were single cell sorted on a FACSAria (BD Biosciences, San Diego, USA) into 96-round bottomed well plates containing 100 μ l T-cell medium supplemented with 100 IU/ml IL-2, 800 ng/ml PHA and 1×10^5 irradiated feeder cells.

Flow cytometry and T-cell staining. Data acquisition was performed on an LSR-II flow cytometer (BD) with FACS Diva software using the following instrument settings: 488nm laser: 685LP, 695/40; PE: 550LP, 575/26; FITC: 505LP, 530/30; SSC: 488/10. 633nm laser: Alexa700: 685LP, 730/45; APC: 660/20. Approximately 1×10^6 PBMC were stained for each analysis with a final concentration of 2 μ g/mL per MHC-tetramer in 100 μ l Phosphate buffered saline (PBS) with 5% (v/v) pasteurized plasma protein solution (GPO). Next, antibody-mixtures consisting of CD8-Alexa700 (Caltag-MedSystems, Buckingham, UK) and CD4-FITC (BD) were added and cells were incubated for 30 min at 4°C. Prior to flow cytometry, cells were washed twice. TCR β chain (TCR-V β) usage was investigated by flow cytometry using specific monoclonal antibodies as included in the TCR-V β repertoire kit (Beckman Coulter).

Functional analysis. For analysis of IFN- γ production, 5000 T-cells were cocultured with 25.000 target cells loaded with different concentrations of peptides. Peptide loading was performed by incubating target cells for 1 hour in 96 well plates at 37°C and 5% CO₂ in IMDM containing 2% FCS and cells were washed twice before use. After 18 hours, supernatants were harvested, and the concentration of IFN- γ was measured by an enzyme-linked immunosorbent assay (Sanquin Reagents).

REFERENCES

1. Porter DL, Roth MS, McGarigle C, Ferrara J, Antin JH. Induction of Graft-versus-Host Disease as Immunotherapy for Relapsed Chronic Myeloid Leukemia. *N Engl J Med* 1994;330:100-106.
2. Kolb HJ, Schattenberg A, Goldman JM et al. Graft-versus-leukemia effect of donor lymphocyte transfusions in marrow grafted patients. European Group for Blood and Marrow Transplantation Working Party Chronic Leukemia [see comments]. *Blood* 1995;86:2041-2050.
3. Goulmy E. Human minor histocompatibility antigens: new concepts for marrow transplantation and adoptive immunotherapy. *Immunol.Rev.* 1997;157:125-140.
4. Marijt WAE, Heemskerk MHM, Kloosterboer FM et al. Hematopoiesis-restricted minor histocompatibility antigens HA-1- or HA-2-specific T cells can induce complete remissions of relapsed leukemia. *Proceedings of the National Academy of Sciences of the United States of America* 2003;100:2742-2747.
5. Falkenburg JH, van de Corp, Marijt EW, Willemze R. Minor histocompatibility antigens in human stem cell transplantation. *Exp.Hematol.* 2003;31:743-751.
6. de Bueger M, Bakker A, van Rood JJ, Van der Woude F, Goulmy E. Tissue distribution of human minor histocompatibility antigens. Ubiquitous versus restricted tissue distribution indicates heterogeneity among human cytotoxic T lymphocyte-defined non-MHC antigens. *J.Immunol.* 1992;149:1788-1794.
7. Reddy P, Ferrara JLM. Immunobiology of acute graft-versus-host disease. *Blood Reviews* 2003;17:187-194.
8. Ferrara JL, Levine JE, Reddy P, Holler E. Graft-versus-host disease. *Lancet* 2009;373:1550-1561.
9. Warren EH, Greenberg PD, Riddell SR. Cytotoxic T-lymphocyte-defined human minor histocompatibility antigens with a restricted tissue distribution. *Blood* 1998;91:2197-2207.
10. Dolstra H, Fredrix H, Maas F et al. A Human Minor Histocompatibility Antigen Specific for B Cell Acute Lymphoblastic Leukemia. *The Journal of Experimental Medicine* 1999;189:301-308.
11. Murata M, Warren EH, Riddell SR. A Human Minor Histocompatibility Antigen Resulting from Differential Expression due to a Gene Deletion. *The Journal of Experimental Medicine* 2003;197:1279-1289.
12. Slager EH, Honders MW, van der Meijden ED et al. Identification of the angiogenic endothelial-cell growth factor-1/thymidine phosphorylase as a potential target for immunotherapy of cancer. *Blood* 2006;107:4954-4960.
13. Warren EH, Otterud BE, Linterman RW et al. Feasibility of using genetic linkage analysis to identify the genes encoding T cell-defined minor histocompatibility antigens. *Tissue Antigens* 2002;59:293-303.
14. de Rijke B, van Horszen-Zoetbrood A, Beekman JM et al. A frameshift polymorphism in P2X5 elicits an allogeneic cytotoxic T lymphocyte response associated with remission of chronic myeloid leukemia. *J Clin Invest* 2005;115:3506-3516.
15. Akatsuka Y, Nishida T, Kondo E et al. Identification of a Polymorphic Gene, BCL2A1, Encoding Two Novel Hematopoietic Lineage-specific Minor Histocompatibility Antigens. *The Journal of Experimental Medicine* 2003;197:1489-1500.
16. van Bergen CAM, Kester MGD, Jedema I et al. Multiple myeloma-reactive T cells recognize an activation-induced minor histocompatibility antigen encoded by the ATP-dependent interferon-responsive (ADIR) gene. *Blood* 2007;109:4089-4096.
17. Rotzschke O, Falk K, Wallny HJ, Faath S, Rammensee HG. Characterization of naturally

- occurring minor histocompatibility peptides including H-4 and H-Y. *Science* 1990;249:283-287.
18. den Haan JM, Sherman NE, Blokland E et al. Identification of a graft versus host disease-associated human minor histocompatibility antigen. *Science* 1995;268:1476-1480.
 19. Spaapen RM, Lokhorst HM, van den Oudenalder K et al. Toward targeting B cell cancers with CD4+ CTLs: identification of a CD19-encoded minor histocompatibility antigen using a novel genome-wide analysis. *The Journal of Experimental Medicine* 2008;205:2863-2872.
 20. Kamei M, Nannya Y, Torikai H et al. HapMap scanning of novel human minor histocompatibility antigens. *Blood* 2009;113:5041-5048.
 21. Kawase T, Nannya Y, Torikai H et al. Identification of human minor histocompatibility antigens based on genetic association with highly parallel genotyping of pooled DNA. *Blood* 2008;111:3286-3294.
 22. Celis E, Tsai V, Crimi C et al. Induction of anti-tumor cytotoxic T lymphocytes in normal humans using primary cultures and synthetic peptide epitopes. *Proc.Natl.Acad.Sci.U.S.A* 1994;91:2105-2109.
 23. van der Bruggen P, Zhang Y, Chauv P et al. Tumor-specific shared antigenic peptides recognized by human T cells. *Immunol.Rev.* 2002;188:51-64.
 24. Maecker B, von Bergwelt-Baildon, Anderson KS, Vonderheide RH, Schultze JL. Linking genomics to immunotherapy by reverse immunology--'immunomics' in the new millennium. *Curr.Mol.Med.* 2001;1:609-619.
 25. Hombrink P, Hadrup SR, Bakker A et al. High-throughput identification of potential minor histocompatibility antigens by MHC tetramer-based screening: feasibility and limitations. *PLoS.One.* 2011;6:e22523.
 26. Ofran Y, Kim HT, Brusica V et al. Diverse patterns of T-cell response against multiple newly identified human Y chromosome-encoded minor histocompatibility epitopes. *Clin.Cancer Res.* 2010;16:1642-1651.
 27. Hunt DF, Henderson RA, Shabanowitz J et al. Characterization of peptides bound to the class I MHC molecule HLA-A2.1 by mass spectrometry. *Science* 1992;255:1261-1263.
 28. Falk K, Rotzschke O, Stevanovic S, Jung G, Rammensee HG. Allele-specific motifs revealed by sequencing of self-peptides eluted from MHC molecules. *Nature* 1991;351:290-296.
 29. Admon A, Barnea E, Ziv T. Tumor antigens and proteomics from the point of view of the major histocompatibility complex peptides. *Mol.Cell Proteomics.* 2003;2:388-398.
 30. Nijveen H, Kester MG, Hassan C et al. HSPVdb--the Human Short Peptide Variation Database for improved mass spectrometry-based detection of polymorphic HLA-ligands. *Immunogenetics* 2011;63:143-153.
 31. Altman JD, Moss PAH, Goulder PJR et al. Phenotypic Analysis of Antigen-Specific T Lymphocytes. *Science* 1996;274:94-96.
 32. Toebes M, Coccoris M, Bins A et al. Design and use of conditional MHC class I ligands. *Nat. Med.* 2006;12:246-251.
 33. Hadrup SR, Bakker AH, Shu CJ et al. Parallel detection of antigen-specific T-cell responses by multidimensional encoding of MHC multimers. *Nat.Methods* 2009;6:520-526.
 34. Stepniak D, Wiesner M, de Ru AH et al. Large-scale characterization of natural ligands explains the unique gluten-binding properties of HLA-DQ2. *J.Immunol.* 2008;180:3268-3278.
 35. Meiring HD, van der Heeft E, ten Hove GJ, de Jong APJM. Nanoscale LC-MS(n): technical design and applications to peptide and protein analysis. *J.Sep.Science* 2002;25:557-568.
 36. Van Bergen CA, Rutten CE, Van Der Meijden ED et al. High-throughput characterization of 10

- new minor histocompatibility antigens by whole genome association scanning. *Cancer Res.* 2010;70:9073-9083.
37. Burrows SR, Kienzle N, Winterhalter A et al. Peptide-MHC Class I Tetrameric Complexes Display Exquisite Ligand Specificity. *J Immunol* 2000;165:6229-6234.
 38. Rodenko B, Toebe M, Hadrup SR et al. Generation of peptide-MHC class I complexes through UV-mediated ligand exchange. *Nat.Protoc.* 2006;1:1120-1132.
 39. Eijssink C, Kester MG, Franke ME et al. Rapid assessment of the antigenic integrity of tetrameric HLA complexes by human monoclonal HLA antibodies. *J Immunol Methods* 2006;315:153-161.
 40. Pruitt KD, Tatusova T, Maglott DR. NCBI reference sequences (RefSeq): a curated non-redundant sequence database of genomes, transcripts and proteins. *Nucleic Acids Res.* 2007;35:D61-D65.
 41. Hiemstra HS, Duinkerken G, Benckhuijsen WE et al. The identification of CD4+ T cell epitopes with dedicated synthetic peptide libraries. *Proc.Natl.Acad.Sci.U.S.A* 1997;94:10313-10318.
 42. Smigielski EM, Sirotkin K, Ward M, Sherry ST. dbSNP: a database of single nucleotide polymorphisms. *Nucleic Acids Res.* 2000;28:352-355.
 43. Dolstra H, de Rijke B, Fredrix H et al. Bi-directional allelic recognition of the human minor histocompatibility antigen HB-1 by cytotoxic T lymphocytes. *Eur.J.Immunol.* 2002;32:2748-2758.
 44. Kawase T, Nannya Y, Torikai H et al. Identification of human minor histocompatibility antigens based on genetic association with highly parallel genotyping of pooled DNA. *Blood* 2008;111:3286-3294.
 45. Valmori D, Fonteneau JF, Lizana CM et al. Enhanced Generation of Specific Tumor-Reactive CTL In Vitro by Selected Melan-A/MART-1 Immunodominant Peptide Analogues. *J Immunol* 1998;160:1750-1758.

SUPPLEMENTARY INFORMATION

Table S1. Eluted MiHA candidates

No.	Gene	mRNA ^α	dbSNP ^β	Sequence ^γ	Inframe
1	APOBEC3F	NM_004900	rs17000697	FL <u>S</u> EHPNVTL	yes
2	APOBEC3F	NM_004900	rs17000697	FLA <u>E</u> HPNVTL	yes
3	ASNS	NM_001673	rs2070159	TLLKQLK <u>E</u> A	yes
4	ATF6	NM_007348	rs2070151	ILL <u>S</u> LLN <u>L</u> V	no
5	ATP10D	NM_020453	rs1058793	TAALF <u>I</u> ILL	yes
6	ATR	NM_001184	rs2227928	<u>M</u> VLTRIIAI	yes
7	BRD3	NM_007371	rs14719	DVRS <u>L</u> LVVM	yes
8	CDC26	NM_139286	rs12248	<u>F</u> VAGTQEVFV	no
9	CHRNA9	NM_017581	rs10022491	TFLK <u>I</u> PML	no
10	CMPK1	NM_016308	rs35687416	TQH <u>S</u> MVNL	no
11	DDX41	NM_016222	rs11555631	SVAEGR <u>A</u> LMSV	yes
12	GPR180	NM_180989	rs9524559	<u>M</u> LKGHLLI	no
13	GTF3C5	NM_001122823	rs1047844	<u>S</u> MYDKVLM	yes
14	GUCA1C	NM_005459	rs6804162	<u>M</u> QEKM <u>E</u> QKL	yes
15	HIVEP1	NM_002114	rs2228220	SLPK <u>H</u> SVTI	yes
16	MAGEF1	NM_022149	rs11554279	ILFPD <u>I</u> ARA	yes
17	MAP4K1	NM_007181	rs35958189	<u>I</u> LNDAGEVRL	yes
18	NISCH	NM_007184	rs887515	ALAPAP <u>A</u> EV	yes
19	NISCH	NM_007184	rs887515	ALAPAP <u>V</u> EV	yes
20	NUFIP1	NM_012345	rs1140993	DTAPPRD <u>S</u> W	yes
21	OR13G1	NM_001005487	rs28556931	ALLSMV <u>M</u> AIA	yes
22	OR6C65	NM_001005518	rs7971073	YTLILK <u>T</u> IL	yes
23	PARP10	NM_032789	rs11136343	GL <u>L</u> GQEG <u>L</u> VEI	yes
24	PEMT	NM_148172	rs897453	LS <u>V</u> TILL	yes
25	PKD1	NM_000296	rs10960	QLA <u>V</u> LLV	yes
26	PLEK	NM_002664	rs1063479	TEWIK <u>A</u> IQM	yes
27	PRH1	NM_006250	rs2416548	MLAPEAV <u>L</u> VLM	yes
28	PRRG2	NM_000951	rs2288920	VASLAVGLT <u>G</u> GIL	yes
29	RNASE8	NM_138331	rs12437266	<u>P</u> LLLLLLGL	yes
30	RPL19	NM_000981	rs11554156	<u>I</u> LMEHIHKL	yes
31	SFI1	NM_014775	rs12171042	PELLLL <u>P</u> L	yes
32	SSTR4	NM_001052	rs3746726	LLN <u>L</u> VVTSL	yes
33	TARS	NM_152295	rs11541416	GLADNT <u>V</u> IAKV	yes
34	TARS	NM_152295	rs11541416	DNT <u>V</u> IAKV	yes
35	TMC06	NM_018502	rs17208187	K <u>T</u> EDAGLEL	yes
36	TRIM9	NM_015163	rs2275462	ATIGVLL <u>D</u> L	yes
37	TYK2	NM_003331	rs34669146	VMEY <u>L</u> PL	yes
38	UCRC	NM_001003684	rs76013375	AIYDH <u>I</u> NEGV	yes
39	USP31	NM_020718	rs10083789	ATVIV <u>S</u> V	no
40	ZNF610	NM_173530	rs321937	<u>V</u> QALLTI	no

^α NCBI messenger RNA transcript

^β NCBI Reference SNP ID

^γ Underlined is polymorphic residue

Table SII. Evaluation peptide selection thresholds

	PPM ^α					BMI ^β					Inframe ^δ	
Score	≤ 1,0	≤ 2,0	≤ 3,0	≤ 4,0	> 4,0	≥ 40	≥ 35	≥ 30	≥ 25	≥ 20	YES	NO
Total peptides	30	34	35	39	40	15	20	32	39	40	33	7
Good	21	23	23	23	23	11	15	20	23	23	19	4
Doubt	4	5	6	7	7	0	0	5	7	7	7	1
False	5	6	6	9	10	4	5	7	9	10	7	2
FPR [%]	17	18	17	23	25	27	25	22	23	25	21	29

^α PPM: Difference between observed and exact ion mass

^β BMI: Match between observed MS spectrum and stated peptide

^δ Normal frame peptide translation

FPR: False positive identification rate in percentage of total peptides

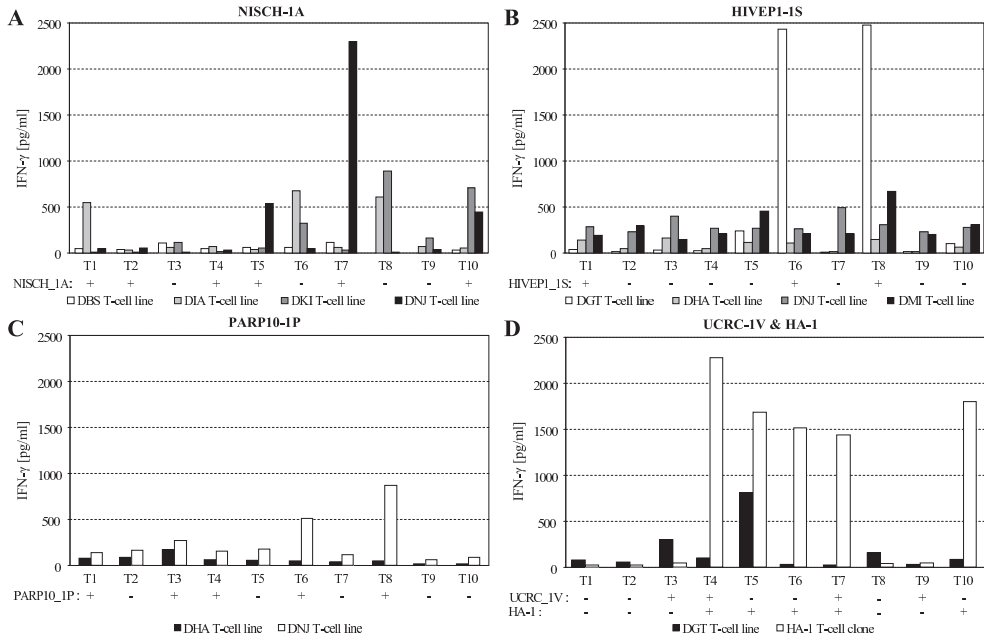
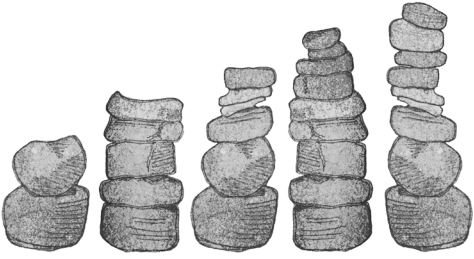


Figure S1. Stimulation assay MHC-tetramer positive T-cell lines. (A) Donor DBS7251, DIA7274, DK17276 and DNJ7281 derived NISCH-1A and (B) DGT7271, DHX7272, DNJ7281 and DMI7280 derived HIVEPI-1S and (C) DHX7272 and DNJ7281 derived PARP10-1P and (D) DGT7271 derived UCRC-1V purified MHC-tetramer positive T-cell lines were stimulated with a panel of 10 HLA-A*0201 positive and SNP genotyped EBV-LCL target cells positive (+) or negative (-) for the indicated MiHA for 18 hours. T-cell reactivity was measured by standard IFN- γ ELISA. As a control for MiHA specific T-cell reactivity a high avidity HA-1 specific T-cell clone was used.



5

Submitted for publication

IDENTIFICATION OF BIOLOGICAL RELEVANT MINOR HISTOCOMPATIBILITY ANTIGENS WITHIN THE B-LYMPHOCYTE DERIVED HLA-LIGANDOME USING A REVERSE IMMUNOLOGY APPROACH

Pleun Hombrink^{1#}, Chopie Hassan^{2#}, Michel G.D. Kester¹, Lorenz Jahn¹, Margot J. Pont¹, Arnoud H. de Ru², Cornelis A.M. van Bergen¹, Marieke Griffioen¹, J.H. Frederik Falkenburg¹, Peter A. van Veelen^{2,§} and Mirjam H.M. Heemskerk^{1,§}

¹ Department of Hematology, Leiden University Medical Center, Leiden, The Netherlands;

² Department of Immunohematology and Blood Transfusion, Leiden University Medical Center, Leiden, The Netherlands

[#] These authors contributed equally

[§] Shared Senior Authorship

T-cell recognition of minor histocompatibility antigens (MiHA) plays an important role in the beneficial graft-versus-leukemia (GVL) effect of allogeneic stem cell transplantation (allo-SCT) but also mediates serious graft versus host disease (GVHD) complications associated with allo-SCT. Using a reverse immunology approach we aim to develop a method enabling the identification of T-cell responses directed against predefined antigens, with the goal to select those MiHAs that can be used clinically in combination with allo-SCT. In this study, we used a recently developed MiHA selection algorithm to select candidate MiHAs within the HLA-presented ligandome of transformed B-cells. From the HLA-presented ligandome, that predominantly consisted of monomorphic peptides, 25 polymorphic peptides with a clinically relevant allele frequency were selected. By high-throughput screening the availability of high-avidity T-cells specific for these MiHA-candidates in different healthy donors was analyzed. With the use of MHC-multimer enrichment, analyses of expanded T-cells by combinatorial coding MHC-multimer flow cytometry, and subsequent single cell cloning, positive T-cell clones directed to 2 new MiHA: LB-*CLYBL*-1Y and LB-*TEP1*-1S could be demonstrated, indicating the immunogenicity of these 2 MiHAs. The biological relevance of MiHA LB-*CLYBL*-1Y was demonstrated by the detection of LB-*CLYBL*-1Y specific T cells in a patient suffering from acute myeloid leukemia (AML) that experienced an anti-leukemic response after treatment with allo-SCT.

INTRODUCTION

Allogeneic HLA-matched hematopoietic stem cell transplantation (allo-SCT) and subsequent donor lymphocyte infusion (DLI) to eradicate persistent or relapsed malignant cells are considered an effective curative treatment for patients with high-risk hematological malignancies or patients who fail to respond to chemotherapy¹. The curative potential of this therapy has been attributed to the recognition of malignant cells by donor T-cells. Detailed analyses of T-cell immune responses in patients responding to DLI have demonstrated that the donor T-cells recognize minor histocompatibility antigens (MiHA) presented in the context of HLA-molecules on malignant cells. MiHA are peptides derived from polymorphic proteins that differ between donor and recipient due to single nucleotide polymorphisms (SNP)²⁻⁵. Previously it has been demonstrated that T-cells directed against MiHA that are ubiquitously expressed can mediate life-threatening graft-versus-host-disease (GVHD)⁶, whereas T-cells directed against MiHA with hematopoietic restriction may mediate graft-versus-leukemia (GVL) response in absence of GVHD⁷.

Although the introduction of various molecular and genomic technologies resulted in an increased number of HLA-class I restricted MiHA identified by forward immunological approaches, the number of MiHA with therapeutic relevance is still limited^{8,9}. A major limitation for clinical implementation of MiHA is the small number of identified MiHA derived from genes that are exclusively expressed in hematopoietic cells. To allow the selective analysis of hematopoietic restricted MiHA, we and others have used reverse immunological approaches in which predicted polymorphic peptides are the starting point and peptide candidates are subsequently screened for their capacity to induce a specific T-cell response. This approach has the potential to specifically screen for T-cells recognizing MiHA that are exclusively expressed by hematopoietic cells. However, it has been reported that when such peptide predictions are solely based on computer algorithms that predict peptide-HLA binding affinity and proteolytic cleavage, the detected T-cell responses are often directed against epitopes that are not naturally processed and presented and therefore fail to lyse malignant target cells¹⁰⁻¹². To circumvent this peptide selection problem we and others previously introduced mass spectrometry (MS) based HLA-ligandomes as a reliable source for naturally processed and presented peptides and developed an algorithm that can be exploited to identify T-cells specific for potential clinically relevant MiHA^{13,14}.

The emerging availability of high quality SNP data in combination with the implementation of HLA-ligandomes provides a large supply of MiHA-candidates with guaranteed processing and HLA-restricted presentation at the cell surface¹⁵. We used our recently established algorithm¹³ to select the top 25 MiHA-candidates from our newly established large set of B-lymphocyte derived HLA-class I eluted peptides¹⁶. To validate these MiHA candidates it is essential to demonstrate their immunogenic potential by isolation of high avidity specific T-cells. We therefore screened the TCR repertoire of 16 unrelated donors for the presence of T-cells specific for these MiHA-candidates. MHC-multimer

positive T-cells lines were generated from peripheral blood mononuclear cells (PBMC) by magnetic activated cell sorting (MACS). Flow cytometric analysis of antigen-specific T-cells, followed by functional testing of MHC-multimer sorted and expanded T-cell clones using both IFN- γ and GM-CSF as readout demonstrated the immunogenic potential of LB-*CLYBL-1Y*, LB-*TEP1-1S* and two previously described MiHA. For one of the newly defined MiHA we were able to confirm the biological relevance by demonstrating MHC-multimer positive T-cells in a patient suffering from AML after treatment with allo-SCT and subsequent DLI. Our data illustrate that with this reverse immunology approach biologically relevant MiHA can be identified as well as MiHA that are not frequently induced *in vivo* but can potentially be used for immunotherapeutic strategies.

RESULTS

5

Selection of high affinity HLA-A*0201 and B*0702 binding MiHA-candidates from a set of HLA-class I eluted peptides

We have recently reported a MiHA selection algorithm to be able to select MiHA candidates from a library of HLA-class I eluted peptides¹³. This MiHA selection algorithm comprises several evaluation steps that are summarized in the material and methods section. This algorithm was used to screen our newly established library of eluted HLA-class I peptides derived from multiple HLA-A*0201 and B*0702 positive EBV-LCLs, to select for potential MiHA candidates¹⁶. To validate this newly established library of approximately 16,000 eluted HLA class I peptides comprising of mainly monomorphic peptides, we first screened for the presence of known MiHA. Peptide sequences or their relevant length variants were identified for 10 out of 13 MiHA that were expressed by the EBV-LCLs as revealed by SNP genotyping (Table S1)^{3,8,9}, illustrating the high quality of this peptide elution library.

In the next step we selected a set of 25 MiHA-candidates using the MiHA selection algorithm, including 22 novel MiHA-candidates as well as the previously reported LB-*NISCH-1A*, LB-*ERAP1-1R* and LB-*GEMIN4-1V* MiHA (Table SII). We first analyzed the capacity of the 25 MiHA-candidates to stabilize a peptide-HLA complex in a HLA-binding assay that is based on UV-induced conditional ligand cleavage as described previously^{10,22,26}. After UV-exchange, the HLA-binding affinity of the tested peptides was normalized to the high-affinity control peptides CMV-*PP65-NLV* and CMV-*PP65-TPR* for HLA-A*0201 and B*0702, respectively (Fig. S1A,B). MiHA-candidates were selected when their HLA-binding affinity exceeded that of the *MART1-WT-AAG* peptide, which binds with low affinity to HLA-A*0201. HLA-binding affinity as measured with HLA-rescue scores exceeded that of the *MART1-WT-AAG* control for 8 HLA-A*0201 and 13 B*0702 binding MiHA-candidates. Peptide sequences and allele frequencies of the MiHA are shown in Table I.

Table I. Validated MiHA candidates.

HLA	Peptide	Sequence ^α	Gene	RS number	SNP	Allele Frequency
A*02:01	P1	GLLGQEG ^α LV ^α EI	<i>PARP10</i>	rs11136343	L/P	0.66%
	P2	ALAPAP ^α AEV	<i>NISCH</i> ^β	rs887515	A/V	0.17%
	P3	AMLERQ ^α FTV	<i>FAM119A</i>	rs2551949	T/I	0.19%
	P4	FLSSANEHL	<i>GLRX3</i>	rs2274217	S/P	0.25%
	P5	MMYKDILLL	<i>HNF4G</i>	rs1805098	M/I	0.40%
	P6	SLAAYI ^α PRL	<i>CLYBL</i>	rs17577293	Y/D	0.05%
	P7	SLQEK ^α VAKA	<i>HMMR</i>	rs299295	V/A	0.20%
	P8	VLQ ^α NVAFSV	<i>BCL2A1</i>	rs1138358	N/K	0.69%
B*07:02	P9	APNTGRANQ ^α QM	<i>BFAR</i>	rs11546303	M/R	0.57%
	P10	LPMEVEKNST ^α L	<i>HMGF</i>	rs4399146	L/P	0.40%
	P11	RPRAP ^α TEELAL	<i>C14orf169</i>	rs3813563	A/V	0.40%
	P12	APDGAKVAS ^α L	<i>TEP1</i>	rs1760904	S/P	0.49%
	P13	APAGVRE ^α V ^α M	<i>AKAP13</i>	rs7162168	M/T	0.37%
	P14	KPQQKGLRL	<i>APOBEC3H</i>	rs139298	K/E	0.52%
	P15	LPQKKS ^α NAL	<i>POP1</i>	rs17184326	N/K	0.10%
	P16	LPQQP ^α PLSL	<i>SCRIB</i>	rs6558394	L/P	0.64%
	P17	NPATP ^α ASKL	<i>C18orf21</i>	rs2276314	A/T	0.21%
	P18	SPASS ^α R ^α TDL	<i>MTRR</i>	rs1532268	S/L	0.68%
	P19	S ^α PSLRILAI	<i>LLGL2</i>	rs1671036	R/H	0.50%
	P20	HPRQE ^α QIAL	<i>ERAP1</i> ^β	rs34753	R/P	0.31%
	P21	FPALRFVEV	<i>GEMIN4</i> ^β	rs1045481	V/E	0.20%

^α SNP underlined

^β Published MiHA epitope or length variant

Non- and Immunogenic Allele indicated by amino acid code, allele frequencies are calculated by quantification in a panel of 100 Dutch individuals using SNP genotyping array.

Isolation of peripheral blood derived MHC-multimer positive T-cells by MHC-multimer pull down

To validate the 21 peptides as MiHA with immunogenic potential, we generated MHC-multimers and analyzed the T-cell repertoire of 16 healthy HLA-A*0201 and B*0702 positive donors for MHC-multimer reactive T-cells. MiHA-specific T-cell lines were generated by incubating 100×10^6 peripheral blood mononuclear cells (PBMC) with a specific set of MHC-multimers, followed by enrichment of MHC-multimer positive cells on a magnetic column. To allow the isolation of high avidity T-cell populations, the set of MHC-multimers was specifically adjusted for each PBMC sample to cover only those MiHA for which the encoding SNP was screened homozygous negative in the respective donor, since in this individual's T-cell repertoire high avidity MiHA specific T-cells will not have been deleted due to negative selection. The set of PBMC donors was specifically adjusted to cover as many applicable donors per MiHA candidate. Unfortunately, no homozygous negative donors were found for the *SCRIB*-1L MiHA candidate. The MHC-multimer enriched T-cells were expanded for 14 days in presence of α CD3/28 beads, IL-2 and IL-15. To increase the frequency of MHC-multimer positive T-cells, a second pull down was performed at day 14

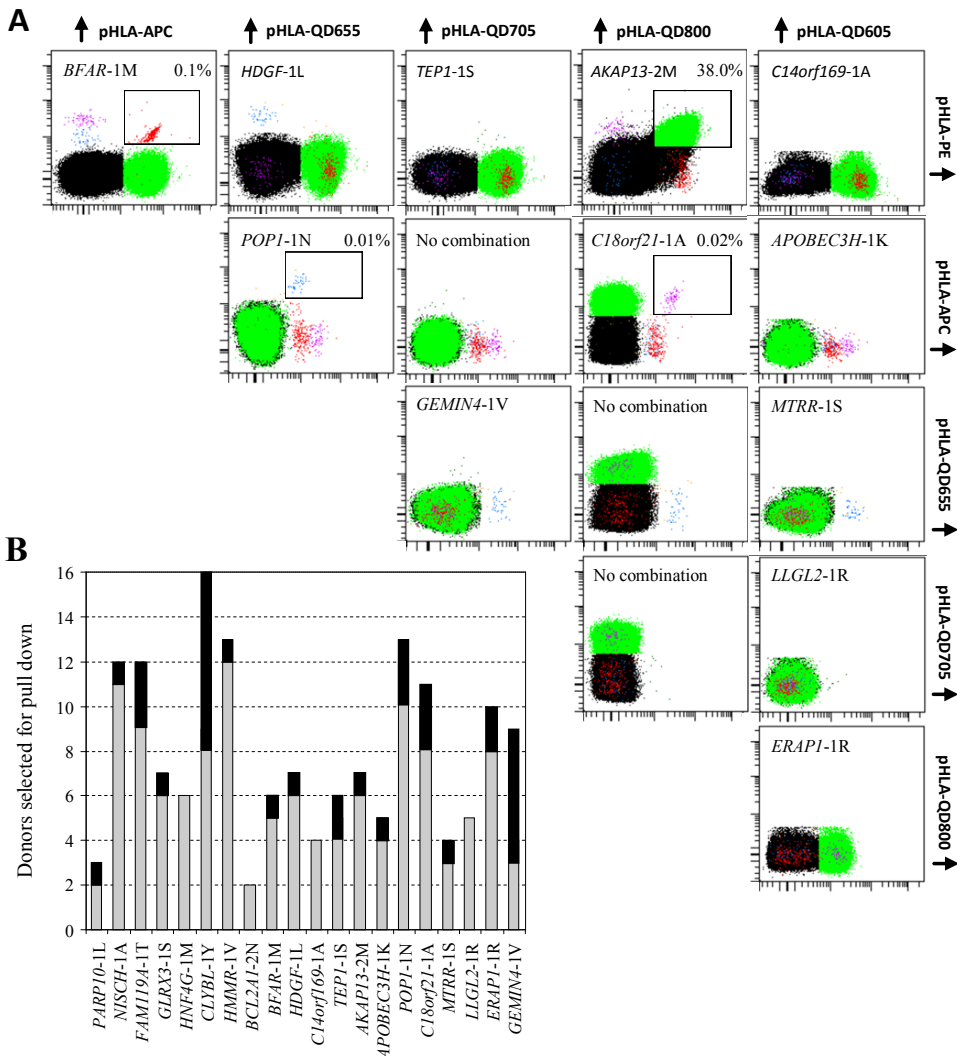


Figure 1. Detection of MiHA-specific T-cells after MHC-multimer enrichment and expansion. FACS analyses were performed to detect MiHA-specific T-cells through combinatorial coding MHC-multimer screening after second pull down and *in vitro* expansion. Each peptide-MHC complex was encoded by a unique combination of fluorochromes. Two HLA-restricted sets of MHC-multimers were used to screen for detection of all MiHA-candidates specific T-cells. (A) Representative analysis of the two times enriched T-cell line derived from donor OMH with the HLA-B*0702 restricted MHC-multimer set. Total CD8⁺ T-cells are shown and MHC-multimer negative cells or cells staining with more than 2 fluorochromes are indicated in black. All dot plots are shown with bi-exponential axes and display fluorescence intensity for the fluorochromes indicated on each axis. Frequencies indicate MHC-multimer positive T-cells of total CD8⁺ cells. (B) Total MHC-multimer positive T-cell populations detected in 16 tested PBMC donors after second pull down by combinatorial coding MHC-multimer screen. Bars indicate the number of donors homozygous negative for the indicated SNP encoding MiHA and applicable for MHC-multimer pull down. The number of MHC-multimer positive T-cell populations detected per MiHA candidate is indicated in black. No homozygous negative donors were found for *SCRIB-1L*, and therefore *SCRIB-1L* is not indicated in the figure. At least two homozygous negative donors were included for the other 20 MiHA-candidates.

using the identical initial set of MiHA candidate specific MHC-multimers. After both rounds of MHC-multimer enrichment we analyzed the expanding T-cell lines for the presence of MHC-multimer positive T-cells by FACS. A representative FACS analysis after two rounds of MHC-multimer enrichment is demonstrated in Fig. 1A in which 4 MHC-multimer positive T-cell populations specific for HLA-B*0702 binding MiHA-candidates are detected in donor OMH. After the first MHC-multimer pull down, MHC-multimer positive T-cell populations were detected specific for 11 of the 20 tested MiHA-candidates in one or more T-cell cultures. MHC-multimer positive T-cell frequencies varied between 0.01% and 5.0% of total CD8⁺ T-cells (Table SIII). These low frequencies are most likely due to the very low frequency of MHC-multimer positive T-cells in the naïve repertoire. After the second MHC-multimer pull down, MHC-multimer positive T-cell populations were detected specific for an increased number of 16 of the 20 tested MiHA-candidates with frequencies up to 85% of total CD8⁺ T-cells (Table SIII). As demonstrated in Figure 1B, T-cells reactive with the *CLYBL-1Y* and *LB-GEMIN4-1V* MHC-multimer were frequently detected in 8 of the 16 and 6 of the 9 enriched T-cell lines, respectively. In contrast, T-cells specific for the other MiHA appeared more restricted to a few donors.

Detection of high avidity T-cell clones by screening for MiHA-specific IFN- γ and GM-CSF production

Next, a total number of 806 MHC-multimer positive T-cell clones representing all detected T-cell populations were generated by FACS sorting. To demonstrate recognition of potential MiHA-candidates, all 806 T-cell clones were stimulated with specific antigen and cytokine production was determined as a measure for antigen specific reactivity. Because the T-cell clones were most likely derived from the naïve T-cell repertoire and have presumably not all acquired the capacity to produce IFN- γ upon antigen encounter, we first screened all T-cell clones for their potential to secrete IFN- γ after α CD3/28 stimulation. As demonstrated in Figure 2A, the generated T-cell clones demonstrated a broad range of IFN- γ secretion. To investigate whether GM-CSF was of additional value to improve the screening efficiency, the GM-CSF production of part of the T-cell clones with variable IFN- γ secretion potential was measured after α CD3/28 stimulation. The results demonstrate that a substantial number of T-cell clones with poor intrinsic IFN- γ production were able to produce pronounced GM-CSF levels (Fig. 2B). Therefore by using both IFN- γ and GM-CSF as a readout we could increase the number of MHC-multimer positive T-cell clones that could be screened. By setting an arbitrary detection limit to 100 pg/ml for both cytokines, 98% of generated T-cell clones could subsequently be screened for MiHA specific reactivity.

To demonstrate the capacity of the isolated MHC-multimer positive T-cell clones to recognize specific MiHA peptides we stimulated all T-cell clones with HLA-A*0201 and B*0702 positive T2 target cells loaded with titrated concentrations of specific peptide. MiHA specific T-cell reactivity was observed for 8 out of 16 tested MiHA-candidates and

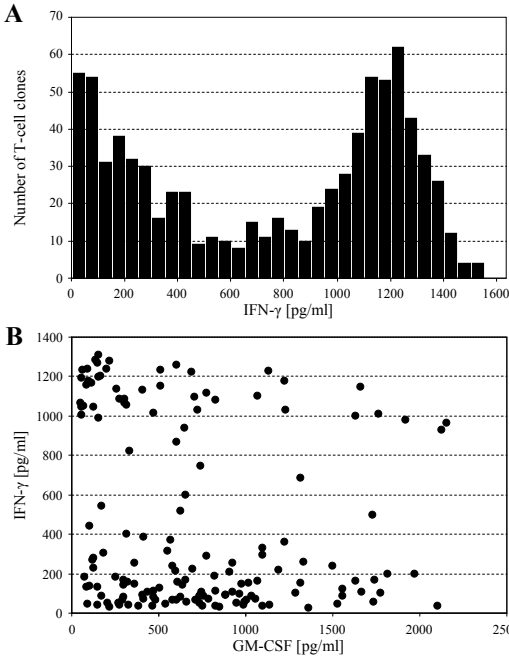
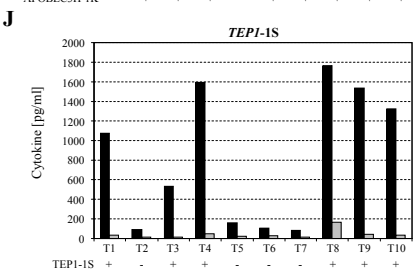
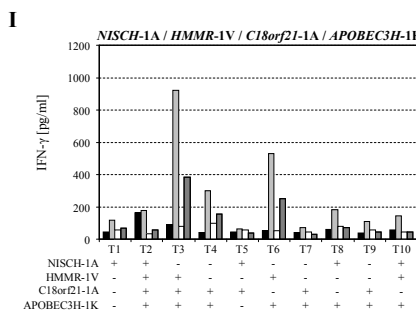
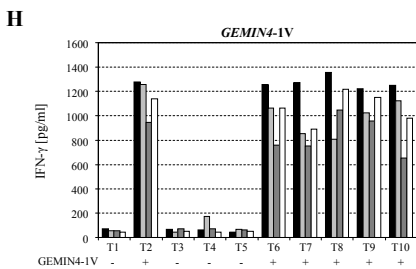
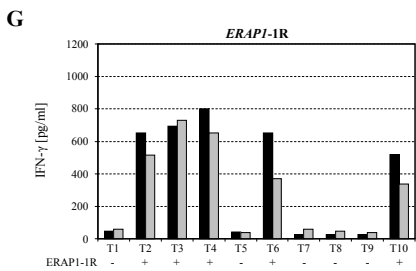
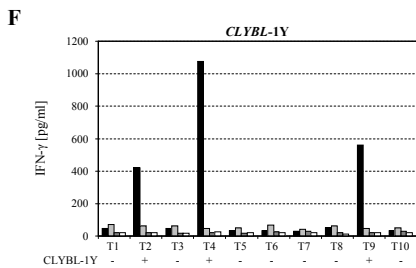
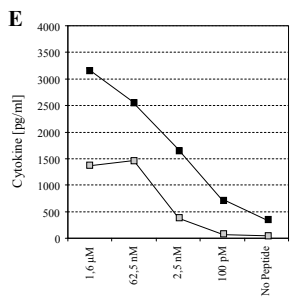
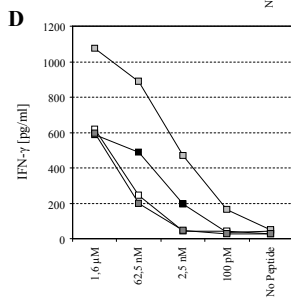
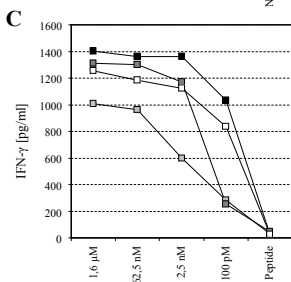
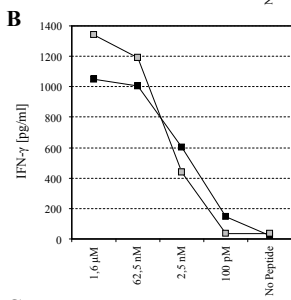
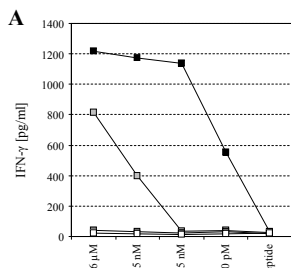


Figure 2. Isolated T-cell clones vary in production of IFN- γ and GM-CSF upon α CD3/28 stimulation. (A) Distribution of the intrinsic IFN- γ secretion capacity of 806 MiHA-specific MHC-multimer positive T-cell clones stimulated with α CD3/28 beads. (B) Production of GM-CSF for 150 selected T-cell clones with variable IFN- γ secretion capacity. MiHA specific MHC-multimer positive T-cell clones were stimulated for 18 hours in presence of α CD3/28 beads and GM-CSF and IFN- γ secretion was measured by standard ELISA.

Figure 3. MHC-multimer positive T-cell clones demonstrate MiHA specific reactivity. Isolated MHC-multimer positive T-cell clones were stimulated with HLA-A*0201 and B*0702 positive T2 cells loaded with titrated concentrations of peptides for 18 hours [E:T] 5,000:25,000. For each donor the MiHA specific T-cell clone that demonstrated the highest peptide avidity is shown for the respective cytokine. MiHA specific IFN- γ production was observed for T-cell clones specific for (A) *CLYBL-1Y*, (B) *ERAP1-1R*, (C) *GEMIN4-1V* (D) *NISCH-1A*, *HMMR-1V*, *C18orf21-1A*, *APOBEC3H-1K*, and (E) *TEP1-1S* MiHA-candidates. For the *TEP1-1S* specific T-cell clone K091 derived from donor EPP both the peptide induced IFN- γ and GM-CSF secretion are shown. (F,G,H,I,J) To measure the reactivity of the MiHA specific T-cell clones against endogenously processed and presented antigens, all MiHA specific T-cell clones that demonstrated IFN- γ or GM-CSF production in response to specific peptide were stimulated with a panel of 10 HLA-A*0201 and B*0702 positive EBV-LCL target cells positive (+) or negative (-) for the indicated MiHA for 18 hours. Cytokine secretion was measured by standard ELISA.



either IFN- γ or GM-CSF was detected after stimulation with *CLYBL-1Y*, *ERAP1-1R*, *GEMIN4-1V*, *NISCH-1A*, *HMMR-1V*, *C18orf21-1A*, *APOBEC3H-1K* and *TEP1-1S* MiHA peptides. For each donor the MiHA specific T-cell clone that demonstrated the highest peptide avidity is shown (Fig. 3A-E). MiHA specific T-cell clones demonstrated variable peptide avidity and half maximum cytokine production (IC₅₀) varied between an IC₅₀ of ± 100 pM for the high avidity T-cell clone K156 specific for *GEMIN4* (Fig. 3C) and an IC₅₀ of ± 62.5 nM for the low avidity T-cell clone K337 specific for *C18orf21* (Fig. 3E). For the *CLYBL-1Y* MiHA candidate, MHC-multimer positive T-cell clones were successfully isolated from 4 different donors. High avidity *CLYBL-1Y* specific T-cell clones were isolated from donor ABM, whereas only low avidity or non-reactive T-cells were isolated from donor UDN, EPP and FHT respectively (Fig. 3A). For the previously described MiHA *ERAP1-1R*, both high and low avidity T-cell clones were isolated from the 2 donors that demonstrated MHC-multimer positive T-cell populations after pull down. For the previously described MiHA *GEMIN4-1V*, high avidity T-cell clones were only isolated from 4 out of 6 donors that demonstrated MHC-multimer positive T-cell populations after pull down (Fig. 3B,C; low-avidity T-cell clones not shown). The *NISCH-1A*, *HMMR-1V*, *C18orf21-1A* and *APOBEC3H-1K* specific T-cell clones were each successfully isolated from one donor and exhibited high (*HMMR-1V*) to low peptide avidity (*NISCH-1A*, *C18orf21-1A* and *APOBEC3H-1K*) (Fig. 3D). For the *TEP1-1S* MiHA candidate high avidity T-cell clones were isolated from donor EPP. T-cell clone K091 demonstrated high peptide specific GM-CSF production and low IFN- γ production (Fig. 3E). No peptide specific T-cell clones specific for the other MiHA-candidates were observed.

All T-cell clones that demonstrated peptide specific cytokine production were stimulated with a panel of 10 SNP genotyped HLA-A*0201 and B*0702 positive EBV-LCL target cells to screen for reactivity against endogenously processed and presented peptide. As demonstrated in Figure 3F,G,H and J all high avidity T-cell clones specific for *CLYBL-1Y*, *TEP1-1S*, *ERAP1-1R* and *GEMIN4-1V* demonstrated recognition of all target cells that endogenously process and present their respective MiHA, whereas targets that were negative for the MiHA were not recognized. Surprisingly, the high avidity T-cell clone K508 specific for *HMMR-1V* did not show a recognition pattern that correlated with MiHA expression. This may be caused by the absence of endogenously presented MiHA peptide by some of the SNP positive EBV-LCL or by the recognition of allo-HLA molecules expressed by EBV-LCL. No or only marginal target cell recognition was observed for the *NISCH-1A*, *C18orf21-1A* and *APOBEC3H-1K* specific T-cell clones (Fig. 3I). These results indicate that the MiHA *CLYBL-1Y* and *TEP1-1S* represent potentially immunological relevant MiHA-candidates.

Detection of MiHA specific T-cell responses in patients after allo-SCT

To validate the biological relevance of the MiHA-candidates we analyzed the peripheral blood of patients suffering from various hematopoietic malignancies that received an allo-

SCT and DLI and demonstrated a clinical response revealed by declining patient chimerism, for the detection of MiHA specific T-cells. Patients were only screened with MiHA-specific MHC-multimers when they were positive for the MiHA and received a DLI from a donor who was homozygous negative for the SNP encoding MiHA (Table SIII). Tested patient samples were obtained during or after the peak response, 5 to 8 weeks after treatment with DLI. For the newly identified *CLYBL-1Y* MiHA, MHC-multimer positive T-cells were detected in 1 of the 3 screened patients (Fig. 4A) with a frequency of 0.34% of total CD8⁺ T-cells at day 41 after DLI (AML patient MBF, Fig. 4B). For the previously described *ERAP1-1R* and *GEMIN4-1V* MiHA, MHC-multimer positive T-cells were detected in 1 of the 2 and 1 of the 4 screened patients (both multiple myeloma (MM) patient CUB at day 86), respectively (Fig. 4A,B). Detected frequencies of circulating MHC-multimer positive T-cells ranged between 0.04% and 0.34% of total CD8⁺ T-cells. For the other 17 MiHA-candidates with validated HLA-binding affinity and SNP occurrence, including the newly identified MiHA *TEP1-1S*, no MHC-multimer positive T-cells were detected in the peripheral blood of 1 to 5 screened patients (Fig. 4A,B, Table SIII).

To investigate whether the MHC-multimer enriched T-cell clones exerted comparable peptide specific avidity as the *in vivo* generated patient derived MiHA specific T-cells, we generated *CLYBL-1Y* specific T-cell clones by single cell sorting of *CLYBL-1Y* MHC-multimer positive T-cells from patient MBF. After expansion the T-cell clones were stained with the MHC-multimer and TCR-V β mAbs. The T-cell clone K264, which was generated by MHC-multimer enrichment from donor ABM, demonstrated similar MHC-multimer staining intensity as the patient derived K2-339 clone (Fig. 5A), but a difference in TCR V β usage; clones derived from donor ABM expressed TCR V β 22 and patient MBF derived clones were TCR-V β 1 positive. Clone K264 and K2-339 were stimulated with T2 cells loaded with titrated concentrations of either the specific or the allelic variant peptide and IFN- γ production was measured (Fig. 5B). Both T-cell clones demonstrated high *CLYBL-1Y* specific peptide reactivity, with IC50 varying between 1-4 pM, whereas the allelic *CLYBL-1D* variant was not or hardly recognized by both T-cell clones, demonstrating that T-cell clones derived from an unprimed setting can be equally potent as T-cells derived from an *in vivo* primed setting.

***CLYBL-1Y* and *TEP1-1S* specific T-cell recognition of hematopoietic malignant cells**

To investigate the expression pattern of the *CLYBL* and *TEP1* genes we performed a microarray gene expression array using a panel of primary and cultured malignant (and non-malignant) hematopoietic and non-hematopoietic cells (Fig. S1C,D). The data showed that the *CLYBL* gene is broadly expressed in hematopoietic and non-hematopoietic cells. Expression of the *TEP1* gene was not significantly measured in the majority of the samples. To investigate whether the *CLYBL-1Y* and *TEP1-1S* specific T-cell clones were able to recognize hematopoietic malignant cells they were stimulated with primary CML, AML and

ALL cells derived from different MiHA positive and negative patients that were positive for the restricting HLA-molecule. As a control, T-cell clones were also tested for recognition of EBV-LCL generated from the same individuals. Both the high avidity T-cell clones *CLYBL* K264 and *TEP1* K091 demonstrated MiHA specific recognition of primary hematopoietic malignant cells (Fig. 6A,C). No reactivity was observed against MiHA negative target cells. These data indicate that the tested MiHA can be presented in the context of HLA at the surface of leukemic cells and may therefore serve as direct targets of CD8⁺ T-cells involved in a GVL response. In addition, the potential of the MiHA to serve as target in GVHD was estimated and the MiHA specific T-cell clones were tested for recognition of

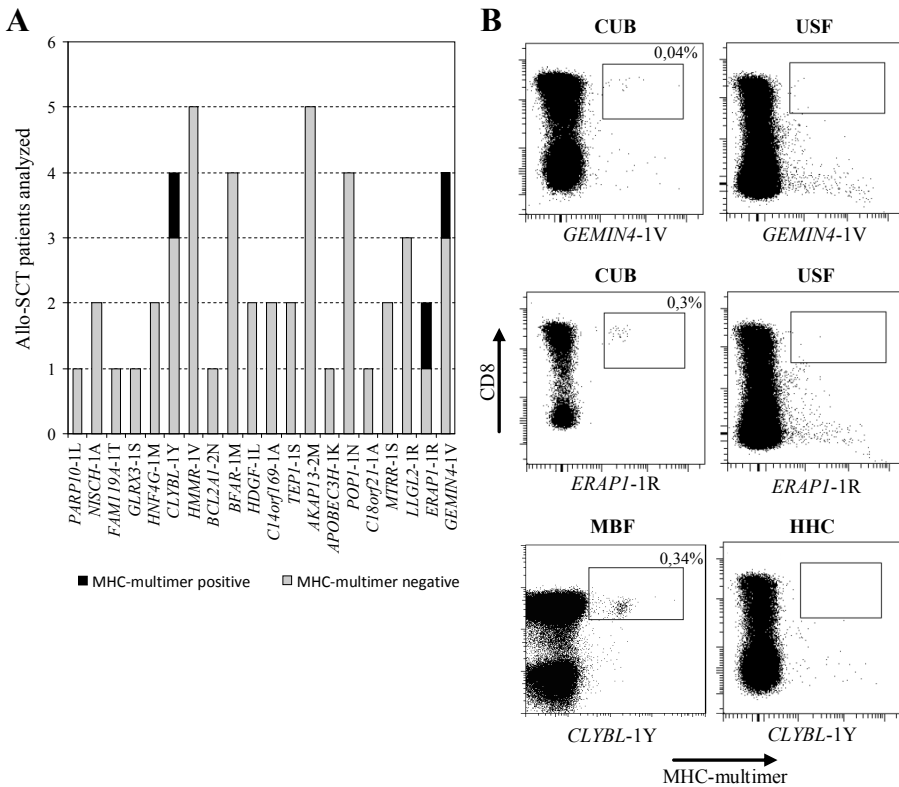


Figure 4. MHC-multimer positive T-cell populations detected in patients after allo-SCT.

(A) Number of MHC-multimer positive T-cell populations detected by combinatorial coding MHC-multimer analysis in peripheral blood samples of 16 patients with various hematologic malignancies that received an allo-SCT and demonstrated a clinical response to DLI. Patients were only screened when they were positive for the SNP encoding MiHA and received a DLI from a donor that was homozygous negative for the SNP encoding MiHA. Bars indicate the number of patients applicable for MiHA-specific MHC-multimer screening. The number of MHC-multimer positive T-cell populations detected per MiHA candidate is indicated in black. (B) Representative FACS analysis of MHC-multimer positive T-cell populations detected in the indicated patients. All dot plots display fluorescence intensity for CD8 and specific MHC-multimer staining. Total lymphocytes are shown. Frequencies indicate MiHA specific T-cells of total CD8⁺ T-cells.

non-hematopoietic fibroblasts. To mimic the pro-inflammatory cytokine milieu, early after transplant or during potent GVHD responses, fibroblasts were pretreated with IFN- γ . Although both the *CLYBL* K264 and *TEP1* K091 T-cell clone poorly recognized non treated fibroblasts they clearly recognized those that were IFN- γ pretreated (Fig. 6B,D). These data indicate that both *CLYBL*-1Y and *TEP1*-1S may be considered as MiHA with potential therapeutic value under non-inflammatory conditions, but they may participate in toxic GVHD responses in a pro-inflammatory environment.

DISCUSSION

In this study we demonstrate the identification of two biologically relevant MiHA by a reverse immunology approach. We started our approach by selecting MiHA-candidates from our recently generated B-lymphocyte derived HLA-class I eluted peptide library(13,16). By MiHA candidate specific MHC-multimer enrichments and subsequent single cell sorting of MHC-multimer positive T-cells, high avidity MiHA specific T-cell clones directed against the MiHA *TEP1* -1S and *CLYBL*-1Y could be identified that recognize primary hematological

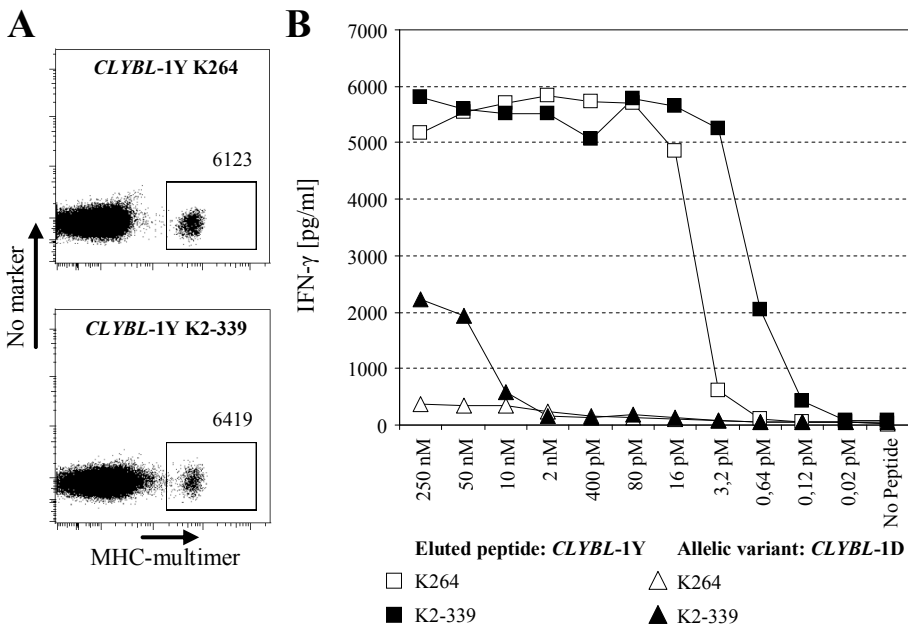


Figure 5. Functional avidity of patient and donor derived *CLYBL*-1Y specific T-cell clones. (A) FACS analysis of MHC-multimer positive *CLYBL*-1Y specific T-cell clones. To prevent doublet formation, *CLYBL*-1Y specific T-cell clones were mixed with CD4 T-cell blasts. Dot plots display fluorescence intensity for MHC-multimer staining. Total lymphocytes are shown. (B) *CLYBL*-1Y specific T-cell clones derived from donor ABM (K264; white) or from patient MBF (K2-339; black) were stimulated with HLA-A*0201 positive T2 target cells loaded with titrated concentrations of *CLYBL*-1Y peptide (squares) or allelic variant (triangles) for 18 hours [E:T] 5,000:25,000. IFN- γ secretion was measured by standard ELISA.

malignancies expressing the respective MiHA, indicating the immunogenicity of the two MiHA. In addition, we were able to demonstrate an *in vivo* induced immune response against the new *CLYBL*-1Y MiHA in a patient suffering from AML that experienced an anti-leukemic response after allo-SCT and subsequent DLI treatment, demonstrating that by using this reversed immunology approach, biologically relevant MiHA can be identified. For the *CLYBL*-1Y MiHA, MHC-multimer analysis revealed the presence of T-cells specific for this MiHA in one of the 3 patients screened. These *in vivo* primed T-cells demonstrated to be high avidity T-cells specific for the *CLYBL*-1Y allelic MiHA variant. For the *TEP1*-1S MiHA only two patients could be screened for the presence of *TEP1*-1S specific MHC-multimer

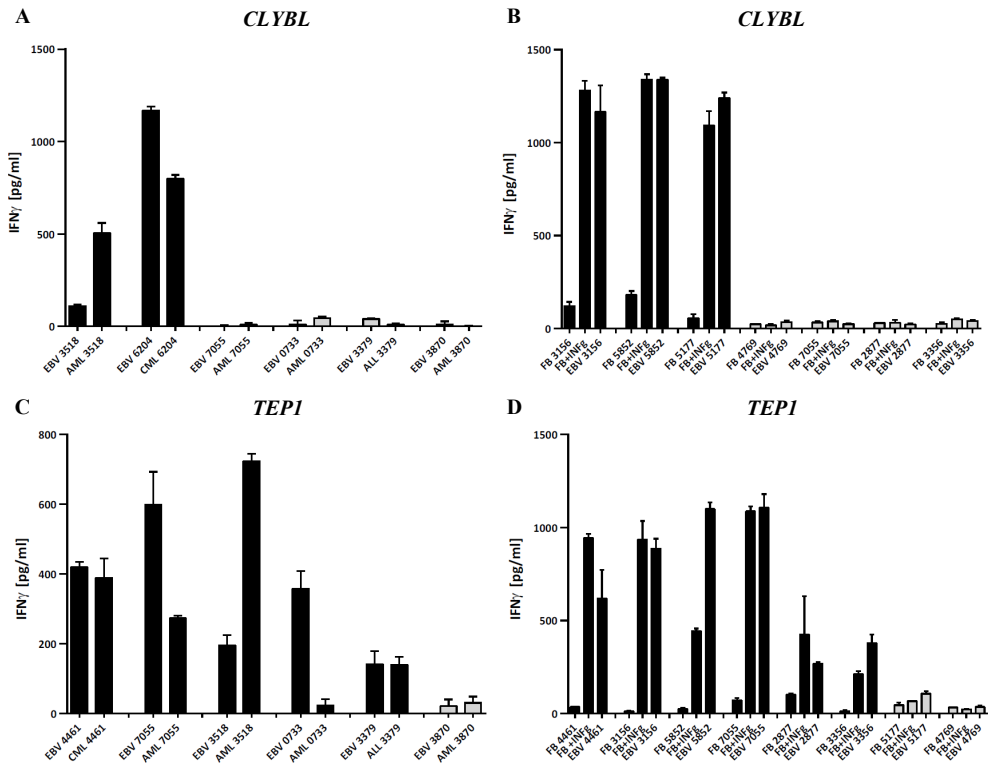


Figure 6. MiHA specific T-cell reactivity towards hematopoietic malignancies and fibroblasts. Isolated MHC-multimer positive T-cell clones were screened for recognition of various primary hematopoietic malignancies and non-hematopoietic fibroblasts isolated from different individuals. As a control for T-cell recognition, all T-cell clones were also stimulated with EBV-LCL generated from the same individuals. (A) *CLYBL*-1Y clone K264 and (C) *TEP1*-1S clone K091 were stimulated with HLA-A*0201 or B*0702 positive primary AML, CML and ALL cells either positive (black bars) or negative (gray bars) for the specific MiHA, directly after isolation of malignant cells for 18 hours [E:T] 1,000:5,000. To measure the recognition of non-hematopoietic cells, (B) *CLYBL*-1Y clone K264 and (D) *TEP1*-1S clone K091 were stimulated with fibroblasts either pre-treated with IFN- γ (100 IU/ml) or not. MiHA specific recognition of target cells was measured by standard IFN- γ ELISA.

positive cells. Therefore, the absence of an *in vivo* induced immune response against *TEP1*-1S could either be due to the low number of patients that could be screened or due to subdominance of *TEP1*-1S in the immune response. Our reverse immunology approach has the advantage to allow identification of subdominant MiHA as the T-cell repertoire of patients that are screened in forward immunology approaches is skewed towards highly immunodominant MiHA specific responses. Subdominant MiHA, however, may be of therapeutic interest as they can be exploited in potential peptide vaccination or adoptive T-cell therapies when they demonstrate promising gene expression patterns.

A major limitation for the identification of large numbers of MiHA using a reverse immunology approach may be the low frequency of high avidity MiHA specific T-cells within an individual's T-cell repertoire. By performing two rounds of MHC-multimer enrichments each followed by a 10 days expansion step we increased the number of MHC-multimer positive T-cells that was isolated, since we observed that after the second enrichment round previously undetected MHC-multimer positive T-cell populations were found. In addition, by measuring GM-CSF in addition to IFN- γ as readout for T-cell reactivity, we were able to increase the number of MHC-multimer positive T-cell clones that could be screened for functional activity. However, the failure to isolate high-avidity T-cells for the previously identified LB-*NISCH*-1A MiHA indicates that isolation of high avidity T-cells may still be a matter of chance¹³. Alternatively, T-cells may be tolerant for some MiHA due to molecular mimicry with non-polymorphic epitopes or due to their failure to discriminate between both allelic variants of a SNP encoding MiHA²⁷, explaining why not all MiHA-candidates will be of clinical relevance.

For 8 of the 20 MiHA-candidates MHC-multimer positive T-cell clones were isolated that demonstrated MiHA specific peptide reactivity. The different MHC-multimer positive T-cell clones however demonstrated functional heterogeneity. We have recently demonstrated that CMV-specific MHC-multimer positive T-cells isolated from CMV negative individuals by MHC-multimer enrichments also demonstrated a large variation in functional avidity²⁸. This heterogeneity in functional activity of the MHC-multimer positive T-cell populations may be specific for T-cells isolated from the naïve repertoire as memory T-cells are skewed toward a high-avidity range as a result of antigen encounter *in vivo*. Non-responsiveness of MHC-multimer positive T-cell clones has also been reported by others for T-cells derived from the naïve repertoire^{29,30}. The discrepancy between MHC-multimer reactivity and T-cell functionality can most likely be explained by the staining with multimerized MHC-peptide complexes. Multimerization of MHC-peptide complexes alters the TCR-MHC-peptide dissociation on- and off-rate kinetics and will result in increased binding avidity of the multimerized MHC-peptide complex to surface TCR. By measuring the strength of TCR binding to monomeric peptide-MHC complexes using the *Streptamer* K_{off} rate assay, we recently demonstrated that the dissociation kinetics correlated with the observed functional avidity of different MHC-multimer positive T-cell clones, and that

T-cells demonstrating lower dissociation rates confer significantly better antigen specific reactivity than those with fast dissociation rates^{28,31}.

For the high throughput isolation of antigen specific T-cells using recombinant MHC-peptide complexes the use of MHC-multimer complexes is necessary, since MHC-monomers do not stably bind to TCRs. However, multimerization of MHC-peptide complexes may false positively increase the binding avidity of the multimerized MHC-peptide complex to T-cells. The analysis of conventional MHC-multimer based TCR dissociation kinetics is complicated by multivalent binding and dissociation rates, even when competitor reagents or cold MHC-multimer staining are used³². The controlled disassembly of MHC-multimers to monomers directly after MHC-multimer based T-cell isolation and subsequent FACS sorting of T-cells expressing a TCR with a low MHC-peptide dissociation rate may further increase the efficiency of future reverse immunology approaches³³.

In conclusion, with this reverse immunology approach we have demonstrated the immunogenic potential of two newly identified MiHA; LB-*CYBL*-1Y and LB-*TEP1*-1S. The biological relevance of LB-*CYBL*-1Y was demonstrated by the detection of MHC-multimer positive T-cells with equally high peptide avidity in a patient suffering from AML who experienced an anti-leukemic response after treatment with allo-SCT and subsequent DLI. The identification of LB-*TEP1*-1S demonstrated the feasibility of our reverse immunology approach to identify MiHA that are not frequently induced *in vivo* but can potentially be used for immunotherapeutic strategies. In addition, these results demonstrate that this approach will enable the identification of clinically relevant MiHA when MiHA candidates are selected based on a hematopoietic restricted gene expression pattern.

MATERIAL AND METHODS

Cell collection and culture conditions. Peripheral blood was obtained from different individuals after informed consent (Sanquin Reagents, Amsterdam and Leiden University Medical Center, Leiden, The Netherlands). All experiments were approved by the local medical ethics committees. Blood samples were HLA-typed by high-resolution genomic DNA-typing. Peripheral blood mononuclear cells (PBMC) were isolated by ficoll gradient separation and cryopreserved for further use. T-cells were cultured in T-cell medium consisting of Iscove's Modified Dulbecco's Media (IMDM: Lonza) supplemented with 5% human serum (HS), 5% fetal bovine serum (FBS), 100 IU/ml IL-2 (Proleukin), 2 mM L-glutamine, 100 U/ml penicillin, and 100 µg/ml streptomycin (Invitrogen). Epstein-Barr virus-transformed lymphoblastoid B-cell lines (EBV-LCL) and phytohemagglutinine (PHA; Murex Diagnostics) blasts were generated using standard procedures. The T2 cell line was cultured in IMDM with penicillin/streptomycin and 5% FCS.

Peptide library of HLA-class I eluted peptides. The peptides used for this study are derived from a newly established large peptide library that has been recently described by Hassan et al¹⁶. In short: Peptide elution, reverse phase high-performance liquid chromatography (RP-HPLC), and tandem mass spectrometry (MS/MS) were carried out as previously described^{17,18}. Briefly, 60 x 10⁹ HLA-A*0201 and HLA-B*0702 positive EBV-LCL were washed with ice cold PBS and pellets were stored at -80°C until use. Peptide-HLA-class I complexes were purified from cell lysate by affinity chromatography. Subsequently, peptides were eluted from HLA-molecules, and separated from the HLA heavy chain fragments and β₂-microglobulin by size filtration. The peptide mixture was separated by various first dimension separation techniques, after which the peptides were measured by on-line nanoHPLC-MS/MS.

Selection of MiHA-candidates from a set of eluted peptides. MiHA-candidates were selected based on our recently developed MiHA selection algorithm from the recently established peptide elution library¹³. Briefly, the tandem mass spectra of eluted peptides were submitted to the HSPVdb¹⁹, a database optimized for finding polymorphic peptides. To select for MiHA-candidates within this set we evaluated the polymorphic peptides using strict threshold scores for mass spectrometry defined sequence reliability (BMI≥30, ppm≤2.0), peptide length (8-11 amino acids), predicted peptide-HLA affinity (<500nM), allele frequencies of the SNP encoding polymorphism (0.05-0.7%) and specific gene exclusion criteria (no extreme polymorphic genes). After confirming their integrity by comparing the tandem mass spectra of the synthetic peptides with that of the eluted counterparts the top 25 MiHA-candidates, with the highest threshold scores, were selected for further analysis.

Generation of peptide-MHC complexes. All peptides were synthesized in-house using standard Fmoc chemistry. Recombinant HLA-A*0201 and HLA-B*0702 heavy chain and β_{2m} were in-house produced in Escherichia coli. MHC-class I refolding was performed as previously described with minor modifications²⁰. MHC-class I complexes were purified by gel-filtration HPLC in PBS and stored at 4°C.

The peptide HLA-A*0201 or HLA-B*0702 binding affinity was assessed by subjecting prefolded UV-sensitive peptide-MHC complexes (100µg/ml) to 366nm UV light (Camag) for 1 h in presence of the peptide of interest (200µM)²¹. As controls the CMV PP65 NLVPMVATV, CMV PP65 TPRVTGGAM, modified MART1 ELAGIGILTV and wild-type MART1 AAGIGILTV peptide were used. After exchange, samples were spun at 16,000g for 5 min and supernatants were used to assess HLA-monomer rescue using a bead assay as previously described²².

Isolation of MHC-multimer positive T-cells by MHC-multimer pull down. Prior to isolation PBMC samples were stained with PE-coupled MHC-multimers for 1 hour at 4°C. Subsequently, cells were washed and incubated with anti-PE beads (Miltenyi Biotec, Bergisch Gladbach, Germany). PE-positive T-cells were isolated by magnetic activated cell sorting (MACS), according to the manufacturer's protocol. Positive fraction was cultured with irradiated autologous feeder cells in T-cell medium supplemented with 5ng/ml IL-15 (Biosource) and anti-CD3/CD28 Dynabeads (Invitrogen). After 2 weeks, T-cell cultures were analyzed by MHC-multimer combinatorial coding flow cytometry. Data acquisition was performed on an LSR-II flow cytometer (BD Biosciences, San Diego, USA) and MHC-multimer positive T-cell populations were single cell sorted on a FACSAria (BD) into 96-round bottomed well plates containing 100 µl T-cell medium supplemented with 800 ng/ml PHA and 1×10^5 irradiated feeder cells. T-cell receptor-β variable chain (TCR-Vβ) usage was investigated by flow cytometry using specific monoclonal antibodies as included in the TCR-Vβ repertoire kit (Beckman Coulter).

Cytokine secretion assay. For analysis of IFN-γ and GM-CSF production, 5000 T-cells were stimulated with 20,000 EBV-LCL or 10,000 fibroblasts loaded with different concentrations of peptides in 96-round bottomed well plates. Before stimulation, fibroblasts were either pre-treated with IFN-γ (100 IU/ml) or not for 5 days. For recognition of primary malignant cells, 1000 T-cells were stimulated with 5,000 malignant cells in a 384-well plate. After 18 hours, supernatants were harvested, and the concentration of IFN-γ and GM-CSF were measured by an enzyme-linked immunosorbent assay (ELISA; Sanquin Reagents). An arbitrary detection limit was set to 100 pg/ml for both cytokines.

SNP genotyping and microarray gene expression analysis. A panel of 100 HLA-typed EBV-LCL was selected for SNP screening as previously described⁹. Briefly, genomic DNA was isolated of 5×10^6 EBV-LCL cells using Genra Puregene Cell Kit (Qiagen) and PCR-free whole genome amplification (WGA) was performed. The DNA samples were hybridized to Illumina Human1M-duo arrays. For gene expression analysis, total RNA was isolated using small and micro scale RNAqueous isolation kits (Ambion), and amplified using the TotalPrep RNA amplification kit (Ambion). After preparation using the whole-genome gene expression direct hybridization assay (Illumina), cRNA samples were dispensed onto Human HT-12 v3 Expression BeadChips (Illumina) according to the manufacturer's protocol. Sample collection was performed as previously described²³⁻²⁵. Microarray gene expression data were analyzed using R 2.15.

REFERENCES

1. Appelbaum, F. R. 2001. Haematopoietic cell transplantation as immunotherapy. *Nature* 411: 385-389.
2. Falkenburg, J. H., van de Corp, E. W. Marijt, and R. Willemze. 2003. Minor histocompatibility antigens in human stem cell transplantation. *Exp. Hematol.* 31: 743-751.
3. Feng, X., K. M. Hui, H. M. Younes, and A. G. Brickner. 2008. Targeting minor histocompatibility antigens in graft versus tumor or graft versus leukemia responses. *Trends Immunol.* 29: 624-632.
4. Goulmy, E. 1997. Human minor histocompatibility antigens: new concepts for marrow transplantation and adoptive immunotherapy. *Immunol Rev* 157: 125-140.
5. Mullally, A., and J. Ritz. 2007. Beyond HLA: the significance of genomic variation for allogeneic hematopoietic stem cell transplantation. *Blood* 109: 1355-1362.
6. Ferrara, J. L., J. E. Levine, P. Reddy, and E. Holler. 2009. Graft-versus-host disease. *Lancet* 373: 1550-1561.
7. Warren, E. H., P. D. Greenberg, and S. R. Riddell. 1998. Cytotoxic T-lymphocyte-defined human minor histocompatibility antigens with a restricted tissue distribution. *Blood* 91: 2197-2207.
8. Bleakley, M., and S. R. Riddell. 2011. Exploiting T cells specific for human minor histocompatibility antigens for therapy of leukemia. *Immunol. Cell Biol.* 89: 396-407.
9. van Bergen, C. A., C. E. Rutten, E. D. van der Meijden, S. A. van Luxemburg-Heijs, E. G. Lurvink, J. J. Houwing-Duistermaat, M. G. Kester, A. Mulder, R. Willemze, J. H. Falkenburg, and M. Griffioen. 2010. High-throughput characterization of 10 new minor histocompatibility antigens by whole genome association scanning. *Cancer Res.* 70: 9073-9083.
10. Hombrink, P., S. R. Hadrup, A. Bakker, M. G. Kester, J. H. Falkenburg, P. A. von dem Borne, T. N. Schumacher, and M. H. Heemskerk. 2011. High-throughput identification of potential minor histocompatibility antigens by MHC tetramer-based screening: feasibility and limitations. *PLoS. One.* 6: e22523.
11. Ofran, Y., H. T. Kim, V. Brusic, L. Blake, M. Mandrell, C. J. Wu, S. Sarantopoulos, R. Bellucci, D. B. Keskin, R. J. Soiffer, J. H. Antin, and J. Ritz. 2010. Diverse patterns of T-cell response against multiple newly identified human Y chromosome-encoded minor histocompatibility epitopes. *Clin. Cancer Res.* 16: 1642-1651.
12. Popovic, J., L. P. Li, P. M. Kloetzel, M. Leisegang, W. Uckert, and T. Blankenstein. 2011. The only proposed T-cell epitope derived from the TEL-AML1 translocation is not naturally processed. *Blood* 118: 946-954.
13. Hombrink, P., C. Hassan, M. G. Kester, A. H. de Ru, C. A. Van Bergen, H. Nijveen, J. W. Drijfhout, J. H. Falkenburg, M. H. Heemskerk, and P. A. van Veelen. 2013. Discovery of T cell epitopes implementing HLA-peptidomics into a reverse immunology approach. *J Immunol* 190: 3869-3877.
14. Gilchuk, P., C. T. Spencer, S. B. Conant, T. Hill, J. J. Gray, X. Niu, M. Zheng, J. J. Erickson, K. L. Boyd, K. J. McAfee, C. Oseroff, S. R. Hadrup, J. R. Bennink, W. Hildebrand, K. M. Edwards, J. E. Crowe, Jr., J. V. Williams, S. Buus, A. Sette, T. N. Schumacher, A. J. Link, and S. Joyce. 2013. Discovering naturally processed antigenic determinants that confer protective T cell immunity. *J Clin. Invest* 123: 1976-1987.
15. The 1000 Genomes Project Consortium. 2010. A map of human genome variation from population-scale sequencing. *Nature* 467: 1061-1073.
16. Hassan, C., M. G. Kester, A. H. de Ru, P. Hombrink, J. W. Drijfhout, H. Nijveen, J. A. Leunissen, M. H. Heemskerk, J. H. Falkenburg, and P. A. van Veelen. 2013. The human leukocyte antigen-

- presented ligandome of B lymphocytes. *Mol. Cell Proteomics*. 12: 1829-1843.
17. den Haan, J. M., N. E. Sherman, E. Blokland, E. Huczko, F. Koning, J. W. Drijfhout, J. Skipper, J. Shabanowitz, D. F. Hunt, V. H. Engelhard, and . 1995. Identification of a graft versus host disease-associated human minor histocompatibility antigen. *Science* 268: 1476-1480.
 18. van Bergen, C. A., M. G. Kester, I. Jedema, M. H. Heemskerck, S. A. van Luxemburg-Heijs, F. M. Kloosterboer, W. A. Marijt, A. H. de Ru, M. R. Schaafsma, R. Willemze, P. A. van Veelen, and J. H. Falkenburg. 2007. Multiple myeloma-reactive T cells recognize an activation-induced minor histocompatibility antigen encoded by the ATP-dependent interferon-responsive (ADIR) gene. *Blood* 109: 4089-4096.
 19. Nijveen, H., M. G. Kester, C. Hassan, A. Viars, A. H. de Ru, J. M. de, J. H. Falkenburg, J. A. Leunissen, and P. A. van Veelen. 2011. HSPVdb--the Human Short Peptide Variation Database for improved mass spectrometry-based detection of polymorphic HLA-ligands. *Immunogenetics* 63: 143-153.
 20. Burrows, S. R., N. Kienzle, A. Winterhalter, M. Bharadwaj, J. D. Altman, and A. Brooks. 2000. Peptide-MHC Class I Tetrameric Complexes Display Exquisite Ligand Specificity. *J Immunol* 165: 6229-6234.
 21. Rodenko, B., M. Toebes, S. R. Hadrup, W. J. van Esch, A. M. Molenaar, T. N. Schumacher, and H. Ovaa. 2006. Generation of peptide-MHC class I complexes through UV-mediated ligand exchange. *Nat. Protoc.* 1: 1120-1132.
 22. Eijssink, C., M. G. Kester, M. E. Franke, K. L. Franken, M. H. Heemskerck, F. H. Claas, and A. Mulder. 2006. Rapid assessment of the antigenic integrity of tetrameric HLA complexes by human monoclonal HLA antibodies. *J Immunol Methods* 315: 153-161.
 23. Nauta, A. J., H. S. de, B. Bottazzi, A. Mantovani, M. C. Borrias, J. Aten, M. P. Rastaldi, M. R. Daha, K. C. van, and A. Roos. 2005. Human renal epithelial cells produce the long pentraxin PTX3. *Kidney Int.* 67: 543-553.
 24. Griffioen, M., M. W. Honders, E. D. van der Meijden, S. A. van Luxemburg-Heijs, E. G. Lurvink, M. G. Kester, C. A. van Bergen, and J. H. Falkenburg. 2012. Identification of 4 novel HLA-B*40:01 restricted minor histocompatibility antigens and their potential as targets for graft-versus-leukemia reactivity. *Haematologica* 97: 1196-1204.
 25. Kremer, A. N., E. D. Van Der Meijden, M. W. Honders, J. J. Goeman, E. J. Wiertz, J. H. Falkenburg, and M. Griffioen. 2012. Endogenous HLA class II epitopes that are immunogenic in vivo show distinct behavior toward HLA-DM and its natural inhibitor HLA-DO. *Blood* 120: 3246-3255.
 26. Toebes, M., M. Coccoris, A. Bins, B. Rodenko, R. Gomez, N. J. Nieuwkoop, W. van de Kastelee, G. F. Rimmelzwaan, J. B. Haanen, H. Ovaa, and T. N. Schumacher. 2006. Design and use of conditional MHC class I ligands. *Nat. Med.* 12: 246-251.
 27. Macdonald, W. A., Z. Chen, S. Gras, J. K. Archbold, F. E. Tynan, C. S. Clements, M. Bharadwaj, L. Kjer-Nielsen, P. M. Saunders, M. C. Wilce, F. Crawford, B. Stadinsky, D. Jackson, A. G. Brooks, A. W. Purcell, J. W. Kappler, S. R. Burrows, J. Rossjohn, and J. McCluskey. 2009. T cell allorecognition via molecular mimicry. *Immunity*. 31: 897-908.
 28. Hombrink, P., Y. Raz, M. G. Kester, B. R. de, B. Weissbrich, P. A. von dem Borne, D. H. Busch, T. N. Schumacher, J. H. Falkenburg, and M. H. Heemskerck. 2013. Mixed functional characteristics correlating with TCR-ligand k-rate of MHC-tetramer reactive T cells within the naive T-cell repertoire. *Eur. J Immunol*.
 29. Ford, M. L., B. H. Koehn, M. E. Wagener, W. Jiang, S. Gangappa, T. C. Pearson, and C. P. Larsen. 2007. Antigen-specific precursor frequency impacts T cell proliferation, differentiation, and requirement for costimulation. *J. Exp. Med.* 204: 299-309.
 30. Moon, J. J., H. H. Chu, M. Pepper, S. J. McSorley, S. C. Jameson, R. M. Kedl, and M. K. Jenkins.

2007. Naive CD4(+) T cell frequency varies for different epitopes and predicts repertoire diversity and response magnitude. *Immunity*. 27: 203-213.
31. Nauerth, M., B. Weissbrich, R. Knall, T. Franz, G. Dossinger, J. Bet, P. J. Paszkiewicz, L. Pfeifer, M. Bunse, W. Uckert, R. Holtappels, D. Gillert-Marien, M. Neuenhahn, A. Krackhardt, M. J. Reddehase, S. R. Riddell, and D. H. Busch. 2013. TCR-Ligand koff Rate Correlates with the Protective Capacity of Antigen-Specific CD8+ T Cells for Adoptive Transfer. *Sci Transl Med* 5: 192ra87.
32. Wang, X. L., and J. D. Altman. 2003. Caveats in the design of MHC class I tetramer/antigen-specific T lymphocytes dissociation assays. *J Immunol Methods* 280: 25-35.
33. Knabel, M., T. J. Franz, M. Schiemann, A. Wulf, B. Villmow, B. Schmidt, H. Bernhard, H. Wagner, and D. H. Busch. 2002. Reversible MHC multimer staining for functional isolation of T-cell populations and effective adoptive transfer. *Nat. Med.* 8: 631-637.

SUPPLEMENTARY INFORMATION

5

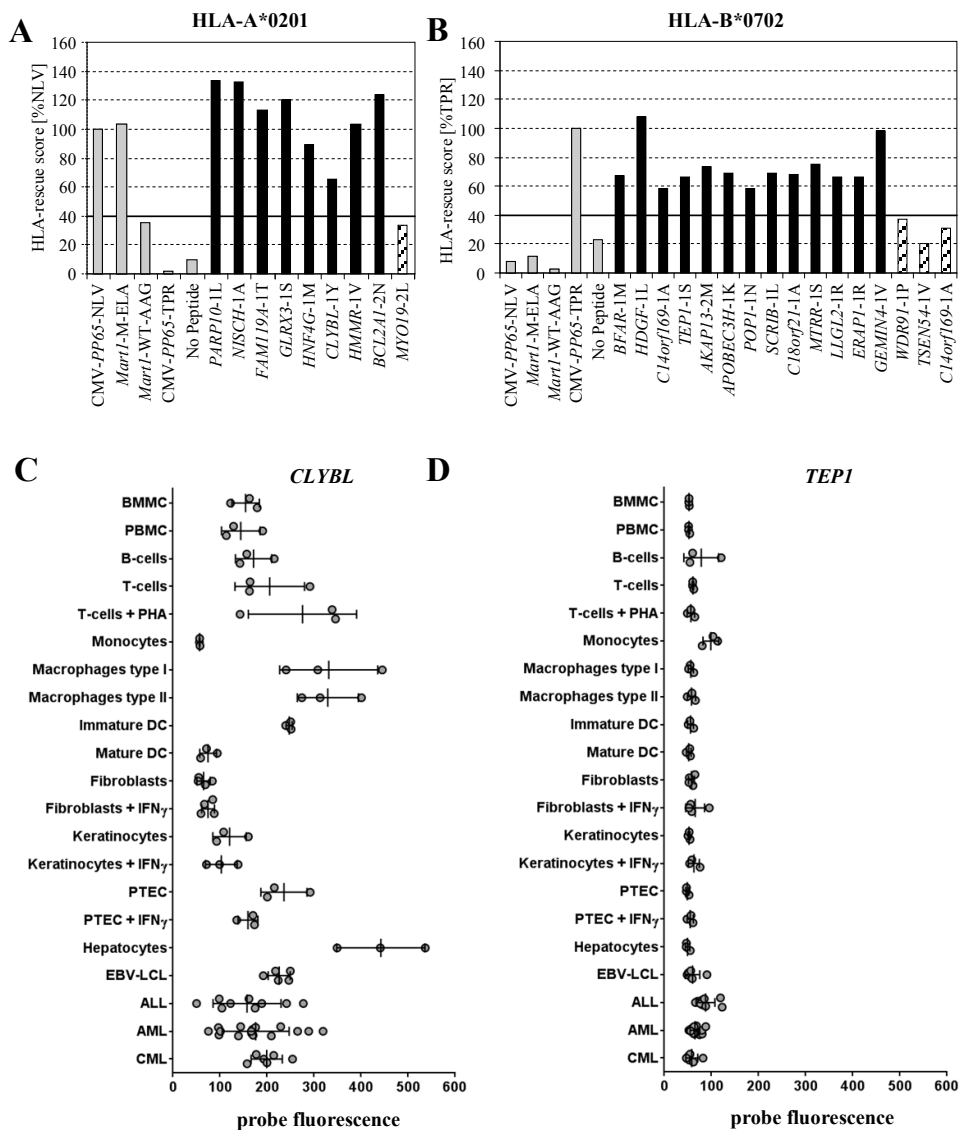


Figure S1. The HLA-binding affinity of 25 eluted highly potential MiHA candidates was analyzed by a binding assay that is based on HLA-recovery after UV-exchange monomer technology. After UV-exchange the HLA-monomer rescue score was normalized to the peptides CMV *PP65*-NLV and CMV *PP65*-TPR that exhibit a high binding affinity for HLA-A*0201 or B*0702, respectively. Peptides with a higher HLA-recovery score (>40%) compared to the low affinity HLA-A*0201 binding *MART1*-WT-AAG were selected for further analysis. As negative control no rescue peptide was added. All control peptides are indicated in grey. The percentage of HLA-recovery as a measure for HLA-binding affinity for 9 HLA-A*0201 (A) and 16 HLA-B*0702 (B) restricted MiHA candidates was shown. MiHA candidates with HLA-recovery score above the selection threshold of 40% are indicated in black. MiHA candidates that demonstrated a HLA-recovery below 40% were removed from the study and are indicated with stripes. (C,D) Gene expression of *CLYBL* and *TEP1* were analyzed. Normal hematopoietic T-cells, monocytes, B-cells and hematopoietic stem cells (HSC) were isolated from (G-CSF mobilized) peripheral blood and bone marrow mononuclear cells (PBMC and BMNC) from donors by flow cytometry cell sorting based on expression of CD3, CD14, CD19 and CD34, respectively. Skin derived fibroblasts (FB), keratinocytes (KC) and PTEC were cultured with and without IFN- γ (100 IU/ml) and hepatocytes were freshly isolated from liver specimen. AML, ALL and CML cells were isolated from peripheral blood and bone marrow samples from patients by flow cytometry cell sorting based on expression of CD33, CD19 and CD34, respectively. EBV-LCL and PHA blasts were generated using standard procedures. Total RNA was isolated and whole-genome gene expression assay was performed as previously described²⁶. The probe fluorescence for the indicated genes are shown for each sample, and the mean with SD is indicated for each cell type.

Table S1. Eluted published MiHA epitopes.

HLA	Genotyped MiHA	Eluted Sequence ^α	MiHA positive EBV-LCL	Eluted and matched	BMI [*]
A*02:01	HA-2V	YIGEVLVSV	JY, ALY, HHC	JY, HHC	50.4
	HA-8R	RTLDKVLEV	JY, ALY	JY, ALY	33.8
	LB-SSR1-1S	VLFRGGPRGSLAVA	HHC	HHC	28.6
	LB-PRCP-1D	MWDVAEDLKA ^β	HHC	HHC	14.3
	LB-WNK1-1I	TLSPFIITV ^β	JY, HHC	HHC	28.4
	LB-NISCH-1A	ALAPAPAEV	JY	JY	39.0
	SMCY-A2	FIDSYICQV	JY	ND ^γ	-
B*07:02	LB-EBI3-1I	RPRARYYIQV	ALY	ALY	14.3
	LB-ERAP1-1R	HPRQEQIAL ^β	JY, HHC	JY, HHC	36.2
	LB-GEMIN4-1V	FPALRFVEV	JY	JY	42.5
	LB-PDCD11-1F	GPDSSTFLCL	ALY, HHC	ND	-
	SMCY-B7	SPSVDKARAEI	JY	JY	57.8
	LB-APOBEC3B-1K	KPQYHAEMCF	ALY, HHC	ND ^γ	-

Total detected MiHA

^α Sequence confirmed by matching the MS spectra of synthetic and eluted peptide

^β Length variant of published MiHA epitope

^γ Not Detected (ND)

^{*} Highest detected Best Mascot Ion Score (BMI)

Table SII. Validation scores MiHA candidates.

HLA	Peptide	Sequence ^a	Gene	PPM ^b	BMI ^γ	netMHC ^μ (nM)
A*02:01	P1	GL <u>L</u> GQEGLVEI	<i>PARP10</i>	0,7	56	96
	P2	ALAPAP <u>A</u> EV	<i>NISCH</i>	0,9	40	12
	P3	AMLERQ <u>F</u> TV	<i>FAM119A</i>	0,1	35	3,4
	P4	FL <u>S</u> SANEHL	<i>GLRX3</i>	0,6	36	10,6
	P5	MMYKDILL <u>L</u>	<i>HNF4G</i>	0,1	63	6,9
	P6	SLAAY <u>I</u> PRL	<i>CLYBL</i>	0,8	40	4,1
	P7	SLQEK <u>V</u> AKA	<i>HMMR</i>	0,5	46	356,4
	P8	VLQ <u>N</u> VAFSV	<i>BCL2A1</i>	1,1	40	12,7
	#	RLLEAI <u>I</u> RL	<i>MYO19</i>	0,1	50	10
B*07:02	P9	APNTGRAN <u>Q</u> QM	<i>BFAR</i>	0,6	44	55,8
	P10	LPMEVEKN <u>S</u> T <u>L</u>	<i>HDGF</i>	0,1	50	49,7
	P11	RPRAPTEEL <u>A</u> L	<i>C14orf169</i>	0,1	38	3,3
	P12	APDGAKV <u>A</u> SL	<i>TEP1</i>	0,3	45	73,1
	P13	APAGVRE <u>V</u> M	<i>AKAP13</i>	0,1	72	20,5
	P14	KPQQ <u>K</u> GLRL	<i>APOBEC3H</i>	0,3	36	19,6
	P15	LPQKKS <u>N</u> AL	<i>POP1</i>	0,3	38	6,2
	P16	LPQQP <u>P</u> LSL	<i>SCRIB</i>	0,4	54	14,2
	P17	NPATP <u>A</u> SKL	<i>C18orf21</i>	0,1	43	71,6
	P18	SPASSR <u>T</u> DL	<i>MTRR</i>	0,8	45	11,1
	P19	SPSLR <u>I</u> LAI	<i>LLGL2</i>	0,1	48	20,4
	P20	HPRQ <u>E</u> QIAL	<i>ERAP1</i>	1,3	36	9
	P21	FPALRFV <u>E</u> V	<i>GEMIN4</i>	0,5	43	33
	#	SPRVGF <u>L</u> SSL	<i>WDR91</i>	0,6	56	17
	#	LPDGG <u>V</u> RLL	<i>TSEN54</i>	0,2	46	135
	#	RPRAPTEEL	<i>C14orf169</i>	0,1	36	12

Low HLA-affinity peptides

^a SNP underlined^b Parts-Per-Million: Difference between observed and exact ion mass^γ Best-Mascot-Ion-Score: Match between observed MS spectrum and stated peptide^μ Predicted netMHC affinity (nM), Strong binder ≤50; Weak binder ≤500

Table SIII.

Expanded T-cell lines after first MHC-multimer pull down

Donor ID	PARP10-1L	NISCH-1A	FAM119A-1T	GLRX3-1S	HNF4G-1M	CLYBL-1Y	HMMR-1V	BCL2A1-2N	BFAR-1M	HDGF-1L	C14orf169-1A	TEP1-1S	AKAP13-2M	APOBEC3H-1K	POP1-1N	C18orf21-1A	MTRR-1S	LLGL2-1R	ERAPI-1R	GEMIN4-1V	
FHT						0,5															0,2
EPP		0,01				0,2						0,01				0,01				0,01	
UBE						0,2															
AKH																					
JSB																					2,8
DSP																					
USQ																					
ABM						5,0	0,01													0,01	2,0
UDN						0,2															
OMH													0,01								
UBF						0,1				0,1	0,1										
OGV						0,01									0,01						
MMY																					0,01
CLO																					
UHR																					
ADB	0,2																				0,2

Expanded T-cell lines after second MHC-multimer pull down

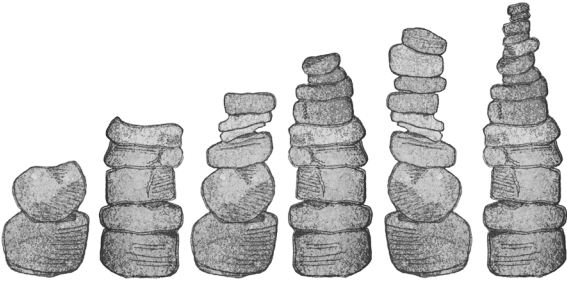
Donor ID	PARP10-1L	NISCH-1A	FAM119A-1T	GLRX3-1S	HNF4G-1M	CLYBL-1Y	HMMR-1V	BCL2A1-2N	BFAR-1M	HDGF-1L	C14orf169-1A	TEP1-1S	AKAP13-2M	APOBEC3H-1K	POP1-1N	C18orf21-1A	MTRR-1S	LLGL2-1R	ERAPI-1R	GEMIN4-1V	
FHT						0,8											0,1				65
EPP		28	0,3	0,01		8,4						2,0				6,7				3,6	
UBE						0,5															
AKH																					
JSB																					2,8
DSP																					
USQ																					
ABM						28,3	0,2							0,3						0,2	5,6
UDN						85															
OMH								0,1					38		0,01	0,02					
UBF						0,1			0,1	0,1					0,01	0,02					
OGV			0,2			54									0,01						
MMY																					0,04
CLO			0,1																		
UHR																					85
ADB	0,2																				0,2

Screening for MHC-tetramer positive T-cell populations in expanded T-cell lines after one or two rounds of MHC-multimer pull down. All T-cell populations screened for in PBMC donors homozygous negative for the indicated SNP encoding MiHA are indicated in grey. Frequencies indicate MHC-multimer positive T-cells out of total CD8⁺ T-cells as revealed by FACS analysis

Circulating MHC-multimer positive T-cell frequencies detected in allo-SCT patients

Allo-SCT Patient	Disease	Days After DLI	PARP10-1L	NISCH-1A	FAM119A-1T	GLRX3-1S	HNF4G-1M	CLYBL-1Y	HMMR-1V	BCL2A1-2N	BFAR-1M	HDGF-1L	C14orf169-1A	TEF1-1S	AKAP13-2M	APOEC3H-1K	POF1-1N	C18orf21-1A	MTRR-1S	LLGL2-1R	ERAP1-1R	GEMIN4-1V	
BWB	CML	83																					
AZP	CML	62	■																		■		■
BDV	MM	49						■															
MDD	RCC	67																					
HHC	MDS	49			■			■															
CUB	MM	86																					
MBS	CMMOL	54																					
USF	PCL	95																					
JBZ	CML	59																					
OBG	CML	172	■																				
ASQ	AA	35				■																	
RBH	CML	106																					
MBF	AML	41																					
YKV	CML	50																					
JLW	CML	90																					
MHU	MM	100																					

Screening for MHC-tetramer positive T-cell populations in 16 MiHA positive patient that received a DLI of a donor that was homozygous negative for the SNP-encoding MiHA. All T-cell populations screened for are indicated in gray. Frequencies indicate detected MHC-multimer positive T-cells out of total CD8⁺ T-cells as revealed by FACS analysis



6

SUMMARY AND GENERAL DISCUSSION

SUMMARY

T-cell recognition of MiHA plays an important role in the GVT effect of allo-SCT. Selective infusion of T-cells reactive for hematopoiesis-restricted MiHA presented in the context of HLA-class I molecules may help to separate the beneficial GVT effects from GVHD after allo-SCT. To date, only a few MiHA that form attractive targets for adoptive immunotherapy have been characterized and the number of patients that can be treated with such MiHA-selective cell therapy remains limited. In this thesis we focused on “reverse immunology” as an attractive strategy to identify clinically relevant MiHA and other T-cell epitopes. In this approach peptide predictions are the starting point and peptide candidates are subsequently screened for their capacity to induce a T-cell response. We investigated the feasibility of computational genome-wide prediction of hematopoietic MiHA and alternatively implemented mass spectrometry based HLA-peptidomics as source for candidate peptides. T-cells that reacted with these antigens were collectively isolated by MHC-tetramer pull down. Subsequently, the composition of MHC-tetramer positive T-cell populations was characterized and tested for reactivity against any of the predicted epitopes that was included in the initial MHC-tetramer panel. We generated an algorithm that could be exploited to selectively target T-cells specific for clinically relevant MiHA.

In **chapter 2** we demonstrated the technical feasibility of high-throughput analysis of antigen-specific T-cell responses in small patient samples. Using three different peptide-HLA binding algorithms a set of 973 peptides that contained a SNP and where theoretically expressed by hematopoietic stem cells was produced and screened for HLA-A*0201 binding. After synthesis all peptides were tested for true peptide-HLA affinity in two separate assays resulting in a set of 333 high affinity HLA-A2 peptides that was used to generate MHC-tetramers. Subsequently, post-transplantation samples from allo-SCT patients were screened for T-cell populations reactive to any of these predicted peptides. MiHA-specific T-cell lines were generated by incubating patient PBMC samples, regardless of patient SNP status, with the collective set of 333 MHC-tetramers, followed by enrichment of MHC-tetramer positive cells on a magnetic column. Isolated T-cells were expanded and analyzed for MHC-tetramer reactivity by multi-color flow cytometry. Although a promising number of 71 peptide-reactive T-cell populations were generated by FACS sorting of MHC-tetramer positive cells, with the exception of the defined MiHA HMHA1, none of the other T-cell populations that were generated demonstrated recognition of endogenously MiHA expressing target cells, even though recognition of peptide-loaded targets was often observed. On basis of the result that the high avidity HMHA1 specific T-cell population was isolated from a transplantation setting in which both donor and recipient were homozygous negative for the MiHA phenotype we assumed that these cells were derived from the naïve T-cell repertoire. We concluded that the unbiased screening for T-cell reactivity against large sets of predicted MiHA that are solely based on epitope binding, irrespective of peptide processing data and SNP status of donor and recipient, did not result in the identification of

a novel biological relevant MiHA and we speculated that a more reliable source of naturally processed and presented peptide candidates could overcome this problem.

In **chapter 3** we optimized our MHC-tetramer pull down approach to isolate antigen-specific T-cells derived from a naïve T-cell repertoire. For this purpose we took CMV as a model and aimed to generate functional CMV-specific T-cell lines from seronegative individuals within four weeks. Generated T-cell lines consisted of a variety of immunodominant CMV-epitope specific oligoclonal T-cell populations restricted to various HLA-molecules. Although all CMV-specific T-cells were isolated based on their reactivity towards a specific peptide-MHC complex, we observed a large peptide avidity variation within the isolated T-cell populations. Specifically, in addition to high-avidity T-cells, clones were also present that lacked functional reactivity. In addition, MHC-tetramer staining was not always predictive for the observed T-cell reactivity and we demonstrated that this was caused by altered MHC-peptide-TCR interaction dynamics due to the multimerized nature of MHC-tetramer complexes. Surprisingly, while the frequent isolation of naïve T-cells specific for the immunodominant A1-pp65-YSE epitope correlated with the frequent detection of a memory T-cell response in seropositive individuals, this correlation was absent for the immunodominant A2-pp65-NLV epitope, for which no high avidity T-cells could be isolated from any seronegative individuals. Based on the variable functionality of the isolated T-cell populations we put a critical note to the direct monitoring of the shape of the peripheral T-cell repertoire independent of the analysis of functional activity.

In **chapter 4** we established a method for the identification of naturally processed MiHA by implementing mass spectrometry based HLA-peptidomics into a reverse immunology approach. For this purpose HLA-class I binding peptides were eluted from transformed B-cells, analyzed by mass spectrometry and matched with a database dedicated to identify polymorphic peptides. This peptide source guarantees identification of naturally processed and presented peptides. MiHA-specific T-cell lines were generated by incubating large numbers of PBMC from healthy donors with a specific set of MHC-tetramers, followed by enrichment of MHC-tetramer positive cells on a magnetic column. To increase the isolation frequency of high-affinity T-cell populations, the set of MHC-tetramers was specifically adjusted to each donor to cover only those MiHA for which the encoding SNP was screened homozygous negative in the respective donor. The identification of the LB-NISCH-1A MiHA demonstrated the feasibility of this approach. Based on these results we generated an algorithm that could be exploited to efficiently identify T-cells specific for MiHA and used this in **chapter 5** to identify 2 new MiHA: LB-CLYBL-1Y and LB-TEP1-1S. Detailed analysis of the cytokine secretion profiles of the isolated T-cells demonstrated that these cells were not fully differentiated towards high IFN- γ secreting T-cells after several weeks of *in vitro* culture and that GM-CSF could be used as readout for T-cell reactivity to further improve the efficiency of the approach. Although the clinical relevance was only demonstrated for LB-CLYBL-1Y by the detection of MHC-multimer

positive T-cells in a patient with hematologic malignancy after allo-SCT, we underline that the identification of LB-TEP1-1S demonstrated the feasibility of our reverse immunology approach to identify MiHA that are not frequently induced *in vivo*. We speculate that these so called “subdominant” MiHA can still be of interest for immunotherapeutic strategies.

GENERAL DISCUSSION

Donor T-cells contribute to the success of allo-SCT and both MiHA specific CD8 and CD4 positive T-cells play a crucial role in the eradication of malignant leukemic cells. Although preclinical adoptive T-cell approaches directed against single MiHA antigens provided promising results¹⁻³, the proof of principle for the effectiveness of MiHA specific immunotherapy should be provided by currently ongoing and future clinical studies. Although since the first molecular characterization of MiHA, 21 years ago⁴, 50 MiHA have been characterized⁵, only a few of them demonstrated to be expressed on hematopoietic cells, including leukemic stem cells, but not on tissues affected by GvHD. The tissue restricted expression of MiHA is crucial to enable the separation of GvL from GvHD upon adoptive transfer of T-cells specifically recognizing these MiHA to treat leukemia. Currently, there are 15 MiHA identified that are stated to be selectively expressed in hematopoietic cells^{6,7}. In reality, this number is lower as T-cells reactive to several of these MiHA, recognized at least some non-hematopoietic cells. The low number of validated hematopoietic-restricted MiHA limits the broad clinically application of MiHA specific immunotherapy. Due to unbalanced population MiHA allele frequencies and HLA-restriction elements, the number of patients that could potentially be treated with MiHA based immunotherapy remains low. As a consequence the discovery of hematopoietic MiHA remains a high priority.

Future prospects for the identification of clinically relevant MiHA by reverse immunology

Although only 3 out of the 50 characterized MiHA were discovered by reverse immunology⁸⁻¹⁰, in theory this is the most efficient methodology towards identification of hematopoietic MiHA. Typical for this approach is the screening for T-cells reactive against predicted antigens. In theory this approach circumvents the need to screen isolated T-cells for unwanted reactivity against non-hematopoietic screening and allows focusing on SNP encoding MiHA with a favorable allele frequency and presented in a HLA molecule with high population coverage. Unfortunately, the historical low sensitivity and yield of every prediction step required a compensatory up-scaling of the initial numbers of candidate sequences to be screened. This resulted in a rather complex approach and several attempts failed to identify biologically relevant epitopes¹¹⁻¹⁴. The efficacy of reverse immunology approaches is dependent on the quality of peptide predictions and the capacity to screen for peptide specific T-cell reactivity. As the prediction of MiHA critically relies on the identification of polymorphisms, new molecular developments that allow robust gene expression profiling and high resolution genome sequencing will help to separate reliable polymorphisms from sequence errors and increase the efficacy of valid MiHA candidate predictions. In addition, characterization of proteosomal cleavage sites and improvement of peptide-HLA binding prediction algorithms enables to better understand the process

of antigen processing and presentation. Due to the emerging availability of these bioinformatics data an increasing number of MiHA candidates may be predicted. However, only when these predictions are linked to high quality gene expression profiling of virtually all organs and tissue types to select for MiHA candidates that are exclusively expressed by the hematopoietic compartment, MiHA reactive T-cell libraries can be established that may broaden the clinical application of MiHA specific immunotherapy. Ultimately this may result in “off the shelf” personalized MiHA-based therapies.

When the predicted MiHA library that was used in chapter 2 was compared with the eluted peptide libraries used in chapter 4 and 5 that yield a significant part of the B-cell HLA-ligandome, the minimal amount of coverage was striking. Length variants of fewer than 5 out of the 1000 predicted peptides were found after sequencing of eluted ligands. Although we only used genomic sequence data, gene expression profiling and peptide-HLA prediction algorithms for MiHA prediction, no significant improvement was observed when we screened a putative MiHA library that included proteosomal cleavage and TAP translocation predictions (unpublished data). These low yields indicate that either the current knowledge of antigen processing and presentation is insufficient to efficiently predict cell-surface presentation of specific peptide-MHC complexes or that the analysis of HLA-ligandomes is far from perfect. HLA-ligandome analysis by mass spectrometry may be strongly biased towards the most abundantly expressed genes (e.g. over presented housekeeping genes) and genes with a lower abundant but favorable gene expression profile may be lost in background noise. In addition, the efficiency of HLA-ligandome analysis drastically decreases when low numbers of cells, in the range of millions, are used as starting material. Ideally, large primary tumor samples should be analyzed and healthy tissues of the patient, for example, peripheral blood cells, can serve as a source of reference material at least for excluding abundant normal self-peptides from consideration¹⁵.

Although the identified HLA-eluted peptides may be a fraction of the total naturally processed peptide pool, we demonstrate in chapter 4 and 5 that this may serve as a reliable source for MiHA identification, when successfully implemented into a reverse immunology approach. As the correlation between the transcriptome and HLA peptidome has been demonstrated to be low¹⁶, it remains questionable how much efficiency gain may be expected when new methods to generate genome, gene or transcript sequence data are used to predict relevant T-cell epitopes. Although demonstrated to be technically feasible, even the state-of-the-art high resolution exome sequencing (only coding regions of the genome are sequenced) of patient hematopoietic or malignant cells alone may not be sufficient to identify large amounts of clinically relevant T-cell epitopes¹⁷⁻¹⁹. Alternatively, strategies that focus on ribosome bound mRNA profiling, also called polysome profiling, may boost the efficiency of T-cell epitope predictions one step further as it maps the translation of proteins and thereby underscoring measurements of mRNA expression levels only^{20;21}. Polysome profiling revealed thousands of translational pause sites and

unannotated translation products indicating an unanticipated complexity to mammalian proteomes²². In yeast, comparing the rate of translation with mRNA abundance from the same samples revealed a roughly 100-fold range of translation efficiency (as measured by the ratio of ribosome footprints to mRNA reads). In addition, translation was demonstrated for approximately 85% of genes for which mRNA abundance was measured suggesting that a 15% efficiency gain may be expected when epitope predictions are based on polysome profiling compared to total mRNA sequencing. Establishing hematopoietic cell or tumor specific polysome profiling sequencing libraries and merge them with a well established HLA-peptide affinity prediction algorithm may theoretically boost the efficiency of reverse immunology based MiHA prediction.

Although both exome and polysome sequencing methods, in contrast to HLA peptidome analysis have the benefit to be applicable on limited size malignant samples and may identify disease related mutations and genomic translocations, the unpredictability of post-translational modifications and proteosomal degradation of cellular proteins into peptides remain a bottleneck for efficient epitope prediction. As proteasomes are responsible for generation of the majority of MHC class I presented T-cell epitopes, the development of new prediction algorithms that are more accurate than those currently in use will be crucial to boost the efficacy of reverse immunology based epitope predictions²³⁻²⁵. In addition, ongoing and future technical developments in the field of mass spectrometry that enable more sensitive peptide detection in limited material samples will greatly boost the efficiency in which eluted peptide libraries can be used to predict reliable T-cell epitopes. Novel developments may also enable a more efficient identification of peptides eluted from limited size samples such as specific primary cell subsets or hematopoietic malignancies.

Rationale for the characterization of new MiHA by reverse immunology

Based on the fact that approximately 3 million SNP were identified per individual genome, irrespective of MiHA phenotype frequencies, each allo-SCT HLA-matched donor and recipient pair is mismatched for thousands of SNP and it is likely that many MiHA have yet to be discovered. The recurrent characterization of identical MiHA specific T-cell responses in various patients after allo-SCT suggests a strong role for immunodominance²⁶. Dissecting the mechanism of immunodominance whereby the donor T-cells responds to only a few of the many possible MiHA may become very relevant for future immunotherapy as some MiHA specific T-cell responses that are frequently induced *in vivo* may induce GVL whereas others can mediate GVHD. It remains to be investigated whether this phenomenon is regulated by high to borderline presence of MiHA specific precursor T-cells or by other mechanisms such as tolerance induction to molecular mimicry epitope^{27,28}. The identification of LB-NISCH-1A and LB-TEP1-1S in chapter 4 and 5 illustrates that our approach allows the identification of highly immunogenic MiHA that are not frequently

induced *in vivo* as no MHC-tetramer positive T-cell populations were observed in the blood of patients that were positive for the MiHA and received an allo-SCT and subsequent DLI from a donor who was homozygous negative for the SNP encoding MiHA. The identification of subdominant MiHA may be restricted to reverse immunology approaches as the T-cell repertoire of patients that are screened in forward immunology approaches is skewed towards *in vivo* induced high immunodominant MiHA. If the identified MiHA is restricted to a favorable gene expression profile, subdominant MiHA may be of therapeutic interest as they can be exploited in potential peptide vaccination or adoptive T-cell therapies.

Increasing the yield of MHC-tetramer pull down and FACS analysis

In our approach the MHC-multimer based enrichment and analysis of the generated T-cell lines is crucial for the validation of MiHA and other T-cell epitopes. The absence of MHC-multimer positive T-cells however, does not necessarily indicate the non-immunogenicity of a specific peptide candidate. Precursor frequencies of antigen specific T-cells in an unchallenged donor PBMC sample vary and may be so low that the identification of these cells may be a matter of chance^{29,30}. In addition, potential antigen specific T-cells may be lost during the first 10 days of *in vitro* culture after MHC-multimer isolation. To prevent potential loss of MiHA specific T-cell populations during culture we, as an alternative, performed a single cell sort of MHC-tetramer positive T-cell population directly after MHC-tetramer pull down. Unpublished results have shown that this approach resulted in an increased number of unique MHC-tetramer positive T-cells to be screened. To allow selection of high-avidity T-cell clones in a high-throughput manner we isolated T-cells that express the surface activation marker CD137 after challenge with endogenously processed and presented antigen. This activation marker is in contrast to other activation markers upregulated by all T-cells, regardless of differentiation stage, 24 hours after *in vitro* antigen activation. As a consequence, recently activated *in vitro* primed naïve T-cells can be easily isolated based on their CD137 expression by FACS sorting^{31,32}.

The detection efficiency of MHC-multimer positive T-cells by combinatorial coding FACS analysis is depending on the number of fluorescent labels with sufficient intrinsic fluorescent capacity. The quantum dots that were used in chapter 2, 3, 4 and 5 allowed the use of two-color combinations. The competition for cell surface peptide-MHC complex resulted in a decreased intensity for all MHC-multimers combinations. As a consequence, the MHC-tetramer staining intensity of antigen-specific T-cell populations with a low affinity for the MHC-multimer complex may drop below threshold, especially when combinations of the lowest intensity Qdots were used. Although this may serve as an additional selection step to bias our selection strategy towards T-cell populations with a moderate to high affinity for the MHC-tetramer complex we show in chapter 3 that MHC-tetramer staining was not always predictive for T-cell avidity and therefore potential T-cell populations of interest may also be lost. The recent availability of new fluorochromes with increased fluorescent

intensities and smaller emission spectra, such as brilliant (ultra)violet dyes³³, may be used to further expand the complexity of combinatorial coding MHC-tetramer analysis by either adding or replacing to the number of fluorochromes used in two-color combinations or by designing a three- or four-color combination matrix³⁴. Increasing the complexity of combinatorial coding MHC-tetramer analysis will only serve purpose if T-cell recognition of large sets of potential clinically relevant peptides needs to be screened in either unbiased T-cell repertoires or limited size patient PBMC samples. In the case of dissecting patient-specific T-cell reactivity towards tumor associated neoantigens, T-cell responses were demonstrated to be biased towards a few epitopes derived from highly expressed genes, suggesting that it may be feasible to analyze patient-specific T-cell reactivity towards these type of antigens with relatively small peptide sets¹⁷. If only a few peptide candidates needs to be screened, the complexity of combinatorial coding MHC-tetramer analysis may be downgraded towards a few optimal fluorescent labels to facilitate analysis of larger groups of patient and donor samples and thereby increasing the change of finding rare but useful T-cell clones.

Isolation of naïve antigen-specific T-cells by MHC-tetramer pull down

Characterization of antigen specific T-cells within the naïve repertoire can be of clinical relevance for various reasons. Detection of naïve T-cell populations may contribute to optimize rational vaccine design or to select cord blood samples with pre-existing MiHA or tumor specific T-cells prior to umbilical cord transplantation. However, due to extreme low frequencies, characterization of naïve T-cell populations requires enrichment of MHC-tetramer positive cells prior to analysis, in contrast to memory T-cell populations that expanded *in vivo* after antigen encounter. In chapter 2, 3, 4 and 5 we demonstrate the successful isolation of high-avidity MiHA and CMV specific T-cells from an unprimed setting. Although direct phenotypic characterization to demonstrate their naïve phenotype was lacking due to the low frequency of these cells directly after MHC-tetramer isolation, we demonstrate that these cells were not terminally differentiated towards high IFN- γ producing T-cells, unlike memory T-cells. The *in vitro* generated T-cell clones and lines were solely selected based on TCR-MHC-tetramer with no subsequent selection for T-cell reactivity. As the TCR diversity in the naïve repertoire has been reported to be at least 100-fold higher compared to the memory T-cell repertoire and high avidity T-cells are selectively enriched in the memory subset a substantial part of the isolated T-cells will be of low avidity³⁵. The composition of the isolated T-cell populations most likely reflected the broad MHC-tetramer positive T-cell repertoire before antigen driven T-cell selection.

In chapter 3 we demonstrate that no strict correlation between MHC-tetramer reactivity and T-cell avidity exist by studying various A1-pp65-YSE and A1-pp50-VTE specific T-cell clones. Although controversial, this discrepancy may be explained by the staining with multimerized MHC-peptide complexes. Multimerization of MHC-peptide

complexes alter the TCR-MHC-peptide dissociation on- and off-rate kinetics and may result in increased binding affinity of the multimerized MHC-peptide complex to surface TCR³⁶. This discrepancy may however not be observed when solely monitoring the memory T-cell repertoire which is dominated by a few antigen-experienced immunodominant high avidity T-cell clones³⁷.

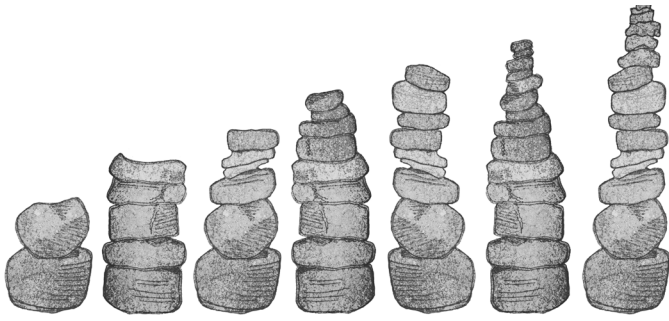
Currently, the numbers of MiHA that are characterized by forward immunology exceed those that are characterized by reverse immunology, but our efforts doubled the number of MiHA identified by reverse immunology in only a small time period. Although our results did not meet the expectations that were set at the start of this project in 2007, they indicate that T-cell epitope predictions are of unexpected complexity and that new technical implementations can turn reverse immunology into a more successfully approach. In the coming years, it will be interesting to assess how new bioinformatics information can be used to improve the efficiency of reverse immunology strategies. If successful, reverse immunology based strategies can be of great value to make “off the shelf” personalized MiHA-based therapies a realistic option.

REFERENCES

1. Marijt WAE, Heemskerk MHM, Kloosterboer FM et al. Hematopoiesis-restricted minor histocompatibility antigens HA-1- or HA-2-specific T cells can induce complete remissions of relapsed leukemia. *Proceedings of the National Academy of Sciences of the United States of America* 2003;100:2742-2747.
2. Li N, Matte-Martone C, Zheng H et al. Memory T cells from minor histocompatibility antigen-vaccinated and virus-immune donors improve GVL and immune reconstitution. *Blood* 2011;118:5965-5976.
3. Warren EH, Fujii N, Akatsuka Y et al. Therapy of relapsed leukemia after allogeneic hematopoietic cell transplantation with T cells specific for minor histocompatibility antigens. *Blood* 2010;115:3869-3878.
4. van Els CA, D'Amato J, Pool J et al. Immunogenetics of human minor histocompatibility antigens: their polymorphism and immunodominance. *Immunogenetics* 1992;35:161-165.
5. Warren EH, Zhang XC, Li S et al. Effect of MHC and non-MHC donor/recipient genetic disparity on the outcome of allogeneic HCT. *Blood* 2012;120:2796-2806.
6. Bleakley M, Riddell SR. Exploiting T cells specific for human minor histocompatibility antigens for therapy of leukemia. *Immunol.Cell Biol.* 2011;89:396-407.
7. Oostvogels R, Minnema MC, van EM et al. Towards effective and safe immunotherapy after allogeneic stem cell transplantation: identification of hematopoietic-specific minor histocompatibility antigen UTA2-1. *Leukemia* 2012
8. Dolstra H, de Rijke B, Fredrix H et al. Bi-directional allelic recognition of the human minor histocompatibility antigen HB-1 by cytotoxic T lymphocytes. *Eur.J Immunol* 2002;32:2748-2758.
9. Mommaas B, Kamp J, Drijfhout JW et al. Identification of a novel HLA-B60-restricted T cell epitope of the minor histocompatibility antigen HA-1 locus. *J Immunol* 2002;169:3131-3136.
10. Kawase T, Akatsuka Y, Torikai H et al. Alternative splicing due to an intronic SNP in HMSD generates a novel minor histocompatibility antigen. *Blood* 2007;110:1055-1063.
11. Hombrink P, Hadrup SR, Bakker A et al. High-throughput identification of potential minor histocompatibility antigens by MHC tetramer-based screening: feasibility and limitations. *PLoS.One.* 2011;6:e22523.
12. Broen K, Greupink-Draaisma A, Woestenenk R et al. Concurrent detection of circulating minor histocompatibility antigen-specific CD8+ T cells in SCT recipients by combinatorial encoding MHC multimers. *PLoS.One.* 2011;6:e21266.
13. Popović J, Li LP, Kloetzel PM et al. The only proposed T-cell epitope derived from the TEL-AML1 translocation is not naturally processed. *Blood* 2011;118:946-954.
14. Ofrañ Y, Kim HT, Brusica V et al. Diverse patterns of T-cell response against multiple newly identified human Y chromosome-encoded minor histocompatibility epitopes. *Clin.Cancer Res.* 2010;16:1642-1651.
15. Rammensee HG, Singh-Jasuja H. HLA ligandome tumor antigen discovery for personalized vaccine approach. *Expert.Rev Vaccines.* 2013;12:1211-1217.
16. Hillen N, Stevanovic S. Contribution of mass spectrometry-based proteomics to immunology. *Expert.Rev Proteomics.* 2006;3:653-664.
17. van Rooij N, van Buuren MM, Philips D et al. Tumor exome analysis reveals neoantigen-specific T-cell reactivity in an ipilimumab-responsive melanoma. *J Clin.Oncol.* 2013;31:e439-e442.
18. Hong D, Gupta R, Ancliff P et al. Initiating and cancer-propagating cells in TEL-AML1-associated

childhood leukemia. *Science* 2008;319:336-339.

19. Matsushita H, Vesely MD, Koboldt DC et al. Cancer exome analysis reveals a T-cell-dependent mechanism of cancer immunoeediting. *Nature* 2012;482:400-404.
20. Weiss RB, Atkins JF. Molecular biology. Translation goes global. *Science* 2011;334:1509-1510.
21. Ingolia NT, Ghaemmaghami S, Newman JR, Weissman JS. Genome-wide analysis in vivo of translation with nucleotide resolution using ribosome profiling. *Science* 2009;324:218-223.
22. Ingolia NT, Lareau LF, Weissman JS. Ribosome profiling of mouse embryonic stem cells reveals the complexity and dynamics of mammalian proteomes. *Cell* 2011;147:789-802.
23. Nussbaum AK, Kuttler C, Hadelor KP, Rammensee HG, Schild H. PProC: a prediction algorithm for proteasomal cleavages available on the WWW. *Immunogenetics* 2001;53:87-94.
24. Hakenberg J, Nussbaum AK, Schild H et al. MAPP: MHC class I antigenic peptide processing prediction. *Appl.Bioinformatics.* 2003;2:155-158.
25. Nielsen M, Lundegaard C, Lund O, Kesmir C. The role of the proteasome in generating cytotoxic T-cell epitopes: insights obtained from improved predictions of proteasomal cleavage. *Immunogenetics* 2005;57:33-41.
26. Hobo W, Broen K, van der Velden WJ et al. Association of disparities in known minor histocompatibility antigens with relapse-free survival and graft-versus-host-disease after allogeneic stem cell transplantation. *Biol.Blood Marrow Transplant.* 2012
27. Ford ML, Koehn BH, Wagener ME et al. Antigen-specific precursor frequency impacts T cell proliferation, differentiation, and requirement for costimulation. *J Exp.Med* 2007;204:299-309.
28. Hiemstra HS, van Veelen PA, Geluk A et al. Limitations of homology searching for identification of T-cell antigens with library derived mimicry epitopes. *Vaccine* 1999;18:204-208.
29. Moon JJ, Chu HH, Pepper M et al. Naive CD4(+) T cell frequency varies for different epitopes and predicts repertoire diversity and response magnitude. *Immunity.* 2007;27:203-213.
30. Alanio C, Lemaitre F, Law HK, Hasan M, Albert ML. Enumeration of human antigen-specific naive CD8+ T cells reveals conserved precursor frequencies. *Blood* 2010;115:3718-3725.
31. Watanabe K, Suzuki S, Kamei M et al. CD137-guided isolation and expansion of antigen-specific CD8 cells for potential use in adoptive immunotherapy. *Int.J Hematol.* 2008;88:311-320.
32. Wolf M, Kuball J, Ho WY et al. Activation-induced expression of CD137 permits detection, isolation, and expansion of the full repertoire of CD8+ T cells responding to antigen without requiring knowledge of epitope specificities. *Blood* 2007;110:201-210.
33. Chattopadhyay PK, Gaylord B, Palmer A et al. Brilliant violet fluorophores: a new class of ultrabright fluorescent compounds for immunofluorescence experiments. *Cytometry A* 2012;81:456-466.
34. Hadrup SR, Bakker AH, Shu CJ et al. Parallel detection of antigen-specific T-cell responses by multidimensional encoding of MHC multimers. *Nat.Methods* 2009;6:520-526.
35. Arstila TP, Casrouge A, Baron V et al. A direct estimate of the human alphabeta T cell receptor diversity. *Science* 1999;286:958-961.
36. Knabel M, Franz TJ, Schiemann M et al. Reversible MHC multimer staining for functional isolation of T-cell populations and effective adoptive transfer. *Nat.Med.* 2002;8:631-637.
37. Busch DH, Pamer EG. T cell affinity maturation by selective expansion during infection. *J Exp. Med* 1999;189:701-710.





NEDERLANDSE SAMENVATTING
DANKWOORD
LIST OF PUBLICATIONS
CURRICULUM VITAE

&

NEDERLANDSE SAMENVATTING

Hematopoïese en het ontstaan van leukemie

In het bloed bevinden zich verschillende celpopulaties. Veel van deze populaties hebben een relatief korte levensduur en worden constant vernieuwd door nieuwe cellen die differentiëren uit *hematopoïetische stamcellen* (HSC) in de medula van het beenmerg. Deze constante vorming van nieuwe bloedcellen wordt *hematopoïese* genoemd. HSC's hebben de unieke eigenschap om zichzelf te kunnen vernieuwen. Dit houdt in dat er na iedere celdeling altijd een nieuwe HSC ontstaat naast een voorlopercel die verder kan differentiëren naar een specifiek type bloedcel. Het differentiëren van een 'onrijpe' voorlopercel naar een 'rijpe' functionele bloedcellen gebeurt op specifieke locaties zoals het beenmerg, de thymus, lymfklieren en de milt en staat onder stricte regulatie van groeifactoren. Bloedcellen kunnen in verscheidene groepen worden ingedeeld, waaronder een *myeloïde* groep waarin zich onder andere *erythrocyten* (rode bloedcellen), granulocyten en *trombocyten* (bloedplaatjes) bevinden die nodig zijn voor zuurstoftransport, afweer en bloedstolling. Daarnaast de *lymfoïde* groep waarin zich *B-lymfocyten* (B-cellen) en *T-lymfocyten* (T-cellen) bevinden die een belangrijke specifieke rol in ons immuunsysteem spelen. Dagelijks worden er biljoenen nieuwe bloedcellen aangemaakt. Meestal gaat dit goed maar gedurende hematopoïese kunnen er incidenteel op verschillende momenten *DNA mutaties* ontstaan. Deze vorm van DNA schade is een biologisch proces dat kan worden veroorzaakt door normale metabolische processen van delende cellen. Daarnaast kunnen omgevingsfactoren zoals UV- en radioactieve straling en blootstelling aan toxische stoffen hier ook aan bijdragen. Meestal leidt een mutatie tot een abrupte delingsstop van de betrokken cel waarna deze in *apoptose* gaat, een gereguleerde manier van celdood. Wanneer een mutatie leidt tot een ongecontroleerde groei van *abnormale, maligne* cellen in het beenmerg en bloed wordt dit *leukemie* genoemd. Er zijn verschillende verschijningsvormen van leukemie. Bij een opeenhoping van onrijpe snel delende maligne cellen noemt men dit acute leukemie en wanneer het rijpere, meer gedifferentieerde maligne cellen betreft ontwikkelt zich een chronisch leukemie.

Allogene stamceltransplantatie als behandeling van leukemie

Afhankelijk van het type leukemie, de leeftijd van de patiënt en de prognose wordt er een initiële behandeling gekozen die gericht is op het vernietigen van de maligne cellen. Vaak omvat deze behandeling intensieve chemo- en radiotherapie waarbij met behulp van medicijnen of straling zoveel mogelijk maligne cellen worden vernietigd. Omdat een '*remissie*' van de ziekte zelden compleet is, blijven er vaak lage frequenties van maligne cellen achter in het beenmerg of bloed, en is de kans op een *recidief* (terugkomen van

de leukemie) groot. Er is dan ook vaak nog additionele behandeling nodig. Dit kan het uitvoeren van een *allogene stamceltransplantatie* (alloSCT) zijn. Bij een *allogene stamceltransplantatie* (alloSCT) worden stamcellen uit het beenmerg van een gezonde donor naar de patiënt getransplanteerd. De donor kan een verwante donor (directe familie) maar ook een niet-verwante donor zijn met een overeenkomende *HLA-typing*, de genen die coderen voor het *major histocompatibility complex* (MHC). Aan de alloSCT gaat een intensieve pre-conditioning vooraf waarin met behulp van chemo- en radiotherapie naast achtergebleven maligne cellen ook de gezonde HSC in het beenmerg van de patiënt worden vernietigd. Vervolgens worden gezonde HSC van de donor in de patiënt getransplanteerd. De toegediende stamcellen zullen de patiënt herkoloniseren en het hematopoïetische systeem herstellen. Naast het vervangen van potentiële maligne stamcellen heeft een alloSCT ook een aanvullend extra voordeel ten opzichte van een *autologe stamceltransplantatie* waarin de HSC afkomstig zijn van de patiënt zelf T-cellen in het transplantaat kunnen een sterke immuunreactie vormen tegen de achtergebleven hematopoïetische cellen, en wellicht chemotherapie resistente maligne cellen van de patiënt opruimen. Deze zogenoemde *Graft versus Tumor* (GvT ofwel transplantaat versus tumor) reactie ontstaat doordat de toegediende T-cellen de tumorcellen als lichaamsvreemd herkennen. Daarnaast kunnen donor T-cellen in het transplantaat ook een immuunreactie vormen tegen de gezonde weefsels van de patiënt. Deze potentieel levensbedreigende *Graft versus Host Disease* (GvHD) manifesteert zich vooral in de darmen, lever, huid, en longen. Om ernstige GvHD te voorkomen wordt gezocht naar een stamcel donor met een zo identiek mogelijke HLA-typing. Om het risico op GvHD te verminderen kan na alloSCT ervoor gekozen worden om donor T-cellen uit het transplantaat te verwijderen (*T-cel depletie*). Een nadeel van deze T-cel depletie is een vergrote kans op een recidief. Naast een vermindering van het GvT effect leidt verwijdering van T-cellen ook tot een verhoogde kans op opportunistische virale complicaties. Als er geen virus-specifieke T-cellen in het transplantaat van de donor aanwezig zijn, kunnen latent in de immuungecompromitteerde patiënt levende virussen zoals Epstein-Barr virus (EBV) en Cytomegalovirus (CMV) reacteren en ernstige, potentiële levensbedreigende infecties veroorzaken. Het manipuleren van de immuunrespons na alloSCT om gewenste en ongewenste effecten van elkaar te scheiden vormt de basis van veel immuuntherapieën.

&

Donor lymfocyten infusie na allogene stamceltransplantatie

Indien er na een alloSCT nog steeds of opnieuw hematopoïetische cellen van patiënt herkomst worden aangetroffen spreekt men van een onvolledig *donor chimerisme*. Deze achtergebleven cellen kunnen leiden tot een recidief van de leukemie en dienen ideaal gezien te worden vernietigd. Om dit te bereiken of te voorkomen (profylactisch) dat een recidief optreedt, kan de patiënt na alloSCT worden behandeld met T-cellen van de oorspronkelijke donor. Deze therapie noemt men een *donor lymfocyten infusie* (DLI). Als

het gewenste effect van een DLI uitblijft, kan meermalig DLI worden toegediend. Als vroeg na alloSCT een recidief optreedt of de kans daarop groot is, is de keuze om DLI te geven vaak lastig. Aangezien in de patiënt, als gevolg van pre-conditioning geïnduceerde weefselschade en infecties, een proinflammatoire cytokine milieu kan zijn gecreëerd is er een verhoogde kans op GvHD. Voor het bereiken van het gewenste therapeutische effect na een DLI is het dus belangrijk om de goede balans tussen de kansen op het optreden van GvT en GvHD te vinden. Veel onderzoek is er op gericht om T-cellen te kunnen selecteren, die uitsluitend antigenen herkennen die specifiek door maligne of patiënt hematopoïetische cellen worden aangeboden. Net zoals het selecteren en toedienen van virus specifieke T-cellen kan helpen bij het voorkomen en terugdringen van opportunistische virale infecties, kan het toedienen van geselecteerde T-cellen die slechts aan GvT bijdragen, leiden tot een langdurige immuunreactie tegen deze kwaadaardige cellen in de afwezigheid van ernstige GvHD.

De basis van T-cel reactiviteit

T-cellen kunnen lichaamsvreemde cellen herkennen met behulp van een *T-cel receptor* (TCR). Het TCR repertoire in onze T-cel populatie is enorm divers en elke TCR is in principe specifiek voor een bepaald antigeen. Een TCR is een heterodimeer die bestaat uit een *TCR α* en *TCR β* keten. In deze ketens vinden willekeurige mutaties en recombinaties plaats in de *complimentarity determining regions* (CDR3) die bepalen welke specifieke structuur (epitoot) de betreffende T-cel kan herkennen nadat deze is aangeboden door HLA-moleculen. Deze TCR gen recombinaties vormen de basis voor de diversiteit in ons *TCR repertoire* en vormen evolutionair gezien een belangrijke overlevingsstrategie. Voordat een gematureerde T-cel met zijn unieke TCR de thymus kan verlaten en in de bloedbaan kan worden opgenomen, wordt deze gecontroleerd op zijn vermogen om interacties met eigen HLA-moleculen aan te kunnen gaan. Herkenning van lichaamsvreemde epitopen, zoals die afkomstig van virussen en bacteriën, maar ook die van patiëntenweefsel met een vreemd HLA-type, kan de T-cel doen activeren. Vervolgens zal de T-cel de potentieel geïnficeerde cel doorboren met perforines om toegang te verschaffen voor de door de T-cel uitgescheiden *cytotoxische moleculen* zoals granzymes en granulysin. Deze zullen vervolgens de geïnficeerde cel aanzetten tot *apoptose*.

T-cellen zijn op basis van de expressie van het type *coreceptor* molecuul te onderscheiden in twee categorieën. Deze coreceptor kan tijdens het herkennen van een vreemd HLA-peptide complex door de TCR ook aan het HLA van de geïnficeerde cel binden. Door deze interactie verankert de T-cel zich aan de geïnficeerde cel en kan er een cascade van intracellulaire signalering ontstaan die noodzakelijk is om de T-cel te activeren. Onderscheid wordt gemaakt tussen T-cellen die een *CD4* of *CD8* co-receptor op hun oppervlak presenteren. In deze studie wordt gefocust op de *CD8* positieve T-cellen die beperkt zijn tot het herkennen van epitopen in *HLA klasse I*. HLA klasse I moleculen

komen in tegenstelling tot klasse II constant tot expressie op alle kernhoudende cellen. CD8 positieve T-cellen die in de context van HLA klasse I antigenen kunnen herkennen zijn overwegend effector T-cellen met een cytotoxische activiteit die vreemde cellen kunnen liseren.

Minor-antigenen

Voor het slagen van een stamceltransplantatie is het relevant om de juiste donor te selecteren. Wanneer er een verschil in HLA-typering bestaat tussen patiënt en donor, een zogenoemde 'major mismatch', zal een groot gedeelte van de geïntroduceerde donor T-cel immuniteit zich richten tegen epitopen die worden gepresenteerd door het vreemde HLA-molecuul. Het T-cel compartiment van een individu bestaat uit T-cellen die alleen lichaamsvreemde en niet lichaameigen epitopen in eigen HLA moleculen mogen herkennen. T-cellen zijn tijdens hun selectie in de thymus in de donor niet zijn geselecteerd om te voorkomen dat zij lichaamseigen epitopen in de context van vreemd patiënt HLA herkennen. Hierdoor kunnen de geïntroduceerde T-cellen de door dit vreemde HLA aangeboden lichaamseigen epitopen herkennen als lichaamsvreemd en zodoende gezonde cellen aanvallen. Als gevolg hiervan kan er een zeer ernstige GvHD optreden. Echter, in de context van een HLA-identieke stamceltransplantatie kan er nog steeds T-cel immuniteit optreden tegen cellen van de patiënt. Deze allo-activiteit wordt veroorzaakt door lichaamsvreemde peptiden afkomstig van de patiënt die in hetzelfde type HLA worden aangeboden, en door donor T-cellen kunnen worden herkend.. In dit geval kan de T-cel immuniteit worden verklaard door de herkenning van zogenoemde *minor-antigenen*. Deze potentieel immunogene epitopen zijn het product van polymorfe genen, het gevolg van kleine variaties in het DNA tussen twee individuen. Er zijn talrijke verschillen in het DNA tussen individuen. Verschillen in nucleotide kunnen aminozuurveranderingen opleveren met als gevolg dat andere peptides door het HLA gepresenteerd kunnen worden. Wanneer een polymorf peptide door T-cellen van een ander individu herkend kan worden spreekt men van een minor-antigeen. De zogenoemde *single nucleotide polymorphisms* (SNP) die coderen voor minor-antigenen komen met een bepaalde frequentie in een populatie voor. Afhankelijk van deze frequentie, zal een specifieke T-cel populatie gericht tegen dit minor-antigeen in veel of weinig patiënten te vinden zijn na een alloSCT en DLI.

Wanneer een minor-antigeen breed tot expressie komt op gezonde weefsels (zowel hematopoïetische als niet-hematopoïetische cellen) van de patiënt kan de T-cel reactiviteit van de donor bijdragen aan GvHD omdat de T-cellen deze gezonde cellen als vreemd zullen herkennen en liseren. Als het minor-antigeen alleen gepresenteerd wordt op alle hematopoïetische cellen of preferentieel op de maligne cellen van de patiënt kan deze echter bijdragen aan GvT. Het elimineren van de hematopoïetische cellen van de patiënt waar de leukemiecellen een onderdeel van zijn, leidt namelijk niet tot problemen aangezien de normale hematopoïese na de transplantatie van donor herkomst is, en dus niet door

donor T-cellen zal worden aangevallen. Therapeutisch relevante minor-antigenen worden daarom preferentiël door hematopoïetische of maligne cellen tot expressie gebracht. Om de weefseldistributie van minor-antigenen te karakteriseren is een uitgebreide genexpressie analyse noodzakelijk. Een infusie van T-cellen die reactief zijn tegen minor-antigenen die uitsluitend worden gepresenteerd door het hematopoïetische systeem van de patiënt, en zodoende reactief zijn tegen de hematopoïetische cellen, inclusief de maligniteit, is een ideale manier om langdurige genezing van leukemie te induceren. Deze *minor-antigeen-specifieke immunotherapie* kan, zoals onderzoek heeft aangetoond, effectief zijn. Er zijn echter nog maar een beperkt aantal minor-antigenen geïdentificeerd die uitsluitend door het hematopoïetische systeem worden gepresenteerd. Om minor-antigeen-specifieke immunotherapie tot een realistische optie te maken voor veel patiënten met leukemie dienen er meer geschikte minor-antigenen te worden geïdentificeerd.

Dit proefschrift

In dit proefschrift zijn methoden onderzocht om op een innovatieve wijze minor-antigeen-specifieke CD8 positieve T-cellen te identificeren. De conventionele, '*voorwaartse methode*' om nieuwe minor-antigenen te identificeren is sinds zijn ontdekking drastisch veranderd en geoptimaliseerd maar is in essentie niet veranderd. T-cellen met een onbekende specificiteit worden geïsoleerd uit het bloed van patiënten die een HLA-identieke stamceltransplantatie hebben ondergaan. Met behulp van verschillende moleculaire methoden kan vervolgens het herkende minor-antigeen geïdentificeerd worden. Met behulp van de voorwaartse methode is er de afgelopen jaren een grote hoeveelheid minor-antigenen met uiteenlopende weefseldistributies geïdentificeerd. Helaas zijn er hiervan veel niet therapeutisch relevant vanwege een ongunstige weefseldistributie van het minor-antigeen coderende gen. Om de identificatie van therapeutisch relevante minor-antigenen efficiënter te maken is in dit onderzoek de mogelijkheid onderzocht om met een '*terugwaartse methode*' minor-antigenen en de bijbehorende specifieke T-cellen te identificeren. Het fundamentele verschil tussen deze en de voorwaartse methode is de keuze voor het epitoom dat herkend dient te worden. Het uitgangspunt van deze methode is gebaseerd op het kunnen voorspellen van perfecte, hematopoïese-specifieke minor-antigenen door het gebruik van *datbanken* en *bioinformatica*. Als een voorspeld minor-antigeen op theoretische wijze voldoet aan alle opgestelde criteria kan vervolgens in het bloed van gezonde donoren gezocht worden naar een T-cel die uitsluitend dit epitoom herkend. Het isoleren van deze voorspelde minor-antigeen-specifieke T-cellen is het einddoel van deze methode. Gebleken is dat de kans om dit soort T-cellen te isoleren uit de totale T-cel populatie erg klein is. Daarom moeten verschillende verrijkmethode worden ontwikkeld om tot dit resultaat te komen. Omdat de TCR de specificiteit van de minor-antigeen-specifieke T-cellen bepaalt, kan de TCR worden gekloneerd en worden gebruikt in een immunotherapie waarin deze wordt geïntroduceerd in donor T-cellen van

een ander individu. Door met de terugwaartse methode op grote schaal nieuwe minor-antigeen-specifieke T-cellen te isoleren kan er een *TCR-bank* worden aangelegd die in de toekomst patiënten die een allogene stamceltransplantatie ondergaan mogelijk kan voorzien van een minor-antigeen-specifiek T-cel product met gewenste anti-leukemie reactiviteit.

In **hoofdstuk 2** wordt onderzocht of het haalbaar is om met de op dat moment beschikbare technieken op een efficiënte manier de specificiteit van grote hoeveelheden T-cellen te analyseren. Met behulp van publieke *SNP en genexpressie databanken* en drie verschillende *peptide-HLA-binding algoritmes* kan een groot aantal minor-antigenen worden voorspeld. Vervolgens worden bloedmonsters van patiënten die een succesvolle alloSCT en DLI hebben ondergaan geanalyseerd met complexen van vier recombinante HLA-moleculen (MHC-tetrameren) die een specifiek voorspeld peptide aanbieden. T-cellen die deze zogenoemde '*MHC-tetrameren*' herkennen kunnen op basis van een fluorescent label worden geïdentificeerd. Hoewel het technisch haalbaar blijkt om met de ontwikkelde methode op grote schaal peptide-specifieke T-cellen te isoleren – er worden T-cellen geïsoleerd voor 71 voorspelde minor-antigenen – blijkt geen van deze T-cellen in staat te zijn de door de patiënt van nature gepresenteerde peptiden te herkennen. Op basis van dit hoofdstuk kunnen twee belangrijke conclusies getrokken worden die voor het verdere verloop van het onderzoek relevant zijn. Allereerst blijkt dat het willekeurig analyseren van patiënten op de aanwezigheid van minor-antigeen reactieve T-cellen, in de context van een epitooop-gedreven terugwaartse methode, zonder hun *SNP status* in overweging te nemen, een zeer lage efficiëntie op te leveren. Het grootste deel van de geïsoleerde MHC-tetrameer positieve T-cellen blijkt niet in staat minor-antigeen presenterende cellen te kunnen herkennen. Vermoedelijk komt dit doordat de geïsoleerde T-cellen in de thymus van de oorspronkelijke donor zijn geselecteerd om lichaamseigen epitopen *niet* te herkennen. T-cellen geïsoleerd in deze categorie hebben een overwegend lage aviditeit voor de voorspelde minor-antigenen. Daarnaast worden er ook T-cellen geïsoleerd uit donoren die het voorspelde minor-antigeen *wel* met een hoge aviditeit herkennen. Dit wordt aangetoond door op een artificiële manier dit antigeen door antigeen-negatieve cellen tot expressie te laten brengen. Deze cellen worden alleen dan herkend. Omdat cellen van de patiënt niet herkend worden geeft dit aan dat een groot deel van de voorspelde minor-antigenen niet van nature wordt gepresenteerd door het HLA op de cellen van de patiënt.

In **hoofdstuk 3** wordt onderzocht of het met de ontwikkelde MHC-tetrameer verrijkmethode mogelijk is om laag-frequente peptide-reactieve T-cellen effectiever te isoleren uit perifere bloed en wat hun vermogen is goed hun epitooop te herkennen. Van de geselecteerde virale peptiden is eerder aangetoond dat ze van nature worden gepresenteerd door geïnfecteerde cellen in één van de veel voorkomende HLA allelen; A1, A2, B7, B8 en B40, en dat T-cel immuniteit tegen deze epitopen bestaat. Met de isolatie van laag-frequente

T-cellen uit het 'naïeve' repertoire willen we de gevoeligheid van de isolatiemethode bepalen. Voor dit doeleinde zijn donoren met een negatieve serologische status voor het humane herpesvirus CMV geselecteerd en is met behulp van de MHC-tetrameer verrijkmethode getracht CMV-specifieke naïeve T-cellen te isoleren. Het blijkt mogelijk om in twee opeenvolgende MHC-tetrameer verrijkingstappen duidelijk aantoonbare MHC-tetrameer-positieve T-cel populaties op te kweken voor 8 van de 10 geselecteerde epitopen. Door het V-beta keten gebruik van de TCR van MHC-tetrameer-positieve T-cel populaties te analyseren laten we zien dat deze van een complexe samenstelling zijn. Het meermaals uitvoeren van een zelfde isolatie experiment laat zien dat de frequentie van CMV specifieke voorloper cellen in het naïeve T-cel repertoire een grote invloed heeft op de samenstelling van de expanderende T-cel populaties. Door de verschillende populaties functioneel te testen op de herkenning van cellen die beladen zijn met peptide of die het peptide endogeen presenteren blijkt dat veel geïsoleerde T-cel klonen niet reactief zijn tegen het specifieke CMV-peptide. Blijkbaar correleert de MHC-tetrameer aankleuring van een T-cel populatie niet altijd met *functionele reactiviteit*, zeker wanneer T-cellen worden verkregen uit het naïeve repertoire aangezien deze nog niet zijn geselecteerd op een hoge aviditeit zoals antigeen-ervaren T-cellen. Dit gebrek aan correlatie kan worden verklaard door de manier waarop een recombinant MHC-multimeren complex (MHC-tetrameer) zich aan een T-cel bindt. Door de *associatie- en dissociatiekinetiek* van het MHC-peptide-TCR-complex te bestuderen met behulp van een innovatieve *streptameer* techniek blijkt dat deze kinetiek tussen een TCR en een MHC-tetrameer op een onnatuurlijke wijze verstoord is door de multimerisatie van MHC-peptide moleculen. Met behulp van streptameren, een complex dat sterk lijkt op een MHC-tetrameer maar waarvan de sterptavidine-biotine anker-residuen van het complex na de binding met een T-cel verbroken kunnen worden, tonen we aan dat de dissociatiekinetiek van een TCR met een enkel MHC-peptide molecuul wel correleert met de functionaliteit van de geïsoleerde T-cel kloon. We laten zien dat van vier T-cel klonen met een relatief vergelijkbare hoge MHC-tetrameer aankleuring er maar twee daadwerkelijk functioneel zijn. Door deze analyse kunnen functionele en niet-functionele T-cel klonen in de toekomst van elkaar worden onderscheiden.

In **hoofdstuk 4** wordt een nieuwe methode beschreven die ontwikkeld wordt om minor-antigenen te voorspellen en de bijbehorende T-cellen te isoleren. In deze methode wordt een andere bron van minor-antigenen geïntegreerd in de terugwaartse identificatiemethode. Peptiden die van nature gepresenteerd worden door het HLA van cellen worden door een zuurbehandeling geëluëerd en vervolgens geïdentificeerd op basis van hun *moleculaire massa* met behulp van *massaspectrometrie*. Deze bron van geëluëerde peptiden garandeert dat de peptiden van nature gepresenteerd kunnen worden in het HLA op het celmembraan van cellen. Om minor-antigenen te identificeren die van nature door hematopoïetische cellen kunnen worden gepresenteerd is gebruik gemaakt van *geïmmortaliseerde B-cellijnen* als peptidenbron. De identificatie van de

biologisch relevante en immunogene *LB-NISCH-1A* minor-antigeen-specifieke T-cel uit het bloed van een gezonde donor toont aan dat deze nieuwe methode haalbaar is. Deze nieuwe methode wordt vervolgens in **hoofdstuk 5** op grotere schaal gebruikt om vanuit een nieuwe databank van geëluëerde peptiden minor-antigenen te voorspellen en daar vervolgens immunogene T-cellen voor te isoleren. Dit leidt tot de identificatie van de minor-antigenen *LB-CLYBL-1Y* en *LB-TEP1-1S*. De klinische relevantie van *LB-CLYBL-1Y* wordt aangetoond door de aanwezigheid van MHC-tetrameer-positieve T-cellen in het bloed van een patiënt na alloSCT. Hiermee is de cirkel rond en tonen we aan dat met de in dit proefschrift ontwikkelde terugwaartse methode T-cellen met een gewenst minor-antigeen herkenningspatroon geïdentificeerd kunnen worden.

Tot op heden is het aantal minor-antigenen dat geïdentificeerd werd met een voorwaartse methode groter dan die resulteren uit een terugwaartse methode. In dit proefschrift tonen we aan dat het voorspellen van klinisch relevante T-cel epitopen onverwacht complex is. De identificatie van drie nieuwe minor-antigenen met de in dit proefschrift ontwikkelde terugwaartse methode geeft de mogelijkheid aan maar de lage efficiëntie maakt deze nog niet tot een volwaardige concurrent van de voorwaartse methode. In de komende jaren kan het gebruik van nieuwe bioinformatische informatie de efficiëntie van terugwaartse epitoom identificatie methoden verhogen. Hierdoor kan een grote collectie van T-cel producten worden aangelegd waardoor het realistischer wordt om patiënten met een minor-antigeen specifieke therapie op maat te behandelen.



&

DANKWOORD

Op een vroege decemberochtend in 2011 kreeg ik vlak voor mijn eerste praatje op het grootste internationale hematologiecongres een belangrijk advies. “Houdt de spanning tot het einde vast en laat deze niet direct los bij het uitspreken van je laatste woorden, een goed optreden tijdens de vragenronde bepaalt hoe je bij het publiek blijft hangen”. Ondanks een grote dosis gezonde spanning ging mijn presentatie inclusief vragenronde goed en ik denk nog vaak met plezier terug aan deze indrukwekkende tijd. Dit advies heb ik ook proberen te volgen bij het afronden van mijn promotietraject. Het was niet altijd eenvoudig om in de twee jaar sinds mijn vertrek uit Leiden mijn energie te doseren en verdelen om tot een goed resultaat te komen. Het advies bleek wederom waardevol en ik ben trots op het resultaat, mijn proefschrift is klaar!

Allereerst wil ik graag mijn collega's bedanken van het laboratorium voor Experimentele Hematologie en in het bijzonder die uit “37” voor de geweldige sfeer die ik daar heb ervaren. Het was geweldig om te beleven hoe in het bijzonder de oudgedienden een hechte en warme groep vormen waar de nieuwe PhD studenten zich meteen thuis voelen. Adviezen en ervaringen werden met veel enthousiasme gedeeld en tijdens de koffiepauze op “de brug” werden naast de dagelijkse belevenissen ook vaak de saillantste details besproken.

Michel Kester wil ik speciaal bedanken voor onze geweldige samenwerking gedurende mijn gehele promotietraject. Door onze discussies heb je mijn enthousiasme vergroot voor de wetenschap en vooral voor het biochemische “groffuh gooi- en smijtwerk” waar je echt een kei in bent. Lorenz Jahn wil ik bedanken voor de enorme berg werk die hij verzet heeft tijdens zijn stage en de manier waarop hij hiermee later als PhD student is doorgegaan. Heren, naast goede collega's zijn we ook vrienden geworden en ik ben er trots op straks aan jullie zijde op het Rapenburg te mogen staan.

Daarnaast wil ik alle co-auteurs danken voor hun belangrijke bijdrage aan het tot stand komen van de hoofdstukken. In het bijzonder mijn eerste student Yotam Raz. Ik heb je tijdens je “vrijwillige” stage van puber zien opgroeien tot enthousiaste onderzoeker en ik weet zeker dat je een groot onderzoeker gaat worden. I thank Sine Reker Hadrup. As an experienced Postdoc you took me by the hand during the first difficult phase of my PhD. You showed me the great things that can be done using multi-color flow cytometry that I am still doing today. Thanks for inviting me at your lab in Copenhagen and for having me as a guest at your house.

Mijn ouders wil ik bedanken voor hun onvoorwaardelijke steun en liefde. Ik heb jullie geduld op de proef gesteld maar dit leidde alleen maar tot meer aanmoedigingen.

Lieve Liset, met jou is het iedere dag genieten. Fijn dat we elkaar zo goed begrijpen. Zonder jouw hulp was dit boekje nooit op tijd afgekomen. Op de volgende berg staan we samen!

&

CURRICULUM VITAE

Pleun Hombrink werd geboren op 28 juli 1982 te Eindhoven. Na het behalen van het VWO diploma aan het Over Betuwe College te Bommel in 2001, begon hij in datzelfde jaar met de studie Biomedische wetenschappen aan de Universiteit Utrecht. In 2004 behaalde hij zijn Bachelor of Science titel en begon aan de master Immunititeit en Infectie aan de Universiteit Utrecht. Na een masterstage bij de afdeling Pediatrische Immunologie van het Wilhelmina Kinderziekenhuis, Universitair Medisch Centrum Utrecht (Prof. Dr. A.B.J. Prakken) en een tweede masterstage bij de afdeling Experimentele Virologie van het Academisch Medisch Centrum in Amsterdam (Dr. A.T. Das) behaalde hij in 2006 de Master of Science titel. Vervolgens werd vanaf 2007 tot heden het in dit proefschrift beschreven promotieonderzoek uitgevoerd op het Laboratorium voor Experimentele Hematologie in het Leids Universitair Medisch Centrum onder leiding van Dr. M.H.M. Heemskerk en Prof. Dr. J.H.F. Falkenburg. Tijdens deze periode werd intensief samengewerkt met de massaspectrometriegroep (Dr. P.A. van Veelen) van de afdeling Immunohematologie en Bloedtransfusie.

Vanaf september 2012 is hij werkzaam als post-doctoraal onderzoeker op de afdeling Hematopoïese van Sanquin Research in Amsterdam. Hier werkt hij aan het karakteriseren van primaire T-cellen uit humaan longweefsel.

LIST OF PUBLICATIONS

Hombrink P, Hadrup SR, Bakker A, Kester MG, Falkenburg JH, von dem Borne PA, Schumacher TN, Heemskerk MH. High-throughput identification of potential minor histocompatibility antigens by MHC tetramer-based screening: feasibility and limitations. *PLoS One* 2011;6(8):e22523.

Hombrink P, Hassan C, Kester MG, de Ru AH, van Bergen CA, Nijveen H, Drijfhout JW, Falkenburg JH, Heemskerk MH, van Veelen PA. Discovery of T cell epitopes implementing HLA-peptidomics into a reverse immunology approach. *Journal of Immunology* 2013 Apr 15;190(8):3869-77.

Hombrink P, Raz Y, Kester MG, de Boer R, Weißbrich B, von dem Borne PA, Busch DH, Schumacher TN, Falkenburg JH, Heemskerk MH. *Mixed functional characteristics correlating with TCR-ligand koff -rate of MHC-tetramer reactive T cells within the naive T-cell repertoire.* *European Journal of Immunology* 2013 Nov;43(11):3038-50.

Hombrink P, Hassan C, Kester MG, Jahn L, Pont MJ, Ru AH, Bergen CAM, Griffioen M, Falkenburg JH, van Veelen PA, Heemskerk MH. Identification of biological relevant minor histocompatibility antigens within the B-lymphocyte derived HLA-ligandome using a reverse immunology approach. *Submitted.*

Publications not in this thesis

Hombrink P, Backer RA, Piet B, Jongejan A, Jonkers RE, Helbig C, Amsen D, Moerland PD, van Lier RA. The transcriptional profile of human CD8⁺ lung resident memory T-cells. *Submitted.*

&

Jahn L, Hombrink P, Hassan C, Kester MG, van der Steen DM, Hagedoorn RS, Falkenburg JH, van Veelen PA, Heemskerk MH. Therapeutic targeting of the BCR associated protein CD79b in a TCR-based approach is hampered by aberrant expression of CD79b. *Submitted.*

van Aalderen MC, Remmerswaal EBM, Versteegen NJM, Hombrink P, ten Brinke A, Pircher H, Kootstra NA, ten Berge IJM, van Lier RA. Two dimensions in human CD8⁺ T-cell development: cell surface phenotype in conjunction with T-bet and Eomes expression levels predicts the functional potential of antigen-experienced CD8⁺ T-cells. *Submitted.*

Linnemann C, Heemskerk B, Kvistborg P, Kluin RJ, Bolotin DA, Chen X, Bresser K, Nieuwland M, Schotte R, Michels S, Gomez-Eerland R, Jahn L, Hombrink P, Legrand N, Shu

CJ, Mamedov IZ, Velds A, Blank CU, Haanen JB, Turchaninova MA, Kerkhoven RM, Spits H, Hadrup SR, Heemskerk MH, Blankenstein T, Chudakov DM, Bendle GM, Schumacher TN. High-throughput identification of antigen-specific TCRs by TCR gene capture. *Nature Medicine* 2013 Nov;19(11):1534-41.

Hassan C, Kester MG, de Ru AH, Hombrink P, Drijfhout JW, Nijveen H, Leunissen JA, Heemskerk MH, Falkenburg JH, van Veelen PA. The human leukocyte antigen-presented ligandome of B lymphocytes. *Molecular and Cellular Proteomics* 2013 Jul;12(7):1829-43.

Falkenburg WJ, Melenhorst JJ, van de Meent M, Kester MG, Hombrink P, Heemskerk MH, Hagedoorn RS, Gostick E, Price DA, Falkenburg JH, Barrett AJ, Jedema I. Allogeneic HLA-A*02-restricted WT1-specific T cells from mismatched donors are highly reactive but show off-target promiscuity. *Journal of Immunology* 2011 Sep 1;187(5):2824-33.

de Jong H, Berlo SE, Hombrink P, Otten HG, van Eden W, Lafeber FP, Heurkens AH, Bijlsma JW, Glant TT, Prakken BJ. Cartilage proteoglycan aggrecan epitopes induce proinflammatory autoreactive T-cell responses in rheumatoid arthritis and osteoarthritis. *Annals of Rheumatic Diseases* 2010 Jan;69(1):255-62.

Hadrup SR, Bakker AH, Shu CJ, Andersen RS, van Veluw J, Hombrink P, Castermans E, Thor Straten P, Blank C, Haanen JB, Heemskerk MH, Schumacher TN. Parallel detection of antigen-specific T-cell responses by multidimensional encoding of MHC multimers. *Nature Methods* 2009 Jul;6(7):520-6.